CUTANEOUS LEISHMANIASIS

-SKIN BARRIER PROPERTIES AND DRUG DELIVERY STRATEGIES-

A thesis submitted by

Katrien Van Bocxlaer

For the degree of

Doctor of Philosophy

University College London

School of Pharmacy

Department of Pharmaceutics

29-39 Brunswick Square

London WC1N 1AX

2015

DECLARATION

I, Katrien Van Bocxlaer confirm that the work presented in this thesis is my own. Where information has been derived from other sources, I confirm that this has been indicated in the thesis.

Date:

Printed name:

Signature:

ACKNOWLEDGEMENTS

First, I would like to thank Dr. Sudax Murdan for her helpful advice and support. I also would like to thank my LSHTM supervisors Prof. Simon Croft and Dr. Vanessa Yardley for their enthusiasm, guidance, encouragement and support throughout this entire PhD.

Thank you to Lindsay Stewart for the many times she offered to help and especially for her guidance on the PCR and qPCR method; to Alec, alias babybird, for the overload of sugar and cheerfulness; and Evangelia Piperakis for providing the drawing that summarised this PhD and for the often refreshing intermezzos.

A huge thank you to the entire DMPK team of Scynexis for their patience, help and hospitality. A special thanks to Dr. Steve Wring for his mentorship, calm and patience. Together with the other Scynexians and the Frenchies, Alexis and Corentin, they turned my 3 months in the US into an incredible experience.

I wish to acknowledge Dr. Bob Jacobs and the entire Anacor team for the stimulating telephone conferences, their enthusiasm, help and financial support.

A special thanks to my friend Katie for her continuous support, the evening moral boost sessions and her friendship; to Francisco, Britt, Justine and Shahr for helping me keep my sanity and the incredible nights out.

Many thanks to my colleagues of lab 239: Rose, Andrew, Holly, Oihane, Matt, Emilie, Lisa, Juliana, Chris; and lab 324: Pierfranscesco, Laxmi, Basma and Seen-Wai. I also want to thank other SOP buddies: Jawal, Ina, Mary, Alex, Haydar, and Jonny. Apologies for those who I have forgotten, there are plenty more people who have supported and helped me over the years.

My final thanks are to my mum, sister and brother (alias het 'thuisfront') without whom I would have never gotten here in the first place.
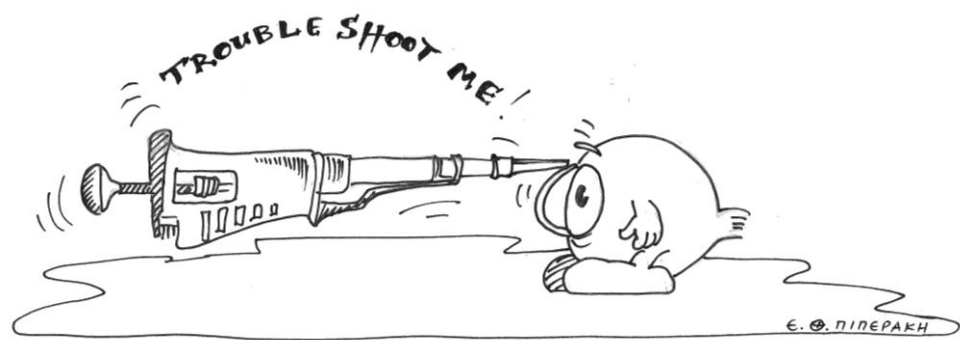
ABSTRACT

Cutaneous leishmaniasis (CL) is a parasitic disease caused by several species of the protozoan parasite *Leishmania* and affects approximately 10 million people worldwide. The drugs currently available such as miltefosine, amphotericin B and pentavalent antimonials, are limited by high cost, considerable side effects and restricted efficacy.

CL could potentially be treated by a topical formulation. In its simplest form CL consists of a single nodule or papule, typically on exposed body parts, with the parasites residing in the lower epidermis and dermis. A topical treatment would minimise possible adverse effects by reducing the amount of drug taken up in the systemic circulation and would be easy to apply which is important for patient compliance.

The overall aim of the work described in this thesis was to explore the use of different drugs in a topical formulation to cure CL. To be efficacious, a topical treatment requires the permeation of the active ingredient through the *stratum corneum* and into the deeper layers of the skin where the *Leishmania* parasites resides. Intact skin is a highly effective barrier against xenobiotics. However many skin diseases are known to affect the skin barrier making it more or less permeable to drugs. An understanding of the permeability of the skin hosting the *Leishmania* parasites is a prerequisite when trying to optimize drug delivery to the skin. Therefore the barrier function of *Leishmania* infected skin in early stages of CL was characterised with respect to histology, transepidermal water loss and drug permeation.

Suitable anti-leishmanial drugs with the potential to permeate into the skin were identified through literature review, taking into account the information obtained from the skin barrier characterisation. The leishmanicidal activity of the drugs was evaluated in an intracellular amastigote-macrophage model and potent compounds were selected for further work.

First, the re-formulation of miltefosine, currently used to treat leishmaniasis via oral administration, into a topical formulation was explored. The effects of different solvents on its permeation through and disposition in the skin was evaluated using *in vitro* Franz diffusion cell permeation studies.

Secondly, a drug discovery approach was used to identify lead benzoxaboroles, a set of interesting anti-leishmanial compounds. In the early stages, *in vitro* ADME studies were conducted to establish basic pharmacokinetic parameters of a range of benzoxaboroles. This information together with previously unpublished data was used to select compounds for further testing such as stability and binding in skin homogenate and permeation evaluation. The three most promising compounds were tested *in vivo* in a CL model.

Table of Contents

LIST OF ABBREVIATIONS

ADME	absorption – distribution – metabolism-excretion
AmB	amphotericin B
b.i.d.	bis in die (twice a day)
BPQ	buparvaquone
CD	cyclodextrin
CL	cutaneous leishmaniasis
DMI	dimethyl isosorbide
FDC	Franz diffusion cell
GM-CSF	granulocyte-macrophage colony-stimulating factor
HAT	human African trypanosomiasis
HePC	hexadecylphosphocholine
HiFCS	heat-infactivated foetal calf serum
HPLC	high performance liquid chromatography
i.m.	intramuscular
i.v.	intraveneous
ICH	immunohistochemistry
LCL	localized cutaneous leishmaniasis
LC-MS/MS	liquid chromatography-tandem mass spectrometry
MA	meglumine antimoniate
MBCL	methylbenzethonium chloride
MCL	mucocutaneous leishmaniaisis
OSAL	octyl salicylate
PBS	phosphate buffered saline
PG	propylene glycol
Pgp	P-glycoprotein
PKDL	post kala-azar dermal leishmaniasis
PK-PD	pharmacokinetics and pharmacodynamics
PM	paromomycin sulphate
RCT	randomised controlled trial
s.c.	subcutaneous
Sb^{III}	trivalent antimony
Sb^{V}	pentavalent antimony
spp.	species
SSG	sodium stibogluconate
UV	ultraviolet
VL	visceral leishmaniasis

LIST OF FIGURES

LIST OF TABLES

1 INTRODUCTION

Today many topical pharmaceutical formulations are on the market. A considerable number of these products are used to treat viral, bacterial or fungal infections whereas only one topical formulation is commercially available to treat cutaneous leishmaniasis (Leshcutan®; Teva, Israel).

Cutaneous leishmaniasis (CL) is a widespread parasitic disease that affects 12 million people worldwide[1] with 0.7-1.2 million new cases every year[1]. It is characterized by a variety of clinical symptoms ranging from defined nodular lesions to gross mucosal destruction. Non-complicated lesions tend to heal spontaneously but this process can take 3 to 18 months and nearly always leave a disfiguring scar[2, 3]. Available treatments are constrained by parenteral drug administration, toxicity, cost and limited efficacy. For example Leshcutan® ointment contains an aminoglycoside drug, paromomycin sulphate (PM) that is formulated with an excipient that solubilizes skin lipids and decreases the skin barrier function. This is necessary to enable the skin permeation of PM and thus treatment efficacy. The excipient is also the main cause of skin irritation that is often reported after application of the ointment[4-6]. Intrinsic insensitivity of *Leishmania* species to drugs may contribute to the variable cure rates observed[3, 7-9].

For localized diseases such as CL, a topical formulation would be easy to apply and local application would reduce the risk of adverse effects and resistance development.

The skin has a unique composition and architecture that forms an efficient barrier that protects the internal environment from the ingress of xenobiotics. The section below describes the different skin layers and how their composition can restrict the permeation of molecules.

1.1 HEALTHY SKIN PHYSIOLOGY

The skin is composed of three main layers (Figure 1-1) and depending on the drug that is being delivered, certain layers might present more of a barrier to permeation than others. The different skin layers and their compositions are described below.
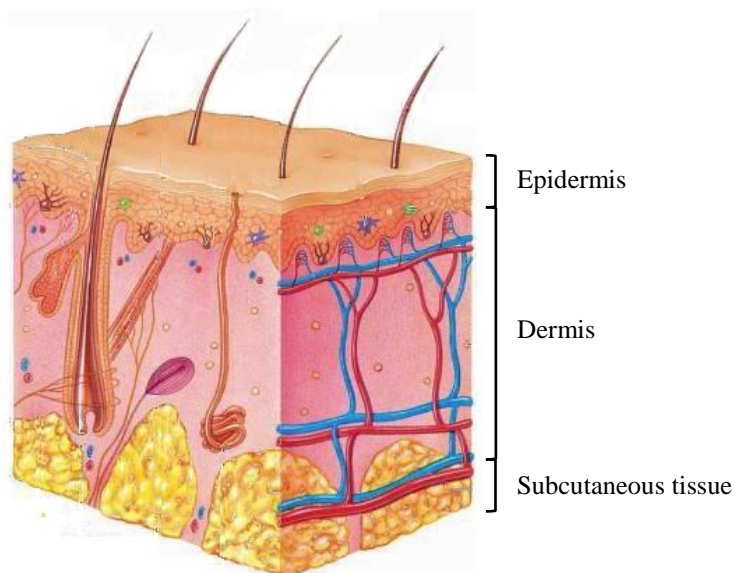
FIGURE 1-1. A CROSS-SECTION THROUGH HUMAN SKIN (ADAPTED FROM[10])

1.1.1 EPIDERMIS

The epidermis is the most superficial layer of the skin (Figure 1-1). It contains different cell types including keratinocytes, Langerhans cells, Merkel cells and melanocytes. The keratinocytes represent 90-95% of the cell volume and their maturation appears as four histologically distinct layers of the epidermis[11]. From the inside out, they are as follows[12]:

> ➢ *Stratum basale* or basal layer
> ➢ *Stratum spinosum* or prickly layer
> ➢ *Stratum granulosum* or granular layer
> ➢ *Stratum corneum* (SC) or cornified layer

The *stratum corneum* is the outermost layer and is considered the rate-controlling barrier for diffusion (outside-inside barrier). It is made up of 10 to 15 stratified layers of dead flattened and keratinized cells (also known as corneocytes) and is around 10-15 μm thick[13, 14]. A complex mixture of intercellular lipids such as ceramides, free fatty acids, cholesterol and cholesterol sulphate is present between the corneocytes [15, 16]. The

lipids are structured into ordered bilayers creating both hydrophilic and hydrophobic regions. As the cells move outward and upward their structure, composition and function changes allowing desquamation.

The viable epidermis is an avascular structure of around 50-100 μm and forms an indispensable barrier to water evaporation (inside-outside barrier)[17]. The *stratum basale* lies adjacent to the basement membrane that forms a well-defined border between the dermis and epidermis. The keratinocytes of the basal layer are attached to the basement membrane by hemidesmosomes. The cells in this layer are similar to cells in other body tissues as they contain typical cell organelles and they undergo mitotic cell division. From the two cells originating from replication, one daughter cell remains in the *stratum basale* whilst the other differentiates and moves upwards during the maturation process. The layer found above the *stratum basale* is the *stratum spinosum*. It is made up of several layers of polyhedral shaped keratinocytes that start to differentiate and synthesise keratins. As the keratinocytes pass to the *stratum granulosum* they continue to differentiate. The cells flatten and contain protein granules called keratohyalin granules[12]. This layer also contains enzymes that start the degradation of the living cell components such as nuclei and organelles[18].

1.1.2 DERMIS

The dermis is 3 to 5 mm thick[12]. This layer consists of a fibrous network of connective tissue mainly collagen fibrils (70%) and elastic tissue, embedded in a semigel matrix of mucopolysaccharides[19, 20]. With regards to transdermal delivery this layer is considered as gelled water and might provide a barrier to highly lipophilic drugs[21]. The superficial dermis contains a rich capillary network and forms the first site of drug uptake into the systemic circulation.

Furthermore, the dermis hosts several epidermally derived appendages such as hair follicles and glands, it contains sensory receptors and an extensive vascular network. The primary cell type is the fibroblast that migrates through the tissue while it produces the precursors of connective tissue components[22]. Other cells include mast cells; they originate in the bone marrow and are involved in the immune and inflammatory responses and melanocytes that are responsible for the production of the pigment melanin.

1.2 SKIN DRUG DELIVERY

Topical and transdermal formulations deliver drugs across the SC but have a different target. Transdermal formulations are designed to achieve drug transport across the skin into the blood circulation with minimal drug retention in the skin. In contrast, topical products are designed to treat local skin diseases and the target is inside the skin[23]. Systemic exposure is avoided as this may not be needed and increases the risk of side effects.

Both types of formulations rely on passive diffusion of the active molecule across the SC and into the epidermis and dermis. The different permeation routes are described below.

1.2.1 SKIN PERMEATION ROUTES

As mentioned above, the SC is designed to be a highly efficient barrier restricting the penetration of xenobiotics through skin. For most compounds this is the rate-controlling barrier for diffusion. Three different pathways for molecules to permeate through the SC: (i) transcellular route, (ii) intercellular route and (iii) transappendageal route are described in literature (Figure 1-2).

Intercellular route   Transcellular route   Transappendageal route
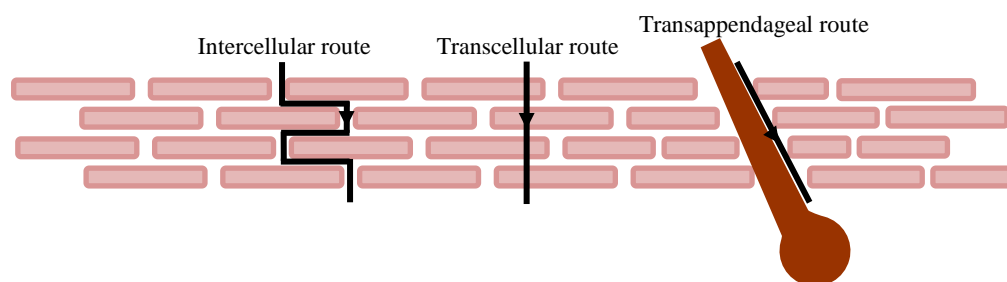
FIGURE 1-2. SCHEMATIC REPRESENTATION OF THE PATHWAYS OF TOPICAL DRUG DELIVERY.

Initially it was believed that the transcellular diffusion route was the main pathway for solutes to pass through the SC[24]. However following research and experimental evidence, it is now generally excepted that the transport through the is mainly by the intercellular route[25]. As described before, the SC is a dense layer of flattened, dead cells that are surrounded by a mixture of lipids, structured in bilayers. The intercellular pathway (Figure 1-2) therefore implies transport of the diffusant through the bilayers and thus through sequential hydrophilic and lipophilic domains[26]. Compared to transcellular transport where the molecule moves directly across the SC and the path

length for permeation is considered the same as the SC thickness. The intercellular transport is highly tortuous and the permeation path length is greater than the SC thickness.

The transappendageal route differs from the other two routes because this pathway circumvents the intact SC barrier using hair follicles and sweat ducts to permeate. It is suggested to be a significant pathway for large polar molecules during the early stages of passive diffusion[27].

1.2.2 PASSIVE DIFFUSION LAWS

The main mechanism of drug permeation through skin is passive diffusion. Essentially, during the diffusion process there is a movement of molecules from a high to a low concentration (Figure 1-3).
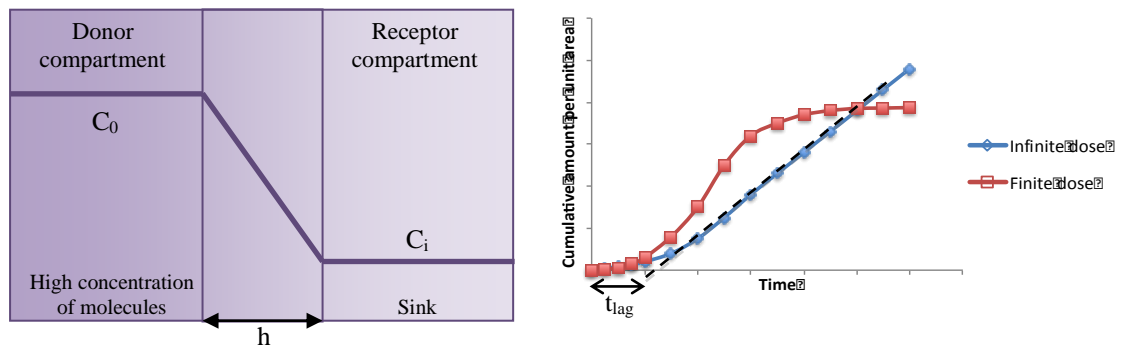
FIGURE 1-3. SCHEMATIC PRESENTATION OF THE PASSIVE DIFFUSION OF A DRUG ACROSS A MEMBRANE.

Fick's first law, applied when steady state conditions have been reached, states that the rate of transfer of the diffusing molecules per unit area is proportional to the concentration gradient measured across the membrane (Equation 1).

$$J = \frac{KD}{h}\left(C_0 - C_i\right)$$

<div align="right">**EQUATION 1**</div>

J is the flux of the permeant per unit area (in mol/(cm^2·s)), K is the *stratum corneum*-formulation partition coefficient, D is the diffusion coefficient of the permeant in the *stratum corneum* (in cm^2/s), h is the path length (in cm), C_0 is the concentration of drug applied to the skin surface (in mol/cm^3) and C_i is the concentration inside the skin.

In most practical situations $C_0 >>> C_i$ [26] and the equation becomes (Equation 2):

$$J = \frac{KD}{h} C_0$$

EQUATION 2

After insertion of the permeability coefficient $K_p = DK/h$ (in cm/s) the equation becomes (Equation 3):

$$J = K_p C_0$$

EQUATION 3

The lag time can be obtained from extrapolation of the steady state portion to the intercept of the time axis (Figure 1-3).

In order to apply the above equations to skin permeation, the experimental design should comply with some assumptions:

- The *stratum corneum* is the rate-limiting barrier;
- Permeation through the appendages is negligible and by passive diffusion only;
- The nature of the *stratum corneum* is not changed by the application of the vehicle of the formulation and the *stratum corneum* is considered isotropic;
- The diffusion is not dependent on concentration, time or distance;
- The diffusing compound dissolves in the *stratum corneum*.

However in real-life situations, patients are more likely to apply finite dose formulations. In time, the amount of drug that permeates through the stratum corneum will reach a plateau and remain constant (Equation 4). The diffusion is mathematically described as follows:

$$\frac{\partial c}{\partial t} = D \frac{\partial^2 c}{\partial x^2}$$

EQUATION 4

It is important to note that Equation 4 can only be used assuming a unidirectional diffusion through an isotropic membrane.

1.3 TOPICAL FORMULATIONS

1.3.1 GENERAL COMPOSITION

A drug is rarely applied to the skin as a pure compound, instead the drug is incorporated in a suitable carrier system.

Topical formulation = active ingredient + non-active carrier system (vehicle+excipients)

1.3.1.1 ACTIVE INGREDIENT

Not all drugs permeate easily through skin. From Fick's first law of diffusion (Equation 1) it can be derived that the main physicochemical determinants of the passive diffusion process are solubility, partition behaviour and diffusion coefficient of the drug.

In general, percutaneous absorption is considered as a series of partition and diffusion processes. Modelling these processes has given more insight in to which physicochemical drug parameters guide these processes. Potts and Guy modelled the permeation of a set of compounds using only the partition coefficient ($K_{oct/water}$) and molecular weight (Mw) to explain the permeability of the range of compounds[28]. In fact, *in vitro* studies that evaluated the permeability of steroids through skin have shown that smaller molecules permeated quicker than large molecules[29]. This inverse relationship between skin permeation flux and molecular weight was confirmed by later research[30] and is now generally accepted. More recent research evaluated the molecular weight of drugs that are currently available in topical formulations and found a molecular weight below 500 g/mol for the majority of drugs[31].

As mentioned before the intercellular route is considered the main route for drug permeation. This involves the permeant to partition and diffuse through the sequential lipophilic and hydrophilic regions of the intercellular lipids and requires thus both lipoidal and aqueous solubilities. *In vivo* studies involving compounds with a variety of lipophilicities indicated an optimal log $K_{oct/water}$ of 2.5 and a range of 1-3 is appropriate for topical drugs[32].

Due to their nature, the partitioning behaviour and solubility of a drug are inversely related. Compounds with a high log $K_{oct/water}$, often have a lower aqueous solubility compared to compounds with a low log $K_{oct/water}$. Passive permeation benefits from a slightly lipophilic compound and therefore a compromise between log $K_{oct/water}$ and

solubility are required. Furthermore research has led to believe that a higher solubility is related to a lower melting point[33].

Further extension of modelling techniques to bigger data sets and thus a wider variety of chemical compounds revealed that a delay in percutaneous permeation could be linked to the presence of H-bonding groups[34]. Moreover functional groups behaving as H-bond donor appeared to have a higher impact on permeation than H-bond acceptors and adding a third H-bond donor group to a molecule, resulted in a large reduction of the diffusion of a compound[35].

Briefly to optimise permeation, a given drug should comply with the following physicochemical properties [26, 34-37]:

> ➢ molecular weight < 500 g/mol[31]
> ➢ log $K_{octanol/water}$ between $1 – 3$[35]
> ➢ low melting point ($< 200°C$)[38]
> ➢ aqueous solubility > 1 mg/ml[37]
> ➢ hydrogen bonding groups < 2[39]

1.3.1.2 NON-ACTIVE CARRIER SYSTEM

The carrier system is regarded as the sum of the ingredients in which the drug is delivered (i.e. the formulation matrix or vehicle and excipients) and is important as it influences the drug delivery, product performance and tolerance profiles of topical formulations. The ideal carrier system is easy to apply and remove, nontoxic, non-irritant, non-allergenic, chemically stable, homogeneous, bacteriostatic, cosmetically acceptable, pharmacologically inert, and should readily release the drug into the stratum corneum [40].

According to the European Pharmacopeia, *vehicles* are divided in three main types: the solids (sticks, powders and patches), semi-solids (ointments, creams and gels) and liquids (solutions, suspensions and lotions). When choosing the vehicle type it is important to consider:

- Skin type: a richer vehicle is preferred for a dry skin for example a water-in-oil cream or an ointment;
- Skin site: when applied on the face the formulation should be aesthetically acceptable;

- Wound type: wet wounds require an absorbing formulation type for instance a gel;
- Compatibility: ionic active ingredients should be compatible with the vehicle components for example when ionic surfactants are used;
- Environmental factors: warm and humid climate increases instability of creams and emulsions.

An *excipient* is part of a formulation as a non-medical agent and help to keep the formulation and active ingredient stable throughout the shelf life, efficacious and safe. It is important that this compound is compatible with the other ingredients of the formulation. The function of excipients can vary widely and sometimes one excipient has multiple functions as indicted in Table 1-1.

TABLE 1-1. TOPICAL FORMULATION EXCIPIENTS AND THEIR FUNCTION(S).

Excipient function	Use	Example
Humectant	Avoids water evaporation from the formulation	Propylene glycol, PEG 400, glycerol
Solvent	Dissolve and increase the solubility of a compound	Propylene glycol, alcohol, glycerol
Antioxidant	Prevent oxidation	Ascorbic acid, tocopherol, butylated hydroxyanisole
Preservative	Prevent growth of micro-organisms	Methylparaben, benzoic acid
Buffer	Weak acid or base that maintains the pH around a certain value	Sodium hydroxide, ascorbic acid, citric acid
Thickening agent	Increase the viscosity of the vehicle	Methylcellulose, Carbomer, tragacanth
Chemical penetration enhancer	Promote the permeation of the active ingredient through the SC	Propylene glycol, dimethyl isosorbide, isopropyl myristate

1.3.2 SKIN PENETRATION ENHANCEMENT

A lot of effort is made to try and circumvent the barrier property and enhance the permeation of drugs. The different strategies can be divided in two main categories: chemical and physical methods[41]. In physical modulation methods a form of electrical, mechanical, magnetic or thermal energy is applied to disrupt the skin barrier[42]. Some

examples include the use of electric current in iontophoresis[43, 44] and electroporation[45], ultrasound[46] and use of micro needles[47, 48]. Drug permeation enhancement via physical methods is not the subject of this project, and physical methods are therefore not discussed further.

This project focuses on chemical modulation of topical permeation enhancement. From Fick's first law (Equation 1 and Equation 2), it is clear that enhanced flux of the drug across the skin can be accomplished by:

- Increasing C_0 by aiming for maximum thermodynamic activity of the permeant in the vehicle or by supersaturation;
- Increasing the diffusion (D) of the drug across the *stratum corneum*
- Increasing the solubility of the permeant in the *stratum corneum* (K)
- Reducing the path length of permeation for instance by tape stripping.

Above, the effects of solvents on the permeation of drugs were categorised, however, practically the mechanisms of action are much more complex and solvents can increase the permeation of a drug by a number of mechanisms.

Increase of diffusivity. Azone®, oleic acid, octyl salicylate and surfactants are examples of chemical penetration enhancers (CPEs) that increase the diffusion of a permeant across the SC by disruption or interaction with skin lipids.

Octyl salicylate (OSAL) is a lipophilic compound that is used as sunscreen in topical formulations and is considered safe in concentrations up to 5%[49]. Its enhancing effect on percutaneous permeation was first described in the 1990's[50, 51]. OSAL increased the flux of testosterone *in vitro* using porcine skin, when used alone and in combination with PG[52]. It was also reported to increase the permeation of fentanyl in spray formulations by enhancing the drug diffusion across the SC[53]. However when using differential scanning calorimetry (DSC) and attenuated total reflectance Fourier transform infrared spectroscopy (ATR-FTIR), no changes in lipid fluidity or molecular conformation in the SC were observed and so it was suggested that OSAL disturbs the skin lipid formation by forming a pool in the SC rather than intercalating with the skin lipids, a mechanism previously described for oleic acid[53, 54].

Increase partitioning. A second category of CPEs increases the solubility of the drug in the outer layers of the skin enhancing the partitioning of the drug into the skin for example propylene glycol and Transcutol®.

Propylene glycol (PG) exhibits mild permeation enhancer properties and is used as a co-solvent to increase solubility of poorly soluble drugs[55-57]. As PG is a small hydrophilic molecule, it is suggested that it readily permeates the skin upon application[58-61], and modifies the solubility of the drug in the SC, thereby enhancing the permeation[57, 62]. Furthermore research has shown that the permeation of drugs can synergistically be enhanced by combining CPEs that influence the diffusivity of the drug and the partitioning of the drug in the SC. For example, a combination of oleic acid and PG was shown to synergistically enhance the permeation of tenoxicam compared to the single solvents[62]. The same synergistic effect was observed when using PG in combination with other fatty acids[63-65]. This is also the reason why PG is often used as a vehicle for other enhancers rather than a standalone permeation enhancer.

Other chemical compounds have shown an effect on the drug flux across the skin but the precise mechanism of action remains unclear. An example would be dimethyl isosorbide (DMI). It has been shown to increase dermal delivery of hydrophilic drugs[66]. Research found it to permeate the skin[60] but no interruption of the intercellular packing was observed and therefore it is thought to not change the skin barrier and the diffusivity of permeants[67].

Water is incorporated in nearly every formulation on the market and the water content of the human skin was shown to influence the permeation of both lipophilic[68] and hydrophilic permeants[69, 70]. The precise mechanism of percutaneous permeation increase by hydration is not known yet. From differential scanning calorimetry (DSC) data, it was initially hypothesized that skin permeation enhancement was caused by intercellular lipid disorder and loosening of the intracellular keratin structure. However later this theory was challenged when Bouwstra et al conducted X-ray diffraction studies and found no changes to the lipid and protein organisation of the SC in the presence of water[71, 72]. These findings were supported by Fourier transform infrared data obtained from skin samples with different levels of hydration[73].

Like other penetration enhancers, water in the SC can alter the solubility of the permeant in the SC and therefore affect its partitioning from the vehicle into the SC. However this mechanism does not explain the effect of hydration and the enhanced delivery of lipophilic compounds. Others however, suggested that the intercellular lipid domains of a highly hydrated SC contain water pools [74].

In order to enhance permeation, CPEs are added to the formulation and are in contact with the skin for a considerable amount of time. Therefore the ideal penetration enhancer complies with the following properties [51, 75]:

- It should have no pharmacological activity of its own.
- It should not cause allergies, be irritating or toxic.
- It should work directly and its effect (duration and activity) should be reproducible and predictable.
- The activity should be reversible meaning that the barrier function of the SC should return to normal once the penetration enhancer is removed.
- It should work unidirectional, meaning that it allows the therapeutic agents to enter through skin without endogenous substances leaving the body.
- It should be odourless, tasteless and colourless.
- It should be compatible with the active ingredients and excipients of the formulation.

1.4 DISEASED SKIN

Although topical treatments are often evaluated using healthy skin, they are designed and developed to treat diseased skin. Many pathological disorders alter the physiology and barrier function of the skin and therefore influence the delivery of drugs to their target site. Research into drug delivery to diseased skin has mainly focused on non-infectious diseases such as atopic dermatitis, psoriasis and eczema. Infectious skin diseases caused by pathogens such as herpes, *Tinea* and *Candida albicans* have been investigated, but to a lesser extent. Limited data on the permeability of cutaneous leishmaniasis-affected skin is available. However this information is vital when trying to develop a topical formulation for the disease. Below three different techniques are described that were used in this project to investigate the barrier function of cutaneous leishmaniasis-affected skin.

1.4.1 TRANSEPIDERMAL WATER LOSS

Transepidermal water loss (TEWL) represents the water that migrates through the epidermis from inside the body to the external environment.

In clinical settings, non-invasive TEWL measurements allow the evaluation of the skin barrier integrity[76]. Healthy skin is a good barrier that retains water inside the body. However in diseased skin, the barrier is compromised and TEWL values are increased (Figure 1-4). Some of the frequently cited pathologies for which an increase of TEWL values was recorded, are atopic dermatitis[77-79], psoriasis[80, 81], ichtyosis[82, 83] and xerosis[84, 85].

Healthy skin   Diseased skin
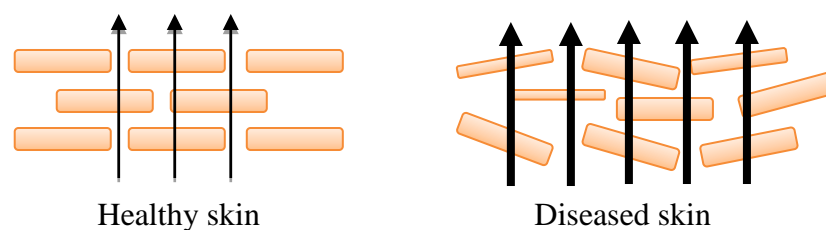
FIGURE 1-4. A SCHEMATIC OF INCREASED TRANSEPIDERMAL WATER LOSS IN IN HEALTHY AND DISEASED SKIN.

Two types of equipment have been designed to measure water evaporation from the skin surface: open and closed chamber tools. The main limitation of an equipment using the open chamber method is the vulnerability to disturbances from ambient air

movements. Practically, this means that this type of equipment can only be used in well controlled laboratories and on horizontal surfaces. In closed chamber equipment, the water evaporation is determined from the time rate of rise of humidity in this chamber.

The Aquaflux AF200 (Biox, UK) used in this study is a ventilated condenser chamber instrument. The condenser is maintained at low temperature and acts as a water vapour sink that maintains a low humidity (Figure 1-5). The test surface acts as a vapour source and creates a higher humidity in the chamber. Basically vapour moves from the test surface to the chamber (sink condition) by passive diffusion and a continuous flux can be measured without purging the chamber.
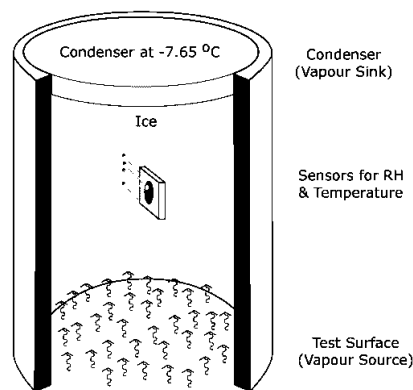
FIGURE 1-5. SCHEMATIC OF A CONDENSOR CHAMBER (ADAPTED FROM WWW.BIOX.BIZ).

1.4.2 HISTOLOGY

Histopathological investigation allows an in depth understanding of the pathological changes of the skin at microscopic level. A variety of stains are available and can be used depending on the target. Haematoxylin and eosin stain (H&E) is a commonly used stain that provides structural information. It colours nucleic acids purplish and proteins such as in the cytoplasm and extracellular matrices pink.

Immunohistochemistry (ICH) is another useful technique that combines immunological and biochemical reactions whereby specific antibodies tagged with a visible label bind to target antigens. This allows the visualization of the distribution and localization of the target within cells and tissues.

Both techniques give a variety of information and are widely used. However the sample preparation is time consuming and in the process the sample is altered restricting its use for other scientific purposes. Furthermore histology does not give dermatopharmacokinetic or -dynamic information.

1.4.3 SKIN PERMEATION

As mentioned in the previous section, pathological skin disorders have been reported to change the cutaneous barrier and pharmacokinetics and dynamics of a topical formulation *in vitro* and *in vivo*. This highlights the importance of efficacy evaluation of a topical formulation on the target population. This is not always possible in early drug development stages due to legal and ethical issues and thus the development and characterization of a model that presents the same cutaneous changes as the target population is essential.

Many models were developed in an attempt to mimic diseased skin and its impaired barrier to drug delivery[86, 87]. However in most models an impaired skin barrier was obtained by mechanically or chemically modifying the SC and are not specific to a particular disease. An extensive review of these methods is written by Chiang et al[87].

Briefly, mechanical damage involves: (i) abrasion that causes the SC to loosen as seen by transmission electron microscopy and (ii) tape stripping that involves removal of SC layers. Freezing the skin also seems to damage the skin barrier integrity and the effect appears to be storage-time dependent[88-90].

The SC consists of corneocytes that are embedded in a matrix of lipids. Therefore it is not surprising that extraction of these intercellular lipids results in increased drug permeation. Several chemical reagents have been reported to de-lipidise the skin and effect its barrier integrity. For example, when evaluating the permeation of skin that was exposed to a chloroform-methanol mixture prior to the experiment using Franz diffusion cells an increase of permeation for drug compounds was observed[91, 92]. This increase was higher for hydrophilic compared to lipophilic compounds. The same was observed when treating the skin with acetone prior to evaluating the permeation of drugs[93].

Diseases such as atopic dermatitis, psoriasis and skin cancer were reported to increase skin permeability. For example when evaluating permeability of psoriasis affected skin *in vitro*, an increase in anthralin[94] and 8-methoxypsoralen[95] permeation was recorded. Shani et al compared the penetration of electrolytes through skin of healthy and psoriatic patients after bathing in the Dead Sea and found increased electrolyte levels only in the psoriatic group[96]. Other *in vivo* studies showed an increase in permeation of a range of molecules indicating that the permeation in psoriatic skin is often increased[87].

Differences may exist in different diseases and with various severity levels within one disease. Moreover data obtained using animal models are not always translatable to humans because of differences in the skin physiology, hair follicle density and even metabolism. Therefore care should be taken of extrapolating from these results.

1.5 LEISHMANIASIS

The leishmaniases are a group of poverty-related diseases with clinical manifestations ranging from small cutaneous nodules to fatal visceral infections.

The parasites are transmitted by the bite of a female sandfly of the genus *Phlebotomus* (in the Old World) or *Lutzomyia* (in the New World). Approximately 100-1000 promastigotes[97] are injected in the skin and engulfed by neutrophils, that are rapidly recruited to the site of infection. Some of the parasites survive in the neutrophils and are internalized in their phagolysosome, where they transform into amastigotes (Figure 1-6). In fact, neutorophils act as a transient host for the amastigotes before they are taken up by macrophages where they replicate[98-100]. Research suggested that the presence of the amastigotes in the phagolysosome (pH 5-5.5) of the macrophage inhibits apoptosis and necrosis of the host cell[101-104] and hence, contributes to the survival of the parasites. Eventually the macrophage ruptures, releasing the pathogens to infect other macrophages. The parasites can stay in the skin or migrate to inner organs (liver, spleen and bone marrow) leading to cutaneous (CL) or visceral leishmaniasis (VL) respectively.
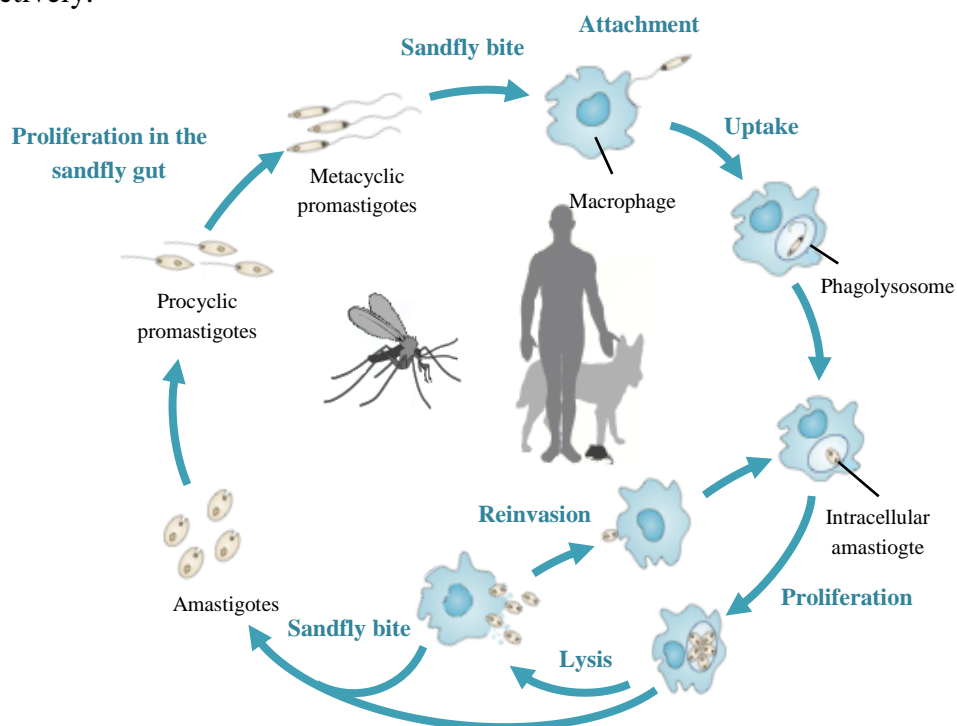
FIGURE 1-6. THE LIFE CYCLE OF *LEISHMANIA* PARASITES (ADAPTED FROM [105]).

The transmission of *Leishmania* species can either be zoonotic when the parasites are transmitted from animal to man or anthroponotic when transmitted from man to man. *L. tropica* and *L. donovani* typically involve anthroponotic transmission.

1.5.1 DISTRIBUTION

Leishmaniasis is endemic in 98 countries over 5 continents and 350 million people are at risk of infection[1]. The reported incidence of VL and CL patients is approximately 58 000 and 220 000 cases a year respectively[1]. The overall magnitude of the problem, however, is estimated to be much higher due to underreporting. The majority (90%) of VL cases are found in six countries: India, Bangladesh, Sudan, South Sudan, Brazil and Ethiopia. In contrast, CL is more widely distributed, with 70-75% of the estimated cases occurring in Afghanistan, Algeria, Colombia, Brazil, Iran, Syria, Ethiopia, North Sudan, Costa Rica and Peru (Figure 1-7)[1]. CL affects an estimated 10 million people and 0.7-1.2 million new cases occur every year[106].
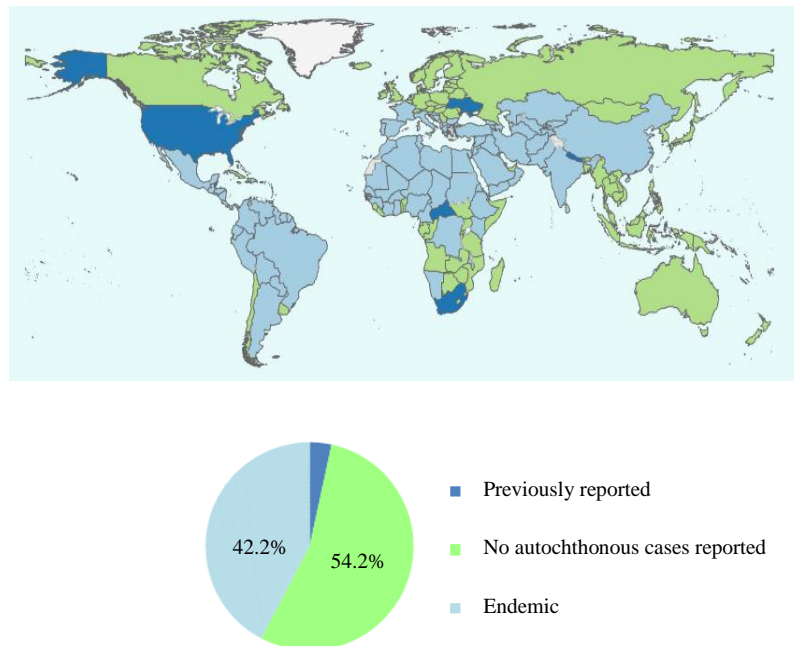
FIGURE 1-7. DISTRIBUTION OF CL IN 2013 (ADAPTED FROM [107]).

The distribution of leishmaniasis has spread over time. This is in part due to environmental changes that favour the dispersion of the reservoir hosts and vector but also importation, travel and emigration[108-111].

1.5.2 CLINICAL SYMPTOMS

Based on the symptoms, leishmaniasis cases can be divided in two groups: VL and CL. Despite this simple classification, a wide spectrum of clinical manifestations are observed.

1.5.2.1 VISCERAL LEISHMANIASIS

Visceral leishmaniasis (also called kala azar) (Figure 1-8 - blue) is the most severe form of leishmaniasis with a fatal outcome if untreated. 70% of VL patients are children younger than 15 years old, who suffer from malnutrition and other illnesses[112]. *L. donovani* (Asia and Africa) and *L. infantum* (Europe, Asia and South America) are the two species causing VL.

Clinical features vary; the infection can remain asymptomatic (patient is infected but shows no signs or symptoms of disease) or can follow an acute or chronic course. The onset of the disease usually occurs two to four months after infection however this can vary. Prolonged and irregular fever, splenomegaly, hepatomegaly, progressive anemia and weight loss are among the major clinical symptoms of an active visceral infection [113].

The further content will focus on cutaneous leishmaniasis.

1.5.2.2 CUTANEOUS LEISHMANIASIS

The clinical features of cutaneous leishmaniasis vary in severity and depend on host, parasite and vector related factors. Old World (Europe, Middle-East, Central Asia and Africa) CL is mainly caused by *L. major*, *L. tropica* and *L. aethiopica,* whereas New World (Central and South-America) species are *L. mexicana*, *L. amazonensis*, *L. panamensis* and *L. braziliensis*.

In its simplest form, CL consists of a single local lesion (marked in green in Figure 1-8). The first sign of a localized infection is a small, itchy erythema at the site of the insect bite. As the erythema develops into a papule*, amastigotes continue to proliferate and multiply in the dermis. The papule expands into a nodule** that reaches its final form and size about two weeks to six months later. When the crust falls off an ulcer typically with raised edges is exposed.

---

* Papules are solid elevated lesions which may be up to 5mm in diameter
** Nodules are a form of papules, but are larger and deeper. They are usually 5mm or more in diameter.
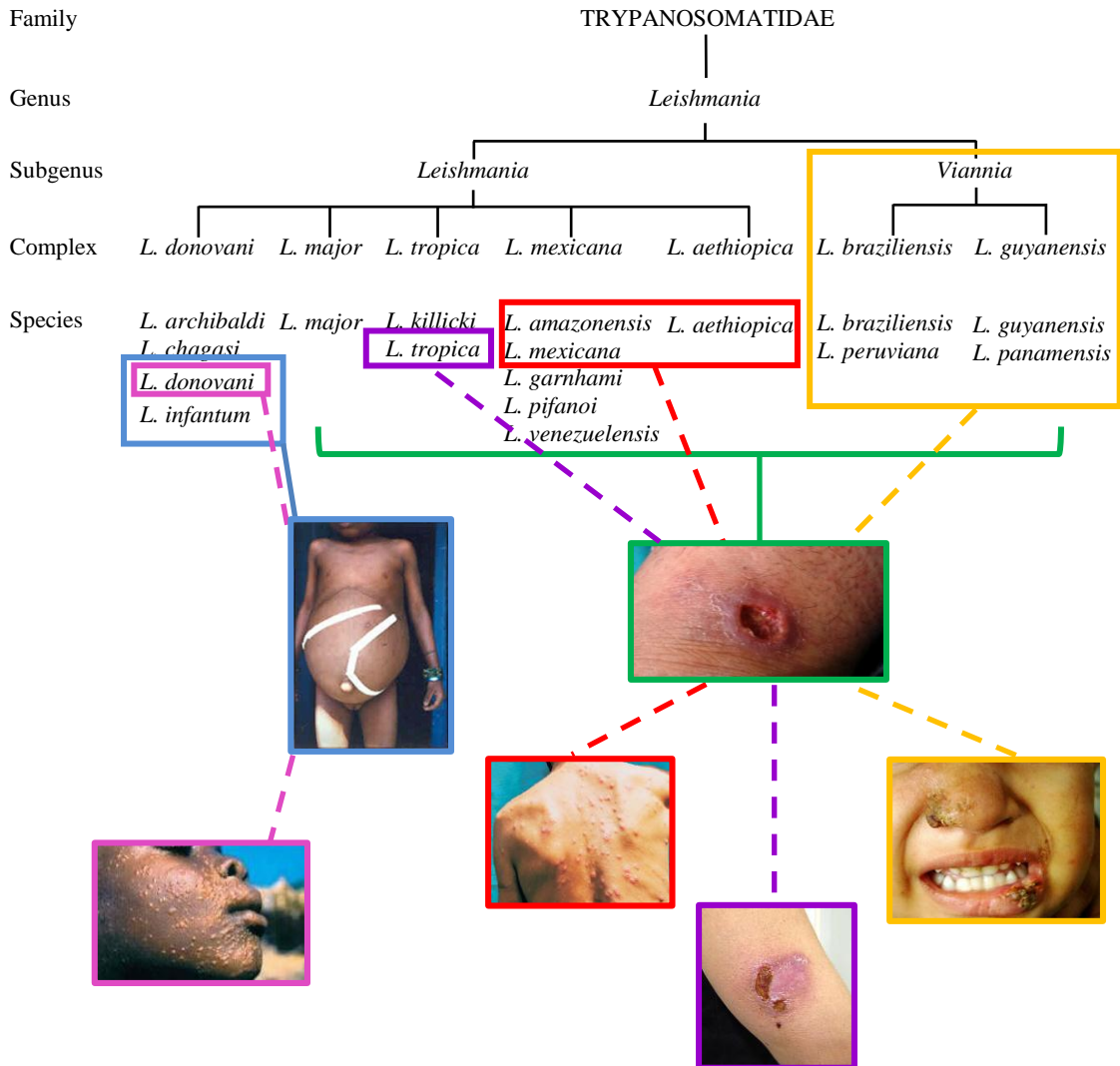
FIGURE 1-8. TAXONOMY OF *LEISHMANIA* PARASITES LINKED TO CLINICAL CL SYMPTOMS (ADAPTED FROM [114]).

Specific species might be associated with a typical clinical form but this can vary. For instance infection with *L. tropica* can evolve to *leishmaniasis recidivans* a chronic form of CL where satellite lesions (Figure 1-8 – purple) appear in the edges of the initial healing lesion. This form is characterized by a sparsity of parasites and can last for years[115-117].

L. aethiopica can cause *diffuse cutaneous leishmaniasis* (DCL), a form that is characterized by widely disseminated non-ulcerated papules, nodules, plaques or by diffuse infiltration of the skin (Figure 1-8- red). In the New World, this anergic form is typically caused by *L. (L.) mexicana* and *L. (L.) amazonensis*[118].This disease does not heal spontaneously and relapses frequently after treatment[119].

Mucocutaneous leishmaniasis (MCL), also called Espundia, occurs mainly after infection with *L. (V.) braziliensis* and *L. (V.) panamensis*[117, 120] (Figure 1-8 - yellow). The majority of the cases present in Bolivia, Brazil and Peru. This form, characterized by destruction of the oral-nasal and pharyngeal cavities can appear years after the onset of CL. Nasal lesions are always present and although the initial symptoms such as nasal inflammation are mild, the disease will evolve leading to infiltration of the anterior cartilaginous septum and later perforation of the septum with collapse and broadening of the nose. The final stage is obstruction and destruction of the nose, pharynx and larynx.

Post-kala-azar dermal leishmaniasis (PKDL) (Figure 1-8 - pink) is a cutaneous sequel of visceral leishmaniasis. This form usually develops when the initial VL infection is cured, although it can appear while the initial VL infection is still active. The clinical spectrum of PKDL varies depending on the geographical area. In Sudan about 50% of the VL cases result in PKDL and mostly affects children[121, 122], while in India 5-10% of VL patients, especially young adults, develop PKDL[123, 124].

1.5.3 CURRENTLY AVAILABLE TREATMENTS

CL is a non-fatal disease, but can cause substantial morbidity and social stigma, related to deformities and disfiguring scars[125, 126]. Furthermore a small percentage of cases advances to long term morbidities like MCL or DCL[127]. The main aim of treatment is to speed up healing and reduce scar formation, and to prevent relapse or parasite dissemination.

The available chemotherapeutics to treat CL can be divided in two groups; (i) systemic treatments, where the drug is taken up in the blood and transported to the target tissue and (ii) local treatments, where the formulation is directly applied to the site of action i.e. the CL lesion. Systemic treatments comes with a higher risk of adverse effects and is therefore typically reserved for patients with more severe or complex form of CL[118] such as:

- Multiple (> 4) or large (> 5cm) lesions
- Disfiguring or disabling lesions typically located on the joints or on the face
- Lesions that are difficult to treat locally (eye, lips, ears)
- CL that does not respond to local treatment
- Leishmaniasis recidivans or diffuse CL

1.5.3.1 Systemic treatments

1.5.3.1.1 *Pentavalent antimonials*

The pentavalent antimonials: sodium stibogluconate (SSG) (Pentostam, GlaxoSmithKline and generic product) and meglumine antimoniate (MA) (Figure 1-9) (Glucantime™, Sanofi) have been first line treatment for CL since their discovery in the 1940s.
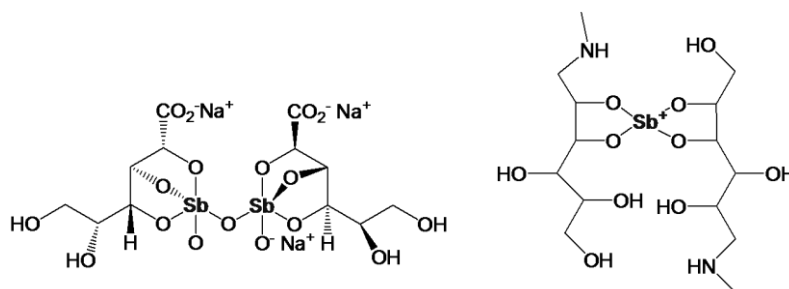
FIGURE 1-9. CHEMICAL STRUCTURE OF SODIUM STIBOGLUCONATE (PENTOSTAM) (LEFT) AND MEGLUMINE ANTIMONIATE (GLUCANTIME™) (RIGHT).

Mechanism of action. The mechanism of action is still not completely understood. Some data suggest that the trivalent form Sb^{III} disturbs the amastigotes' ability to maintain the redox homeostasis by interfering with the trypanothione/trypanothione reductase system that protects the parasite from oxidative damage and toxic heavy metals[128, 129]. Other reported DNA fragmentation and externalization of phosphatidylserine on the surface of the plasma membrane of amastigotes treated with Sb^{III}, leading to parasite apoptosis[130, 131]. This suggests that pentavalent antimonials (Sb^{V}) only act as prodrugs and thus require biological reduction to Sb^{III}.

However, other studies indicate an intrinsic anti-leishmanial activity for Sb^{V} as it forms a complex with adenine ribonucleoside that indirectly inhibits type I DNA topoisomerase causing a depletion of intracellular ATP possibly via inhibition of the glycolysis and fatty acid β–oxidation in the amastigotes[132]. This leads to inhibition of the biosynthesis of macromolecules in amastigotes[133-135].

Administration and treatment regimen. Pentavalent antimonials can be administered locally or systemically depending on the severity of the disease. Local treatment consists of intralesional administration alone (Figure 1-10) or in combination with cryotherapy[118]. During each session, 1-5 ml of pentavalent antimonials is injected in the edges of the lesion, followed by application of liquid nitrogen (-195 °C) if preferred.

The injections with or without liquid nitrogen application can be repeated up to 5 times every 3 to 7 days. Local injections prevent or limit systemic adverse effects; however, these injections are painful and burning, itching and inflammation at the injection site are amongst the reported adverse effects[136].

Antimonials are given systemically through intravenous or intramuscular administration (20 mg/kg per day for 10-20 consecutive days) when patients present with more complex CL[114, 118]. Serious side effects such as hepato- and cardiotoxicity are reported and require patient monitoring[135].

FIGURE 1-10. INTRALESIONAL INJECTION OF A CL LESION WITH ANTIMONIALS[137].

Efficacy. Randomised controlled trials (RCTs) to compare the efficacy of a pentavalent antimonial treatment against placebo are absent or sparse and efficacy-based evidence of pentavalent antimonials against certain species is lacking[136, 138]. *In vitro* studies confirmed species variation in drug sensitivity when tested in promastigotes[139] and intracellular amastigotes[140, 141]. Moreover an *in vivo* study testing the efficacy of pentostam against *L. braziliensis* and *L. mexicana* showed a statistically significant higher cure rate for *L. braziliensis[142]*. It is hypothesised that this variability in drug susceptibility between different *Leishmania* species is responsible for subcurative treatment in certain cases and consequently resistance development.

1.5.3.1.2   *AMPHOTERICIN B*

Amphotericin B (AmB) is the gold standard drug to treat systemic fungal infections and is administered intravenously. It is reserved as second line treatment for CL.

Mechanism of action. AmB is a macrocyclic polyene antifungal drug. Its main mechanism of action is based on the amphiphilic nature of the molecule (Figure 1-11) as the hydrophobic polyene region complexes with sterols in the parasite membrane

forming a transmembrane channel leading to loss of small molecules. Selectivity is obtained because AmB has a higher affinity for the double bonds of ergosterol compared to mammalian cholesterol[143, 144].
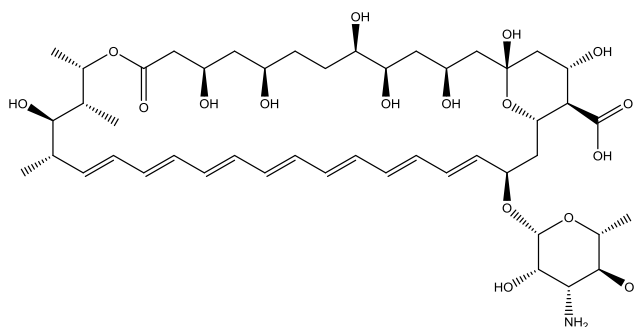
pKa	5.7 and 10
Mol weight (g/mol)	924
Log P	-0.66

FIGURE 1-11. CHEMICAL STRUCTURE AND PROPERTIES[145] OF AMPHOTERICIN B.

Administration and treatment regimen. As a treatment for CL, AmB is reserved for complex forms such as PKDL and mucocutaneous leishmaniasis[138, 146] and is typically administered through slow intraveneous infusion. Amphotericin B deoxycholate is given at 0.7 mg/kg/day for 25-30 doses and liposomal amphotericin B at 2-3 mg/kg/day for a total dose of 20-40 mg/kg. The conventional amphotericin B deoxycholate formulation (Fungizone®) causes acute toxic reactions including renal toxicity, which lipid formulations were developed to reduce. The main disadvantage of these formulations is the high price. Research has been mainly conducted on three lipid formulations:

- Liposomal amphotericin B (AmBisome®)
- A phospholipid complex (Abelcet®)
- A colloidal dispersion with sodium cholesteryl sulphate (Amphocil™)

A study conducted by Yardley and Croft evaluated the *in vivo* and *in vitro* efficacy of four amphotericin B formulations (AmBisome®, Fungizone®, Amphocil™ and Abelcet®) against *L. major* JISH 118 in mice[147]. The *in vitro* assay results showed that Fungizone® was significantly more active against intracellular amastigotes than AmBisome® and Abelcet® and showed a similar level of activity with Amphocil™. *In vivo* results in mice demonstrated a significant reduction in lesion size for Amphocil™ (30%) and AmBisome® (40%) compared to the untreated control after 2 weeks of

treatment with the same total dose of AmB. Complete cure, defined as no visible lesion, was not observed and lesions relapsed after stopping the treatment. Fungizone®, Abelcet® and the standard antimonial sodium stibogluconate (400mg Sb[V]/kg) showed no decrease in lesion size and were found inactive[147].

Efficacy. There is a lack of RCTs that compare AmB treatment with placebo or pentavalent antimonial treatment even though it has successfully been used to treat patients with mucocutaneous leishmaniasis[138, 146, 148]. One RCT compared AmB to AmB in combination with itraconazole but did not report cure rates[149]. In another more recent study, 75% of the patients dropped out due to the obligatory '20 day' admission in the hospital and no cure rate was reported for the patients that completed the study[150].

1.5.3.1.3 *MILTEFOSINE*

Miltefosine is the only oral treatment currently available against CL and VL. Initially, phospholipid derivatives were developed as anti-cancer drugs because they were found to inhibit enzymes involved in cell proliferation and growth factor signal transduction[151]. In the 1980s, a number of research groups independently showed an anti-leishmanial activity for miltefosine and other phospholipid compounds[152-154].

Mechanism of action. Miltefosine, also called hexadecylphosphocholine, is a phospholipid derivative that is structurally related to the phospholipid components of the cell membrane. It interferes with the synthesis of sterols and phospholipids in *Leishmania* parasites and because of its amphiphilic nature (Figure 1-12) it can directly interact with the parasite membrane[155].
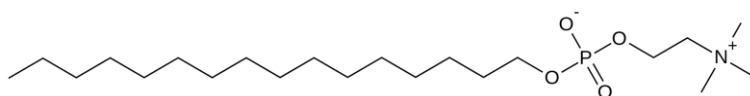
pKa	2
Mol weight (g/mol)	408
Log P	-2.38

FIGURE 1-12. CHEMICAL STRUCTURE AND PROPERTIES[156] OF MILTEFOSINE.

Administration and treatment regimen. Miltefosine is given orally at 2.5 mg/kg/day for 28 days. Gastro-intestinal problems such as vomiting and diarrhoea are the most common side effects. Furthermore it is teratogenic, consequently women of

childbearing age are required to take contraception and pregnancy is contraindicated[114]. The long residence time of the drug in the organism (half-life:150-200 hours) and the long treatment course lead to poor compliance and resistance development[157, 158].

Efficacy. As for the pentavalent antimonials, a difference in intrinsic sensitivity of *Leishmania* species to miltefosine was seen in the laboratory[159, 160] and might explain the variability in clinical response seen in clinical trials conducted in different regions. For example an RCT conducted in Colombia, where *L. panamensis* is most common resulted in a cure rate of 91% compared to 38% for placebo treatment. In contrast in Guatemala, where *L.mexicana* and *L.braziliensis* were identified as CL causing species, the cure rate for miltefosine treatment was only 53% compared to 32% in the placebo group[161]. Another RCT was conducted in Iran and compared the efficacy of oral miltefosine with intramuscular administration of meglumine antimoniate against CL caused by *L. major*. It showed a similar cure rate of approximately 81% for both groups[162]. Miltefosine was also successfully used to treat PKDL in India with a cure rate of 91% after 1 year of treatment[163].

1.5.3.1.4   *PENTAMIDINE ISETHIONATE*

Pentamidine (PMID) (Figure 1-13) is used as alternative treatment for New World CL caused by *L. guyanensis* and *L. panamensis*[118]. The use of this drug is limited and progressively abandoned because of adverse effects such as diabetes mellitus, severe hypoglycemia, shock, myocarditis and renal toxicity[118].

pKa	11.5 and 12.9
Mol weight (g/mol)	592.7
Log P	4
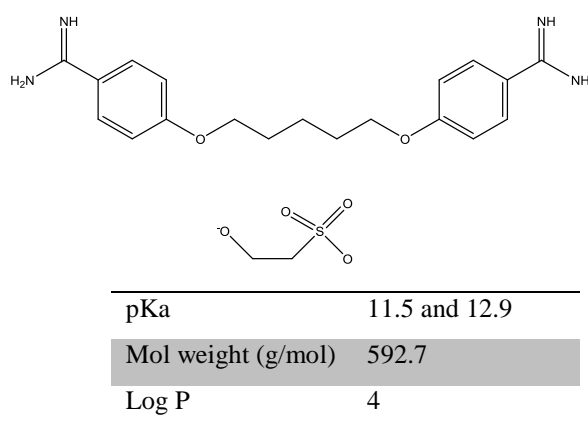
FIGURE 1-13. CHEMICAL STRUCTURE AND PROPERTIES[164] OF PENTAMIDINE ISETHIONATE.

Mechanism of action. The mechanism of action is not fully understood but it is thought to interfere with *Leishmania* DNA synthesis, modify the morphology of the kinetoplast and promote the fragmentation of the mitochondrial membrane[117].

Administration and treatment regimen. 4 mg PMID salt/kg is administered intramuscularly or preferably by intravenous infusion every other day for 3 doses.

Efficacy. In Peru a RCT comprising 80 people compared the treatment efficacies of intravenous administration of pentamidine isethionate (4 mg/kg/every two days for 7 doses) and meglumine antimoniate (20 mg/kg/day for 20 days) against CL caused by *L. braziliensis.* The meglumine antimoniate treatment was significantly more effective with 78% of the patients cured and 17% relapsed compared to 35% cured and 58% relapsed in the pentamidine group[165]. A recent trial evaluated the efficacy of pentavalent antimony treatment with pentamidine against CL caused by *L.guyanensis* and obtained a similar cure rate for both treatments of around 55-58%[150].

1.5.3.1.5 AZOLES

Mechanism of action. The azoles were initially developed to treat fungal infections. Like fungi, *Leishmania* parasites require ergosterol for their cell membrane biosynthesis. Azoles inhibit the ergosterol synthesis and increase the permeability of the *Leishmania* membrane leading to death[3].

Administration and treatment regimen. Fluconazole and ketoconazole are administered orally at 200 mg /day for 6 weeks and 600 mg/day for 28 days respectively. Fluconazole was found efficacious in only one RCT conducted in Saudi Arabia and is therefore only recommended for the treatment of CL caused by *L. major*. Ketoconazole is recommended for the treatment of *L. mexicana* only[118].

Efficacy. Two RCT trials compared the effect of oral ketoconazole to pentavalent antimonials (i.m. MA and i.v. SSG) and placebo in *L. mexicana*, *L. panamensis* and *L. braziliensis* infection. In both studies the ketoconazole group scored significantly higher than placebo and pentavalent antimonial treatments[142, 166]. Moreover fewer adverse effects were reported for the ketoconazole treatment compared to the pentavalent antimonials. Another study compared the anti-leishmanial effect of oral ketoconazole to intralesional MA in Old World CL. The ketoconazole group showed a significant better cure[167]. Fluconazole also seemed effective against Old World CL. After 6 weeks of oral treatment, 59% of complete cure was reported compared with 21% in the placebo group[168].

1.5.3.2 LOCAL TREATMENTS

1.5.3.2.1 *PAROMOMYCIN SULPHATE*

Paromomycin (PM) (monomycin or aminosidine) is an aminoglycoside antibiotic that acts by binding on the small ribosomal unit leading to misreading of the mRNA and inhibition of the protein synthesis in bacteria. In the 1960's it was identified to have antileishmanial activity[169].
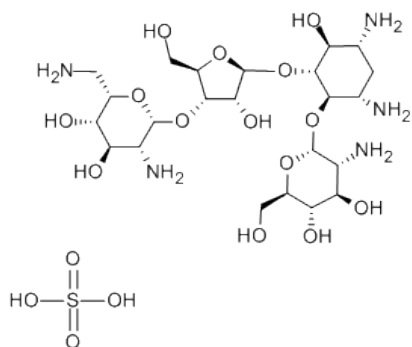
pKa	8.6; 7.6; 5.7; 8.1 and 8.8
Mol weight (g/mol)	714
Log P	-2.9

FIGURE 1-14. CHEMICAL STRUCTURE AND PROPERTIES[170] OF PAROMOMYCIN SULPHATE (LEFT) AND THE COMMERCIALLY AVAILABLE LESHCUTAN® (TEVA, ISRAEL).

Mechanism of action. The mechanism of action of paromomycin against *Leishmania* parasites is not fully understood. Previous research comparing protein expression levels between PM-resistant and -susceptible *L. donovani* promastigotes suggested that PM reduced the protein synthesis by inhibiting the dissociation of the ribosomal subunits[171]. Other studies in *L. mexicana* promastigotes confirmed these results and suggested that PM also led to induction of mistranslation errors[172] and thus altered the accuracy of protein synthesis in *Leishmania* parasites. This increased level of misreading results in defective proteins that affect parasite survival[172, 173]. PM is also believed to affect other cell processes. For example, it was shown to change the lipid metabolism and affect membrane fluidity and alter uptake properties leading to growth arrest of the parasites[174]. Furthermore, dysfunction of the energetic metabolism of the cell caused by defects in the respiratory function was found after exposure of promastigotes to PM[175].

Administration and treatment regimen. PM is a hydrophilic molecule with a high molecular weight (714 g/mol) (Figure 1-14) resulting in poor oral availability. Therefore a parenteral formulation was developed and is mainly used to treat VL and sometimes CL. The majority of CL patients are treated topically with Leshcutan® ointment (Teva, Israel), the only currently available topical formulation that contains 15% PM and 12% methylbenzethonium chloride (MBCL) in soft white paraffin. The efficacy of another topical formulation WR279,396, containing 15% PM and 0.5% gentamycin, was tested in phase 3 clinical trials in 2013. The vehicle of this formulation is more hydrophilic (oil-in-water cream); the ingredients are shown in Table 1-2.

TABLE 1-2. INGREDIENTS OF WR279,396 AND THEIR FUNCTION.

CHEMICAL COMPOUND	FUNCTION
Isopropyl palmitate	Penetration enhancer
Lactic acid	Soothing agent
Propylene glycol	Solvent, humectant, penetration enhancer
Sodium lauryl sulfate	Anionic surfactant (emulsifier)
Sorbitol	Humectant
Stearyl alcohol	Non-ionic emulsifier (fatty alcohol)
Urea	Moisturizing and keratolytic agent
Water	Hydrophilic phase
White petrolatum	Lipophilic phase
Methyl and propyl paraben	Preservative
Paromomycin sulphate/gentamycin	Active ingredients

Efficacy. The topical formulation composed of 15% PM and 12% MBCL in soft paraffin was first tested *in vivo* in mice by El-on et al in the early 1980's[176]. A month after the treatment (two times a day for 10 days) all lesions caused by *L. major* in BALB/C and C/C3H mice were cured. All formulations containing DMSO or quaternary ammonium compounds such as MBCL resulted in cure of the CL lesion in mice but none was more efficient than MBCL. Quaternary ammonium compounds and DMSO are reported to damage the skin by solubilizing SC lipids and hence facilitate drug permeation into the skin (also see chapter 6). This might explain the efficacy of the treatment because based on the physicochemical properties PM is unlikely to go through skin. Moreover MBCL has been shown to be active against *L. major* amastigotes when tested *in vitro* ($ED_{100} = 5$ µg/ml). Further research tested the efficacy of the formulation against New World CL caused by *L. mexicana* and showed no visible lesions after treatment. The formulation only reduced the lesion size in CL caused by *L. panamensis* and *L. amazonensis* in BALB/mice and relapse occurred[177] [178].

Analyses of the subsequent clinical trials (Table 1-3) indicate a higher cure rate for PM with MBCL treatment compared to placebo in patients infected with *L. mexicana*, *L. braziliensis* and *L. major* [136, 138, 179]. However it is important to note that the ointment was applied after manually removing the debris and scab of the wound and hence in the absence of the SC that is the rate limiting membrane to permeation for the majority of topically applied drugs. Because PM has a high molecular weight and physicochemical properties that are unfavourable for skin permeation, the absence of the SC might enhance the permeation of the drug to the bioactive site in the skin. These trial conditions do not reflect the cure rate in patients at onset of the disease where the lesions are still in the nodular stage.

Efficacy data against other species are lacking because of several reasons: (i) trials were not conducted, (ii) causal *Leishmania* species were not identified or (iii) results were inconclusive due to poorly-designed trials.

Local side effects such as burning and irritation of the skin upon application of the PM plus MBCL formulation, have led to the development of a formulation with 15% PM and 10% urea in soft white paraffin[5]. When tested in clinical trials, the formulation showed no higher cure rate over placebo treatment[180, 181] or intralesional MA. The ointment was reported to be safer with fewer adverse effects compared to the ointment containing MBCL[182, 183].

Another more complex paromomycin formulation was developed by the US army. The formulation contains 15% PM and 0.5% gentamycin in a hydrophilic vehicle (also referred to as WR279,396) (Table 1-2). Gentamycin was included in the formulation because the combination of gentamycin (0.5%) with PM (15%) demonstrated a higher efficacy against experimental CL caused by *L. major* compared to PM (15%) alone[176]. Moreover, WR279,396 was more active against experimental CL due to *L. major*, *L. mexicana*, *L. panamensis* and *L. amazonensis* compared to the PM (15%) plus MBCL formulation[184].

As WR279,396 has a hydrophilic base, the aminoglycosides are expected to be more soluble in this formulation compared to the paraffin base used in the previous formulations (15%PM+12%MBCL and 15%PM+10% urea in soft white paraffin). This increases the concentration gradient (Fick's Law - Equation 1) of the drug across the SC

and hence can promote the permeation of the active compounds into the SC. The importance of the vehicle on the permeation of PM was previously demonstrated by Gomes et al in an *in vitro* permeation assay. The PM permeation through a SC that was mechanically damaged by tape stripping was higher for hydrophilic vehicles compared to lipophilic vehicles such as ointments[185].

In clinical studies, the WR279,396 formulation was applied and occluded after cleaning the wound bed of the lesion. Phase 2 and 3 trials, conducted in Tunisia, have shown a statistically significant higher cure rate for WR279,396 compared to vehicle control in CL patients infected with *L. major*[186, 187]. The phase 3 trial data analysis did not indicate a difference in cure rate for the WR279,396 and PM alone formulation. In contrast, a trial in Colombia did not show beneficial effects for the WR279,396 treatment, when applied twice daily, compared to placebo[188]. A study was conducted in Panama where the causative species was *L. panamensis*; the cure rates for the WR279,396 and PM alone formulation were 87% and 53.3% respectively[189].

Briefly, these clinical trials (Table 1-3) indicate that WR279,396 and PM alone are more active than placebo treatment against CL caused by *L. major* but there is a lack of evidence to suggest that the addition of gentamycin to PM enhances treatment. Moreover results obtained from New World CL patients, do not indicate a higher cure rate for WR279,396 compared to placebo even though the efficacy of the formulation was occluded during testing. This technique is known to enhance the permeation of many drugs[69]. Furthermore it should be mentioned that no trials investigated the efficacy of WR279,396 against intralesional MA or PM plus MBCL. When taking into account all the evidence, the WHO decided to only include the PM plus MBCL formulation in their approved CL treatment list.

TABLE 1-3. SUMMARY OF RANDOMIZED CONTROLLED STUDIES EVALUATING TOPICAL PAROMOMYCIN FORMULATIONS IN HUMANS.

Country	Leishmania spp	Patients per group	Experimental/ placebo groups	Treatment regimen per group	Outcome per group	Ref
Iran	*L. major* *L. tropica*	1. 126 2. 125	1. 15%PM+10% urea 2. Placebo	1. 2/day for 14 days 2. 2/day for 14 days	1. 63.5% 2. 63.2% Cure (= complete re-epithelialisation) 2.5 months after treatment	180
Iran	*L. major*	1. 20 2. 20 3. 20	1. 15%PM+12%MBCL 2. Phototherapy 3. placebo topical	1. 2/day for 28days 2. 1/week for 4 weeks 3. 2/day for 28days	1. 41.2% 3. 13.3% Cure (= neg. smear and normal skin texture) 2 months after treatment	190
Iran	*L. major*	1. 117 2. 116	1. 15%PM+10%urea 2. 15%PM+10%urea	1. 2/days for 7 days 2. 2/day for 14 days +14 days placebo	1. 50% 2. 37% Cure (= 50% re-epithelialisation or more) 2.5 months after treatment	191
Iran	*L. major*	1. 48 2. 48	1. 15%PM+10%urea 2. intralesional MA	1. 2/days for 45 days (mean) 2. 1.5g/5ml	1. 16.6% 2. 41.7% Cure (= complete re-epithelialisation) 2 months after treatment	182
Iran	*L. major*	1. 29 2. 27	1. 15%PM+10%urea 2. intralesional MA	1. 2/day for 20 days 2. 20 days	1. 66.7% 2. 60% Cure (= complete re-epithelialisation) one week after treatment	183
Tunisia	*L. major*	1. 66 2. 66	1. 15%PM+10%urea 2. placebo	1. 2/day for 14 days 2. 2/day for 14 days	1. 60.6% 2. 60.6% Cure (= neg. smear and culture, re-epithelialisation and 50% reduction of lesion size) after 2.5months after treatment	181
Iran	*No spec*	1. 40 2. 40	1. 15%PM+10%urea 2. placebo	1. 2/day for 30 days 2. 2/day for 30 days	1. 12.5% 2. 17.5% Cure (= neg. smear and reduction of lesion size and induration by 85%) 1 month after treatment	192
Turkey	*L. tropica*	1. 40 2. 32	1. 15%PM+12%MBCL 2. oral ketoconazole	1. 2/day for 15 days 2. 400mg/day for 30 days	1. 37.5% 2. 0% Cure (= complete re-epithelialisation) 1 month after treatment	193

Tunisia	*L. major*	1. 50 2.42	1. WR279,396 2. Vehicle placebo	1. 2/day for 20 days 2. 2/day for 20 days	1. 94% 2. 71% Cure (= 50% or more reduction of ulcerative size of index lesion by day56 and complete re-epithelialisation) 3 months after treatment	186
Not mentioned	*L. major*	1+2. 32 3+4. 11	1. 15%PM+12%MBCL (2/day for 20 days)+placebo (2/ days for 10 days) 2. placebo (2/ days for 10 days)+ 15%PM+12%MBCL (2/day for 10 days) + placebo (2/ days for 10 days) 3. 15%PM+5% MBCL (2/day for 20 days)+placebo (2/ days for 10 days) 4. placebo (2/ days for 10 days)+15%PM+5%MBCL (2/day for 10 days) +placebo (2/ days for 10 days)		1. 93.1% 2. 76.6% 3. 66.1% 4. not mentioned Cure (no parasites in lesion after treatment and healing lesions 1-4 weeks after treatment)	4
Guatemala	*L. braziliensis* *L.mexicana*	1. 35 2. 33	1. 15%PM+12%MBCL 2. Placebo	1. 2/day for 20 days 2. 2/day for 20 days	1. 91.4% 2. 39.4% Cure (= complete re-epithelialisation and no induration/inflammation by week 13) after treatment	7
Honduras	*L. mexicana* *L. chagasi*	1. 13 2. 22	1. 15%PM+10%urea 2. placebo	1. 3/day for 4 weeks 2. 3/day for 4 weeks	1. 4.3% 2. 3.3% Cure (= complete re-epithelialisation) 2.5 months after treatment	6
Ecuador	*Not specified*	1. 40 2. 40 3. 40	1. 15%PM+12%MBCL 2. 15%PM+10%urea 3. i.m. MA	1. 2/day for 30 days 2. for 30 days 3. 20mg/kg/day for 10 days	1. 79.3% 2. 70% 3. 91.7% Cure (+ complete re-epithelialisation of all lesions 12 weeks after the start of the treatment with no relapse during 52 weeks)	194
Colombia	*L.braziliensis* *L. panamensis*	1. 59 2. 30 3. 30 4. 31	1. 15%PM+12%MBCL+i.v.MA 2. 15%PM+12%MBCL+i.v.MA 3. topical placebo+i.v.MA 4. i.v.MA	1. 2/day for 10 days +i.v.MA for 7 days 2. 2/day for 10 days +i.v.MA for 3 days 3. 2/day for 10 days +i.v.MA for 7 days 4. 20 days	1. 58% 2. 20% 3. 53% 4. 84% Cure (= complete re-epithelialisation without relapse) 1.5 months after treatment	195
Colombia	*L. panamensis*	1. 33 2. 12	1. WR 279,396 2. Placebo	1. 2/day for 20 days 2. 2/day for 20 days	1. 61% 2. 55% Cure (= complete re-epithelialisation	188

					without relaps) 6 months after treatment
Panama	*L.panamensis*	1. 15 2. 15	1. WR 279,396 2. PM (15%) alone	1. 2/day for 20 days 2. 2/day for 20 days	1. 87% 2.53.3% Cure (= 50% or more re-epithelialisation of index lesion by day 63 and no relaps) 6 months after treatment	[189]

Besides the three formulations discussed above, other PM containing formulations were developed in an attempt to enhance PM delivery into the skin for example PM encapsulated in nanoparticles. Nanoparticles as drug carrier have shown to enhance drug permeation through skin[196-198]. However, the ability of nanoparticles to permeate skin as a whole is under discussion and subject of further current research[199, 200].

The level of penetration of liposomes into the epidermis and dermis varies and depends amongst other factors on the type and concentration of phospholipids, the concentration of penetration enhancer that is used and the size of the liposomes[201]. *In vitro* Franz diffusion cell (FDC) permeation studies conducted with tape stripped hairless mouse skin to mimic impaired skin barrier indicated a lower permeation for the liposomal formulations compared to the PM solution. In contrast, the PM concentration retained in the skin was 0.8-1.7% higher for the liposomal formulation[202]. Jaafari et al. showed that treatment with liposomal PM formulations containing 10 or 15% PM (LPMF) (4 weeks; twice daily) induced complete cure of the lesions caused by *L. major* in susceptible BALB/c mice[203]. The difference was statistically significant compared to the vehicle control consisting of empty liposomes or PBS but no liposome-free PM only group was included. Further *in vitro* FDC studies showed a high percentage i.e. over 10% of the PM from the LPMFs permeated across mouse skin after eight hours. To conclude liposomes seem an interesting carrier in order to increase the permeation of PM through skin.

Another approach used to increase the permeation of PM is the use of ion pairing. Molecules with an opposite charge are linked to PM forming a PM salt that is less hydrophilic and more likely to permeate through skin. Noguiera et al compared the permeation of PM free base with PM salts using Franz diffusion cells with full-thickness stripped and intact pig skin[204]. Neither PM free base nor the salt permeated through healthy skin, which is not surprising given its physicochemical characteristics. In skin with reduced barrier properties, the permeation of some PM salts increased significantly compared to the PM free base[204]. It would be interesting to test these formulations *in vivo* in experimental CL models.

1.5.3.2.2 *LOCAL PHYSICAL TREATMENTS – CRYO-AND THERMOTHERAPY*

Cryotherapy and thermotherapy are the most frequently used physical therapies. During cryotherapy a cotton swab with liquid nitrogen is applied on the wound and wound edges for about 10-25 seconds. This treatment is commonly used to treat wart infections but clinical trials have shown it also enhances CL cure. Two studies in Iran were conducted to compare the effect of three different treatments for CL: cryotherapy alone, a combination of cryotherapy with intralesional MA and intralesional MA alone[8, 205]. The first and second studies reported complete cure of patients in 52%, 80% and 52% and 67%, 89% and 75% respectively in the 3 respective groups. The researchers concluded that the combination therapy was significantly better than the two monotherapies. Based on these trials, cryotherapy alone seems to be as effective as intralesional MA alone.

Thermotherapy involves the induction of heat in the superficial layers of the skin. This can be done in several ways for instance by using a radiofrequency generator, ultrasound or infrared radiation. In Iran a randomized controlled study compared thermotherapy and intralesional MA for 4 weeks[206]. In order to localize the warmth a probe was placed on the skin; the resistance of skin to current creates warmth. Warmth of 50°C was applied to the lesions for 30 seconds. This was done once a week for four weeks. Six months after the treatment, 80% of the participants in the thermotherapy group showed complete cure compared with 56% in the intralesional MA group. These results were in agreement with previous studies conducted in Iran.

A trial conducted in Afghanistan compared intralesional SSG for 29 days (2-5 ml every 5-7 days), daily i.m. sodium SSG (20 mg/kg/day) for 21 days and thermotherapy based on radiofrequency (1 session with ≥1 applications of 1 minute of 50°C) for the treatment of CL caused by *L. tropica*[207]. Two months after the treatment the complete cure of patients in the three groups was 47%, 18% and 54% respectively. Treatment with thermotherapy was significantly better than i.m. SSG therapy however no significant difference with intralesional SSG was observed. Some patients that had received thermotherapy experienced superficial second degree burn wounds.

Thermotherapy was also used to treat New World CL. One trial[208] compared thermotherapy (30 seconds of 50°C, 1 session per week for 3 weeks) with i.m. MA (850 mg MA/day for 15 days) with placebo thermotherapy (no heat generation) as potential

treatment for CL. 73%, 59% and 27% of the participants in the respective groups were completely cured two months after the treatment. Again thermotherapy gave significantly better results against CL than the other therapies. Overall the randomised controlled trials (RCTs) showed good results and thermotherapy seems a good treatment option as it is active against all species. However the main limiting factor is the requirement of expensive equipment and electricity which might be unavailable in rural settings. Additionally, thermotherapy requires experienced personnel to apply the treatment to the patient.

1.5.3.2.3 IMMUNOTHERAPY

Research has suggested that immunotherapy can provide a useful adjuvant to chemotherapy in the treatment of CL. In contrast to chemotherapy that aims to kill the parasite, immunotherapy stimulates the host's own immune response in order to clear the parasite from its system.

Imiquimod is an imidazoquinoline and acts as a potent immunomodulator. It is the active ingredient in a topical cream Aldara™ (Meda Pharma, UK) that is used to treat cervical warts caused by human papilloma virus. *In vitro* studies have shown that imiquimod induces a leishmanicidal activity in macrophages[209]. *In vivo* mouse studies compared the Aldara™ cream with a placebo cream without imiquimod and found that the group treated with Aldara™ cream showed a significant reduction in footpad swelling when compared to the placebo group. Furthermore the cream halted the development of visible lesions on the footpad in contrast to the placebo treatment group[209].
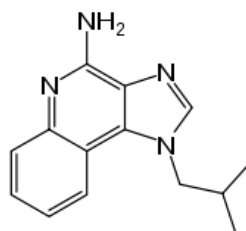
FIGURE 1-15. CHEMICAL STRUCTURE OF IMIQUIMOD

After successful results in mice, imiquimod cream proceeded to clinical trials. Two trials, conducted in Peru compared the activity of standard intraveneous pentavalent animonials (SSG or MA) combined with topical imiquimod to treatment with

antimonials only in patients who had not responded to previous treatment with antimonials only. Both trials indicated that treatment with imiquimod is safe and significantly increased the cure rate compared with antimonials alone in patients. Furthermore imiquimod reduced the residual scarring[210, 211].

Another promising immune adjuvant is the cytokine granulocyte-macrophage colony-stimulating factor (GM-CSF). It is a monomeric glycoprotein of 127 amino acids[212] and an approximate 14 kDa[212] that is secreted by a variety of cell types such as T cells, fibroblasts and macrophages. It is used to prevent neutropenia in cancer patients on chemotherapy and patients that underwent bone marrow transplantation and is administered through subcutaneous injection or intravenous infusion.

GM-CSF seems an interesting immune adjuvant as it can promote proliferation, activation and differentiation of macrophages and dendritic cells[213]. Moreover human studies report increased wound healing and scar formation in diverse wound types upon topical application[214-218].

Regarding leishmaniasis, pretreatment of macrophages with GM-CSF enhanced killing of intracellular *L. tropica[219]*, *L. major[220]* and *L. amazonensis[221] in vitro*. In mice, GM-CSF indicated anti-leishmanial activity by mobilisation of neutrophils and monocytes[222]. RCTs conducted in Brazil have indicated that GM-CSF both after oral[223] or topical[224] administration reduced the healing time of CL lesions when given in combination with intraveneous animonials.

1.5.4 EXPERIMENTAL TOPICAL TREATMENTS

In this section, new drugs that have been tested topically against CL but are currently not recommended by the World Health Organisation due to a lack of efficacy or poorly designed experiments with inconclusive results are discussed.

1.5.4.1 ANTIMONIAL DRUGS

El-On was the first to evaluate the efficacy of a range of drugs with *in vitro* leishmanicidal activity against experimental CL upon topical application[176]. Amongst others, antimonial formulations containing either 1.7% SSG (Sb^V) or 15% stibophen (Sb^{III}) with 12% of MBCL, a penetration enhancer in soft paraffin were evaluated[176]. A month after the last dosing, a mean lesion size of 45.6 and 91.1 mm^2 was reported for

SSG and stibophen respectively compared to a mean lesion size of 40 mm^2 for the untreated control. This suggests that i) the SSG formulation had no activity against CL and ii) the stibophen formulation caused CL to progress. This however does not consider the irritant effect of MBCl that is likely to cause an increase in lesion size. Moreover the stibophen formulation showed toxic effects causing 1 mouse to die during the treatment and an additional 3 to die within 1 month after treatment. Based on the lesion size, death by CL infection should not be excluded.

1.5.4.2 AMPHOTERICIN B

A 15% AmB deoxycholate (Fungizone®) and 12% methylbenzethonium choloride formulation in a soft paraffin base was also tested in mice. The formulation was applied twice a day for 12 days. Thirty days after treatment none of the lesions were cured[176].

Another study tested the topical application of Fungizone®, Amphocil™ and an AmB phospholipid complex in a range of solvents against experimental CL[225]. The application started 24 hours after s.c injection of *L. major* parasites and consisted of 10 µl of a 2 mg AmB (as Fungizone®, Amphocil™ or AmB phospholipid complex)/ml formulation per day for 3 weeks. The application of AmB did not prevent lesion development but a statistically significant reduction in lesion size was measured for Amphocil™ and AmB phospholipid complex, but not Fungizone®, when dispersed in 10% ethanol (EtOH) respectively at the end of the treatment compared to the untreated control. There is no mention of a follow up period.

The use of volatile solvents that evaporate quickly after application potentially increase the thermodynamic activity of the drug, also the driving force for permeation. Ethanol evaporation increased the permeation of fentanyl through this mechanism[226] and might explain the enhanced activity of ethanolic formulations compared to the other solvents used for example glycerol and propylene glycol (PG). Topical application of ethanol is also reported to remove lipids from the skin in humans what potentially can lead to reduced barrier function[227-229].

The effect of a colloidal dispersion of Amphocil™ (5 mg/ml) in 5% ethanol (without glucose) on ulcerated CL lesions in humans was tested. This single blind study was designed so that the placebo and drug-treated ulcers were on the same patient. Nineteen patients were asked to apply the dispersion three times a day. The size of the lesions was used as a measurement of disease progress. All the AmB treated lesions healed

faster than the placebo treated lesions except for one extremely deep lesion[230]. Some case studies also reported successful treatments with topical AmB formulations[231].

Based on its physicochemical profile, AmB is assumed not to permeate into the skin. It (i) has a molecular weight of 924 g/mol; (ii) is amphiphilic at physiological pH; (iii) shows limited water solubility (1µg/ml at ambient temperature); (iv) has a large number of groups capable of hydrogen bonding and (v) has a distribution coefficient of -1.41 at pH 7.4[232]. A possible explanation for the enhanced cure rate seen in some of the studies might be the absence of the SC in ulcers. Because the main barrier to skin permeation is absent, the applied drug can freely diffuse into the dermis and kill the parasite.

The inability of AmB to permeate through skin was shown in both *in vitro*[233, 234] (also see chapter 3) and *in vivo*[225, 235, 236] studies. An *in vitro* study reported limited permeation through rat skin after application of AmB nanoparticles[233]. It should be mentioned that the rat skin tissue was wiped with isopropyl alcohol and the receptor phase contained 2% DMSO. Both solvents can solubilize skin lipids resulting in a damaged barrier function of the skin and possibly enhance permeation. Rat skin is also known to be more permeable than human skin[237, 238]. Another study tested the efficacy of a gel containing AmB-cyclodextrin against CL caused by *L. amazonensis* in hamsters. After 21 days of treatment with the gel (0.125% AmB – twice a day) the growth of the lesion had halted but increased again after treatment was stopped[235].

In conclusion, AmB is a poor drug candidate for topical administration. As explained above, its physicochemical profile is not conducive to skin permeation and *in vitro* studies indicate little or no permeation through healthy skin and only limited permeation through damaged skin. Sometimes low rate of permeation is reported after application on damaged skin[239] or by the use of aggressive solvents as indicated by a study[234], where a number of AmB formulations were tested. AmB permeation through rat skin was only reported for an AmB in DMSO/methanol solution.

Evidence seems to suggest that AmB is not active against CL when applied topically and even if AmB manages to cross the SC, the hydrophilic viable epidermis and dermis can pose a major barrier before it reaches the parasites. In contrast local administration with circumvention of the skin barrier might be a useful approach to treat CL. In fact, Corware et al have shown the activity of an AmB formulation against an early stage and established CL lesion in BALB/c mice upon intradermal administration[240]. In both

models, the formulation was injected 3 times over a 1 or 3 week period in the footpad where the parasites resided, and led to resolution of the CL lesion and a parasite reduction greater than 3 $\log_{10}$[240].

1.5.4.3 MILTEFOSINE

Miltefosine first came to the market as a topical solution (Miltex®- composition Table 1-4) to treat breast cancer metastases. This solution was tested on mice from three different strains (C57BL/6, CBA/J and BALB/c) to evaluate its activity against *L. major* and *L. mexicana* parasites[241]. Treatment for *L. major* and *L. mexicana* were started respectively 3 weeks and 5 months after infections. One drop of Miltex®, containing approximately 1.5 mg miltefosine, was applied 5 days per week for 5 weeks in C57BL/6 and CBA/J mice and for 2 weeks in the BALB/c mice.

After the treatment protocol was finished, no mice showed visible palpable lesions and for BALB/c and C57BL/6 mice the parasite levels in the spleen and the draining lymph nodes were below the assay detection limit, which was not the case for all CBA/J mice[241]. Unfortunately, these results were not reproducible (Yardley and Croft, unpublished data).

TABLE 1-4. COMPOSITION OF MILTEX®.

Chemical compound	Per 100 ml Miltex®
miltefosine	6 g
NaOH	0.227 g
citric acid	0.484 g
3-propyloxypropylene glycol	31.6 g
3-hexyloxypropylene glycol	15.8 g
3-nonyloxypropylene glycol	15.8 g
purified water	30.9 g

1.5.4.4 BUPARVAQUONE

Buparvaquone (BPQ) (Figure 1-16) a hydroxynaphthoquinone is the gold standard treatment against a protozoan disease in cattle called theileriosis. It is a structural analogue of ubiquinone which is also known as coenzyme Q. The latter functions as a carrier of electrons within the mitochondrial membrane in ATP synthesis. Due to its structural resemblance to ubiquinone, BPQ is believed to reduce the intracellular ATP and inhibit the respiratory chain in *Leishmania* parasites[242].
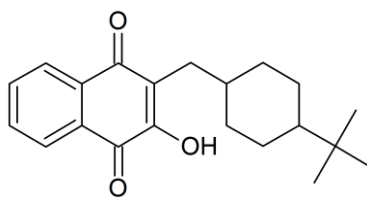
FIGURE 1-16. CHEMICAL STRUCTURE OF BUPARVAQUONE

BPQ demonstrated an activity in the nanomolar and low micromolar range when tested *in vitro* against *Leishmania* species that cause CL or VL[243]. Despite its potent *in vitro* activity, BPQ demonstrated poor *in vivo* efficacy against VL upon oral or subcutaneous administration[244]. This is most likely due to the poor bioavailability and distribution that is related to the low water solubility (<1 mg/L).

Further *in vitro* studies showed no human skin permeation for BPQ after topical application[243]. The use of lipophilic vehicles resulted in BPQ permeation but the rate remained low[245]. In an effort to increase skin permeation, more water soluble anti-leishmanial prodrugs were synthesised. Four optimised topical formulations of BPQ and its prodrug 3-phosphonooxymethyl-BPQ (3-POM-BPQ) were then tested *in vivo* against CL in BALB/c mice induced by *L. major*. The application commenced when the average diameter of the CL lesions measured approximately 2mm. At the end of the treatment, none of the groups showed a statistically significant reduction of the lesion size or parasite load when compared to the untreated control[246].

1.5.5 TREATMENT CHALLENGES

As generally known, all current CL treatments are unsatisfactory. Rather than to criticize them the aim of this section is to highlight the complexity of the challenges that are faced when developing a safe effective and reliable CL treatment, knowing that some are easier to tackle than others.

Drug repurposing. In the 1990's concern was raised about the lack of new chemical entities registered for neglected diseases. The development of an NCE is a long process that takes 9-12 years on average and costs an estimated 802 million US dollars[247, 248]. The pharmaceutical industry is not keen to invest this amount of money in a neglected disease that only offers low return. A study published in the Lancet revealed that only four new chemical entities and 25 products with new indication or formulation for neglected diseases were registered during 2000-2011[249].

Drug repurposing is one of the strategies to overcome the high development costs for a new drug or chemical entity (NCE). It includes drug repositioning, where a known drug is applied to treat a different disease, also referred to as therapeutic switching, and drug reformulation, a process that focusses on the reformulation of the active ingredient in order to administer through a different route. From 2000 to 2011, all three drugs approved to treat leishmaniasis (of which one for CL) were repurposed molecules that were initially used for a different indication. For example, miltefosine was first brought on the market as an anti-cancer drug, amphotericin B was previously used to treat fungal infections and paromomycin that was available as an oral treatment for intestinal amoeba infections was reformulated to a parenteral solution and topical formulation to treat VL and CL respectively.

Actually most of the research conducted on topical formulation development for CL, focusses on reformulating an already existing anti-leishmanial drug. For example DNDi is trying to develop a topical amphotericin B formulation, while Novartis puts effort in reformulating antimonials in a topical preparation.

Even though reformulation of drugs is a useful technique that has led to new treatments, it should be born in mind that the activity of a drug is influenced by the route of administration and different routes impose different physicochemical requirements on a drug. From the previous section it is clear that oral or parenteral drugs are not always the best topical drug candidates and a screening of molecules can prevent time, effort and cost into projects that are likely to lead to partial or unsuccessful results. For example paromomycin, the active drug in Leshcutan®, requires manual removal of the scab prior to application and co-formulation with an aggressive penetration enhancers to increase drug delivery to the bioactive sites in the skin. *In vitro* permeation studies have shown that PM does not penetrate healthy skin and clinical trials using formulations other than PM plus MBCL show limited results. In addition, the combination with MBCL is irritating as it damages the skin but at the same time this agent seems to be necessary for the formulation to be active.

The permeation of amphotericin B from a range of topical formulations was tested but did not show high permeation. Again this is not surprising when comparing the physicochemical properties of amphotericin B with these of compounds that easily permeate the skin such as caffeine and ibuprofen. To conclude, there is no doubt that

new drugs to treat CL are required. However, a careful screening of the available information and drug properties can indicate the feasibility of reformulation for different routes of administration.

One treatment for CL. Depending on host and parasite factors, CL shows a variety of clinical manifestations. One of the main problems of treatment development is finding a treatment that is active against all *Leishmania* parasites. Biochemical and molecular differences between *Leishmania* species lead to differences in drug susceptibility *in vitro*. This correlates with variability in clinical response that is observed when comparing the success rates of treatments given in different geographical regions. Often Old World CL is more responsive to treatment compared to New World CL. However even within Old World CL causing species the sensitivity to drugs varies. Is it possible to find one treatment to treat all CL patients? And if not, will the pharmaceutical industry be interested in manufacturing a treatment that is only active against one species and thus present a smaller market?

Logistics. There are several logistic factors that complicate the development of a treatment for CL. Firstly, CL occurs in tropical climates with sometimes a high humidity. Both a high temperature and humidity are known to cause instability of drug formulations, especially for emulsions and creams that are, by nature, physically unstable systems. Secondly, primary health centres that offer treatment for CL patients can be difficult to reach for people living in rural areas and even when reached, medication availability is not guaranteed.

Cost.

Table 1-5 shows the price per CL treatment estimated by the WHO. This is only the direct cost of the treatment and indirect costs such as inability to work are not included. Moreover Alvar et al reported that the annual income per person in areas that are greatly affected by CL range from 82 to 200 US$. This means that the price of a treatment can exceed the monthly salary for some patients.

TABLE 1-5. PRICE PER CUTANEOUS LEISHMANIASIS TREATMENT(JANUARY 2010)-ADAPTED FROM [118].

Compound	Treatment regimen	Drug cost in US $*
SSG systemic, 20 mg/kg/day	20 days	37
SSG intralesional**	Until lesion is healed	12
MA systemic, 20 mg/kg/day	20 days	40
MA intralesional**	Until lesion is healed	13
Pentamidine	Up to 4 months	Free (donation program)

* For a patient weighing 35kg (leishmaniasis patients often suffer from impaired nutritional status). Calculations for sodium stibogluconate based on exchange rate of 1 GBP= US$ 1.41 (Price based on generic SSG). ** Intralesional treatment is commonly estimated at a third of the cost of systemic treatment.

Treatment seeking behaviour. Patients often seek treatment late after the appearance of the first symptoms because effective and safe treatments are lacking and many patients postpone seeking help by trying herbal or home-made remedies. Only after multiple treatment failures and thus progression of the lesion, they will visit primary health care centres. Research into the treatment seeking behaviour of CL patients reports variable delays between the onset of the symptoms and seeking treatment. A study in Syria reported 2.4 months on average[250], while in Paraguay this was 1-6 months[251]. By this time, the lesion might have progressed to an ulcer which makes it more difficult to treat and increases the risk of scar formation.

1.6 TOPICAL TREATMENTS - RATIONALE

Risk-benefit analysis leads us to conclude that systemic treatment should only be given for the more severe cases with (i) numerous, (ii) large or (iii) disfiguring lesions, (iv) patients at risk of diffuse CL or leishmaniasis recidivans, (v) lesions on places that makes it difficult to treat locally or (vi) when local treatment has failed. This means that about 25-50% of all CL cases worldwide, representing around 150 000 to 550 000 patients require systemic treatment[252] and about 50-75% of all CL patients can be treated with local treatments.

We aim to treat in the early stages of the disease, when the papule is still covered with intact skin mainly because treatment at the onset of the disease might (i) increase the chance of successful treatment; (ii) avoid scar formation by preventing the lesion to progress into an open ulcer; and (iii) reduce spread of the parasites and thus the possibility of satellite lesion development.

Figure 1-17 shows a section of *Leishmania* infected skin and indicates that the parasites reside in the dermis (Figure 1-17).
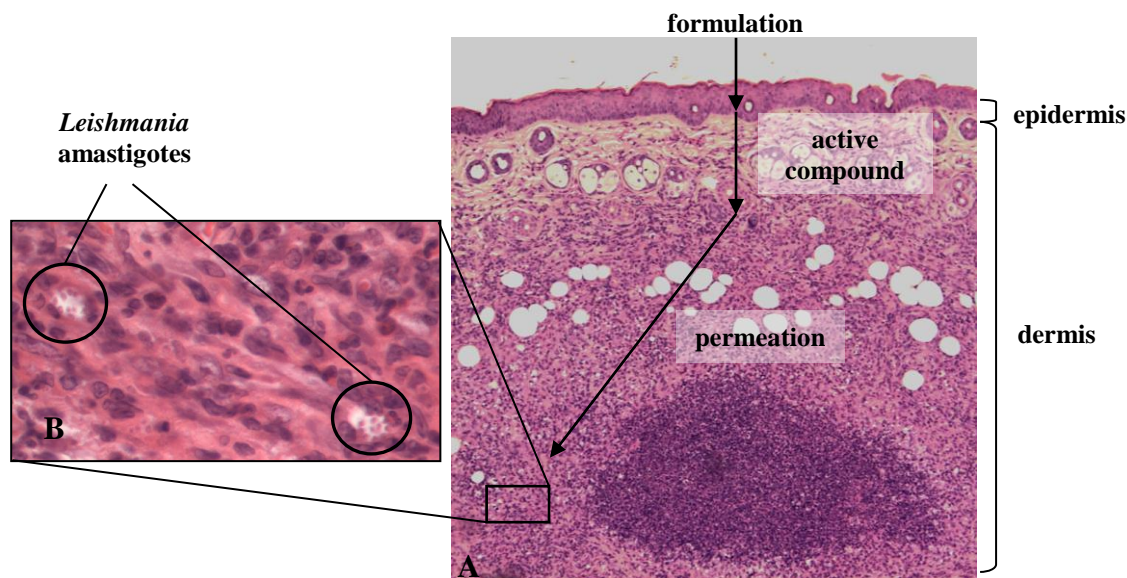
FIGURE 1-17. (A) SHOWS THE ROUTE OF THE ACTIVE INGREDIENT THROUGH *LEISHMANIA* INFECTED BALB/C MOUSE SKIN BEFORE REACHING THE; (B) AMASTIGOTES SITUATED IN THE DERMIS.

The location of *Leishmania* parasites is lower compared to other pathogens that cause skin infections and are treated topically. For example fungi that cause skin infections typically reside in the *stratum corneum* where they can degrade keratin. Only superficial bacterial infections that are limited to the epidermis are treated topically. Infections that extend into deeper skin layers are treated systemically. Herpes simplex is a viral skin infection that originates in the basal layers of the epidermis[253]. Topical treatments are

available indicating that the drug is able to reach the lower layers of the epidermis. For a topical formulation to be active against CL, the drug will have to permeate through the stratum corneum, into the dermis and through the macrophage membrane to reach the parasites that are situated in the phagolysome.

2 AIMS AND OBJECTIVES

The overall aim of this project is to develop a topical treatment for CL. As discussed in the introduction, skin diseases often affect the barrier function of the skin. When targeting the skin, it is thus essential to characterize the impact and extent of the barrier impairment on drug delivery.

In the *first experimental chapter*, *Leishmania* infected skin was compared with uninfected skin in three ways:

- Histology sections of BALB/c mouse skin infected with *Leishmania* parasites were examined for microscopical changes in skin structure.
- The inside-outside barrier integrity was evaluated by repeatedly measuring TEWL as the CL lesion progressed.
- The outside-inside skin barrier impairment was established by measuring the permeation of different model drugs and anti-leishmanial compounds through infected and uninfected skin.

In the *second experimental chapter*, the influence of different solvents on the permeation of miltefosine was determined. The reformulation of miltefosine, already on the market as oral drug, is an attractive development strategy that could save a considerable amount of time and money. It is particularly useful if it concerns neglected diseases that is a domain with poor interest to the pharmaceutical industry.

In the *third experimental chapter*, a drug discovery approach was used to evaluate compounds from 4 different structural classes of benzoxaboroles, for their anti-leishmanial activity and suitability for topical treatment of CL. An array of *in vitro* ADME studies were performed and allowed the selection of 3 favourable compounds.

The *fourth experimental chapter,* describes how the oral and topical activities of these compounds was evaluated *in vivo* in BALB/c mice infected with *L. major*

3 THE BARRIER INTEGRITY OF LEISHMANIA INFECTED MOUSE SKIN - CHARACTERISATION

The skin maintains homeostasis between the inner and outer environment. To do so, it functions as a barrier that prevents water loss and permeation of chemical and infectious agents. It is the largest organ of the body and covers a big surface making it vulnerable to disruption.

By altering the skin physiology, pathological disorders can disrupt the barrier integrity resulting in increased or decreased drug delivery from topical formulations to their target site in the skin[254-256]. For example psoriasis is a common non-infectious skin disorder caused by an uncontrolled division and acceleration of keratinocytes and is characterised by erythematous plaques with overlying silvery scales. Research has shown loss of skin barrier integrity and increase of drug permeation in psoriatic plaques compared to healthy skin[95, 257].

Expanding further, infectious skin disorders were also found to disrupt the physiology and barrier function of the skin. For example, tinea, a fungal skin infection, is caused by dermatophytes that are found on top and in the superficial layers of the epidermis. Evaluation of the barrier integrity in tinea-affected skin reported a reduced SC hydration, enhanced proliferation and disturbed differentiation of the epidermis[255].

This chapter describes the skin physiology changes that occur after infection with *Leishmania* parasites and how they influence the skin barrier integrity and thus the delivery of drugs to the skin. This is especially important because the overall aim of this PhD project is the development of topical formulations to treat CL. The information provided by the experiments described in this chapter can be used to produce more target specific active compounds and better adapted formulations to increase the chance of successful treatment.

First, a histological evaluation of the structural differences between uninfected and *Leishmania* infected skin was performed. The common haematoxylin and eosin (H&E) stain was used to evaluate the different skin tissue layers, whereas an elastic-Van Gieson stain was performed to visualise elastic fibres and collagen, which are 2 dermal components that are important for the support and elasticity of the skin. Finally, a more

specific immunostaining technique was used to see the invasion of macrophage-like cells to the place of infection.

The transepidermal water loss (TEWL) was measured as a function of barrier integrity (section 1.4.1). This technique is a non-invasive method that quantifies the outward diffusion of water through the stratum corneum (SC). Damaged skin is less able to control water movement from the interior to the exterior which translates in a higher TEWL value when compared to healthy skin that is able to restrict water flow. In parallel, skin hydration was measured[258].

The skin pH was measured as it contributes to the maintenance of SC integrity, cohesion and desquamation and seems to be related to the permeability homeostasis of the skin[259-261]. In fact, skin infections caused by fungi such as *Candida*[262] and *Dermatophytes*[263] have been linked to pH increase. Two key serine proteases in the desquamation process, kallikrein 5 and 7 show optimal activity at neutral pH[264-266], whereas β-glucocerebrosidae and acidic sphingomyelinase are active at pH 5.6 and 4.5 respectively[267]. The latter are important enzymes in the synthesis of ceramide, an essential skin lipid that contributes to the SC barrier. When the pH increases, the serine proteases are activated and the activity of the ceramide generating enzymes is reduced by ten-fold[261] causing increased skin desquamation and SC thinning leading to barrier perturbation[268].

Finally, the permeation of two model compounds with different lipophilicities, caffeine (log P = -0.08) and ibuprofen (log D = 3.97) through infected and uninfected skin were compared and subsequently the permeability of three anti-leishmanial drugs amphotericin B, paromomycin sulphate and buparvaquone were evaluated. In contrast to the models commonly used to test drug permeation through diseased skin (section 1.4.3), this model has the advantage of being CL specific.

3.1 MATERIAL AND METHODS

3.1.1 TEST COMPOUNDS AND OTHER REAGENTS

Details and suppliers of the chemicals and solvents used for the experiments of this chapter are listed in the table below (Table 3-1).

TABLE 3-1. DETAILS OF CHEMICALS AND SOLVENTS USED FOR EXPERIMENTS OF THE INFECTED VS. UNINFECTED MODEL

Compound	Specifications	Supplier
Test compounds		
Caffeine	ReagentPlus®; ≥ 99% purity	Sigma Aldrich
Ibuprofen	≥ 98% purity	Sigma Aldrich
Amphotericin B	Molekula, ≥ 99% purity	VWR international
Buparvaquone	Vetranal™, analytical standard	Sigma Aldrich
Paromomycin sulfate	≥ 98% purity	Sigma Aldrich
Chemicals		
Phosphate buffered saline	Tablets, dissolved in 200 ml H_2O - 0.01 M phosphate buffer, 0.0027 M KCl, 0.137 M NaCl, pH 7.4 at 25ºC	Sigma Aldrich
β-cyclodextrin	Hydroxypropyl- β-cyclodextrin	Sigma Aldrich
Formalin solution	10% formalin (approx. 4% formaldehide)	Sigma Aldrich
HPLC solvents/chemicals		
Trifluoroacetic acid	Chromasolv®, HPLC grade	Sigma Aldrich
Disodium EDTA	Disodium dihydrate EDTA, HPLC grade	Sigma Aldrich
Acetic acid	HPLC grade	Sigma Aldrich
Water	HPLC grade	Fisher Scientific
Acetonitrile	HPLC grade	Fisher Scientific
Methanol	HPLC grade	Fisher Scientific
Radiolabeled compound/ scintillation fluid		
Optiphase™ supermix cocktail	N/A	Perkin Elmer
[3H]-paromomycin sulfate	Specific activity: 0.2 Ci/mmol; radiochemical purity: 99.8%; radioactive concentration: 500 μCi/ml; solvent: water	Moravek Biochemicals

3.1.2 PARASITE STRAIN AND ANIMALS

Leishmania major (MHOM/SA/85/JISH118) amastigotes were obtained and isolated from mouse skin lesions. They were allowed to transform to promastigotes and were maintained in Schneiders insect medium (Sigma Aldrich, UK) supplemented with 10% HiFCS (Harlan, UK) at 26°C. The parasites were routinely passaged through BALB/c mice and low passage number promastigotes (typically below passage number 3) were used for this experiment as infectivity was shown to decrease with time of parasite cultivation.

Female BALB/c mice of about 6-8 weeks old, were purchased from Charles River (Margate, UK) and housed in a controlled environment of 55% relative humidity and 26°C. They were provided with tap water and a standard laboratory diet. All *in vivo* experiments were carried out under license (PPL 70/6997) at the London School of Hygiene and Tropical Medicine (LSHTM) after discussion with the veterinarian and according to UK Home Office regulations.

3.1.3 IN VIVO CL MODEL

Five female BALB/c mice (6-8 weeks old; Charles River Ltd., UK) were shaved and one day later, injected with $2x10^7$ stationary phase *L. major* JISH118 promastigotes (200 µl) subcutaneously on the rump above the tail. This inoculum size was selected as previous injection in BALB/c mice had resulted in producible infections in terms of onset of the disease, progression and lesion size evolution. Three control mice were injected with medium that did not contain parasites. The mice were inspected daily for the presence of a papule. After about 7 days, a small papule at the site of injection was visible in the infected mice.

The lesion size was measured every day using digital callipers. Every other day, various skin parameters such as TEWL, SC hydration and skin pH were measured while the mouse was anaesthetised as explained in detail below (section 3.1.5). When an average lesion diameter of 5 mm was reached, the mice were sacrificed and the papule was excised for further histological evaluation or for use in FDC permeation studies. For these permeation studies, uninfected control tissue from above the CL nodule on the back of the same donor mouse was excised (Figure 3-1). Control skin parameter

measurements and histology samples were obtained from mice which received 200 μl of medium without parasites.

uninfected   infected
(control)   (papule)
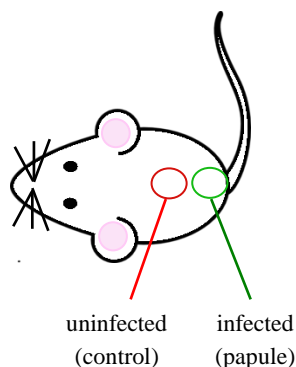
FIGURE 3-1. SCHEMATIC PRESENTATION OF THE ORIGIN OF SKIN USED IN THE FRANZ DIFFUSION CELL PERMEATION ASSAYS.

3.1.4 HISTOLOGY

Skin samples of the infected (papule; ±5 mm diameter) and uninfected skin (mice injected with medium without parasites) were collected and fixed in 10% neutral formalin solutions until they were further processed at the UCL Institute of Neurology (Queen Square, London).

Briefly, the samples were dehydrated using ascending concentrations of ethanol and clear xylene prior to paraffin embedding. The samples were then cut and sections were mounted on slides and stained to allow histological examination by light microscopy. Images were taken using a Leica DMRB microscope (Leica, Germany) (eye piece magnification x1, x1.6, x2.5, x5 and lens magnification x10, x40, x100) equipped with a Leica DFC 420 camera controlled by Leica Application Suite (version 3.1).

3.1.5 TEWL - AQUAFLUX AF102

Transepidermal water loss (TEWL) was measured every other day using the AquaFlux AF102 (Biox, London). The equipment was calibrated (flux density calibration) according to the manufacturer's guidelines prior to starting the experiment and was baseline calibrated prior to use each day.

Mice were left to acclimatise in the room (temperature: 21-22˚C / relative humidity: 50-54% relative humidity) for 1 hour before they were placed in the induction chamber. Anaesthesia were induced at 3% isoflurane with 100% oxygen at a flow rate of 2.5 l/min until no movement was observed. The mice were then removed from the chamber

and placed on tissue with their snout covered by a mask to maintain anaesthesia exposure with 2% isoflurane and 100% oxygen at 2.5 l/min. The probe was placed over the papule and the measurement was recorded when the TEWL stabilised (approx. 30-60 seconds later). For recovery from the anaesthesia, the mask was removed and the mice were gently placed on a warm plate (37˚C) and observed until first movements before being placed back in their cage. Statistical analysis were performed using SPSS software version 19.0.

3.1.6 SKIN HYDRATION AND P*H*

Skin hydration was recorded after the TEWL measurement but prior to determining the skin pH while the mouse was still anaesthetised. The probe (MY-808S, moisture checker, Scalar, Japan) was cleaned carefully and applied to the skin surface, where the parasites had been injected. The value was registered.

Afterwards the Skin-pH-Meter® PH 905 from CK electronics (Köln, Germany) that was calibrated (using pH 4.0 and pH 7.0 buffer solutions) prior to starting the experiment, was rinsed with distilled water. The moist probe was applied to the mouse skin and six consecutive measurements were taken and averaged.

3.1.7 INVESTIGATION INTO PERMEABILITY OF INFECTED VS UNINFECTED SKIN

3.1.7.1 PREPARATION OF DONOR AND RECEPTOR SOLUTIONS

Saturated donor solutions for caffeine, ibuprofen, paromomycin sulphate and buparvaquone were prepared by adding an excess amount of drug to PBS. A magnetic stirrer bar was added to the vial and the mixture was left to stir at 32˚C for 48 hours prior to the experiment. For paromomycin sulphate, the drug suspension was centrifuged at 13000 rpm for 30 minutes and the supernatant was removed and spiked so that it would contain 10 µCi of [3H]-paromomycin sulfate per Franz diffusion cell. Due to stability issues, the amphotericin B donor solution was prepared by adding an excess amount of drug to PBS followed by 1 hour of sonication.

The receptor fluid consisted of a PBS solution that was sonicated for 30 minutes to remove air bubbles prior to adding it to the Franz cell device. For the permeation of the more lipophilic compounds, buparvaquone and amphotericin B, PBS was supplemented

with 2% hydroxypropyl-β-cyclodextrin[245] (CD) in order to ensure sink conditions during the experiment.

3.1.7.2 PERMEATION EQUIPMENT AND DIFFUSION CELLS

For this experiment, Franz cell devices (Figure 3-2) with narrow diameter were developed (Soham Scientific, Fordham, UK) in order to measure the permeation of a drug through a *Leishmania* infected skin area (diameter of receptor and donor compartment: 5 mm). Furthermore the volume of the receptor compartment was approximately 2 ml.
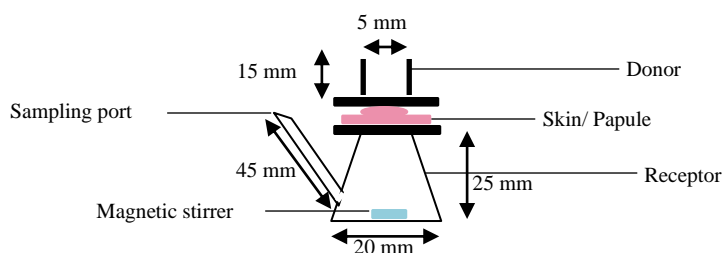
FIGURE 3-2. SCHEMATIC REPRESENTATION OF A FRANZ DIFFUSION CELL (WITH DIMENSIONS).

The cells were placed in a plexiglass waterbath equipped with an immersion thermostat and a Variomag 60 position stirrer supplied by CamLab Ltd. Teflon coated magnetic stirrer bars were obtained from VWR international Ltd. (Leicestershire, UK).

3.1.7.3 SOLUBILITY DETERMINATION OF THE TEST DRUGS

The solubility of the drug compounds in PBS (with or without 2%CD) was determined by adding an excess amount of drug to the appropriate solvent in a clean vial. A magnetic stirrer was added before carefully sealing the vial and the suspension was left to stir for 48 hours at 32°C as per[269]. An aliquot of this mixture containing some solid drug particles was centrifuged at 13000 rpm at 32°C for 15 minutes. The supernatant was taken and analysed by HPLC-UV. This was done in triplicate for each test drug.

HPLC-UV analysis for paromomycin sulfate was not possible due to the absence of chromophores. The solubility in PBS was determined by adding weighed amounts of drugs to a vial containing the appropriate solvent and a magnetic stirrer. Every 2-3 hours the status of the mixture was observed and when a visibly clear solution was obtained a small amount of drug was added. Afterwards the vial was carefully sealed and returned to the warm water bath (32°C). The approximate solubility of the drug was

calculated by taking the sum of the drug added to the solvent until visible drug particles remained present and no longer dissolved.

3.1.7.4 STABILITY OF THE TEST DRUGS IN THE RECEPTOR AND DONOR SOLUTIONS

In order to ensure drug stability during the experiment (32ºC - PBS) and storage (4ºC ±2%CD), drug solutions were prepared in MilliQ water and PBS with or without 2%CD. An aliquot was removed and analysed for the initial concentration at time 0 (t_0) and the remaining solution was either left at 32 ºC in a warm water bath or stored in the fridge protected from light. An aliquot was taken at different time points and analysed by HPLC-UV. Stability was defined as the retention of 90-110% of the initial drug concentration. Paromomycin sulphate was stable for 5 days at 37 ºC according to the supplier.

3.1.7.5 IN VITRO DIFFUSION ASSAY
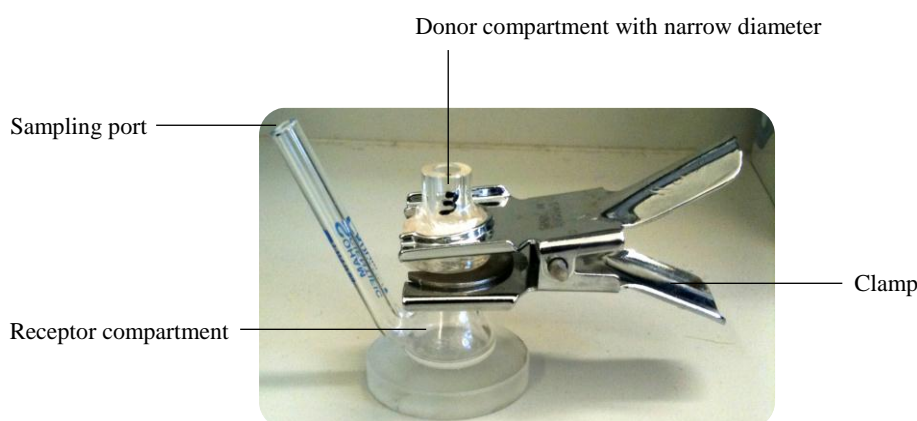
FIGURE 3-3. AN IMAGE OF THE FRANZ CELL DEVICE USED FOR THE PERMEATION STUDIES.

The full-thickness skin pieces, both the control and papule part, were inspected for macroscopic damage and muscle and fat tissue were carefully removed using forceps. Skin pieces were cut in circular discs of about 2 cm diameter. They were then mounted between the donor and receptor compartment of the Franz cell device and kept in place by a clamp (Figure 3-3). The receiver fluid, PBS or water with 2%CD, was sonicated for 30 minutes prior to the experiment before adding to the receptor compartment. A small magnetic stirrer was introduced through the sampling arm, taking care not to introduce bubbles. When ready the cells were incubated in a warm water bath until the skin temperature measured 32°C. The magnetic stirrer plate was set at a speed of 800 rpm. After 1 hour, each cell was checked for leakage and the presence of air bubbles.

250 µl of the donor solution was applied to each donor compartment. Receptor fluid samples were taken at regular time intervals and analyzed by HPLC-UV (Table 3-2) or by liquid scintillation counting. Flux and lag time were calculated using the linear portion of the graph when plotting the cumulative amount of drug permeated in function of time. K_p was determined according to Equation 3. Statistical analysis were performed using SPSS software version 19.0.

3.1.7.6 DRUG QUANTIFICATION

HPLC-UV. All compounds, except for paromomycin sulphate, were analysed in duplicate using a 1260 Infinity Agilent HPLC system. The column and settings used to separate and detect the compounds are summarised below (Table 3-2). The validations of the HPLC-UV methods are described in the Appendix 1.

Liquid scintillation counting. Because paromomycin sulfate lacks ultraviolet absorbing chromophore functions HPLC-UV could not be used to analyse the permeation samples. Therefore the donor solution was spiked with radiolabeled paromomycin sulfate and permeation samples were analysed using liquid scintillation counting. Thus 100 µl of receptor fluid and 100 µl of Optiphase™ supermix cocktail were added to a 96 well flexible PET microplate (Perkin Elmer, Buckinghamshire, UK). The plates were incubated on a plate shaker for 1 hour at room temperature. After this they were fitted in an appropriate support cassette and placed in the MicroBeta® Trilux with two detectors for scintillation counting (1 minute/well).

Each plate included 3 blanks containing water that had been in contact with mouse skin (100 µl of water), 3 negative controls (100 µl of paromomycin sulfate saturated solution without radiolabeled compound) and 12 standards prepared by serially diluting one in five. Additionally 3 samples of the donor solution were analysed to confirm homogeneous distribution of the radiolabeled compound in the solution. The cpm readings obtained for the samples were converted to mg of paromomycin sulfate/ml using the standard curve.

TABLE 3-2. HPLC-UV METHOD SPECIFICATIONS (FOR METHOD VALIDATION SEE APPENDIX 1).

Compound ID	HPLC column	Injection volume (µl)	Flow rate (ml/min) / condition	Mobile phase A	B	Detector wavelength (nm)	Retention time (min)
Caffeine	Phenomenex; Synergi–Hydro RP (250x4.6 mm; 5 µm)	20	1.3 / Isocratic	0.1% TFA in water (15%)	ACN (85%)	273	5.8
Ibuprofen	Phenomenex; Synergi–Hydro RP (250x4.6 mm; 5 µm)	20	1 / Isocratic	0.1% TFA in water (30%)	ACN (70%)	227	5.6
Amphotericin B	Phenomenex; Synergi–Hydro RP (250x4.6 mm; 5 µm)	80	1/ Isocratic	2.5mM EDTA in water (68%)	ACN (37%)	407	8.2
Buparvaquone	Luna C18 (4.6x250 mm; 5 µm) with Luna guard column	20	1.7 / Isocratic	5% Water+ acetic acid (pH3.5) (5%)	MeOH (95%)	250	5.4

3.2 RESULTS AND DISCUSSION

3.2.1 EVALUATION OF HISTOLOGICAL SECTIONS OF INFECTED AND UNINFECTED MOUSE SKIN

A histological examination of the epidermal and dermal layers was performed to identify skin structure changes upon infection with *Leishmania* parasites. Figure 3-4 shows an H&E stain of BALB/c mouse skin approximately 11 days after injection with either plain medium (A) or medium containing *Leishmania major* promastigotes (C). The magnification shown in Figure 3-4 (E) confirms infection characterised by the presence of amastigotes in the lower layers of the skin; the arrow points towards one amastigote out of many situated in the phagolysosome of the macrophage (circle).
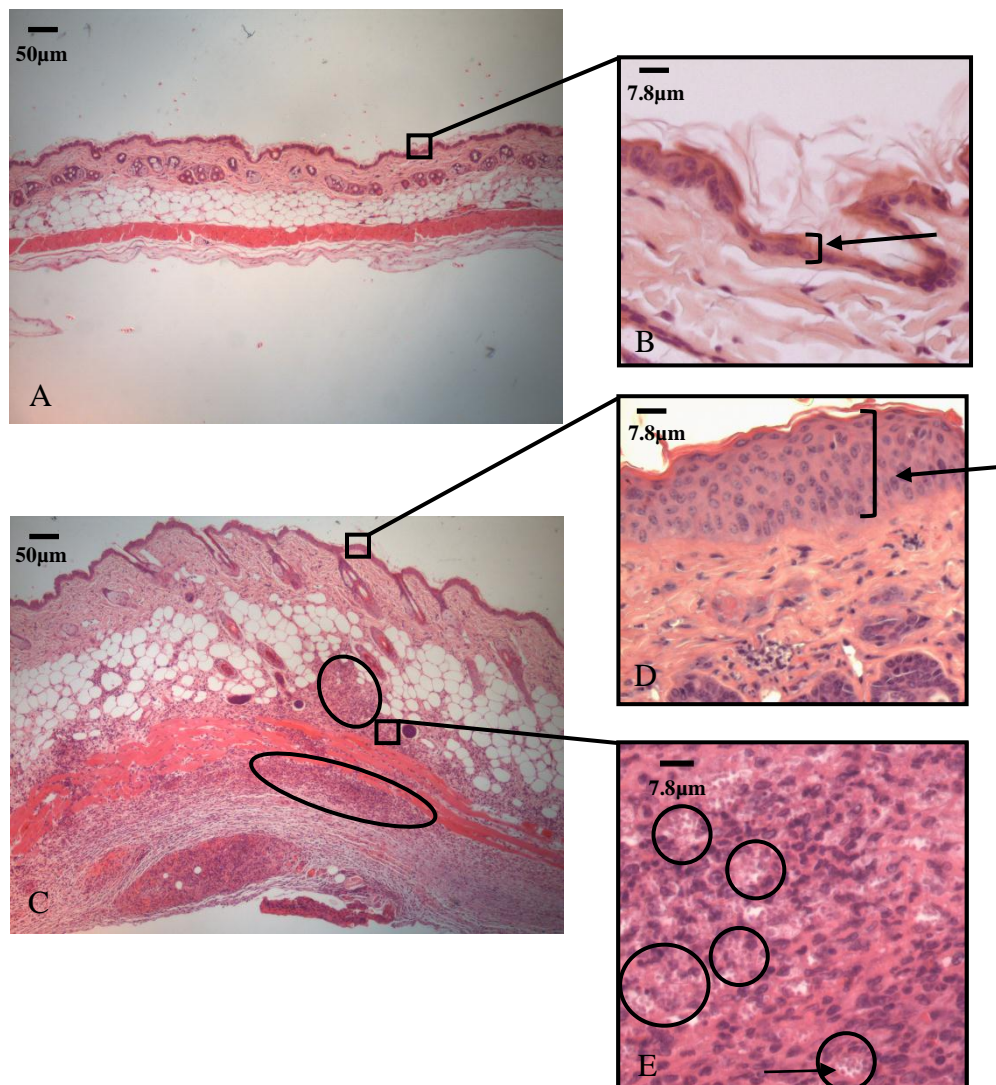
FIGURE 3-4. RUMP SKIN HISTOLOGY. HISTOLOGICAL SECTIONS OF UNINFECTED (N=3) AND *LEISHMANIA* INFECTED (N=5) BALB/C MOUSE SKIN (H&E STAIN). (A AND B) UNINFECTED SKIN AT DAY 11 AFTER INJECTION WITH PLAIN MEDIUM. (C AND D) INFECTED SKIN AT DAY 11 AFTER INFECTION WITH 2x10^7 *L. MAJOR* PROMASTIGOTES. (E) SHOWS THE PRESENCE OF *L. MAJOR* AMASTIGOTES IN THE MACROPHAGES (CIRCLES) SITUATED IN THE LOWER LAYERS OF INFECTED SKIN.

Figure 3-4 (D) and (B) are a magnification of the epidermis of infected and uninfected skin respectively. When comparing the number of cell layers (layers between the half brackets) in the epidermis, the infected skin counts more than the uninfected skin suggesting epidermal hyperplasia.

Infected skin also shows a high infiltration of inflammatory cells in the dermis and underlying tissue and are stained dark blue-purplish by the H&E stain (indicated with ovals in Figure 3-4 (C)). To confirm these findings, an immunostaining with the IBA-1 antibody, a marker for macrophage-like cells was performed. Figure 3-5 (B) shows a high level of macrophages indicated by an abundant brown staining present in the dermis and deeper lying tissues of infected skin compared to uninfected skin (A).
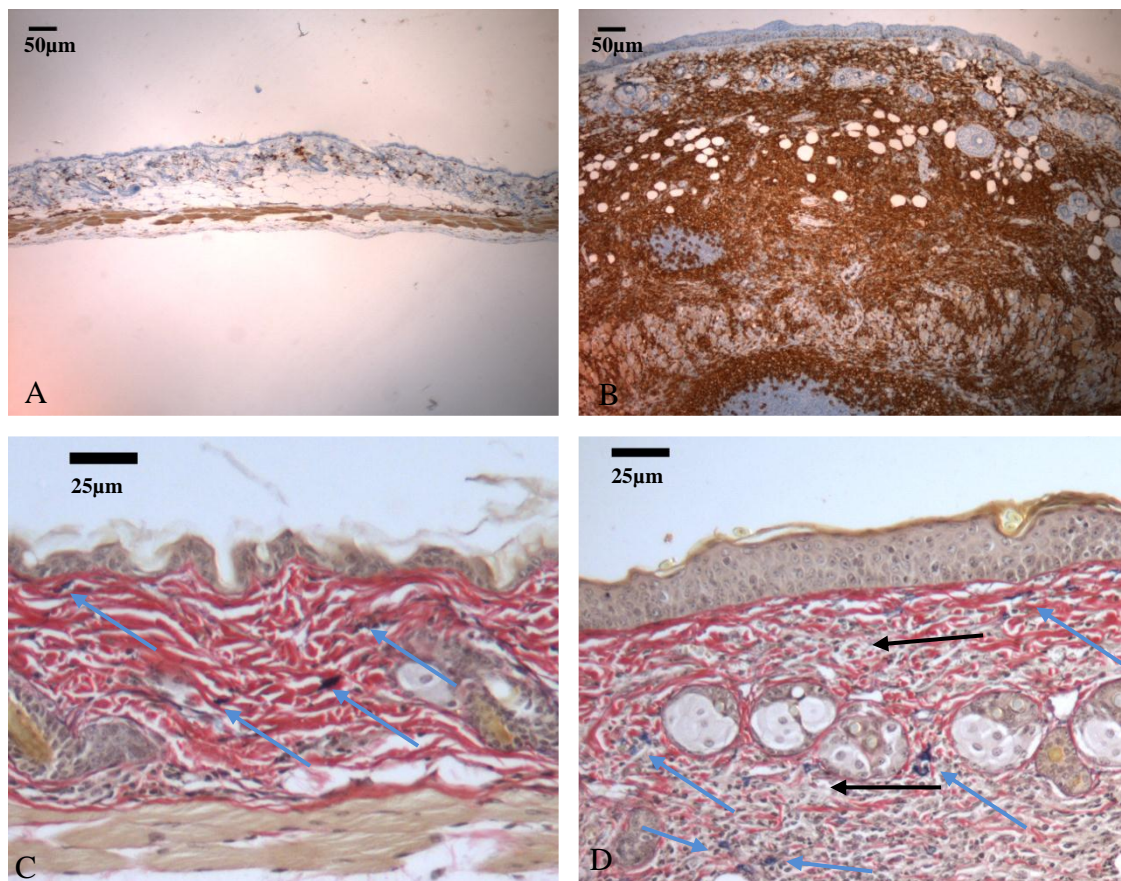
FIGURE 3-5. RUMP SKIN HISTOLOGY. HISTOLOGICAL SECTION OF UNINFECTED (N=3, A AND C) AND *LEISHMANIA* INFECTED (N=5, B AND D) BALB/C MOUSE SKIN AT DAY 11 AFTER INFECTION WITH *L. MAJOR* PROMASTIGOTES. (A AND B) IMMUNOSTAINING WITH IBA-1 ANTIBODIES AND (C AND D) ELASTIC VAN GIESON STAINING.

Elastic and connective tissue in uninfected and infected skin was visualised using an elastic Van Gieson stain (Figure 3-5 (C) and (D) respectively). Collagen and other connective tissue is stained red while elastic fibres are coloured dark blue-black. In uninfected skin, the connected collagen fibres form a dense network with little gaps

characterised by intense red staining as seen in Figure 3-5 (C). On the contrary, infected skin shows a reduced density of collagen fibres as indicated by less intense red staining. The increased space (black arrows, Figure 3-5 (D)) between the fibres is probably due to the infiltration of inflammatory cells.

The elastic fibres are scattered among collagen bundles in the dermis of the uninfected skin (blue arrows, Figure 3-5 (C)). Elastic fibres also seem to be less densely located in infected skin (blue arrows, Figure 3-5 (D)) compared to uninfected skin. However a higher magnification does not allow clear visibility.

3.2.2 COMPARISON OF pH VALUES AND HYDRATION FOR INFECTED AND UNINFECTED SKIN

Figure 3-6 shows the skin hydration and pH as the infection progressed. A one-way repeated measures ANOVA was conducted to compare values of skin pH and hydration between uninfected and infected skin at day 0, 2, 4, 6, 8 and 10 post-infection. There was no significant difference in pH or hydration between the infected and uninfected mice (p>0.05).
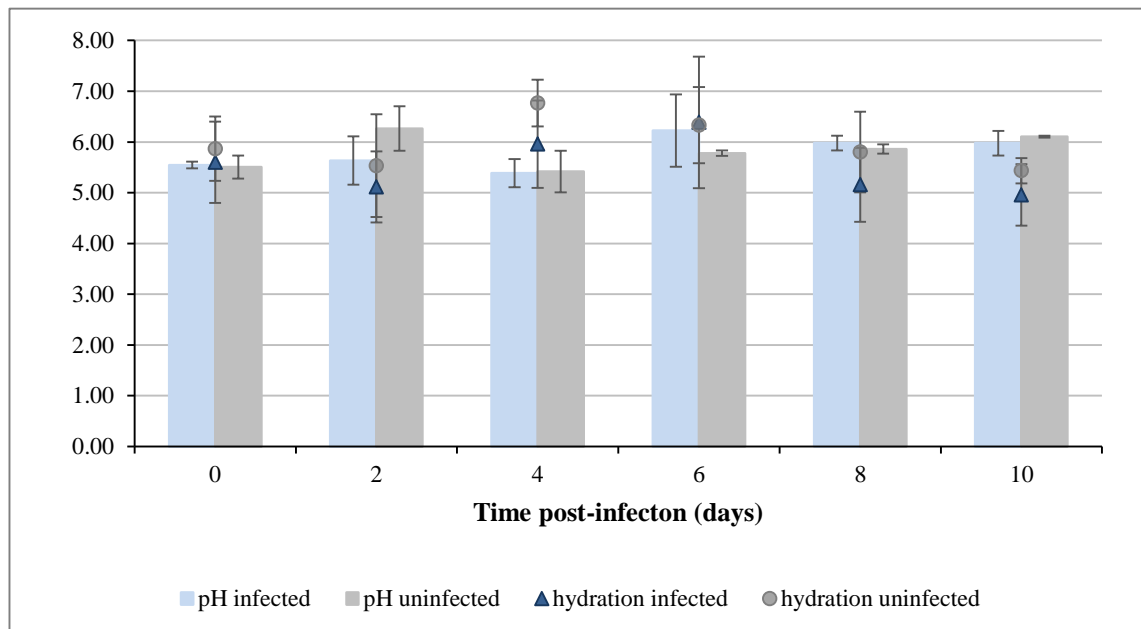
FIGURE 3-6. THE MEAN SKIN pH AND HYDRATION (%) VALUES FOR INFECTED (MEAN±SD; N=5) AND UNINFECTED (MEAN±SD, N=3) MICE AS A FUNCTION OF TIME POST-INFECTION (DAYS) (ONE-WAY ANOVA, P > 0.05).

3.2.3 COMPARISON OF TEWL VALUES FOR INFECTED AND UNINFECTED SKIN

There was no statistical difference in TEWL values for infected and uninfected mice of on day 0 (independent sample t-test; p>0.05) (Figure 3-7).
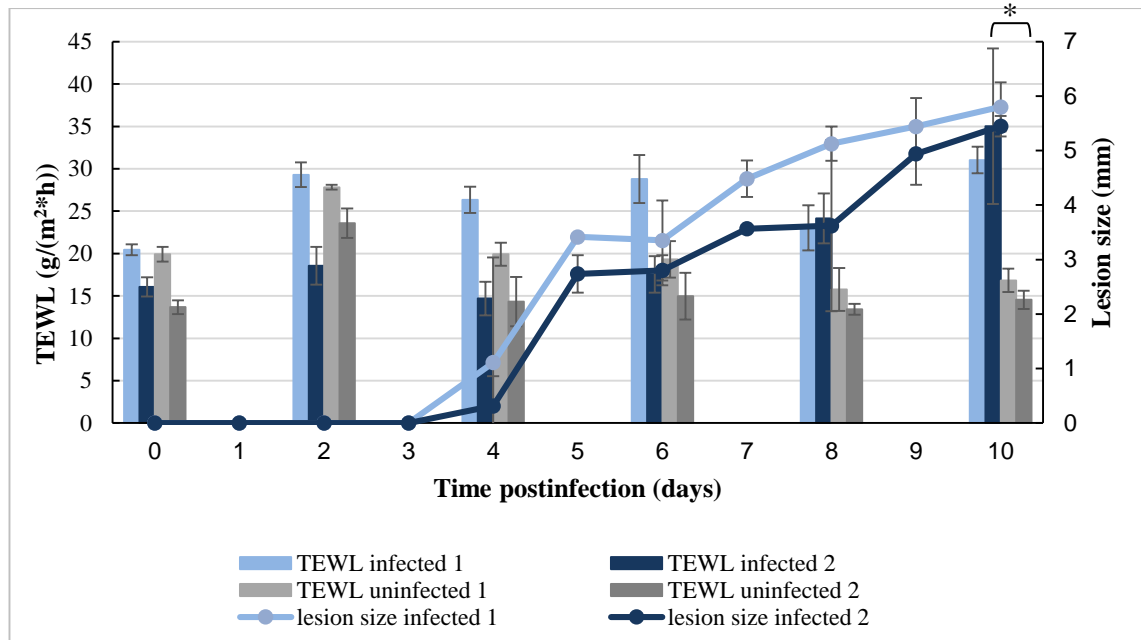
FIGURE 3-7. THE TEWL VALUE (G/(M²H)) AND LESION SIZE (MM) OF *L. MAJOR* INFECTED (MEAN±SD; N=5) AND UNINFECTED (MEAN±SD; N=3) MICE AS A FUNCTION OF TIME POST-INFECTION (REPEATED-MEASURES ANOVA, P < 0.05).

By day 10, when the infected mice had developed a papule with an approximate diameter of 5 mm, the mean TEWL values in the infected group had significantly increased compared to the uninfected group (repeated measures ANOVA, p<0.05) (Figure 3-7). Moreover, an increase of the mean TEWL values for infected mice at day 0 and day 10 was found (paired t-test, p < 0.05).

The relationship between TEWL values and lesion size was investigated using a pearson correlation coefficient. There was no statistically significant correlation between the two variables (r=0.218, p>0.05) while a strong correlation was expected as both lesion size and TEWL increase in time in the infected group. Therefore the relationship between TEWL and time and lesion size and time was investigated. There was no significant correlation between TEWL and time (r=0.186, p>0.05), however there was a strong positive correlation for lesion size and time (r=0.882, p<0.05). Furthermore the correlation between TEWL and hydration was investigated but was weak and not significant (r=-0.124, p>0.05).

3.2.4 EVALUATION OF THE PERMEABILITY OF INFECTED AND UNINFECTED SKIN

3.2.4.1 MODEL COMPOUNDS: CAFFEINE AND IBUPROFEN

Stability. Stability studies performed prior to the permeation studies showed that both compounds, caffeine and ibuprofen were stable in water for 72 hours at 32ºC and in PBS for 4 days at 4ºC allowing sufficient time for analysis.

Solubility. Caffeine has a partition coefficient of -0.08 and a water solubility of approximately 26 mg/ml, while ibuprofen has a partition coefficient of 3.57 and a water solubility of 0.15 mg/ml (Table 3-3).

TABLE 3-3. PHYSICO-CHEMICAL PROPERTIES FOR CAFFEINE AND IBUPROFEN (N=3, MEAN±SD).

	Caffeine	**Ibuprofen**
Solubility (mg/ml) PBS (pH 7.4)	22.74±5.26	0.15±0.01
Log $P_{oct/water}$	-0.08*	3.57*
Mol. weight (g/mol)	194*	206*
H-bond donor	0	1

*Calculated using the software ChemBioDraw Ultra 13.0 (PerkinElmer)

Permeability. The cumulative amount of caffeine and ibuprofen permeated through infected and uninfected mouse skin is shown in Figure 3-8 and Figure 3-9 respectively. It can be seen that more caffeine and ibuprofen permeated through infected than uninfected skin. A paired sample t-test was conducted to evaluate the impact of infection on the permeation of caffeine. There was a statistically significant higher caffeine permeation through infected skin compared to uninfected skin after 48 hours (paired sample t-test, $p<0.05$). The same was observed for ibuprofen (paired sample t-test, $p<0.05$).

At the end of the experiment, the cumulative amount of caffeine that had permeated through infected skin was 1.8 to 47.3 times higher compared to uninfected skin (one-way ANOVA, $p < 0.05$). For ibuprofen this difference was more modest (1.7 to 3.1 higher) but it was still significant (one-way ANOVA, $p < 0.05$).
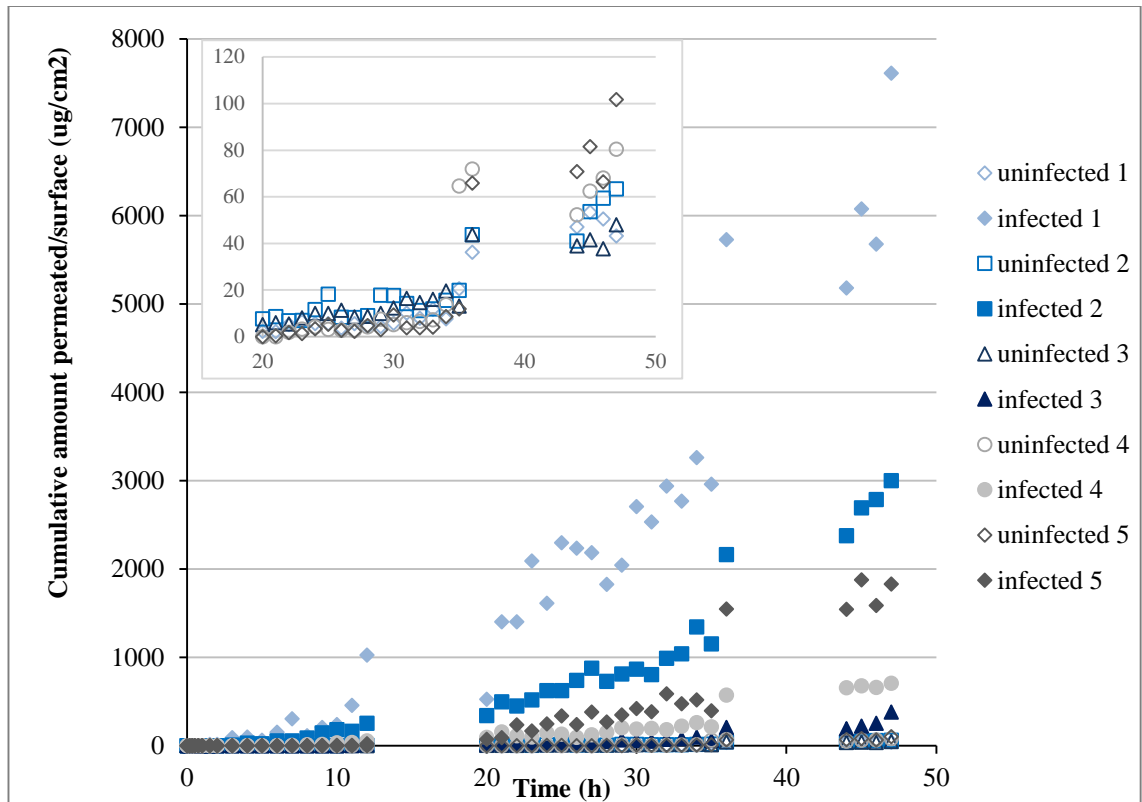
FIGURE 3-8. THE CUMULATIVE AMOUNT OF CAFFEINE PERMEATED PER SURFACE AREA (μG/CM^2) THROUGH UNINFECTED (N=5) AND INFECTED (N=5) SKIN AS A FUNCTION OF TIME (H) (PAIRED T-TEST, P <0.05).
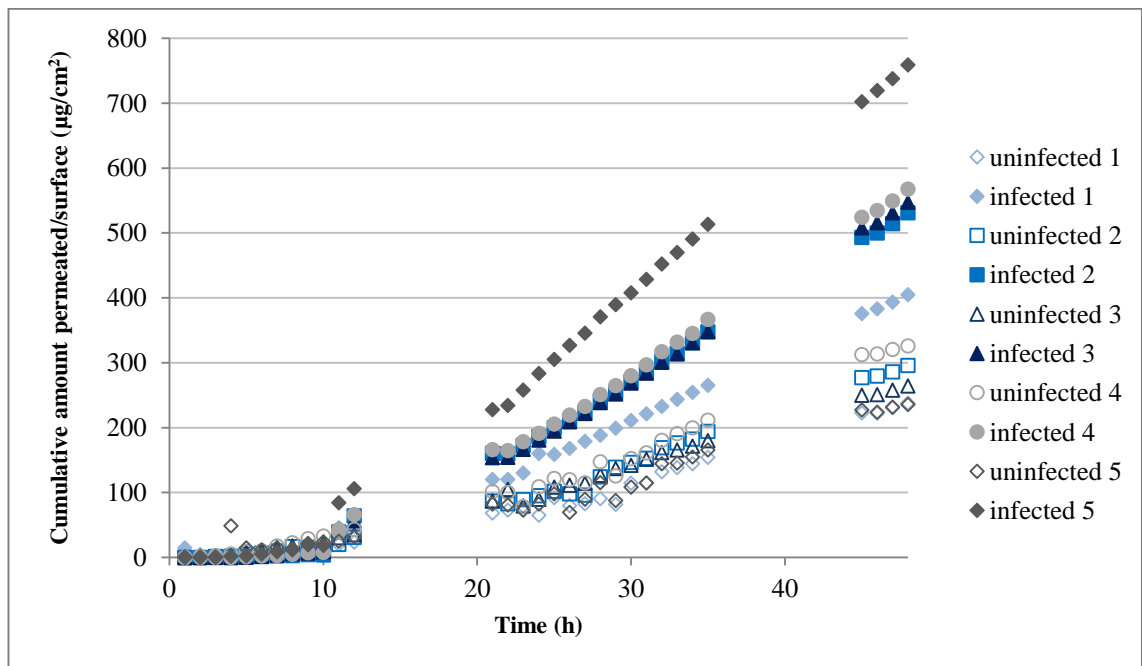
FIGURE 3-9. THE CUMULATIVE AMOUNT OF IBUPROFEN PERMEATED PER SURFACE AREA (μG/CM^2) THROUGH UNINFECTED (N=5) AND INFECTED (N=5) SKIN AS A FUNCTION OF TIME (H) (PAIRED T-TEST, P <0.05).

There was no statistically significant difference in lag time for the model drugs (Table 3-4) for infected skin compared to uninfected skin (independent sample t-test, p >0.05).

The flux of caffeine and ibuprofen through infected skin was respectively about 66 and 2 times higher compared to the uninfected skin (independent sample t-test, p<0.05) (Table 3-4). Both compounds also had a significant higher permeability coefficient for infected compared to uninfected skin (independent sample t-test, p<0.05) (Table 3-4). However, the difference in permeability coefficient for infected compared to uninfected skin was 50 times higher for caffeine while it was only two times higher for ibuprofen. This indicated that both drugs had a higher permeation through infected skin compared to uninfected skin but it also suggested that *Leishmania* infection of the skin enhanced the permeation of hydrophilic drugs to a greater extent than that of lipophilic drugs.

TABLE 3-4. FLUX, LAG TIME AND PERMEABILITY COEFFICIENT FOR CAFFEINE AND IBUPROFEN (MEAN±SD, N=5; INDEPENDENT SAMPLE T- TEST, P<0.05).

	Caffeine	Ibuprofen
Flux (μg/cm^2/h)		
uninfected	0.6±0.1	7.3±1.16
infected	40.1±43.8	15.0±3.7
Lag time (h)		
uninfected	14.9±5.2	11.4±1.1
infected	12.7±3.5	10.7±0.5
K_p (cm/h)		
uninfected	2.3E-05±5.5E-06	0.1±0.0
infected	1.1E-03±8.5E-04	0.1±0.0

3.2.4.2 ANTI-LEISHMANIAL DRUGS: AMPHOTERICIN B, BUPARVAQUONE AND PAROMOMYCIN SULFATE

Stability. Amphotericin B and buparvaquone were stable in PBS at 32ºC for 24 hours and 48 hours respectively. Buparvaquone was stable for 4 days at 4ºC in PBS supplemented with 2% CD whereas amphotericin B was not. Therefore the stability study for amphotericin B in 2% CD was repeated but samples were kept at -20ºC. The amphotericin B samples were stable for 3 days at -20ºC. Paromomycin sulphate was stable for 5 days at 32ºC according to the supplier.

Solubility. The solubility of the test compounds is indicated in Table 3-5. Paromomycin sulphate was highly soluble in PBS. On the contrary, the solubility of buparvaquone and amphotericin B in PBS was low and could not be quantified because it was below the limit of quantification. In an effort to maintain sink condition during the permeation, 2% CD was added to the receptor phase. The solubility of amphotericin B and buparvaquone was 37 and 853 μg/ml in PBS with 2% CD.

TABLE 3-5. PHYSICO-CHEMICAL PROPERTIES FOR PAROMOMYCIN SULPHATE, AMPHOTERICIN B AND
BUPARVAQUONE (N=3, MEAN±SD).

	Paromomycin sulphate	Amphotericin B	buparvaquone
Solubility (µg/ml)			
PBS (pH 7.4)	>650000	< 0.75	<0.1
PBS+2%CD	N/A	37±4	853±25
Log P$_{oct/water}$	-2.9*	-0.66*	3.56*
Mol. weight (g/mol)	714*	924*	326*
H-bond donor	13*	12*	1*

*Calculated using the software ChemBioDraw Ultra 13.0 (PerkinElmer)

Permeation – amphotericin B. Amphotericin B could not be quantified in any of the permeation samples taken (limit of quantification – 750 ng/ml, Appendix 1). Amphotericin B is a large molecule (mol. weight, 924 g/mol) and is practically insoluble in water. Hence it was not expected to permeate through infected or uninfected skin. As discussed in the introduction (section 1.5.4.2), previous studies in mice reported no cure of leishmaniasis lesions after application of amphotericin B topically[176], while it was effective when given intravenously. This led to conclude that amphotericin B as a molecule is unable to permeate through mouse skin. This *in vitro* permeation experiment confirms these findings and suggest that even diseased skin remains impermeable to large molecules.

Permeation – buparvaquone. Buparvaquone did not permeate through uninfected skin (Figure 3-10). Small amounts did permeate through infected skin, however, buparvaquone was only detected in the receptor solution 30 hours after the application of the donor solution. After 48 hours of the permeation study, the mean cumulative amount permeated per surface (n=5) area was 4.5±4.15 µg/cm^2. These results indicate very limited permeation and confirm the limited *in vitro* permeation reported previously[245, 246]. Buparvaquone is a very hydrophobic molecule with a log P of 3.56 and its low water solubility is thought to be an important factor in its limited permeability[245].
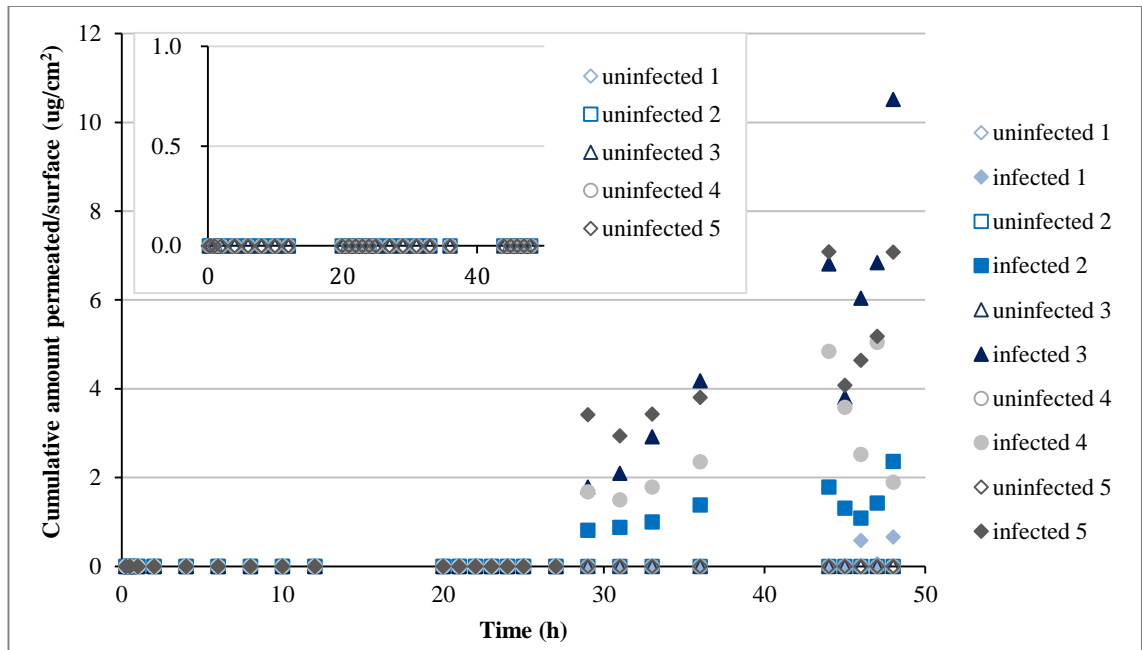
FIGURE 3-10. THE CUMULATIVE AMOUNT OF BUPARVAQUONE PERMEATED PER SURFACE AREA (μG/CM^2) THROUGH UNINFECTED AND INFECTED SKIN OF EACH MOUSE AS A FUNCTION OF TIME (H) (FILLED AND UNFILLED MARKERS REPRESENT VALUES OBTAINED FOR INFECTED AND UNINFECTED MOUSE SKIN RESPECTIVELY, PAIRED T-TEST, P <0.05).

Permeation – paromomycin sulphate. During the entire experiment, paromomycin sulfate did not permeate through uninfected skin. In contrast, it showed a high permeation through infected skin except for one infected skin sample where no permeation was observed (Figure 3-11).
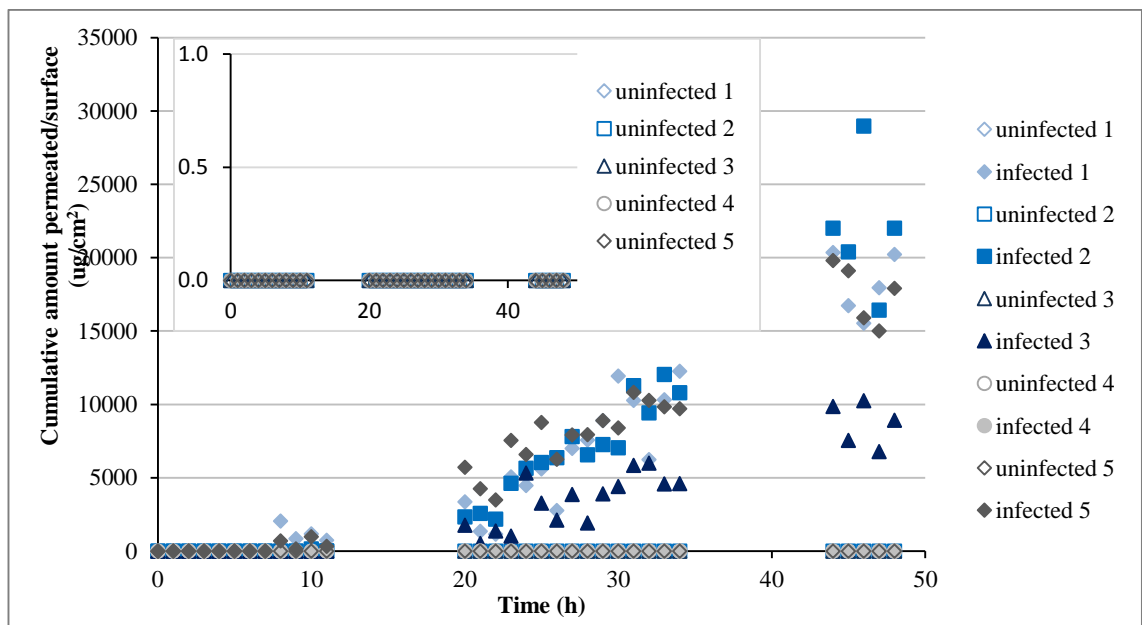
FIGURE 3-11. THE CUMULATIVE AMOUNT OF PAROMOMYCIN SULPHATE PERMEATED PER SURFACE AREA (μG/CM^2) THROUGH UNINFECTED AND INFECTED SKIN OF EACH MOUSE AS A FUNCTION OF TIME (H) (FILLED AND UNFILLED MARKERS REPRESENT VALUES OBTAINED FOR INFECTED AND UNINFECTED MOUSE SKIN RESPECTIVELY, PAIRED T-TEST, P <0.05).

Flux, lag time and approximate K_p value were only determined for the permeation of paromomycin sulphate and buparvaquone through infected skin (Table 3-6) because no anti-leishmanial drug permeated through uninfected skin.

TABLE 3-6. FLUX, PERMEABILITY COEFFICIENT (K_P) AND LAG TIME FOR PAROMOMYCIN SULPHATE, AMPHOTERICIN B AND BUPARVAQUONE (MEAN±SD, N=5 EXCEPT FOR PM WHERE N=4).

	Paromomycin sulphate	Amphotericin B	Buparvaquone
Flux (µg/cm²/h)			
uninfected	-	-	-
infected	548±201	-	0.2±0.1
Lag time (h)			
uninfected	-	-	-
infected	15.4±4.0	-	25.3±3.1
K_p (cm/h)			
uninfected	-	-	-
infected	7.0E-04	-	1.8±1.0

A one-way between-group analysis of variance was conducted to explore the influence of infected skin on the permeation parameters (flux, lag time and K_p) of the different tested drugs. There was a statistically significant difference at the $p<0.05$ level in flux for paromomycin sulphate compared to caffeine and the more lipophilic drugs buparvaquone and ibuprofen but there was no statistical significant difference for caffeine compared to buparvaquone and ibuprofen ($p>0.05$).

The lag time and permeability coefficient (K_p) for buparvaquone permeation through infected skin was significantly higher compared to paromomycin, caffeine and ibuprofen ($p>0.05$ for lag time and K_p). A high permeability coefficient indicates a higher affinity for the membrane than for the vehicle favouring partitioning into the skin. Here it suggests that buparvaquone partitions quickly into the SC but it does not permeate through the skin quickly as is reflected by the low flux. Research already suggested that a highly lipophilic compounds like buparvaquone remain in the stratum corneum and do not tend to permeate into the more hydrophilic dermis[245].

From these findings, it can be hypothesized that the presence of *Leishmania* parasites in the skin triggers a cascade of reactions resulting in inflammation and release of chemokines[98, 270] that subsequently induce oedema because additional fluid accumulates in the interstitial spaces. This hydrophilic environment consequently facilitates permeation of hydrophilic compounds such as caffeine and paromomycin while the permeation of highly lipophilic compounds such as buparvaquone (log P= 3.56) is delayed.

Another possible reason for the enhanced permeation of hydrophilic compounds might be explained using Fick's law. All drugs were applied as saturated solutions and therefore all had the same thermodynamic activity of 1. Furthermore, the permeation rate of the diffusing molecules through a membrane is proportional to the concentration gradient measured over this membrane. In the case of the highly water soluble paromomycin sulfate, this gradient is nearly 25 times higher compared to caffeine and more than 4000 times higher compared to ibuprofen. This is likely to contribute to this increased permeation for more hydrophilic compounds.

Our results are similar to the findings obtained by Tsai et al. who investigated the effect of compound lipophilicity on permeation through acetone damaged mouse skin[93]. Acetone treatment extracts lipids from the skin and was reported to increase TEWL indicating skin barrier damage. The results showed a higher permeation of hydrophilic and amphoteric molecules through damaged skin. The increase in permeation was more modest for lipophilic compounds compared to the hydrophilic compounds. It was hypothesised that the dermis was the rate limiting membrane for permeation of lipophilic compounds and damage to the SC therefore impacted their permeation to a lesser extent than compared to hydrophilic compounds for which the SC is the rate limiting barrier to permeation.

Furthermore it should be mentioned that the variation for permeation experiments described in this chapter was high but this is not uncommon. Intra- and inter-individual variations as high as 45% were reported in *in vivo* studies in humans[271-273]. This was due to differences in skin lipid composition, SC thickness etc. For *in vitro* permeation studies, even larger variations were reported because of the additional modifications introduced by storage and experimental manipulations[274, 275]. Besides the variation between mice, the permeation experiments described in this chapter included an additional factor of variability that is induced by the progression of the infection and was likely to have contributed in the variation observed in these results. An effort was made to try and limit variation by using an inbred strain of mice (BALB/c) and by inducing infection using a standard inoculum of *L. major* parasites.

How these results translate to human skin and particularly to *in vivo* drug permeation is unclear because mouse skin is different from human skin. For example, mouse skin has no sweat glands but has more hair follicles compared to human skin and human skin is thicker than mouse skin (see 6.4)[276] .

3.3 CONCLUSIONS

This chapter describes how we looked at some vital parameters that influence the pharmacokinetics of CL affected skin.

Different stains were used to evaluate skin sections of both infected and uninfected skin and were compared to identify the skin changes in skin physiology upon *Leishmania* infection. It revealed an increase in epidermal cell layers suggesting epidermal hyperplasia. Immunohistochemical staining using IBA-1 antibodies, showed an abundant infiltration of the dermal layer with inflammatory cells and an elastic Van Gieson stain indicated disruption of the connective tissue.

Furthermore, the TEWL, an indicator of barrier integrity was measured and was significantly higher for infected skin compared to uninfected skin indicating the inside-outside barrier was damaged.

Finally the influence of CL drug delivery was evaluated by measuring the permeation of 2 model compounds, caffeine and ibuprofen, and 3 anti-leishmanial drugs, paromomycin sulphate, amphotericin B and buparvaquone through infected and uninfected skin. The permeation of caffeine and ibuprofen was enhanced through infected skin compared to uninfected skin. However, the flux of caffeine was 66 times higher through infected skin while this was only 2-fold higher for ibuprofen. Amphotericin B did not permeate through infected or uninfected skin, which was not surprising due to its high molecular weight. Paromomycin sulphate and buparvaquone did not permeate through uninfected skin but permeated through infected skin and again the permeation increase through infected skin was higher for the hydrophilic paromomycin sulphate. These findings led to the hypothesis that the inflammatory reaction induced by skin damage of the injection and the presence of parasites in the skin, attracted aqueous fluids to the dermis and underlying tissue and hence created a rather hydrophilic environment resulting in more selective permeation enhancement of hydrophilic compounds through infected skin.

3.4 FUTURE WORK

One of the more important future experiments is to extend the drug permeation experiments to drug formulations. In the experiments described in this chapter, the permeation of molecules through infected and uninfected skin was compared. However a drug is rarely applied to the skin as such. It would be interesting to investigate the impact of CL on the permeation of formulations for example fungizone® and Leshcutan®.

Further examination of skin sections using immunostaining could help visualise biomarkers that are known to contribute to skin diseases[255]. This information can be linked to specific biological skin processes that are impaired due to *Leishmania* infection. For instance, the use of Ki-67 antibodies would allow to look for epidermal proliferation.

Above, we also hypothesised about the influence of inflammation on the physicochemical environment of the skin. It would be useful to determine the solubility of compounds in homogenate of infected and uninfected skin and see if there is a difference for the compounds that were tested in this chapter.

Permeation studies with additional compounds with varying partition coefficients would allow to further examine the influence of the physicochemical nature of drugs on permeation enhancement through infected skin.

4 DEVELOPMENT OF A TOPICAL MILTEFOSINE FORMULATION

As described in the general introduction, miltefosine is a known anti-leishmanial drug that is already on the market as an oral formulation. The most frequent reported side effects are:

- gastro-intestinal discomfort that is often the cause of poor therapy compliance[277];
- teratogenicity that calls for adequate contraception throughout the treatment of females of child bearing age;
- hepato- and nephrotoxicity requiring patient monitoring.

Compared to systemic treatment, a topical miltefosine treatment offers certain advantages. The formulation is directly applied to the target site thereby avoiding or at least reducing the potential side effects so that less intense patient follow up is required and it is user friendly increasing patient adherence. Moreover miltefosine is already approved for clinical use and reformulating miltefosine into a topical treatment would save money and time compared to a 'de novo' drug discovery process especially in an area with little financial incentive of big pharma.

The question remains whether miltefosine as a compound can be delivered to the skin. It is a highly water soluble molecule and its physico-chemical properties (molecular weight, solubility, H-bond donors and melting point) are indicative of skin permeation (Table 4-1). Moreover the previous chapter showed that the skin barrier of mice infected with *Leishmania* parasites was damaged and the flux of hydrophilic compounds through skin was increased compared to lipophilic compounds.

In contrast, miltefosine has a similar structure to skin lipids suggesting it might be retained by the SC (Figure 4-1). Also miltefosine is an amphiphilic and zwitterionic molecule at skin pH (pH 5.5) as it contains a permanent positive charge and a negative charge (pKa ≈ 2)[156].
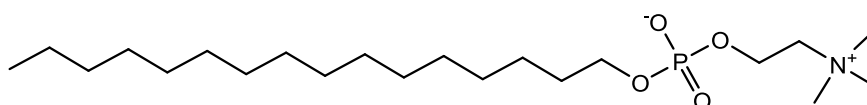
FIGURE 4-1. CHEMICAL STRUCTURE OF MILTEFOSINE

In general, it is accepted that both solubility in the vehicle and the partition coefficient of the molecule influence the permeation process of a molecule into the skin. Often a compromise between both properties is necessary for a molecule to permeate. In the case of ionic compounds with a rather high inherent aqueous solubility, the permeation might be more challenging compared to unionized compounds due to the general lipophilic properties of the stratum corneum. Recent research also suggested that the solubility of the active compound in the vehicle is the main determinant influencing skin permeation in finite dose conditions[278]. The majority of the topical formulations on the market such as creams, gels and sprays are finite dose applications.

TABLE 4-1. PHYSICOCHEMICAL PROPERTIES OF MILTEFOSINE.

Physicochemical properties	Ideal properties	Miltefosine
Molecular weight (g/mol)	< 500[31]	407.6
Aqueous solubility (mg/ml)	-	440
Melting point	$< 200°C$[279]	114°C
H-bond donors/acceptors	< 3 donors[34]	0/4
Partition coefficient	1-3[26, 35]	-2.38*
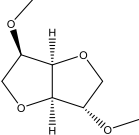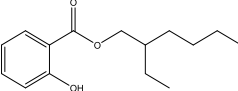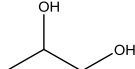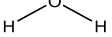
* Clog P octanol –water partition coefficient estimated using ChemBioDraw Ultra software (version 14.0).

A topical solution Miltex®, containing 6% miltefosine (w/v), used to be on the market to treat superficial and flat cutaneous metastases of breast cancer[280] indicating activity upon topical application. Moreover Schmidt-Ott et al tested the efficacy of this solution against *L. major* and *L. mexicana* parasites *in vivo* in mice and after treatment no lesions were visible[241]. This also suggests that miltefosine is able to permeate into the deeper layers of the skin. However, these results were not reproducible when conducted in our lab (Yardley and Croft, unpublished data), even though the activity of miltefosine against a range of *Leishmania* species was confirmed[159].

Two clinical trials were conducted to evaluate the efficacy of Miltex® against CL (Bachmann P., unpublished data). One trial was conducted in Syria and included 16 patients with nodular CL that received treatment twice daily. The other trial was conducted in Colombia where the 19 involved patients received treatment once a day for 4 weeks[281]. Both trials were unable to show efficacy against CL, even though oral administration had been shown to cure CL *in vivo*[161, 282]. This raises the question if miltefosine is able to permeate the skin deep enough to reach parasites and exert its activity.

The aim of the study described in this chapter was to investigate if miltefosine could be used to treat CL upon topical application. In a first stage, the activity of miltefosine against a range of intracellular *Leishmania* amastigotes[159] was evaluated *in vitro*. In a second stage, the permeation of miltefosine when applied on the skin in a range of solvents was investigated. The investigated solvents were propylene glycol (PG), water, dimethyl isosorbide (DMI) and octyl salicylate (OSAL) and are described in the introduction (1.3.2). They were chosen because (i) they had a broad range of physicochemical properties (see Table 4-2) and (ii) they were reported to enhance percutaneous drug delivery through various mechanisms of action (when known).

TABLE 4-2. THE FOUR SOLVENTS USED AND THEIR PHYSICOCHEMICAL PROPERTIES.

	Dimethyl isosorbide	Octyl salicylate	Propylene glycol	Water
Mol. Wt. (g/mol)	174	250	76	18
Log $K_{O/W}$	0.07	5.97	-1.06	-1.38
Solubility parameter $(cal/cm^3)^{1/2}$	9.97	10.87	14.07	22.97
Density at 25°C (g/cm^3)	1.16	1.1	1.04	1.0

In preparation of the permeation experiment, the solubility of miltefosine in these solvents was determined. Fick's law of diffusion describes how the flux of the passive diffusion of molecules through a membrane is directly proportional to the concentration gradient over this membrane. Consequently, the higher the amount of drug dissolved in the vehicle, the higher the flux[283]. However whilst a high solubility in the vehicle potentially increases the flux of the drug through skin, a polarity similar to the SC combined to a low affinity for the vehicle increases the partitioning of the drug into the SC[283]. Hence, the partition coefficient was determined to give an indication of the affinity of miltefosine for the skin. Furthermore computational modelling was used to

estimate the Hoftyzer-Van Krevelen solubility parameter of miltefosine and the solvents. Hadgraft suggested that solvents could enhance skin permeability by shifting the solubility parameter of the skin towards that of the drug[284].

As explained in the introduction, the application of the drug in a binary and even ternary solvent system, this is a mixture of two or three solvents respectively, has shown to enhance percutaneous drug permeation[62-65, 67, 285]. In order to deliver the drug from a stable solvent system, the compatibility of solvents was explored in binary and ternary phase miscibility studies. Finally the effect of the solvents on the permeation of miltefosine through the skin was compared by *in vitro* permeation studies using Franz diffusion cells followed by a mass balance study that allowed the quantification of miltefosine that was inside the skin. A radiolabelled assay was developed to quantify the amount of miltefosine as it lacks chromophores and can therefore not be detected by HPLC-UV.

4.1 MATERIALS AND METHODS

4.1.1 DRUGS AND SOLVENTS

Miltefosine was kindly donated by Paladin Labs Inc. The [^{14}C]-miltefosine was purchased from Nycomed Amersham Pharmacia biotech (Buckinghamshire, UK). Details of the solvents and reagents used, are listed below (Table 4-3).

TABLE 4-3. DETAILS OF SOLVENTS AND REAGENTS USED DURING PERMEATION EXPERIMENTS WITH MILTEFOSINE.

Solvents/ Reagents	Specifications	Supplier
Solvents		
Isosorbide dimethyl ether (DMI)	98% purity	Sigma Aldrich
2-ethylhexyl salicylate (OSAL)	Octyl salicylate, 99% purity	Sigma Aldrich
Propylene glycol (PG)	N/A	Sigma Aldrich
Hydrogen peroxide solution	30% in water	Sigma Aldrich
Phosphate buffered saline	Tablets; NaCl (8g/l), KCl (0.2g/l), Na$_2$HPO$_4$ (1.15g/l), KH$_2$PO$_4$ (0.2g/l), pH 7.3	Oxoid, Thermo Scientific
Methylene blue solution	3.126M	Sigma Aldrich
Radiolabeled assay – reagents/drugs		
Optiphase™ supermix	Liquid scintillation cocktail	Perkin Elmer
Hionic Fluor™	Liquid scintillation cocktail	Perkin Elmer
Solvable™	Aqueous based solubilizer	Perkin Elmer
[^{14}C]-miltefosine	Specific activity: 36mCi/mmol; radiochemical purity: 98.3%; radioactive concentration: 900μCi/ml; solvent: ethanol	Nycomed Amersham
Cell and parasite culture		
RPMI-1640	500ml	Sigma Aldrich
Schneider's insect medium	500ml	Sigma Aldrich
M199 medium	Powder	Sigma Aldrich
Penicillin-streptomycin solution	10000 units penicillin- 10mg streptomycin/ml	Sigma Aldrich
Heat-inactivated foetal calf serum	500ml	Harlan Sera-Lab

4.1.2 FRANZ DIFFUSION CELLS AND EQUIPMENT

Franz cell devices with an approximate diameter of 9 mm and a receptor volume of approximately 2.5 ml were obtained from Soham Scientific (Fordham, UK). The other equipment used for this study is the same as described in 3.1.7.2.

4.1.3 LEISHMANIA PARASITES AND CELL CULTURE

Promastigotes of *L. major* (MHOM/SA/85/JISH118); *L. panamensis* (MHOM/PA/67/BOYNTON); *L. aethiopica* (MHOM/ET/84/KH); *L. mexicana* (MNYC/ BZ/62/M379) and *L. tropica* (MHOM/IR/2013/HTD4) were taken from liquid nitrogen stocks. All species except *L. panamensis* were cultured and maintained in

Schneider's Insect medium plus 10% heat-inactivated fetal calf serum (HiFCS) at 26°C. *L. panamensis* was cultured in M199 medium supplemented with 10% HiFCS. KB and THP-1 cells were maintained in RPMI-1640 medium supplemented with L-glutamine and 10% HiFCS. Both human-derived cell lines were left in an incubator at 37ºC and 5% CO_2 and passaged to new medium once a week (1/10 ratio).

4.1.4 EVALUATION OF THE ANTI-LEISHMANIAL ACTIVITY OF MILTEFOSINE IN THE INTRACELLULAR AMASTIGOTE – MACROPHAGE MODEL

Mouse peritoneal macrophages (PEM) were isolated from CD-1 mice (Charles River, Margate, UK) by abdominal lavage with RPMI-1640 medium containing 1% penicillin and streptomycin. The collected cells were washed, re-suspended and seeded in 16-well Lab-Tek™ slide in RPMI-1640 supplemented with 10% HiFCS at a density of $4x10^4$ per well. After 24 hours incubation at 37°C and 5% CO_2/95% air mixture, the adhered PEMs were infected with stationary phase promastigotes at a ratio of 3 (for *L. tropica* and *L. major*) or 5 (for *L. mexicana*, *L. aethiopica* and *L. panamensis*) promastigotes to 1 macrophage and maintained at 34°C in a 5% CO_2/95% air mixture. These ratios were chosen in order to ensure that at least 75% of the macrophages were infected after 72 hours of incubation in the untreated controls.

After 24 hours, the cultures were washed to remove extracellular promastigotes and one slide was fixed with methanol and stained with Giemsa to determine the initial level of infection. If a sufficient level of infection (i.e. > 75%) was obtained, PBS - miltefosine solutions over a range of 30, 10, 3 and 1 µM were added in quadruplicate at each concentration. Amphotericin B (Fungizone®) was included as control drug. After 72 hours incubation, all slides were methanol-fixed and Giemsa-stained.

The percentage inhibition was determined by microscopically (400x magnification) counting the infected macrophages in drug treated cultures compared to untreated cultures microscopically. The Hill coefficient, ED_{50} and ED_{90} values were calculated by non-linear sigmoidal curve fitting (variable slope) using Prism Software (GraphPad, Surrey, UK).

4.1.5 CYTOTOXICITY TESTING AGAINST KB AND THP-1 CELLS

KB/ THP-1 cells were harvested, washed and counted in serum free medium. The cell density was adjusted to 5×10^4/ml in RPMI-1640 supplemented with 10% HiFCS. 100 µl of the cell suspension was plated in each well of a 96-well plate followed by incubation at 37°C and 5% CO_2 for 24 hours.

Stock drug solutions of 20 µM in PBS were prepared and diluted to 600 nM in RPMI-1640 with 10% HiFCS. 300 nM was the top concentration tested and five-fold serial dilutions were performed across the plate. Podophyllotoxin was included as positive control drugs. Untreated controls and blanks, containing only medium were also included. Each test compound was tested in triplicate. Plates were incubated for a further 72 hours at 37°C and 5% CO_2.

After incubation, the wells were assessed microscopically and 20 µl Alamar Blue® was added to each well. The plates were incubated for a further 2-4 hours before reading at EX/EM 560/585 (cut off 570) in a Spectramax™ M3 Plate reader. The ED_{50} value was calculated by non-linear sigmoidal curve fitting (variable slope) using Prism Software (GraphPad, Surrey, UK).

4.1.6 EVALUATION OF THE PHYSICOCHEMICAL PROPERTIES OF MILTEFOSINE THAT RELATE TO THE PERMEATION PROFILE

4.1.6.1 DISTRIBUTION COEFFICIENT

The slow stirring method was adopted to determine the distribution coefficient for miltefosine. Prior to the experiment 1-octanol and water (buffered to pH 5 with acetic acid) were left to equilibrate for 48 hours at 32°C. Eight ml of the water was used to dissolve 100 µg of miltefosine and was placed in a clean vial. Two ml of 1-octanol was added and the mixture was left to equilibrate at 32°C for 24 hours. 100 µl aliquots from both phases were taken and diluted prior to analysis by LC-MS (conducted by the chemistry department at UCL School of Pharmacy). The experiment was conducted in triplicate.

The distribution coefficient was calculated according to the formula below:

$$\log D_{\frac{octanol}{water}} = log \left[\frac{[miltefosine]_{octanol}}{([miltefosine]_{water-ionised} + [miltefosine]_{water-neutral})} \right]$$

<div align="right">EQUATION 5</div>

4.1.6.2 SOLUBILITY PARAMETER MODELLING AND MEASUREMENTS OF DRUG SOLUBILITY

The solubility parameter (δ) of miltefosine and the solvents/CPEs were calculated according to the Van Krevelen-Hoftyzer method using the Molecular Modelling Pro software (version 6.0, Chemistry Software Ltd., Surrey, UK).

The solubility of miltefosine in PG, DMI, OSAL and water was determined using two different methods

Method 1. The solubility of miltefosine in the different solvents was determined by adding an excess amount of drug to the appropriate solvent in a clean vial. A magnetic stirrer was added before carefully sealing the vial and the suspension was left to stir for 48 hours at 32°C[269]. An aliquot of this mixture containing some solid drug particles was centrifuged at 13000rpm at 32°C. The supernatant was taken and analysed by LC-MS.

Method 2. The solubility was determined by adding weighed amounts of drugs to a vial containing the appropriate solvent (1.5 ml) and a magnetic stirrer. Every 2-3 hours the status of the mixture was observed and when a visibly clear solution was obtained an additional amount of drug was added. Afterwards the vial was carefully sealed and returned to the warm water bath (32°C). The approximate solubility of the drug after 48 hours was calculated by making the sum of the drug added to the solvent until visible drug particles remained present and no longer solubilized.

4.1.7 EVALUATION OF SOLVENT MISCIBILITIES

Binary and ternary mixtures of the four solvents: PG, DMI, OSAL and water were prepared and their miscibilities were determined by adding the appropriate volume and ratio of solvents (v/v) into a clean vial (see Appendix 4). The vial was vigorously mixed for 2 minutes and left at room temperature. After one hour, the samples were observed and marked as immiscible (when phase separation was visible) or miscible (when a homogeneous phase mixture was seen). If necessary, Sudan dye red or methylene blue

was added to the mixture to non-polar and polar solvents respectively to aid the determination of miscibility/immiscibility. Ternary phase diagrams were drawn using the OriginPro software (version 9.1; Northampton, USA).

The stability of the miscible binary and ternary solvent mixtures that were selected for the permeation study was tested over a period of 48 hours at 32ºC to ensure no phase separation would occur during the permeation experiment.

4.1.8 THE EFFECT OF SOLVENTS AND SOLVENT SYSTEMS ON THE PERMEATION AND DISPOSITION OF MILTEFOSINE IN BALB/C MOUSE SKIN

An initial permeation study using single solvents was conducted in order to compare the effect of the different solvents on the permeation of miltefosine through full-thickness mouse skin. The most efficient permeation enhancing solvents were then used as such or combined in binary and ternary mixtures as a drug carrier. Skin disposition studies were performed to quantify the amount of miltefosine that permeated into skin.

4.1.8.1 PREPARATION OF DONOR SOLUTIONS

Binary and tertiary system combinations within the miscible area were chosen to assure the donor solution did not show phase separation. The solutions/ suspensions were prepared by adding the solvent(s) to miltefosine so that a concentration of 6% (w/v) (same as Miltex®) was obtained. The mixture was sonicated for 30 minutes after which it was left to stir overnight at 32°C. Before application, the solutions were spiked with [^{14}C]-miltefosine to a final concentration of 4 µCi/ml and vortexed for 2 minutes. A volume of 0.5 ml of donor solution was applied to each cell.

4.1.8.2 RAPID EVALUATION OF SKIN DAMAGE POST-PERMEATION

For each tested formulation, two extra Franz diffusion cells were prepared and included to test for skin damage after the permeation experiment. After the 48 hours permeation, the formulation was removed and 500 µl of a methylene blue-water (1:9) solution was applied in the donor compartment. After one hour, the colour of the receptor fluid was verified and compared to evaluate skin damage.

4.1.8.3 QUANTIFICATION OF AMOUNT OF MILTEFOSINE PERMEATED THROUGH FULL THICKNESS MOUSE SKIN

The experiment was set up as described in section 3.1.7.5. The permeation study was conducted over a duration of 48 hours. At regular time intervals, 200 µl of receptor phase was removed and replaced with fresh PBS at 32°C. For the quantification of miltefosine, 100 µl of the sample was transferred in a 96-well flexible Microbeta plate and 100 µl of Optiphase™ supermix was added. A standard curve was prepared by double-diluting the donor solution in PBS for PG and water and methanol for DMI and OSAL, as the latter two solvents are not miscible with water. A blank consisting of 100 µl PBS or methanol and 100 µl of Optiphase™ supermix was added to each plate. The plates were left to incubate on a shaking plate at room temperature for 1 hour. Scintillation counting was conducted using a Microbeta2 plate reader equipped with 2 detectors (Perkin Elmer).

The cumulative amount permeated per surface area was plotted as a function of time. The slope and thus mean flux was calculated by linear regression of the data points obtained between 20 and 36 hours following application. Statistical analysis were performed using SPSS software version 19.0.

4.1.8.4 QUANTIFICATION OF THE AMOUNT OF MILTEFOSINE LEFT ON THE SKIN.

After 48 hours, the remaining donor solution was transferred into a clean vial. The remaining fractions on the skin and the donor compartment were removed by carefully swiping the surface with a cotton swab, followed by repeatedly pipetting up and down with a 1 ml methanol – water solution (3:7(v/v)). This was repeated 3 times. To extract the miltefosine absorbed in the cotton, 1ml of a methanol – water solution (3:7(v/v)) was added to the recipient that contained the swab. The mixture was left on a shaking plate for 5 hours, after which 100 µl was transferred to a flexible Microbeta 24-well plate. To quantify the amount of miltefosine, 400 µl of Hionic-fluor™ scintillation fluid was added and left to acclimatise before reading with a Microbeta2 plate reader. For each donor solution, a standard curve of 12 serial 1:2 dilutions was included and each plate also contained 3 methanol – water blanks. The amount of miltefosine in each

sample was calculated by linear regression analysis using the miltefosine standard curve. Statistical analysis were performed using SPSS software version 19.0.

4.1.8.5 EXTRACTION AND QUANTIFICATION OF THE AMOUNT OF MILTEFOSINE IN THE SKIN

After dismantling the Franz cell, the skin was transferred to a clean vial and together with 1 ml of Solvable™, it was incubated at 50°C and vortexed regularly until a homogenous mixture was obtained. A sample of this homogenate was mixed with Hionic-fluor™ in a 1:4 ratio followed by analysis using the Microbeta2 plate reader (Perkin Elmer). An untreated piece of skin was spiked with a known amount of miltefosine to assure no drug breakdown occurred during the extraction procedure and was included in triplicate. Also an untreated piece of skin was included in triplicate to correct for absorption due to skin components. The amount of miltefosine in each sample was calculated by linear regression analysis using the miltefosine standard curve. Statistical analysis were performed using SPSS software version 19.0.

4.2 RESULTS

4.2.1 EVALUATION OF ANTI-LEISHMANIAL ACTIVITY OF MILTEFOSINE

The ED_{50} and ED_{90}s of miltefosine against a panel of *Leishmania* parasites are shown in Table 4-4 and ranged from 7.8 to 45.9 µM and 19.5 to 166.3 µM respectively. The rank order for the ED_{50}s was *L. aethiopica < L. tropica < L. panamensis < L. major < L. mexicana*. These results were similar to previously obtained sensitivities in our lab[159, 246] except for the ED_{50} values for *L. mexicana*. Escobar et al found an ED_{50} of 6.8 and 10.1 µM compared to 31.0 and 45.9 µM in this study[159]. When excluding the results for *L. mexicana,* the rank order was the same in both studies. The difference in ED_{50}s obtained for *L. mexicana* was probably due to the different strains that were used. Escobar et al used *L. mexicana* MHOM/BZ/82/BEL21, while *L. mexicana* MNYC/ BZ/62/M379 was used in this study. The variation in intrinsic susceptibility between and within species is not surprising given the molecular and biochemical differences between strains and species. Additionally, different test settings might also contribute to differences in ED_{50}s obtained[286].

Amphotericin B was highly active against all species. *L. mexicana* was less susceptible to amphotericin B compared to the other species and again confirmed previously obtained results[159].

TABLE 4-4. *IN VITRO* ANTI-LEISHMANIAL ACTIVITY AS DETERMINED BY MICROCOPIC COUNTING OF *LEISHMANIA* INFECTED MACROPHAGES TREATED WITH MILTEFOSINE (30, 10, 3.3 AND 1.1 UM; N= NUMBER OF EXPERIMENTS). CYTOTOXICITY AS DETERMINED USING THE FLUORESCENT ALAMAR BLUE.

Compound	n	Amphotericin B		Miltefosine	
		ED_{50} (µM) (95% CI)	ED_{90} (µM)	ED_{50} (µM) (95% CI)	ED_{90} (µM)
L. tropica	1	0.07 (0.06-0.07)	0.29	20.0 (17.4-23.0)	25.1
	2	0.08 (0.08-0.09)	0.30	9.4 (7.78-11.5)	-
L. major	1	0.12 (0.11-0.14)	0.22	44.9 (26.02-77.3)	163.1
	2	0.05 (0.04-0.06)	-	26.6 (21.30-33.2)	29.4
L. aethiopica	1	0.12 (0.11-0.12)	0.25	7.8 (6.2-9.8)	19.5
	2	0.11(0.10-0.12)	0.24	8.0 (7.26-8.7)	22.0
L. mexicana	1	0.43 (0.39-0.46)	1.10	31.0 (28.56-33.7)	38.0
	2	0.69 (0.55-0.69)	1.21	45.9 (36.61-57.5)	102.8
L. panamensis	1	0.14 (0.13-0.16)	0.29	20.0 (16.17-24.7)	151.3
	2	0.12 (0.09-0.14)	0.15	23.1 (20.41-26.2)	166.3
KB-cells				**0.7 (0.5-1.0)**	
THP-1 cells				**12.9 (7.6-22.0)**	

The ED_{50} value of miltefosine against THP-1 and KB cells was 12.9 and 0.7 μM respectively and indicated that miltefosine was more toxic to KB cells compared to THP-1 cells. This was expected because KB cells were already reported to be very sensitive to miltefosine ($ED_{50} = 1.6$ μM)[287, 288]. The cytotoxicity values are in the same range compared to the anti-leishmanial activity (ED_{50} and ED_{90}) which indicated that the concentrations required to kill parasites also damage macrophages. In fact when using 40 μM as top concentration for miltefosine in the intracellular amastigote-macrophage assay, clear macrophage damage was observed when evaluating microscopically. Ideally, the therapeutic index for a drug is high meaning that there is a big difference between the concentration that induces toxicity and the concentration required for efficacy. This is not the case for miltefosine.

4.2.2 SOLUBILITY OF MILTEFOSINE IN DIFFERENT SOLVENTS

The saturated solubility concentration of miltefosine in different solvents are shown in Table 4-5. In general, both methods gave similar results except for the solvent propylene glycol. The PG solution saturated with miltefosine was very viscous compared to the other miltefosine saturated solvents and it is hypothesized that pipetting errors caused deviations when preparing the sample for analysis. The use of a positive displacement pipette would allow to correct for this mistake.

Miltefosine was highly soluble in water and PG, while its solubility in OSAL and DMI was approximately 4 and 5 orders of magnitude lower respectively. Miltefosine is an ionic compound as it is permanently charged and was therefore expected to be more soluble in hydrophilic solvents such as water and PG and less soluble in lipophilic solvents such as OSAL.

TABLE 4-5. SOLUBILITY OF MILTEFOSINE IN PG, H₂O, DMI AND OSAL (MEAN, N=3) AS DETERMINED USING LC-MS (METHOD 1) OR BY WEIGHT (METHOD 2). THE SOLUBILITY PARAMETERS WERE GENERATED USING MOLECULAR MODELLING PRO.

	Saturated solubility (mg/ml) method 1	Saturated solubility (mg/ml) method 2	Solubility parameter $(cal/cm^3)^{1/2}$
Miltefosine	-	-	8.88
PG	738	1249 - 1342	14.07
H₂O	440	394 - 494	22.97
DMI	0.005	< 1	9.97
OSAL	0.036	<1	10.87

The solubility parameter of miltefosine was estimated at 8.88 $(cal/cm^3)^{1/2}$. DMI and OSAL have a solubility parameter close to miltefosine, whereas the solubility parameter of PG and water are higher (Table 4-5). The solubilities of miltefosine in the respective solvents are expected to be greater when the solubility parameters are close together[289]. According to this theory, miltefosine should be more soluble in DMI than in water, but the contrary was observed. Previous studies have reported similar outcomes and the limitations of this theory in formulation design are discussed in the literature[53, 290]. Another explanation might be the fact that miltefosine is an zwitterionic molecule that acts as a surfactant and forms micelles (CMC_{milt} in H_2O: 1.1-1.2 µg/ml[291]). Ionized molecules have a reduced solubility in solvents with low dielectric constant (DMI) and high solubility in a solvent with high dielectric constant such as water[292].

4.2.3 DISTRIBUTION COEFFICIENT OF MILTEFOSINE

The experimental determined distribution coefficient (log D) of miltefosine in water buffered at pH 5 was found to be 3.74 (±0.17). In contrast, ChemBioDraw software (Perkin Elmer, Coventry, UK) estimates the distribution coefficient at -2.38 indicating it is a highly hydrophilic molecule.

Miltefosine is an amphiphilic molecule composed of a long lipophilic C16 alkane chain and a polar phosphocholine group (Figure 4-1). It has surface activity properties and will migrate to the interface of non-miscible solvents (octanol and water) to reduce the surface tension. Moreover miltefosine spontaneously forms micelles as a result of unfavourable interaction between the hydrophobic regions and aqueous solvents. This heterogeneous distribution is likely to have interfered with the determination of an accurate concentration of the molecule in the two phases when applying the slow stirring method to determine the log D. An alternative experimental method to determine the distribution coefficient is the HPLC method as described in the OECD guidelines[293].

The partition coefficients of the solvents used in this study are shown in Table 4-6. When ranked according to increasing lipophilicity, the order is as follows: H_2O < PG < DMI < OSAL.

TABLE 4-6. ESTIMATED VALUES FOR THE PARTITION COEFFICIENTS OF THE SOLVENTS.

Solvent	Log $K_{o/w}$
PG	-1.06
H_2O	-1.38
DMI	0.07
OSAL	5.97

4.2.4 SOLVENT MISCIBILITIES

Miscibilities of two solvents are shown in Table 4-7. OSAL is only miscible (✓) with DMI but is immiscible (✗) in water and PG. DMI, PG and H2O are miscible.

TABLE 4-7. MISCIBILITY OF BINARY SOLVENT MIXTURES.

	OSAL	DMI	H_2O	PG
OSAL		✓	✗	✗
DMI	✓		✓	✓
Water	✗	✓		✓
PG	✗	✓	✓	

The miscibilities of the ternary mixtures are shown in Figure 4-2. The effects of two ternary phase solvent systems on the delivery of miltefosine were tested. The compositions (indicated with a pink dot in Figure 4-2) were as follows: OSAL–DMI–PG (2:5:3) and H_2O–DMI–PG (3:4:3). The ratio of the three solvents where chosen so that they were away from the miscible/immiscible border. This is also the reason why no OSAL–DMI–H2O combination was tested.
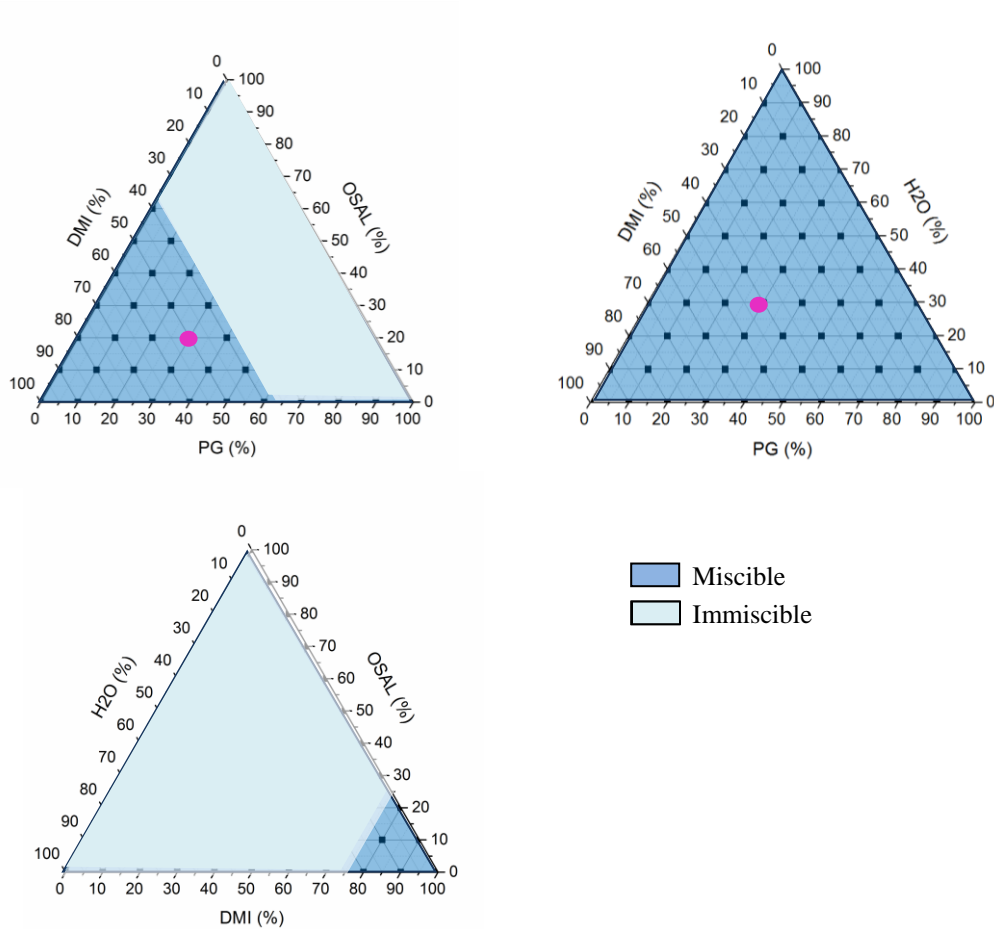
FIGURE 4-2. MISCIBILITIES OF TERNARY SOLVENT MIXTURES.

4.2.5 COMPARISON OF THE EFFECT OF THE SOLVENTS ON THE PERMEATION OF MILTEFOSINE UPON INFINITE DOSE APPLICATION

Ten formulations all containing 6% miltefosine were tested. Four of these formulations were applied as suspensions (Table 4-8) because 6% miltefosine exceeded the saturation limit. Hence the thermodynamic activity is not the same for all the formulations (Table 4-8)[294-296].

TABLE 4-8. THE COMPOSITION AND SATURATION LEVEL OF THE TEST FORMULATIONS.

Formulations tested	Miltefosine concentration (w/v)	Saturated? Yes/no (% saturation if known)	Thermodynamic activity
Single solvent			
H$_2$O	6%	14%	<1
PG	6%	5%	<1
DMI	6%	Yes	1
OSAL	6%	Yes	1
Binary solvent system			
PG-DMI (1:1)	6%	No	<1
H$_2$O-DMI (1:1)	6%	No	<1
H$_2$O-PG (1:1)	6%	No	<1
OSAL-DMI (1:1)	6%	Yes	1
Ternary solvent system			
OSAL-DMI-PG (2:5:3)	6%	Yes	1
H$_2$O-DMI-PG (3:4:3)	6%	No	<1

4.2.5.1 PERMEATION

Only 4 out of 10 tested formulations resulted in miltefosine permeation through BALB/c mouse skin. Three formulations were single solvent mixtures and 1 formulation was a binary solvent mixture. The cumulative amount of miltefosine that permeated per surface area as function of time is shown in Figure 4-3.
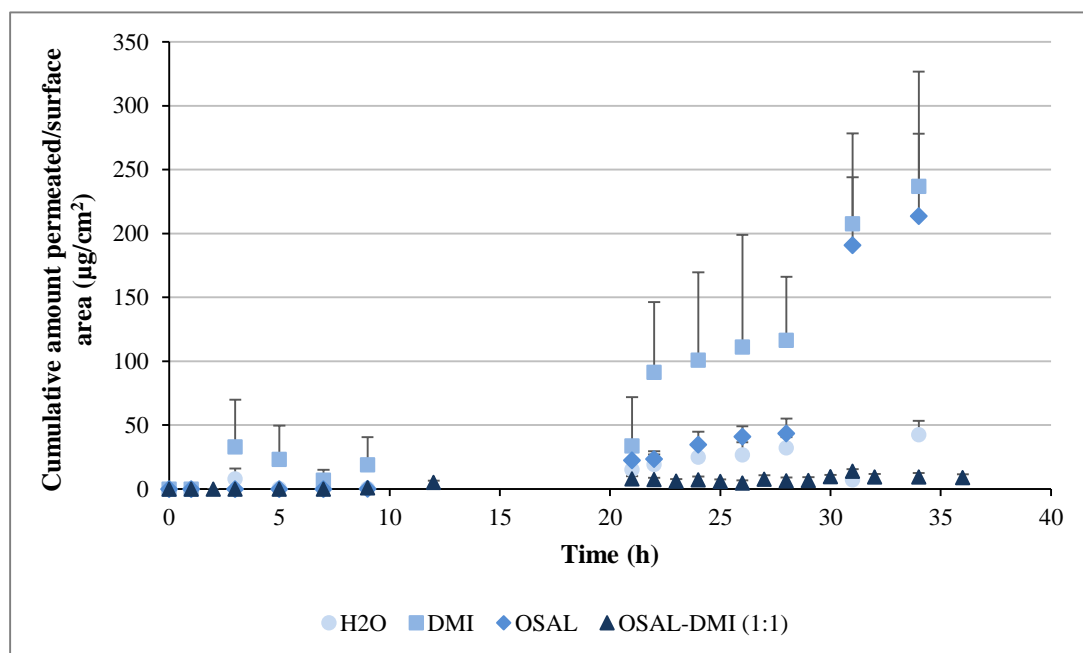
FIGURE 4-3. FOR THE 4 OUT OF 10 FORMULATIONS THAT RESULTED IN MILTEFOSINE PERMEATION, THIS GRAPH SHOWS THE CUMULATIVE AMOUNT PERMEATED PER SURFACE AREA AS A FUNCTION OF TIME (MEAN±SD, N=4).

Single solvents. Miltefosine did not permeate when applied in PG, while permeation was seen when applied in water, DMI and OSAL. The permeation parameters are shown in Table 4-9. A one-way between group analysis of variance was conducted to explore the effect of the solvent on the flux of miltefosine through skin. There was no statistically significant difference at the $p<0.05$ level. This is probably due to the high variation that was observed because the average miltefosine permeation when applied in DMI and OSAL was higher compared to when applied in water.

The thermodynamic activity of the active compound in its vehicle is the driving force for a diffusion across the $SC^{294, 295}$. Two of the formulations that gave permeation (OSAL and DMI) were applied as a suspension and thus the thermodynamic activity was equal to 1. Consequently the thermodynamic activity for the miltefosine in water or PG solution, that were only at 14% and 5% of the saturated solution respectively, was considerably lower than the DMI and OSAL formulation. This might explain why the miltefosine permeation was lower when applied in PG or water compared to DMI and OSAL.

The permeability coefficients (K_p) for the water formulation was statistically significant lower compared to K_p for the DMI and OSAL formulation. This indicated that miltefosine when formulated in water had a low affinity for the skin but a high affinity for the vehicle as was reflected by the high solubility of miltefosine in water. Moreover the high permeability coefficients for miltefosine in DMI and OSAL indicated a high affinity for the skin and favoured partitioning into the BALB/c skin.

TABLE 4-9. SKIN PERMEATION PARAMETERS OF MILTEFOSINE AND THE INFLUENCE OF CHEs (H_2O, DMI, OSAL OR DMI-OSAL (1:1)) (MEAN ± SD (N=4)).

6% miltefosine in	H_2O	DMI	OSAL	OSAL-DMI
Permeation parameters				
J_{ss} (µg/cm²/h)	3.1±2.4	16.6±5.6	15.6±12.4	0.4±0.2
t_{lag} (h)	16.2±2.1	18.0±4.7	21.0±0.5	5.2±4.1
K_p (cm/h)	7.1E-06±5.4E-06	2.7±1.3	0.6±0.4	0.02±0.01

Binary solvent mixtures. The OSAL-DMI formulation was the only binary solvent mixture that was applied as a suspension and thus had a thermodynamic activity of 1. There was no statistically significant difference in miltefosine flux when compared to the single solvent mixtures water, DMI and OSAL (one-way ANOVA; $p>0.05$). The lag

time for this binary solvent formulation was statistically significant lower compared to the single solvent formulations (one-way ANOVA; $p<0.05$). The K_p for miltefosine applied in this OSAL-DMI formulation was significantly lower than the DMI formulation and thus indicated a relatively lower affinity for the skin (one-way ANOVA; $p<0.05$).

When ranking the flux of miltefosine through skin for the different vehicles, the order from high to low was DMI > OSAL > H2O > OSAL-DMI (1:1). The flux obtained from the binary solvent system is considerably lower compared to the single solvent systems but there is no statistically significant difference. Hence, it could be concluded that there was no synergetic effect obtained for the flux of miltefosine through mouse skin when using a combination of solvents. This was confirmed by other studies that had investigated the effect of a combination of solvents on the permeation of drugs and had found that not all combinations showed additional or synergetic effects[297, 298].

Based on the cumulative amount that had permeated, it could be stated that only a very low fraction of the drugs had permeated for all formulations over 36 hours (<2%). Due to an increase in skin permeability 36 hours after application of the formulations, an increase in permeation was seen for most formulations in particular for the miltefosine in water formulation. This was correlated to the methylene blue test as the receptor phase for most formulations had coloured slightly blue, except for the water-miltefosine formulation where a heavy blue coloration of the receptor phase was observed. This was not unexpected as surfactants and more in particular ionic surfactants such as miltefosine are known skin irritants and were reported to damage the skin.

Research has shown that surfactants cause protein denaturation[299] and swelling of the stratum corneum[300] through keratin interaction. They also have the ability to solubilise and deplete lipids from the stratum corneum[79]. Furthermore contact of epidermal keratinocytes with surfactants triggered the release of inflammatory mediators[301]. All these mechanisms contribute to skin barrier impairment[302] and sometimes enhancement of permeation of drugs[303].

In addition, Alonso et al showed an increased fluidity of the intercellular lipids of the SC upon contact with miltefosine[304]. The changes occurred at the interface with the polar heads and the lipophilic regions of the lipids and suggested that miltefosine functions as an acyl-chain spacer. This would suggest that miltefosine on its own functions as a chemical penetration enhancer.

4.2.5.2 MASS BALANCE

The results of the mass balance study are visualised in Figure 4-4 and the values are shown in Table 4-10. Total recovery ranged from 76%-102% which is slightly below the generally accepted recovery of 100±20%. This might be explained by the relatively high limit of quantification for these radiolabeled assays where the kinetic energy of radioactive nuclei (^{14}C-miltefosine) is transformed into light energy (fluorophore) that is then quantified. In contrast, direct detection methods for example HPLC-UV or LC-MS do not require intermediate steps causing loss or quenching of the signal and would therefore be more accurate, allowing a more sensitive drug detection.
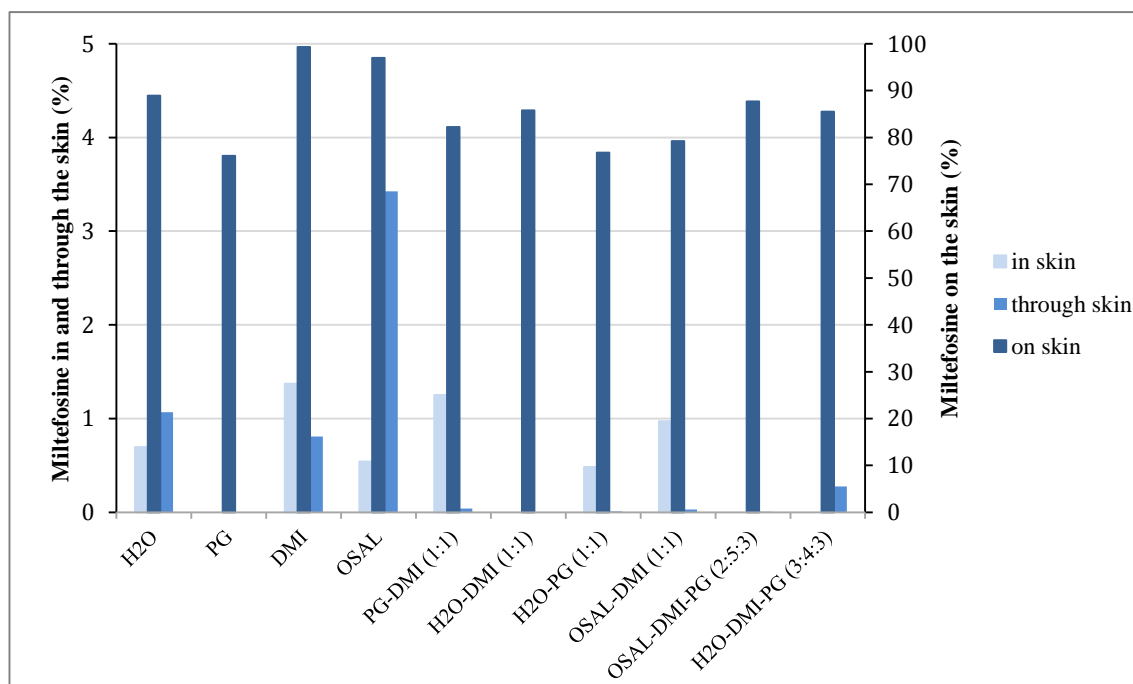
FIGURE 4-4. THE RESULTS OF THE MASS BALANCE STUDY FOR THE 10 TESTED FORMULATIONS (MEAN; N=4).

TABLE 4-10. MASS BALANCE RESULTS FOR THE MILTEFOSINE FORMULATIONS TESTED (MEAN ± SD (N=4)).

	On skin (%)	In skin (%)	Through skin (%)	Total Recovery (%)
Single solvent				
H$_2$O	89 ± 10	0.7 ± 0.3	1.1 ± 1.2	91 ± 12
PG	76 ± 7	0	0	76 ± 3
DMI	99 ± 3	1.4 ± 0.9	0.8 ± 0.6	102 ± 3
OSAL	97 ± 10	0.5 ± 0.7	3.4 ± 2.8	101 ± 6
Binary solvent system				
PG-DMI (1:1)	82 ± 4	1.3 ± 1.0	0	84 ± 3
H$_2$O-DMI (1:1)	86 ± 7	0	0	86 ± 7
H$_2$O-PG (1:1)	77 ± 3	0.5 ± 1.0	0	77 ± 4
OSAL-DMI (1:1)	79 ± 11	0.9 ± 0.3	0	80 ± 9
Ternary solvent system				
OSAL-DMI-PG (2:5:3)	88 ± 8	0	0	88 ± 8
H$_2$O-DMI-PG (3:4:3)	86 ± 11	0	0.3 ± 0.5	86 ± 9

As expected, the majority of the drug for all formulations was found on the skin. Furthermore only small fractions of miltefosine ranging from 0.48-1.37% were found in the skin. The differences were not statistical significant probably due to the large standard deviation (one-way ANOVA; $p < 0.05$). For 4 formulations, no miltefosine was detectable in the skin (PG, H$_2$O-DMI, and the two ternary phase solvent systems). This was not unexpected as miltefosine is an ionised compound that shows little affinity for lipophilic vehicles. The SC, composed of lipid bilayers seems to be a major barrier for miltefosine permeation.

4.3 CONCLUSIONS

This chapter described how we evaluated the permeation of miltefosine when applied on the skin in different vehicles. Four solvents, H2O, DMI, PG and OSAL were chosen based on their physico-chemical properties and previously reported effects on percutaneous drug permeation. The solubility of miltefosine in these solvents was determined and indicated that miltefosine exhibited high solubility in water and PG, but low solubility in DMI and OSAL. The miscibilities of the solvents were evaluated and indicated that OSAL was not miscible with water and PG. DMI, PG and water were miscible.

In a first permeation assay, miltefosine was applied on the skin in single solvent vehicles. No miltefosine permeation was detected for the PG formulation, whereas permeation was detected when it was applied in water, DMI and OSAL. The flux obtained for the OSAL formulation was similar to that of the DMI formulation. Both were approximately 5-fold higher than the flux obtained for the water formulation, however this difference was not statistically significant. The permeability coefficient indicated a significantly lower affinity of miltefosine for the skin when applied in water compared to DMI and OSAL. This was expected because miltefosine exhibited a high solubility in water, favouring retention of miltefosine in the vehicle.

OSAL, DMI and water were then combined in miscible binary and ternary mixtures and consequently the influence of combination vehicles on the permeation of miltefosine was tested. Out the 6 formulations tested, only the vehicle containing equal amounts of DMI and OSAL had led to miltefosine permeation. However the flux of miltefosine permeation for the binary solvent mixture was 40 times lower than the flux obtained when using DMI or OSAL alone. This indicates that the combination of solvents does not always lead to permeation enhancement.

Furthermore, this study showed that regardless of the formulation, only very low concentrations of miltefosine were found in the skin. This was probably due to its low affinity for the skin as the compound is ionised.

4.4 FUTURE WORK

In this study, the solvents were evaluated using infinite dose applications. However in clinical settings, a topical formulation is often applied in a finite dose and depletion of solvent and drugs will influence the skin disposition and permeation. Furthermore, mouse skin is different from human skin for example mouse skin counts more hair follicles and the composition of intercellular lipid mixtures is different. Therefore, the next step would be to repeat the permeation and mass balance studies using human skin and finite dose applications. Quantification of the amount of miltefosine extracted from the skin upon finite formulation application could be linked to the ED_{90} values obtained for the different strains of *Leishmania* parasites.

Finite dose application studies require a very sensitive method of analysis. Radiolabelled studies require an intermediate step where viscous scintillation fluid is added to the analytical sample introducing more error. A more sensitive detection method such as LC-MS/MS should be developed.

Since we have shown that miltefosine permeates, an *in vivo* study where miltefosine is applied in the single solvents OSAL and DMI will be conducted:

- To verify if any of the single solvent formulations allow permeation of miltefosine in a sufficient amount to kill *Leishmania* parasites and cure CL in our *in vivo* model;
- To verify if our *in vitro* permeation data confirm *in vivo* results;
- To see if the formulation is well tolerated in BALB/c mice;
- To compare how these results relate to pharmacokinetic parameters.

5 DRUG DISCOVERY–BENZOXABOROLES FOR A TOPICAL CL TREATMENT

Please note that the chemical structures of the compounds described below are not shown in this thesis as they are subject to confidentiality agreements prior to patent evaluation. All compounds were given an LSH number that is different from the Anacor Pharmaceuticals number.

5.1 GENERAL BACKGROUND

A literature review with the main search criteria for compounds with (i) activity against *Leishmania* parasites or related kinetoplastids, (ii) favourable physico-chemical properties to permeate into the skin, (iii) novelty and (iv) availability, was conducted. A relatively new group of compounds, the benzoxaboroles were identified as possible candidates for a topical CL formulation.

5.1.1 ACTIVITY OF THE BENZOXABOROLES

In the 1970s, boron containing drugs were found to react with the serine hydroxyl in the active site of certain enzymes resulting in potent inhibition of these enzymes, including β-lactamases[305-308] and proteasomes[309-312]. Proteasomes are involved in the degradation of misfolded, damaged or no longer useful proteins. *In vitro* studies have shown that their inhibition resulted in apoptosis induction and growth inhibition in multiple myeloma cells *in vitro*[312]. Bortezomib, a boron containing proteasome inhibitor was FDA approved for the treatment of multiple myeloma cancers in 2003.

Benzoxaborole compounds (Figure 5-1) are different from previously synthesised boron based compounds because the boron atom is incorporated in a ring system fused to an aromatic ring[313]. As other boron containing compounds, the benzoxaboroles were found to inhibit β-lactamases and proteasomes but they also exhibited activities against bacteria, fungi and protozoans such as *Trypanosoma brucei* and *Plasmodium falciparum*[313-318].
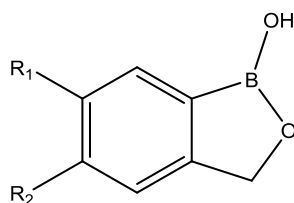
FIGURE 5-1. GENERAL CHEMICAL STRUCTURE OF BENZOXABOROLES.

In S*treptococcus pneumoniae*, the benzoxaborole ZCL039 inhibits leucyl-tRNA synthetase (LeuRS), an enzyme that holds an important role in cellular translation[317]. The same enzyme in dermatophytes is targeted by tavaborole, a drug used to treat onychomycoses. Tavaborole blocks tRNA translocation and blocks protein synthesis leading to cell death[319].

Compounds belonging to another benzoxaborole class, the 6-carboxamides have shown *in vitro* and *in vivo* activity against *T. brucei,* the causative agent of human African trypanosomiasis (HAT). Moreover, they cured mice with infection of the central nervous system indicating that the drugs were able to pass the blood brain barrier. An oral treatment for human African trypanosomiasis (HAT) containing the benzoxaborole SCYX-7158 is in Phase 1 clinical development[7].

Due to parasite similarities, compounds active against *T. brucei* were also screened against *T. cruzi,* the causative agent of Chagas disease. Amongst an array of compounds, the 6-amido oxaborole compounds showed potent *in vitro* activity and the lead compound, SCYX-6759 demonstrated complete removal of blood parasitaemia in mice[314, 320].

A phenotypic screening of a benzoxaborole library against *Plasmodium falciparum* identified potent compounds (defined as $IC_{50} < 1\mu M$) belonging to five chemical benzoxaborole classes[315, 316]. Further tests such as *in vitro* potency, cytotoxicity, drug-linked-bioavailability predictors and structure-activity relationship (SAR) analysis narrowed the selection to two lead scaffolds for further anti-malarial drug discovery research[316, 321, 322].

Finally, a high throughput screening was conducted to identify benchmark compounds to treat VL. The *in vitro* inhibitory activity of more than 2000 compounds were tested against *L. donovani* amastigotes in THP-1 cells and resulted in several hits ($IC_{50} < 1.1$ µM) (Unpublished data).

The majority of the bioactive benzoxaboroles are relatively small molecules (Mw <500g/mol) with a log P between 1-3 and few H-bond donors minimizing interactions with skin components during permeation. In fact, tavaborole (AN2690; Figure 5-1, $R_1 =$ H and $R_2 =$ F) is the active ingredient in a recently-FDA-approved topical treatment for onchychomycosis, Keridyn™[4,5] and AN2728, an investigational topical anti-inflammatory benzoxaborole is in development for the treatment of mild-to-moderate atopic dermatitis and psoriasis[6]. Results from the phase 2 clinical studies indicated a good dermal penetration profile[323, 324].

The aim of this drug discovery project was to evaluate compounds from different structural classes of benzoxaboroles, for their anti-leishmanial activity and suitability for topical treatment of CL.

The experiments discussed in this chapter were mainly conducted at SCYNEXIS Inc. (Research Triangle, NC) as part of a collaboration with Anacor Pharmaceuticals Inc. (Palo Alto, CA). Some of the work was performed by other team members. This is clearly indicated in the sections concerned.

5.1.2 FROM DRUG DISCOVERY TO A TOPICAL TREATMENT FOR CL – STRATEGY

During the pharmaceutical profiling in the early stages of drug discovery, multivariate techniques are used to assess the physicochemical and physiological properties that allow prediction of the performance of the test compounds against hurdles that are to be faced by the pharmaceutical agent. The information is used to optimise and select lead compounds. It is important to highlight that the required drug profile depends on the route of administration.

The timeframe during which the data are provided should be consistent with the fast-paced decisions of the early discovery stage. Figure 5-2 indicates the experiments that were conducted to profile an array of benzoxaborole compounds and the stages at which compounds were eliminated because they exhibited unfavourable properties for a topical treatment.
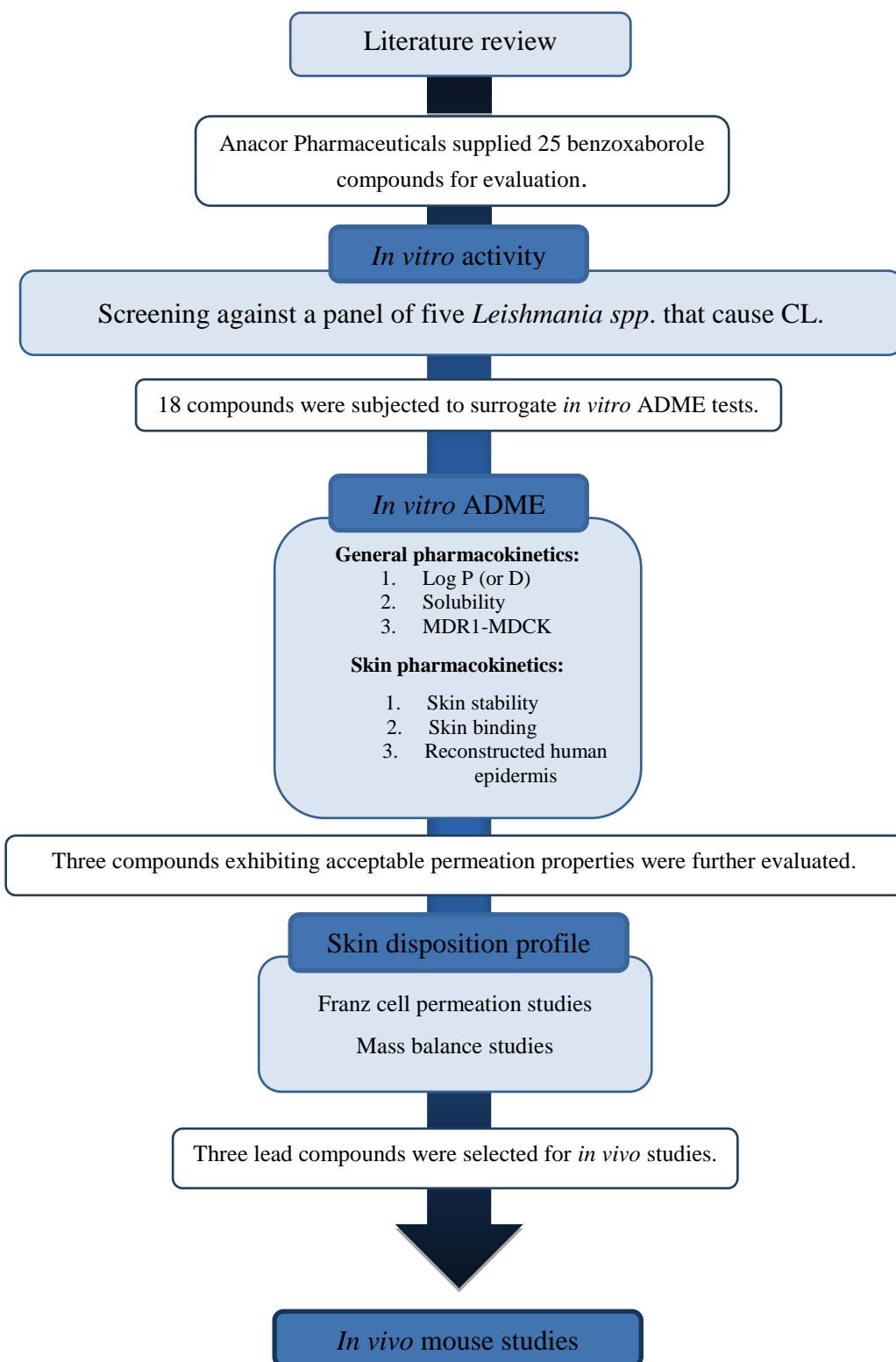
FIGURE 5-2. FROM DRUG DISCOVERY TO A TOPICAL TREATMENT FOR CL – STRATEGY.

5.1.2.1 ANTI-LEISHMANIAL ACTIVITY TESTING

Anacor Pharmaceuticals Inc. provided 25 benzoxaboroles for *in vitro* anti-leishmanial activity testing against a range of five *Leishmania* species. Species selection was based on the geographical distribution, symptoms upon infection and the abundance of infections they cause. *L. tropica* and *L. major* were selected because together they cause the majority of Old World CL. *L. aethiopica* is the main CL causing agent in Ethiopia and causes both LCL and DCL[325, 326]. *L. mexicana* and *L. panamensis* are two New World species that belong to different subgenera *Leishmania* and *Viannia* respectively. *L. mexicana* can cause DCL, an anergic form that is difficult to treat with frequent relapses whereas *L. panamensis* can lead to MCL also difficult to treat.

The *in vitro* assay could not be optimized for *L. braziliensis*, the principal agent of mucocutaneous leishmaniasis. Insufficient infection rates, typically 40% or lower were obtained or abundant extracellular promastigotes made microscopic evaluation of infection difficult. This species was therefore not included in the screenings.

Based on the obtained data, 18 compounds belonging to four different chemical subclasses of benzoxaboroles were selected for surrogate absorption, distribution, metabolism and excretion (ADME) studies. These time-sensitive assays allow a preliminary evaluation of simple physicochemical and biophysical parameters that are important to profile the disposition of the drug within the body.

Figure 5-3 (A) shows the general structure of benzoxaboroles. The subclasses are:
(B) Benzoxaborole-5-amides

(C) Pyrazole-carboxamides

(D) Simple benzoxaborole 6-carboxamides

(E) Benzoxaborole-oxaborininols
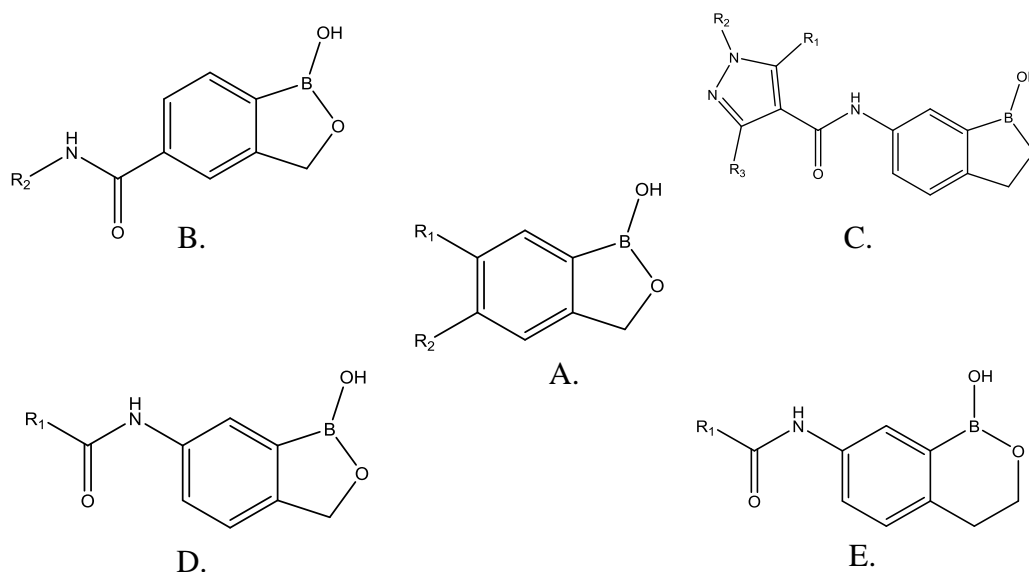
FIGURE 5-3. A: GENERAL STRUCTURE OF BENZOXABOROLES, B-D ARE CHEMICAL SUBCLASSES.

5.1.2.2 IN VITRO ADME ASSAYS.

General physicochemical properties. Computationally and *in vitro* experimentally derived general physico-chemical properties include H-bond donors and acceptors, solubility, log P and general permeability using Madin-Darby canine kidney cells transfected with the human mdr1 gene (MDCK-MDR1).

- The importance of the partition coefficient, aqueous solubility, molecular weight, melting point and H-bond donors was already highlighted in the Introduction (1.3.1.1).

- The MDCK-MDR1 assay. The MDCK-MDR1 assay was used to evaluate the passive (transcellular) permeability of the test compounds while highlighting potential permeability issues. This simple model is composed of a monolayer of cells linked by tight junctions and is used as a surrogate for the multi-layered reconstructed human epidermis (RHE) model in the early stages of drug discovery as it is considerably less expensive. Furthermore, this test allows identification of P-glycoprotein (Pgp) substrates. Pgp is an efflux transporter that is reported to reduce the intracellular concentration of numerous drugs[327, 328]. In man, *Leishmania* parasites survive and divide inside macrophages meaning that Pgp substrate drugs might potentially be less active compared to drugs that are not Pgp substrates as they are transported from the inside to outside the marcophages.

Skin pharmacokinetics. In a second stage, more skin specific biochemical characteristics such as drug stability and binding in skin homogenate supernatant and permeation through RHE were evaluated.

- Drug stability. Most attention in topical treatment development goes to assuring the drug permeates through the SC and reaches the target. Drug degradation by metabolising skin enzymes is reported to influence permeation but is often neglected in the early stages of development. Kao et al evaluated the metabolism of testosterone and benzopyrene during permeation through skin from different species, including mouse and human, and detected a variety of drug metabolites in the receptor phase[329]. Further research using other drugs confirmed the presence of metabolic activity in the skin[330-333].

  For this project the stability of the compounds was tested in full-thickness mouse skin homogenate supernatant. The epidermis appears to be the main site of enzyme activity[331, 334]. This is consistent with findings that suggest that keratinocytes contain the highest amount of drug metabolising enzymes compared to other skin cells[335, 336]. Skin supernatants have previously been used to investigate drug stability[332].

- Drug binding to skin components. It is important to determine the fraction of unbound drug present in the skin as it is only the free drug which is available to exert anti-parasitic activity. The device used in this project to measure the unbound drug fraction is based on equilibrium dialysis and allows the evaluation of the affinity of a drug for skin macromolecules. Essentially two chambers, one containing skin homogenate supernatant and drug and the other containing PBS are separated by a membrane with a particular molecular weight cut-off. After equilibration and analysis of the drug concentration in each chamber, the unbound drug fraction can be calculated. Equilibrium dialysis has already been shown to accurately predict the binding of drugs to tissues such as brain, muscle and adipose tissue[337].

- Permeation prediction using reconstructed human epidermis. Artificial skin tissue is grown by seeding skin keratinocytes with dermal growth factors and leaving them to differentiate at the air-liquid interface. Three RHEs are most commonly used for drug permeation testing: EpiSkin® (L'Oréal), SkinEthic® (SkinEthic has now been acquired by L'Oréal) and EpiDerm® (MatTek). While

the RHEs are similar to human epidermis in terms of structure and composition, they are more permeable to drugs[338]. The permeation of two model compounds, testosterone and caffeine through the 3 RHE's were investigated and compared. The Epiderm® model was the only one to show similar caffeine permeation compared to human epidermis but all models were able to reproduce the same rank order in permeation as when using human epidermis[339]. In addition a slightly lower variability in permeation results was observed compared to excised skin[340]. It should also be mentioned that these models contain metabolising enzymes[341]. In this project, the permeation of the test compounds was evaluated using the Epiderm® model.

5.1.2.3 *In vitro* permeation studies using Franz Diffusion Cells.

The data were analysed and 3 compounds were selected for more stringent permeation tests using full-thickness BALB/c mouse skin. Full-thickness skin was preferred over separated epidermis as although the *stratum corneum* is considered the main barrier to drug permeation, the largely aqueous dermis can act as a significant barrier for lipophilic drugs. The skin disposition profile of the benzoxaborole compounds was established by analysing the amount of drug left in and on the skin. These results were combined with the *in vitro* ADME study results and three lead compounds were selected for *in vivo* evaluation against CL in BALB/c mice.

5.2 MATERIALS AND METHODS

5.2.1 TEST COMPOUNDS

The test compounds were synthesised by Anacor Pharmaceuticals Inc. and SCYNEXIS Inc. (Research Triangle, NC) and submitted to LC-MS* and ^{1}H-NMR* analysis for identification and characterisation before use. One mM stock solutions in dimethyl sulfoxide (DMSO) were prepared and used for the *in vitro* absorption, distribution, metabolism and excretion experiments.

*** The chemical synthesis team at Anacor Pharmacueticals Inc. and SCYNEXIS conduct these assays as part of their standard compound characterisation. The analyses were not conducted by the PhD candidate.**

5.2.2 REAGENTS AND OTHER DRUGS

HPLC grade solvents were purchased from Fisher Scientific (Pittsburgh, PA). Formic acid (≥98% purity, Fluka), caffeine, testosterone, 1-octanol, high grade vacuum silicone grease (Dow Corning) were acquired from Sigma-Aldrich (St. Louis, MO). Ammonium formate (99% purity, Alpha Aesar) was purchased from VWR International, LLC (West Chester, PA). Miglyol 840 (propylene glycol dicaprylate / dicaprate) was obtained from Sasol Germany GmbH (Witten, Germany). Phosphate buffered saline (PBS) was supplied by Gibco (Invitrogen Corporation, Carlsbad, CA) as well as the Dulbecco's modification of Eagle's medium with GlutaMAX, the trypsin-EDTA and the Fetal Bovine Serum. Penicillin-Streptomycin solution, Hank's balanced salt solution and HEPES buffer were obtained from Sigma Aldrich.

5.2.3 LEISHMANIA PARASITES AND CELL CULTURE

MDCKII-hMDR1 cells (Netherlands Cancer Institute, Amsterdam, Netherlands) were maintained in Dulbecco's Modified Eagles Medium (DMEM) and KB cells in RPMI-1640 medium supplemented with L-glutamine and 10% HiFCS. Both human-derived cell lines were left in an incubator at 37ºC and 5% CO_2 and passaged to new medium once a week (1/10 ratio). The parasite cultures were maintained as explained in section 4.1.3.

5.2.4 IN VITRO SENSITIVITY ASSAYS AGAINST LEISHMANIA PARASITES

5.2.4.1 INTRACELLULAR AMASTIGOTES

Mouse peritoneal macrophages (PEM) were isolated from CD-1 mice (Charles River, Margate, UK) by abdominal lavage with RPMI-1640 medium containing 1% penicillin and streptomycin. The collected cells were washed, re-suspended and seeded in 16 well Lab-Tek™ plates (VWR International, Leicestershire, UK) in RPMI-1640 supplemented with 10% HiFCS at a density of $4x10^4$ per well. After 24 hours incubation at 37°C and 5% CO_2/95% air mixture, the adhered PEMs were infected with stationary phase promastigotes at a ratio of 3 (for *L. tropica* and *L. major*) or 5 (for *L. mexicana*, *L. aethiopica* and *L. panamensis*) promastigotes to 1 macrophage and maintained at 34°C in a 5% CO_2/95% air mixture. After 24 hours, the cultures were washed to remove extracellular promastigotes and one slide was fixed with methanol and stained with Giemsa to determine the initial level of infection. If a sufficient level of infection (i.e. > 75%) was obtained, DMSO - oxaborole solutions over a range of 30, 10, 3 and 1 μM were added in quadruplicate at each concentration. Miltefosine and amphotericin B were included as control drugs. After 72 hours incubation, all slides were methanol-fixed and Giemsa-stained. The percentage inhibition was determined microscopically (400x magnification) by counting the infected macrophages in drug-treated cultures. This was only conducted if the 72 hours untreated control slide showed at least 75% infection. The Hill coefficient, ED_{50} and ED_{90} values were determined by non-linear sigmoidal curve fitting (variable slope) using Prism Software (GraphPad, Surrey, UK).

5.2.4.2 PROMASTIGOTES

20 mM drug stock solutions were prepared by dissolving the benzoxaborole compounds in DMSO. The final drug concentrations were obtained by serially diluting (1:3) the stock solutions in RPMI-1640 medium plus 10% heat-inactivated fetal calf serum (HiFCS). Amphotericin B and miltefosine were included as positive controls and each plate contained a 72 hours control, a DMSO and a medium only control.

Exponential phase promastigotes were centrifuged at 2100 rpm for 10 min (4°C) and re-suspended in RPMI-1640 medium supplemented with 10% HiFCS to a $1x10^7$/ml density. 100 μl of promastigote suspension was added to the 100 μl of benzoxaborole solutions reaching final oxaborole concentrations of 300-0.27 μM. The plates were left to incubate at 26°C for 72 hours.

Four hours before the fluorescence reading to measure cell viability, 20 μl of Alamar Blue® solution (Invitrogen™, Thermo Fisher, Loughborough, UK) was added to each well. The fluorescence (λext/em 544/590 nm, cut off 570 nm) was read using a Spectramax™ M3 microplate reader (Molecular Devices, California, US) and the EC_{50} values were determined by non-linear sigmoidal curve fitting (variable slope) using Prism Software (GraphPad, Surrey, UK).

5.2.5 CYTOTOXICITY TESTING AGAINST KB CELLS

KB cells were harvested, washed and counted in serum-free medium. The cell density was adjusted to 5 x 10^4 / ml in RPMI-1640 supplemented with 10% HiFCS. 100 μl of the cell suspension was plated in each well of a 96-well plate followed by incubation at 37°C and 5% CO_2 for 24 hours.

Stock drug solutions of 20 μM in DMSO were prepared and diluted to 600 nM in RPMI-1640 with 10% HiFCS. 300 nM was the highest concentration tested and five-fold serial dilutions were performed across the plate. Podophyllotoxin was included as a positive control drug. Untreated controls and blanks, containing medium only were also included. Each test compound was tested in triplicate. Plates were incubated for a further 72 hours at 37°C and 5% CO_2.

After incubation, the wells were assessed microscopically and 20 μl Alamar Blue® was added to each well. The plates were incubated for a further 2-4 hours before reading at λext/em 544/590 nm (cut off 570 nm) in a Spectramax™ M3 Plate reader. EC_{50} values were calculated by non-linear sigmoidal curve fitting (variable slope) using Prism Software (GraphPad, Surrey, UK).

5.2.6 IN VITRO ADME STUDIES−GENERAL PHARMACOKINETIC PREDICTIONS

5.2.6.1 COMPUTATIONALLY DERIVED PHYSICOCHEMICAL PROPERTIES

The following descriptors of the test compounds, molecular weight, aqueous solubility and number of H-bond donors present were estimated using modelling software ChemBioDraw Ultra 13.0 (PerkinElmer, Waltham, MA).

5.2.6.2 SOLUBILITY IN PBS (PH 7.4)

For the solubility determination, 200 μl of PBS (pH 7.4) was transferred into an Eppendorf tube. Excess drug was added and the vial was left to shake (800 rpm) at

32°C for 48 hours. Subsequently, the mixtures were centrifuged at 13000 rpm for 15 minutes (32°C). An aliquot of the supernatant was removed and analysed by LC-MS/MS. Due to the limited availability of the drug, the study was only conducted once per test compound. Therefore the results should be considered as an indication rather than as an absolute value.

5.2.6.3 DETERMINATION OF LOG D

Equal volumes of octanol and PBS (pH 7.4) were left to equilibrate on a shaking plate at 32°C for 48 hours. The test compound was dissolved in 1-octanol at a concentration of 1 μg/ml and left to equilibrate with an equal volume of PBS on a shaking plate at 32°C for 48 hours. For the experiment to be successful the amount of drugs in each phase should not exceed 10% of the solubility limit of that compound in each phase. Aliquots of each phase were taken and diluted in mobile phase followed by LC-MS/MS analysis. The experiment was conducted in triplicate. The distribution coefficient was calculated as shown in Equation 6:

$$\log D \, (pH\, 7.4) = \log\left[\frac{[\textbf{solute}]_{\textbf{oct}}}{[\textbf{solute}]_{\textbf{pbs}}^{\textbf{ion}} + [\textbf{solute}]_{\textbf{pbs}}^{\textbf{neutral}}}\right]$$

EQUATION 6

5.2.6.4 MELTING POINT DETERMINATION BY DIFFERENTIAL SCANNING CALORIMETRY

Differential scanning calorimetry (DSC) is a technique that measures heat flow to and from a sample as a function of time and temperature and is used to determine the melting point of the sample. DSC analysis were conducted in duplicate and only for the 3 lead compounds because it is a destructive method that requires a drug sample in the mg range which is quite high for drugs in the developmental stage.

Before starting the experiment, the instrument was calibrated with indium using the Tzero™ calibration wizard. Non-hermetic aluminium Tzero pans (TA instruments, Herts, UK) were loaded with the sample and placed in the Q2000 DSC instrument (TA instruments, Herts, UK) together with an empty aluminium pan that served as a reference. Nitrogen at a flow rate of 50 ml per minute was used as a purge gas. The samples were left to equilibrate at -20˚C followed by increasing the temperature to 300˚C in increments of 10˚C. The results were analysed using the Universal Analysis 2000 version 4.7A (TA instruments LLC).

5.2.6.5 EVALUATION OF PERMEABILITY AND PGP-MEDIATED EFFLUX TRANSPORT USING THE MDCK-MDR1 ASSAY[*]

*** This assay was conducted by Dr. Seong Hee Park and Mrs. Sara Schock (Scynexis, Research Triangle Park, Durham, NC) and not by the PhD candidate.**

For the experiment (Figure 5-4), the cells were seeded in the apical chamber of a 12-well Transwell® plate (Corning Inc., Lowell, MA) at a density of 6.6×10^6 cells/well and 1.5 mL of medium was applied in the basolateral chamber. After 24 hours, the non-adhered cells were washed away and new medium was applied in both chambers. The cells were left for another 48 hours at 37°C to form confluent monolayers.

Prior to the addition of the test compounds, the cell culture medium was removed and replaced with transport medium that consists of Hanks's balanced salt solution with 24 mM of glucose and 24 mM of HEPES buffer. The integrity of the monolayers was assured by measuring the trans-epithelial resistance (TEER) for each insert (TEER > 160 Ω cm^2). Assays were performed in triplicate by adding 3 μM drug solutions (1 mM DMSO stock solutions diluted in transport medium) in the absence or presence of 2 μM GF918 (a potent Pgp inhibitor[342]) in the transport buffer of the apical chamber. Reference drugs for transcellular transport and Pgp efflux, propranolol and amprenavir respectively were included in the assay. The Transwell® plates were incubated on a shaking plate (160 rpm) at 37°C and 5% CO$_2$ for 1 hour. After incubation, aliquots from both chambers were removed for analysis by LC-MS/MS.
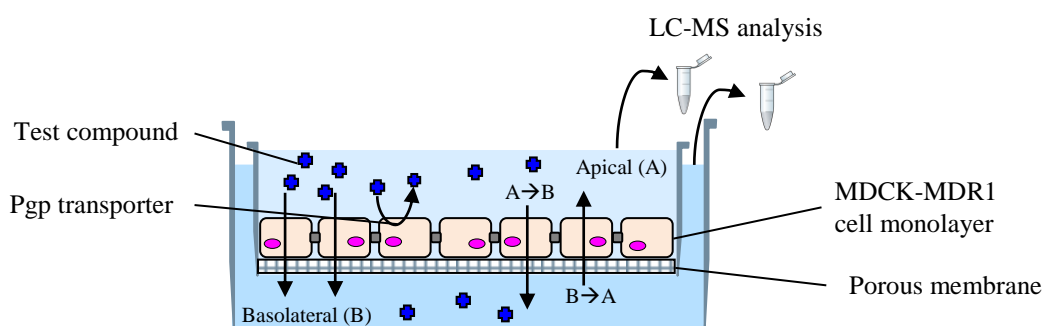
FIGURE 5-4. SCHEMATIC REPRESENTATION OF THE MDCK-MDR1 ASSAY FOR PERMEATION.

Values for mass balance, apparent permeability value for the apical to the basolateral side (P_{app}) (Equation 7), apparent permeability value for the apical to the basolateral in presence of GF+918 ($P_{app+GF918}$) (Figure 5-5), and the absorption quotient (AQ) (Equation 8) were calculated for each compound[343-345]. Test compounds with an AQ $\leq$

0.3 were considered no Pgp substrates, while AQ > 0.3 were considered Pgp substrates[344, 345]. Acceptance criterion for mass balance was 70–120%.

$$P_{app} = \frac{dQ/dt}{C_0 \times A}$$

<div align="right">EQUATION 7</div>

$$AQ = \frac{P_{app+GF918} - P_{app}}{P_{app+GF918}}$$

<div align="right">EQUATION 8</div>
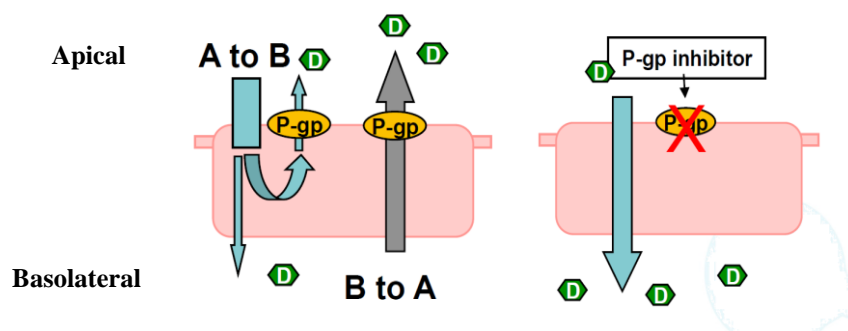
FIGURE 5-5. SCHEMATIC REPRESENTATION OF THE EFFECT OF A PGP GLYCOPROTEIN ON THE PERMEATION OF A PGP SUBSTRATE DRUG.

5.2.7 IN VITRO ADME STUDIES−SKIN PHARMACOKINETICS PREDICTION

5.2.7.1 SKIN HOMOGENATE SUPERNATANT PREPARATION

For the preparation of the homogenate, 20 ml of ice-cold Dulbecco's modified PBS (pH 7.4) was added to fine pieces of approximately 2 g of shaved dorsal full-thickness BALB/c skin (Bioreclamation LLC., Westbury, NY). The mixture was homogenized using an OMNI probe homogenizer (Kennesaw, GA) and centrifuged for 10 minutes at 800g to remove big pieces. The protein content of the supernatant was determined using the Pierce BCA protein assay kit (Pierce, Rockford, IL) and adjusted to 2.5 mg/ml. The supernatant was stored at -80°C until further use.

5.2.7.2 IN VITRO DRUG STABILITY IN MOUSE SKIN HOMOGENATE SUPERNATANT

The stability of the compounds was measured at two different protein concentrations namely 0.6 mg/ml and 2.5 mg/ml. Each compound (10 μM) was incubated in mouse skin homogenate on a shaking plate at 32°C. An aliquot of the fortified supernatant was

taken at 0, 10, 20, 30 minutes, 1 hour and 2 hours and quenched with 4 volumes of ice-cold methanol containing 0.1% formic acid. After centrifugation at 3000xg for 10 minutes at 15°C, the obtained supernatant was analysed for the parent compound by LC-MS/MS. Prism 6 (GraphPad, La Jolla, CA) was used to fit the data and to estimate the half-lives. Ethyl- and propylparaben, ester compounds known to undergo degradation due to enzymatic hydrolysis to yield hydroxybenzoic acid were included as positive controls.

5.2.7.3 IN VITRO BINDING TO SKIN COMPONENTS

Rapid equilibrium dialysis (RED) devices (Pierce, Rockford, IL - Figure 5-6) were used to investigate the drug binding to the skin homogenate supernatant.
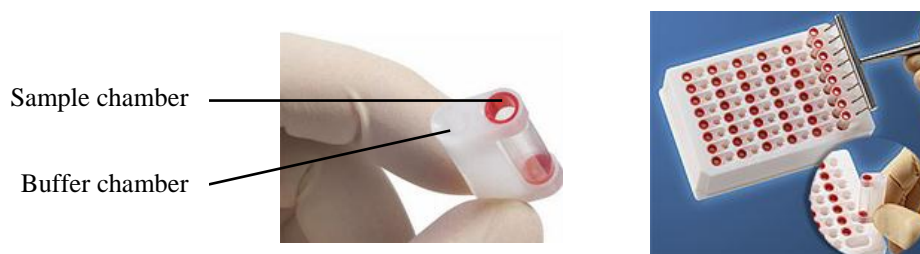
FIGURE 5-6. SHOWS A RED DEVICE INSERT (LEFT) AND THE 96 WELL PLATE HOLDER (RIGHT).

A day prior to the experiment, the Teflon plate was washed with 30% ethanol and rinsed twice with deionized water before leaving it to dry. On the day of the experiment, skin supernatant was thawed and the drug compound was added to a final concentration of 10 μM. After adding 300 μl of fortified tissue in the sample chamber and 500μl of PBS (Pierce, Rockford, IL) to the buffer chamber, the plate was incubated on a shaking plate at 32°C for 2 hours. Aliquots of both phases were collected and treated with 4 volumes of ice-cold methanol with 0.1% of formic acid to precipitate proteins. After 10 minutes of centrifugation at 3000xg at 15°C, the supernatants were assayed for the parent drug by LC-MS/MS.

5.2.7.4 IN VITRO PERMEABILITY EVALUATION THROUGH RHE

The EpiDerm™ Skin Model EPI-606-X was obtained from MatTek Corporation (Ashland, MA, USA). The EPI-606-X model is characterised by an enhanced barrier function and was specifically designed to conduct permeability assays. Upon receipt, the skin tissue (lot 17860) was stored overnight at 2-8°C. On the day of the experiment, the skin inserts were transferred to a 6 well plate containing 2ml of Dulbecco's

modified PBS and left to acclimatise on a heated shaking plate. The temperature was set at 36.6°C which corresponded to a skin temperature of 32°C.

Due to a low water solubility, the test compounds were applied in an ethanol/ Miglyol 840 (1:9) vehicle, a solution that has been used for permeation studies for poorly soluble drugs[346]. After 1 hour, 1.14 ml of a 100 µg/ml donor solution was applied on the model skin using a positive displacement pipette. The plates were left to shake at 95 rpm. Two reference permeation drugs with different lipophilicities were included; caffeine is a hydrophilic compound (log P= -0.08), while testosterone is more lipophilic (log P= 3.32). They were applied at the same concentration and in the same vehicle as the test compounds, except for caffeine was dissolved in Dulbecco's modified PBS. Aliquots were removed from the receiver fluid and replaced with fresh PBS at regular time points over a period of 6 hours. The samples were analysed by LC-MS/MS. The permeation of each compound was tested in triplicate. Statistical analysis were performed using SPSS software version 19.0.
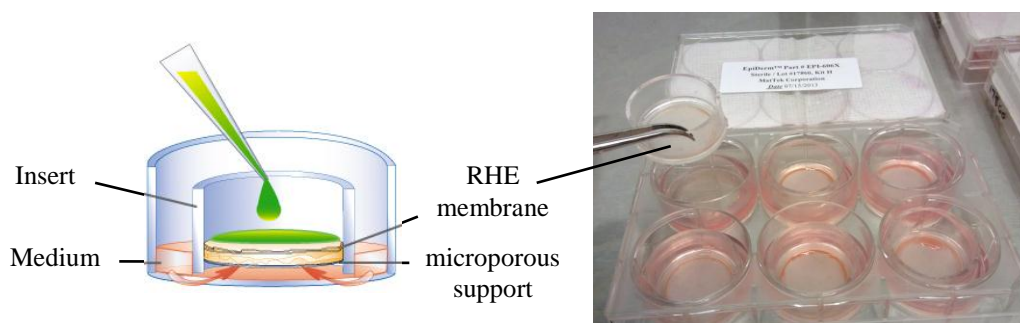
FIGURE 5-7. A SCHEMATIC REPRESENTATION (LEFT- ADAPTED FROM[347]) AND PICTURE (RIGHT) OF THE SETUP OF THE RHE PERMEATION ASSAY.

5.2.8 *IN VITRO PERMEATION THROUGH FULL-THICKNESS BALB/C MOUSE SKIN USING FRANZ DIFFUSION CELLS*

Two FDC studies were conducted. The first FDC study evaluated the permeation of the test compounds through BALB/c mouse skin in order to compare them to the results obtained with the RHE assay. Therefore, the experimental conditions of the RHE and FDC 1 study were similar. The objective of the second FDC study was to evaluate the permeation of the test compounds upon real-life topical treatment i.e. using a low application volume and a 1% (w/v) drug formulation.

Skin of female BALB/c mice was ordered from BioreclamationIVT (Westbury, NY, USA) and stored at -80°C. Prior to the experiment the skin was thawed and clipped carefully to avoid skin damage. Any excess fat and muscle tissue was removed and skin discs of approximately 2.5cm diameter were cut. The skin was mounted between the donor and receptor compartment and kept in place by the use of a clamp. Vacuum silicone grease was applied to seal gaps and prevent leakage. The cells were left to equilibrate until the skin temperature stabilised at 32°C.

The donor and receptor solutions (Table 5-1) were prepared as described in paragraph 5.2.7.4. For FDC 1, the test compounds were mixed together so that LSH001 and LSH002 were applied to skin samples 1 to 3; and LSH003 and LSH0034 (good permeating benzoxaborole control compound) were applied to skin samples 4 to 6. Receptor fluid samples were taken at time intervals over a period of 6 hours. Each test compound was tested in triplicate. Statistical analysis were performed using SPSS software version 19.0.

TABLE 5-1. SUMMARY OF THE EXPERIMENTAL CONDITIONS FOR THE DIFFERENT PERMEATION EXPERIMENTS.

Permeation experiment	Compounds	Donor vehicle	Concentration (μg/ml)	Volume/ skin surface (μl/cm^2)
RHE 1	LSH011; LSH012; LSH029; LSH001: LSH031; LSH034; LSH023; LSH024; LSH003; caffeine; testosterone	Ethanol – Miglyol 840 (1:9) Except for caffeine	100	300
FDC 1	Mix1: LSH001; LSH002 Mix2: LSH003; LSH034	Ethanol – Miglyol 840 (1:9)	100	300
FDC 2	LSH001; LSH002; LSH003	Ethanol – PG (1:1)	10 000 (1% w/v)	28.4

Permeation studies were conducted in a semi-automated system with 6 static vertical type Franz Cells from Logan Instruments Ltd. (Somerset, NJ) (Figure 5-8).
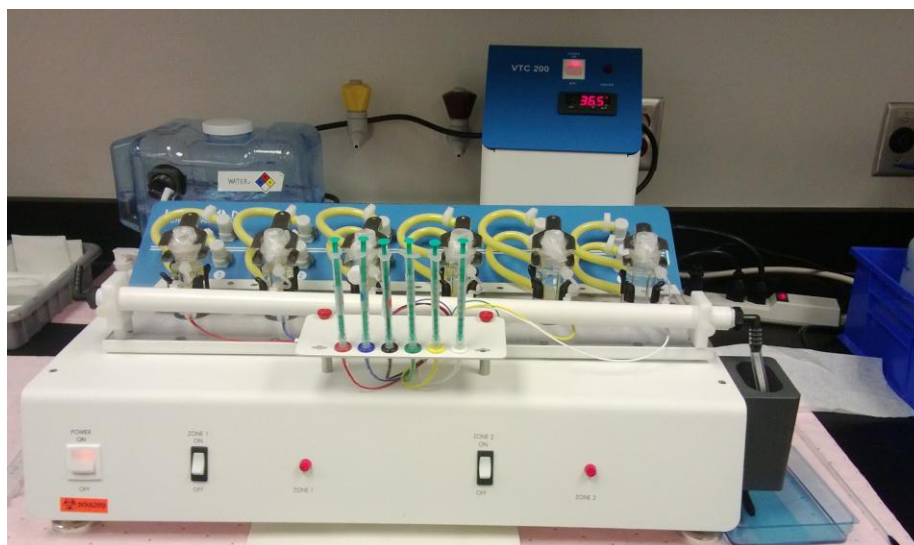
FIGURE 5-8. THE SEMI-AUTOMATED LOGAN SYSTEM WITH SIX STATIC FRANZ CELLS, THE WATER RESERVOIR AND TEMPERATURE CONTROL UNIT.

5.2.9 DETERMINATION OF THE BENZOXABOROLE CONCENTRATION IN THE SKIN

A mass balance study was conducted for the FDC 2 permeation experiment. The amount of drug that did not permeate into or through the skin was obtained by gently swabbing the skin surface with a cotton bud at the end of the permeation experiment. This was repeated a second time. The cotton buds were placed in a tube with 1ml of MeOH/PBS (70:30) and left overnight on a shaker (800 rpm). An aliquot of the extraction fluid was analysed by LC-MS/MS.

The cells were dismantled and the mouse skin was removed and placed in a vial. Three rounds of extraction with 1ml of MeOH-PBS (7:3) were conducted. At each time, the vial was left to shake overnight before analysis by LC-MS/MS to extract the amount of drug that permeated into the skin. A drug recovery of 80-120% was decided to be acceptable. Statistical analysis were performed using SPSS software version 19.0.

5.2.10 LC-MS/MS - METHOD DEVELOPMENT AND OPTIMISATION

Sample analysis was performed by high-performance liquid chromatography with tandem mass spectrometry (LC-MS/MS). The instrumentation consisted of a CTC Pal Autosampler (Leap Technologies, Carrboro, NC), two Agilent 1100 series pumps (Agilent Technologies Inc., Santa Clara, CA), a CH-30 column heater (Eppendorf, Hauppauge, NY) and an API-3000 triple quadrupole mass spectrometer (Applied

Biosystems, Foster City, CA) equipped with a turbo-ion electrospray interface for detection (Figure 5-9). Samples were loaded and separated on a Luna C18 column (50 x 2 mm; 3 µm) from Phenomenex (Torrance, CA) protected by a corresponding guard column. The instrument and peripheral devices were controlled using Analyst® Software version 1.4.2 (Applied Biosystems, Foster City, CA). The mobile phase used to elute the compounds consisted of 5 mM ammonium formate and 0.1% (v/v) formic acid in water (A) and 5 mM ammonium formate and 0.1% (v/v) formic acid in methanol (B).

FIGURE 5-9. THE LC-MS/MS INSTALLATION AT SCYNEXIS (RESEARCH TRIANGLE PARK, NC).

5.3 RESULTS AND DISCUSSION

5.3.1 IN VITRO SENSITIVITY ASSAYS

Amastigotes. All compounds were screened against intracellular amastigotes, the most clinically relevant *Leishmania* form. The ED_{50} values for each compound tested against five *Leishmania* species are indicated in Table 5-3. It is observed that the majority of the test compounds exhibited higher activity against *L. tropica* compared to other species. 40% of the compounds had an ED_{50} below 5μM compared to 24% when tested against *L. major* and 3% for *L. panamensis* (Table 5-2). *L. mexicana* and *L. aethiopica* were least susceptible to the tested benzoxaboroles; no compounds had an ED_{50} below 5μM and 86% and 72% had an ED_{50} above 25μM respectively.

TABLE 5-2. ED_{50} VALUES OF THE BENZOXABOROLE COMPOUNDS AGAINST INTRACELLULAR AMASTIGOTES SORTED BY ACTIVITY RANGE.

	Activity range		
	< 5μM	5-25μM	> 25μM
L. tropica	40%	33%	27%
L. major	24%	29%	48%
L. aethiopica	0%	28%	72%
L. mexicana	0%	14%	86%
L. panamensis	3%	21%	76%

In the amastigote assay, LSH001, LSH023, LSH024, LSH003 and LSH025 were the only compounds active against at least one Old World (*L. major*, *L. tropica* and *L. aethiopica*) and one New World (*L. mexicana* and *L. panamensis*) species. For these compounds, the rank order of sensitivity was *L. tropica* > *L. major* > *L. panamensis* > *L. aethiopica* and *L. mexicana*.

Promastigotes. The drug sensitivity of benzoxaboroles against extracellular promastigotes was only tested for LSH001, LSH002 and LSH003, the three compounds that were selected for *in vivo* studies (Table 5-4) to complete the data. The compounds were about 100 times more active against *L. tropica* promastigotes than amastigotes. There was little difference in sensitivity between the other *Leishmania* strains for LSH001 and LSH003 with ED_{50}s ranging from 1.28 to 5.24 and 2.57 to 5.30 respectively. The ED_{50}s for LSH002 against *Leishmania* promastigotes are in general higher compared to the other two lead compounds. In the promastigote assay, the rank order of sensitivity was the same for the tested compounds and was different to the sensitivity rank order in

the amastigote assay: *L. tropica > L. panamensis > L. aethiopica > L. major > L. mexicana.*

Control drugs. Amphotericin B, included as positive control, had a high activity (nanomolar range) across the promastigotes and amastigotes of different species. The ED_{50}s for the latter ranged from 0.049 to 0.685μM, indicating a tenfold difference in sensitivity between *L. major*/*L. tropica* and *L. mexicana.* For promastigotes, the ED_{50} values ranged from 0.011 to 0.300μM and are similar to the ED_{50}s described by Escobar et al[159]. Miltefosine was less active than amphotericin B against *Leishmania* amastigotes and promastigotes with ED_{50}s ranging from 7 to 45 μM and 10 to 35 μM respectively. The ED_{50}s for both control drugs were similar to values reported in literature bearing in mind that differences in assay methodology and *Leishmania* species can cause shifts in ED_{50} values.

The Hill coefficient shown in Table 5-5 is an indicator of the steepness of the dose response curves and is also an indicator of cooperativity in drug binding to the receptor. The coefficient was well below 1 for all the test compounds which indicated that there was a negative cooperative binding. This suggests that upon binding with the first molecule, the affinity of the drug target (likely an enzyme) for other drugs will decrease. Only for the activity testing of amphotericin B against *L. tropica* a Hill coefficient higher than 1 was obtained. This suggests that the binding of amphotericin B to the target increases its affinity for other drug molecules. Moreover this might indicate that the target in this *L. tropica* strain differs from the target in the other strains.

Cytotoxicity. Cytotoxicity of the benzoxaborole compounds was tested against the human KB cell line and ED_{50}s for LSH001, LSH002 and LSH003 were 46.28, 61.58 and 10.09 μM respectively (Table 5-5). The ratio of the ED_{50} against amastigotes to the ED_{50} against KB cells for LSH001, LSH002 and LSH003 ranged from 2-23, 2-4 and 0-4 respectively. This shows that the margin between efficacy and toxicity is largest for LSH001 >LSH002 >LSH003 based on these *in vitro* assays. However research has highlighted the limited relevance of *in vitro* data as they correlate poorly to *in vivo* data[348], which is not surprising as there are many factors that influence both efficacy and toxicity in humans.

The results described above were discussed with all the collaborators and based on the findings, 18 compounds were selected for in vitro ADME studies.

TABLE 5-3. ACTIVITY OF BENZOXABOROLE COMPOUNDS AGAINST INTRACELLULAR *LEISHMANIA* AMASTIGOTES - ED$_{50}$ VALUES (μM) AND 95% CI.

Compound ID	n	*L. tropica*	*L. major*	*L. aethiopica*	*L. mexicana*	*L. panamensis*
Amphotericin B	1	0.066 (0.062-0.070)	0.043 (0.037-0.049)	0.115 (0.107-0.122)	0.430 (0.394-0.460)	0.143 (0.131-0.156)
	2	0.083 (0.078-0.089)	0.049 (0.043-0.056)	0.107(0.096-0.119)	0.685 (0.553-0.692)	0.115 (0.093-0.142)
Miltefosine	1	19.99 (17.40-22.97)	44.85 (22.02-77.28)	7.79 (6.20-9.78)	31.04 (28.56-33.73)	19.98 (16.17-24.69)
	2	9.44 (7.78-11.45)	26.58 (21.30-33.15)	7.95 (7.26-8.69)	45.86 (36.61-57.45)	23.11 (20.41-26.18)
LSH001	1	2.01 (1.52-2.67)	4.26 (2.97-6.11)	22.10 (15.07-32.41)	23.04 (15.99-33.19)	18.82 (14.08-25.14)
	2	3.12 (2.38-4.09))	7.61 (5.48-10.57)	26.83 (19.40-37.11)	16.94 (9.62-29.83)	13.96 (10.06-19.44)
LSH002	1	14.96 (11.38-19.67)	16.52 (11.56-23.61)	> 30	> 30	> 30
LSH003	1	2.46* (1.78-3.41)	3.93 (3.32-4.64)	11.12 (7.67-16.13)	18.94 (10.78-33.29)	8.09 (6.56-9.96)
	2	3.94 (2.96-5.25))	3.10 (2.25-4.26))	> 30	> 30	19.05 (15.03-24.16)
LSH004	1	16.08 (13.70-18.80)	-	29.97 (19.04-47.16)	> 30	> 30
LSH005	1	6.81 (5.84-7.94)	-	21.25 (13.18-34.26)	> 30	> 30
LSH006	1	> 30	-	25.36 (15.88-40.50)	> 30	> 30
LSH007	1	5.71 (4.39-7.43)	-	27.18 (17.16-43.04)	> 30	> 30
LSH008	1	> 30	-	> 30	> 30	> 30
LSH009	1	3.08 (2.51-3.79)	-	17.66 (12.10-25.76)	> 30	> 30
LSH010	1	6.23 (5.49-7.06)	> 30	11.71 (7.22-19.00)	> 30	> 30
LSH011	1	2.31 (1.73-3.08)	9.92 (8.49-11.59)	> 30	> 30	> 30
	2	3.08* (2.12-4.48)	-	19.47 (11.41-33.23)	> 30	28.09 (22.50-35.07)
LSH012	1	24.61 (14.31-42.30)	9.52 (6.80-13.32)	> 30	> 30	> 30
	2	4.61* (3.53-6.01)	-	> 30	> 30	> 30
LSH013	1	> 30*	> 30	> 30	> 30	> 30
LSH014	1	5.91* (4.63-7.54)	4.15 (3.42-5.04)	> 30	> 30	29.59 (20.59-42.53)
LSH015	1	6.92 (4.95-9.66)	> 30	> 30	> 30	> 30
LSH016	1	5.40 (4.02-7.26)	> 30	21.84 (14.60-32.66)	> 30	> 30
LSH017	1	> 30	> 30	> 30	> 30	> 30
LSH018	1	> 30	> 30	> 30	> 30	> 30
LSH019	1	21.01 (4.07-108.4)	> 30	> 30	> 30	> 30
LSH020	1	> 30	> 30	> 30	> 30	> 30
LSH021	1	28.81 (17.03-48.74)	> 30	> 30	> 30	> 30
LSH022	1	> 30	> 30	> 30	> 30	> 30
LSH023	1	1.19* (0.78-1.80)	1.57 (1.17-2.10)	23.05 (10.09-52.62)	6.31 (4.18-9.54)	2.98 (2.28-3.90)
LSH024	1	4.72* (3.31-6.74)	13.96 (11.52-16.91)	> 30	> 30	22.34 (17.66-28.25)
LSH025	1	2.21* (1.51-3.25)	5.93 (5.08-6.92)	> 30	25.39 (15.81-40.78)	15.85 (12.85-19.56)

* The ED$_{50}$ was obtained using a clinical isolate of *L. tropica* instead of the *L. tropica* AO21/p strain that is generally used for screening purposes.
Where possible, the experiment was repeated. Clearly inactive compounds were not repeated. N=number of experiment repeats

TABLE 5-4. ACTIVITY OF BENZOXABOROLE COMPOUNDS AGAINST *LEISHMANIA* PROMASTIGOTES - ED$_{50}$ VALUES (µM) AND 95% CI.

Compound ID	n	*L. tropica*	*L. major*	*L. aethiopica*	*L.mexicana*	*L. panamensis*
Amphotericin B	1	0.011(0.002-0.066)	0.19 (0.16-0.22)	0.021 (0.018 0.023)	0.29 (0.22-0.39)	0.035 (0.030-0.042)
	2	0.040 (0.036-0.044)	0.032 (0.030-0.035)	0.048 (0.047-0.048)	0.30 (0.19-0.49)	0.041 (0.040-0.041)
Miltefosine	1	10.90 (10.32-11.46)	33.64 (26.25-43.10)	10.19 (9.50-12.21)	23.48 (18.82-29.28)	17.64 (15.27-20.39)
LSH001	1	0.030 (0.010-0.060)	3.80 (3.00-4.82)	2.27 (2.00-2.58)	5.24 (5.14-5.33)	1.28 (1.10-1.49)
LSH002	1	-	52.71	15.57 (13.54-17.91)	57.5	0.66 (0.50-0.85)
LSH003	1	0.03 (0.010-0.037)	4.55 (3.87-5.33)	3.76 (3.22-4.40)	5.30 (5.23-5.36)	2.57 (2.14-3.07)

TABLE 5-5. SUMMARY OF THE ED$_{50}$, ED$_{90}$, HILL COEFFICIENT AND CYTOTOXICITY AGAINST KB CELLS FOR THE THREE LEAD BENZOXABOROLE COMPOUNDS.

Compound ID	*L. tropica*	*L. major*	*L. aethiopica*	*L.mexicana*	*L. panamensis*
Amphotericin B					
EC$_{50}$	0.066; 0.083	0.049; 0.043	0.115; 0.107	0.430; 0.685	0.413; 0.115
EC$_{90}$	0.290; 0.297	0.216	0.247; 0.239	1.095; 1.211	0.286; 0.150
Hill coefficient (EC$_{50}$)	2.1/1.5	0.47/0.34	0.21; 0.19	0.26; 0.29	0.39; 0.42
Miltefosine					
EC$_{50}$	19.99; 9.44	26.58; 44.85	7.79; 7.95	31.04/45.86	19.98; 23.11
EC$_{90}$	25.13	29.44; 163.1	21.99; 19.50	38.02/102.8	166.3; 151.3
Hill coefficient (EC$_{50}$)	0.27	0.21; 0.18	0.18; 0.19	0.58/0.59	0.65; 0.67
LSH0014					
EC$_{50}$	2.01; 3.12	4.26; 7.61	22.10/26.83	23.04/16.94	18.82; 13.96
EC$_{90}$	48.49	12.74; 37.14	26.85	82.16	85.61; 84.74
Hill coefficient (EC$_{50}$)	0.08	0.14; 0.10	0.12; 0.10	0.09; 0.10	0.13; 0.16
Cytotoxicity ED$_{50}$	*46.28*	*46.28*	*46.28*	*46.28*	*46.28*
LSH002					
EC$_{50}$	14.96	16.52	>30	> 30	> 30
EC$_{90}$	-	17.79	95.46	25.47	-
Hill coefficient (EC$_{50}$)	0.05	0.09	-	-	0.22
Cytotoxicity ED$_{50}$	*61.58*	*61.58*	*61.58*	*61.58*	*61.58*
LSH003					
EC$_{50}$	2.46; 3.94	3.93; 3.10	11.12; > 30	18.94; > 30	8.09; 19.05
EC$_{90}$	19.74	14.21; 12.70	10.10	-	365.7
Hill coefficient (EC$_{50}$)	0.07	0.10; 0.07	0.11; 0.27	0.10; 0.94	0.09; 0.11
Cytotoxicity ED$_{50}$	*10.09*	*10.09*	*10.09*	*10.09*	*10.09*

5.3.2 IN VITRO ADME STUDIES-GENERAL PHARMACOKINETIC PREDICTIONS

Overall the benzoxaborole compounds had a good physicochemical profile for skin permeation (Table 5-6). All compounds had the desirable properties (1.3.1.1): a molecular weight below 500 g/mol, a log D (at pH 7.4) between 1-3, except for LSH002 and LSH032 and no more than 2 H-bond donor groups.

The experimental solubility of the test compounds in PBS (pH 7.4) ranged from 0.356 to over 250 μg/ml. Logically, the compounds with a more lipophilic character indicated by a high log D, demonstrated limited solubility in PBS as was seen for LSH001 and LSH031. On the other hand test compound LSH002 on the other hand exhibited a low log D and a high solubility in PBS.

TABLE 5-6. PHYSICOCHEMICAL PROPERTIES OF BENZOXABOROLE COMPOUNDS.

Compound	Molecular weight	H bond donor/acceptor*	Aqueous solubility** (μg/ml)	Aqueous solubility*** (μg/ml)	Log D (pH 7.4)
LSH011	273	2/3	304	259	1.56±0.03
LSH012	339	2/7	31	105	2.24±0.03
LSH026	306	2/4	22	29.5	1.86±0.07
LSH027	325	2/8	103	ND	1.53***
LSH028	334	2/6	53	ND	1.86±0.02
LSH029	393	2/11	14	ND	1.95±0.10
LSH001	387	2/5	9	0.356	> 2.63
LSH030	373	2/5	13	ND	1.94±0.06
LSH031	433	2/5	31	0.529	> 2.72
LSH002	421	2/5	37	> 250	0.44±0.06
LSH032	386	2/5	11	21.4	0.88±0.15
LSH033	400	2/5	7	122	1.70±0.15
LSH023	334	2/5	103	2.63	2.45±0.04
LSH024	368	2/6	45	6.69	2.16±0.07
LSH003	321	2/7	165	6.24	2.18±0.08

*/** Data obtained using ChemBio 3D Ultra 13.0 modeling software
*** Experimental data, based on 1 sample

DSC analysis revealed an endothermic peak indicating a melting point at 220ºC, 244ºC and 196º for LSH001, LSH002 and LSH003 respectively (see Appendix 2 for the respective DSC profiles).

The MDCK-MDR1 assay was conducted to assess the *in vitro* intrinsic permeability of the test compounds and to identify Pgp substrates. Compounds with a $P_{app+GF918}$ >50 nm/s were reported to have high intrinsic permeability across the intestine[345]. The intrinsic permeability of all compounds ranged from 141-699 nm/s and is considered high. Only compound LSH002 showed a low intrinsic permeability of 16.5 nm/s, Based on the AQ test results, it was suggested that there were no Pgp substrates (indicated by

an AQ value < 0.3) amongst the test compounds, except for LSH031 and LSH002 that had an AQ of 0.598 and 0.492 respectively. Amprenavir, the Pgp substrate control showed an AQ value of 0.846.
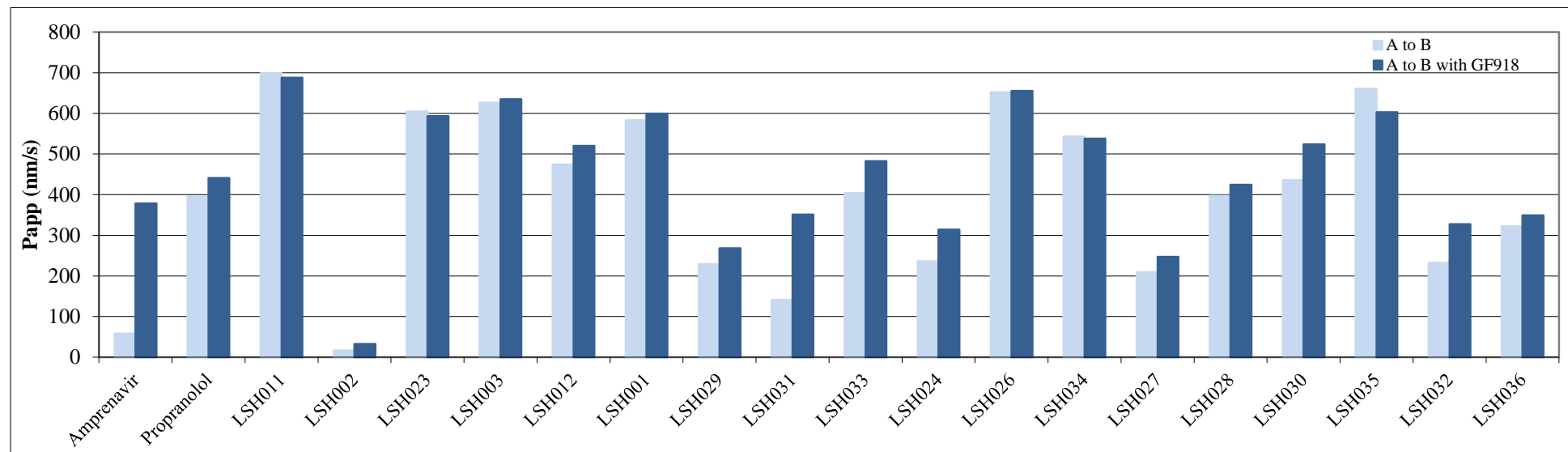
FIGURE 5-10. MDCK – MDR1 ASSAY – P$_{APP}$ (AB) VS P$_{APP}$ (AB IN PRESENCE OF GF918) FOR EACH TEST COMPOUND.

TABLE 5-7. SHOWS THE P$_{APP}$ VALUES WITH AND WITHOUT GF918 AND THE ABSORPTIVE QUOTIENT (AQ) FOR THE MDCK-MDR1 ASSAY

Compound	P$_{app}$(nm/s)	P$_{app}$ +GF918 (nm/s)	AQ	Compound	P$_{app}$ (nm/s)	P$_{app}$ +GF918 (nm/s)	AQ
Amprenavir	58.3	378	0.846	LSH030	436	524	0.168
Propranolol	395	441	0.104	LSH031	141	351	0.598
LSH011	699	688	-0.016	LSH002	16.5	32.5	0.492
LSH012	474	520	0.088	LSH035	660	603	-0.095
LSH026	652	655	0.005	LSH032	232	327	0.291
LSH034	543	538	-0.009	LSH033	404	482	0.162
LSH027	209	247	0.154	LSH023	605	593	-0.020
LSH028	397	424	0.064	LSH024	236	314	0.248
LSH029	229	268	0.146	LSH003	626	635	0.014
LSH001	583	599	0.027	LSH036	322	349	0.077

5.3.3 IN VITRO ADME STUDIES-SKIN PHARMACOKINETIC PREDICTIONS

5.3.3.1 METABOLISATION IN SKIN HOMOGENATE SUPERNATANT

The metabolisation of the test compounds in skin supernatant at 0.6 and 2.5 mg/ml protein content shown in Figure 5-12 and Figure 5-13 respectively. The paraben compounds are known substrates for skin esterases and were expected to break down quickly in presence of the skin supernatant (Figure 5-11). Propyl paraben was metabolised more quickly than ethyl paraben. This correlates with a previous report of its faster breakdown compared to butyl-and ethyl-paraben by rat skin microsomes where a series of parabens were tested[332]. The skin fractions were prepared using a similar methodology except for the extra step necessary to isolate the microsomes.

FIGURE 5-11. STRUCTURES OF ETHYL PARABEN (LEFT) AND PROPYL PARABEN (RIGHT).

Rapid drug metabolisation was seen during the first 30 minutes, followed by slower drug metabolism. As expected drug degradation occurred at a faster rate and to a greater extent at the higher skin protein concentration (2.5 mg/ml); the supernatant with lower protein concentrations is likely to contain less metabolising enzymes quickly leading to saturation. After two hours, compound recovery was 40 to 80% for the 0.6mg/ml and 25 to 60% for the 2.5mg/ml protein content skin supernatant respectively (Figure 5-12 and Figure 5-13).
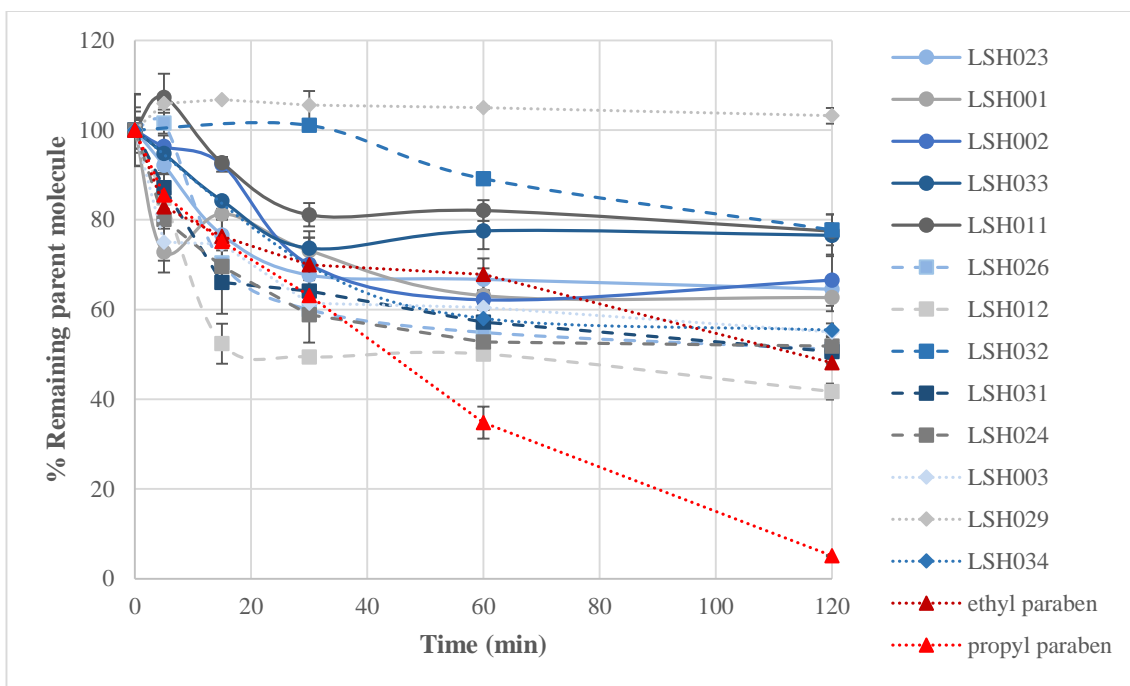
FIGURE 5-12. REMAINING TEST COMPOUND (%) IN SKIN SUPERNATANT (PROTEIN CONTENT 0.6MG/ML) AS A FUNCTION OF TIME (MEAN±SD; N=3).
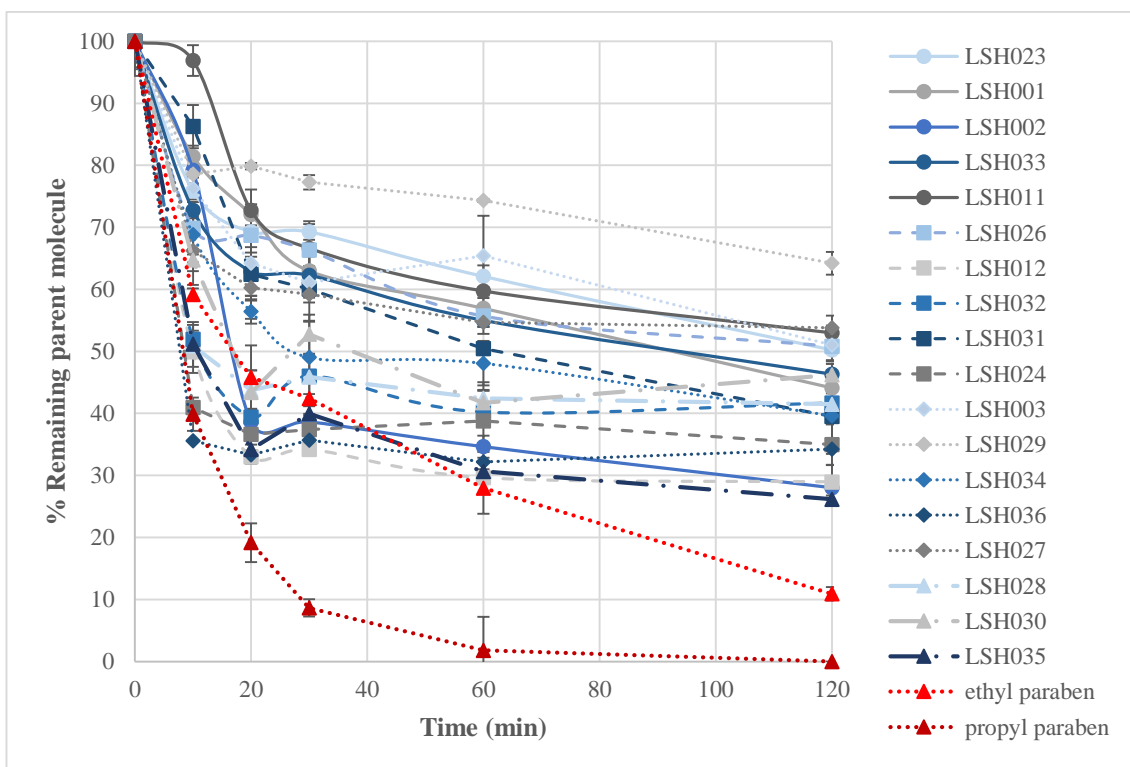
FIGURE 5-13. REMAINING TEST COMPOUND (%) IN SKIN SUPERNATANT (PROTEIN CONTENT 2.5MG/ML) AS A FUNCTION OF TIME (MEAN±SD; N=3).

Full-thickness BALB/c mouse skin was used to prepare skin tissue homogenate for two main reasons. First, epidermal membranes were reported to have reduced enzymatic activity in previous studies[349]. The process of heat separation was thought to have

damaged the enzymes and therefore care was taken to not overheat the skin homogenate at any stage of preparation. Second, the efficacy study will be conducted in female BALB/c mice and full-thickness female mouse skin was used to assure consistency between the *in vitro – in vivo* data set.

As for other *in vitro* pharmacokinetic data, these results should be interpreted with caution especially when translating to *in vivo* animal and human studies. The stability results presented here were obtained by incubating drugs in skin homogenate supernatant. Due to the homogenate preparation methodology, intracellular enzymes might have been released contributing to the breakdown of drugs in which case these results represent an overestimation of drug metabolism[333]. Furthermore the difference in mouse and human skin might contribute to additional error. A study comparing paraben breakdown in rat and human skin, observed a higher metabolism, in the order of magnitudes, for rat skin[350].

5.3.3.2 DRUG BINDING TO SKIN COMPONENTS

The binding assay showed large variations in unbound fractions among the benzoxaboroles; unbound fractions from 34% to 92% were observed (Table 5-8). In general, a high percentage unbound drug is preferable as it is the free fraction of the drug that is available to exert anti-parasitic activity[351]. However, contrary to oral drugs where tissue binding decreases the concentration of systemically available drugs, the binding of topically applied drug to skin components might be desirable as it could prolong the drug residence in the skin, preventing the drug being taken up in the bloodstream, which would lead to its eventual metabolism and excretion. In addition, drug binding to skin could provide a sustained release of free drug and thus sustained anti-parasitic activity.

TABLE 5-8. FRACTIONS OF UNBOUND COMPOUND AFTER 2 HOURS
INCUBATION WITH MOUSE SKIN SUPERNATANT.

Compound	% unbound
LSH011	85
LSH012	77
LSH026	92
LSH027	62
LSH028	60
LSH029	79
LSH001	87
LSH030	67
LSH031	92
LSH002	59
LSH035	74
LSH032	57
LSH033	65
LSH023	34
LSH024	50
LSH003	44
LSH036	66

No clear tendency was visible when trying to link stability or binding data to the structures of the compounds. A greater selection of test compounds would help to identify trends amongst the influences of different functional groups.

5.3.3.3 IN VITRO PERMEATION EXPERIMENT USING THE RHE MODEL

The permeation profiles of the compounds through RHE membrane are shown in Figure 5-14. The permeation of LSH002 was statistically significant higher compared to LSH001, LSH012, LSH029, LSH031 and LSH033 (one-way ANOVA, $p < 0.05$). Caffeine showed the highest permeation which was significantly higher compared to all the test compounds and testosterone after 6 hours (one-way ANOVA; $p < 0.05$).

When ranking the cumulative amount permeated over 6 hours, the rank order from high to low was as follows: caffeine > LSH002 > LSH003 > LSH011 > LSH023 > testosterone > LSH024 > LSH033 > LSH001 > LSH012 > LSH029 > LSH031.

The compounds caffeine and LSH002 were the two more hydrophilic compounds amongst the test compounds as was indicated by their log D value of -0.08 and 0.44 respectively. Hence, LSH002 even though in solution, might have been closer to saturation in the ethanol-Miglyol 840 (1:9) vehicle exhibiting a higher thermodynamic activity compared to the test compounds with a higher log D. Additionally, the higher permeation of LSH002 could involve the higher affinity of this compound for the RHE compared to the lipophilic vehicle thereby stimulating its partitioning into the RHE membrane.
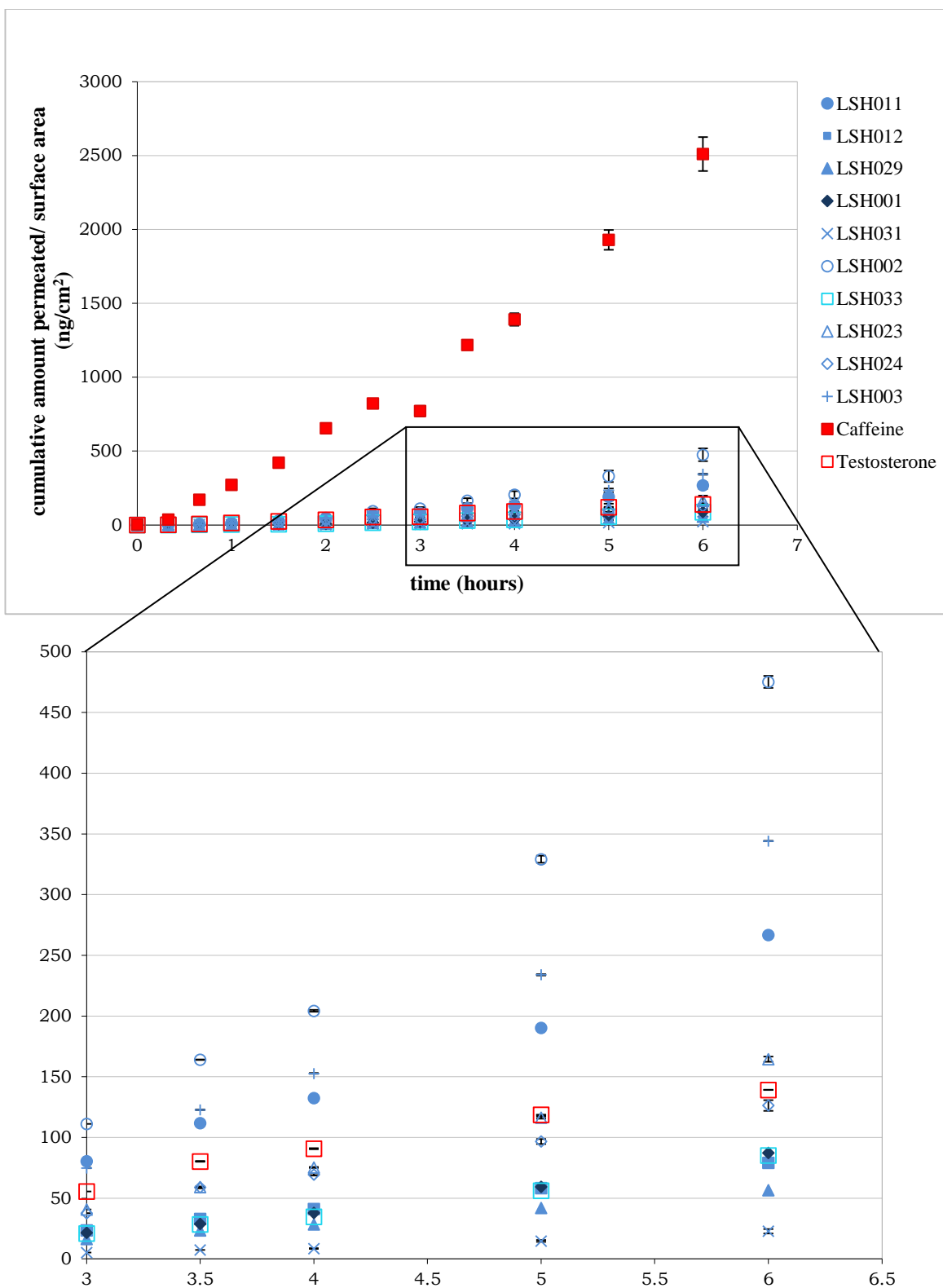
FIGURE 5-14. PERMEATION OF THE BENZOXABOROLE COMPOUNDS ACROSS THE RHE EXPRESSED AS THE CUMULATIVE AMOUNT PERMEATED PER SURFACE AREA AS A FUNCTION OF TIME (MEAN±SD; N=3).

Based on the overall data set collected at this stage, it was decided to select three compounds for further study. These compounds were LSH001, LSH002 and LSH003. LSH002 was included despite the fact that its activity against intracellular amastigotes was not evaluated but due to its higher solubility in water. LSH003 was selected because it was active against the 5 *Leishmania* species tested and it was ranked second from the top in the permeation assay. LSH001 was included because it showed good anti-leishmanial activity and was a more lipophilic compound compared to the other two selected compounds. Its permeation, however, was slightly below the permeation of our lipophilic reference permeant testosterone.

LSH023 was not selected as there was conflicting interest with a different project that was ongoing at Anacor Pharmaceuticals. Limited availability of LSH036 meant that this compound could not be taken further.

5.3.4 IN VITRO PERMEATION EXPERIMENTS USING BALB/C MOUSE SKIN

The objective of the first permeation study (FDC 1) was to verify the rank order of the three selected compounds and compare them with the results obtained from the previous permeation experiment where a RHE model was used. Therefore the experimental conditions were similar to the RHE experiment (Table 5-1). The results are shown in Figure 5-15 and indicate that the rank order LSH002 > LSH003 > LSH001 is maintained when using BALB/c mouse skin instead of the RHE membrane. Furthermore, the permeation of LSH002 through BALB/c mouse skin was significantly higher compared to LSH001, LSH003 and testosterone (one-way ANOVA, $p < 0.05$).
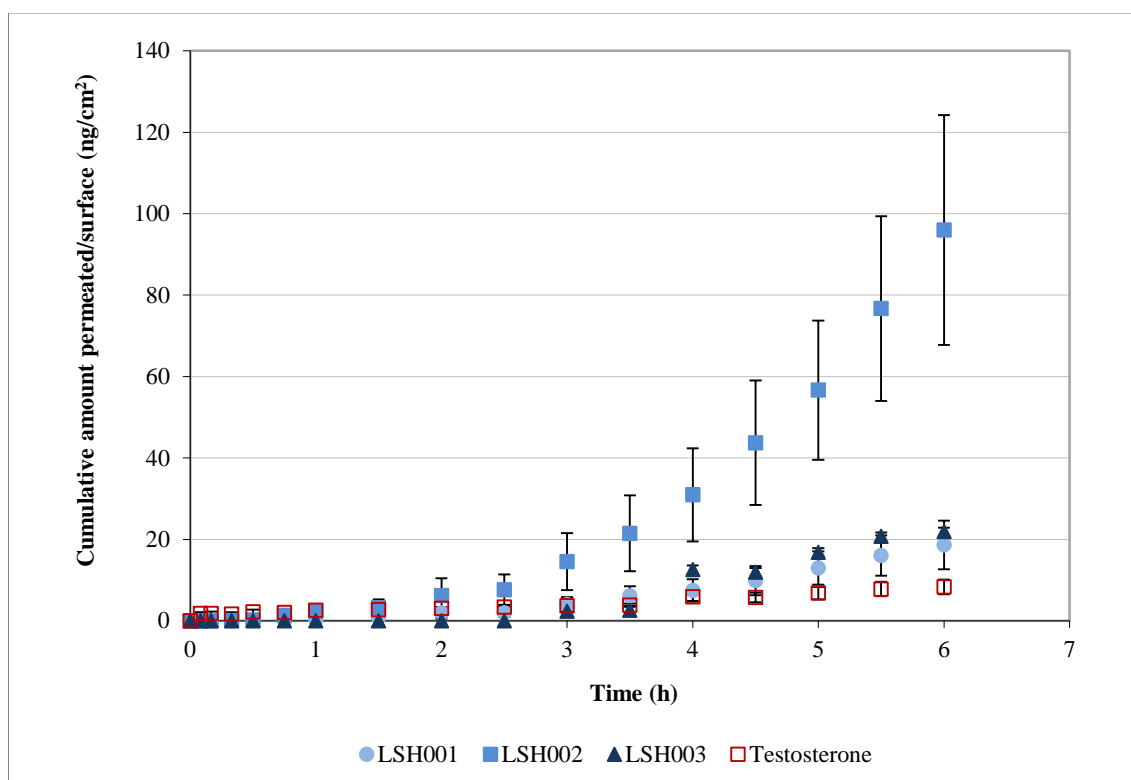
FIGURE 5-15. PERMEATION PROFILES OF THE 3 SELECTED BENZOXABOROLE COMPOUNDS THROUGH BALB/C MOUSE SKIN MEASURED IN FRANZ DIFFUSION CELLS (FDC 1) (MEAN±SD; N=3).

The overall permeation and thus flux of the test compounds and testosterone were lower when using mouse skin compared to the RHE (one-way ANOVA, $p < 0.05$) (Table 5-9). The lag time was not statistically significant for the test compounds when using different skin membranes (ANOVA, $p > 0.05$). This is not surprising as several studies have indicated that RHE is more permeable than animal or human skin[339, 352, 353].

TABLE 5-9. THE PERMEATION PARAMETERS: FLUX AND LAG TIME WHEN USING RHE AND BALB/C MOUSE SKIN (MEAN±SD; N=3 EXCEPT FOR * WHERE N=2)

	RHE	BALB/c
testosterone		
flux (ng/cm^2/h)	28.0±0.8	2.2±0.8
lag time (h)	0.7±0.1	1.1±0.6
LSH001		
flux (ng/cm^2/h)	21.8±0.1	6.6±0.3*
lag time (h)	2.2±0.1	2.4±0.4
LSH002		
flux (ng/cm^2/h)	143.9±44.2	35.8±0.9*
lag time (h)	1.7±0.8	2.8±0.3
LSH003		
flux (ng/cm^2/h)	45.1±5.9	8.0±1.5*
lag time (h)	2.1±0.1	2.5±0.3

A second permeation (FDC 2) using BALB/c mouse skin aimed to assess the permeation and skin disposition of the compounds after application of 1% drug in Ethanol-PG (1:1) solution ($28\mu l/cm^2$). The permeation of the test compounds is shown in Figure 5-16. A one-way between groups analysis of variance was conducted to explore the permeation differences between the test compounds. There was a statistically significant difference at the $p<0.05$ level for LSH001 compared to LSH002.
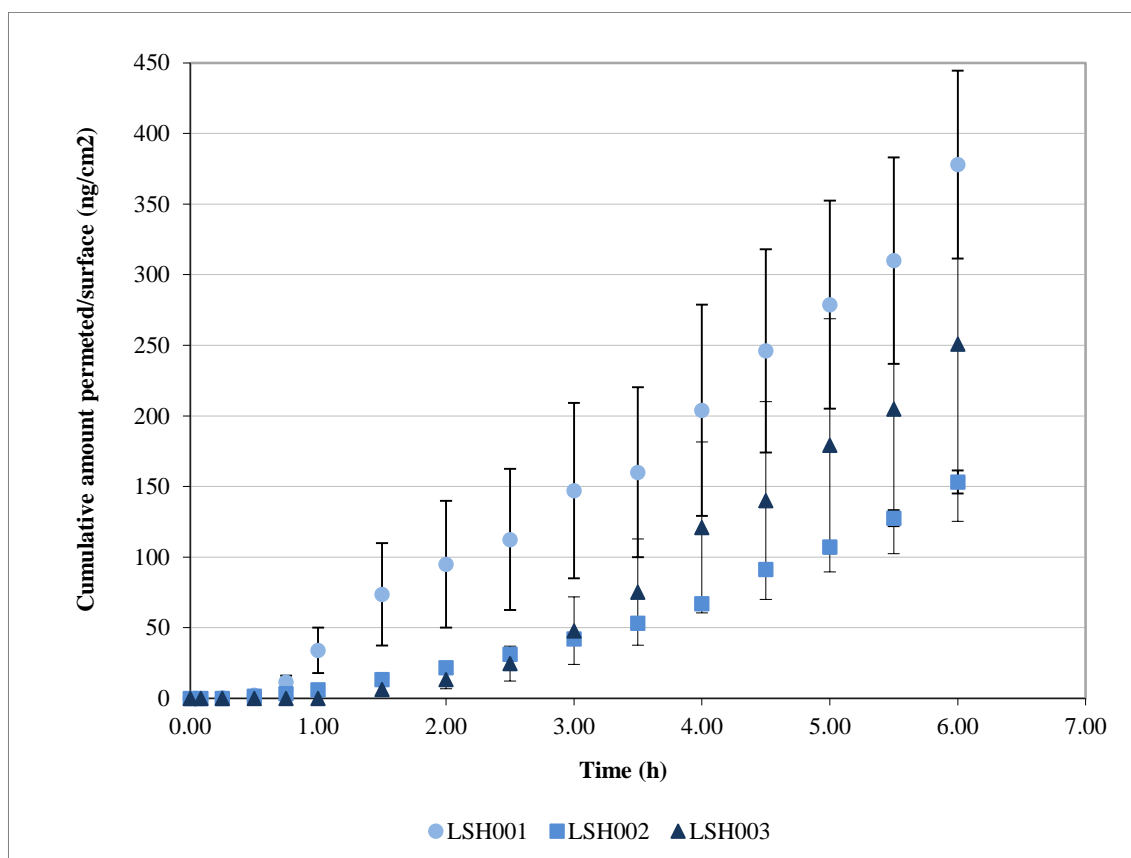
FIGURE 5-16. PERMEATION PROFILES OF THE 3 SELECTED BENZOXABOROLE COMPOUNDS ACROSS BALB/C MOUSE SKIN MEASURED IN FRANZ DIFFUSION CELLS (FDC2) (MEAN±SD; N=3).

The flux and lag time for the 3 different benzoxaboroles are indicated in Table 5-10. When ranking the flux from high to low, there is a difference in order when compared to the previous permeation experiments: LSH001 > LSH003 > LSH002. Interestingly the permeation for LSH002 was statistically significant lower compared to the other two compounds (one-way ANOVA; $p < 0.05$), in contrast to its higher permeation shown in Figure 5-14 and Figure 5-15.

TABLE 5-10. THE PERMEATION PARAMETERS: FLUX AND LAG TIME FOR FDC2
(MEAN±SD; N=3 EXCEPT FOR * WHERE N=2).

	Flux (ng/cm²/h)	Lag time (h)
LSH001	88.7±8.8	2.7±0.5*
LSH002	13.5±8.7*	2.7±0.7
LSH003	71.8±18.0	2.7±0.9

LSH001 and LSH003 where applied as suspensions with a maximal thermodynamic activity, while LSH002 was applied as a solution at about 80% of saturation and thus a suboptimal thermodynamic driving force (Table 5-11). Furthermore due to its hydrophilic nature, LSH002 is likely to have a higher affinity for the Ethanol-PG vehicle compared to the skin causing the drug to remain in the vehicle on the skin surface. There was no difference observed in the lag time for the different compounds (ANOVA; p >0.05).

TABLE 5-11. SOLUBILITY OF LSH001, LSH002 AND LSH003 IN THE PG/ETHANOL (1:1) VEHICLE (N=1).

	Solubility in PG (mg/ml)	Solubility in PG-Ethanol (1:1) (mg/ml)
LSH001	1.74	7.90
LSH002	5.87	12.63
LSH003	5.02	7.90

A mass balance study was conducted to quantify the amount of test compound that had permeated, was left on or inside the skin. The results are shown in Figure 5-17. Whilst there was no statistical significant difference between the amounts of compounds that had permeated over 24 hours, the amount of LSH001 in the skin was significantly higher in comparison to LSH002 and LSH003 (one-way ANOVA; p<0.05). In fact, about half of the applied drugs had permeated into the skin. Logically, the amount of LSH001 retrieved from the skin surface was significantly lower than for LSH002 and LSH003 (one-way ANOVA; p<0.05). Based on the solubility data presented in Table 5-11, it is clear that LSH001 and LSH003 were applied as a suspension. This means that the driving force for permeation was maximal. There was no statistical significant difference for the amounts of LSH002 and LSH003 that was found in and on the skin.
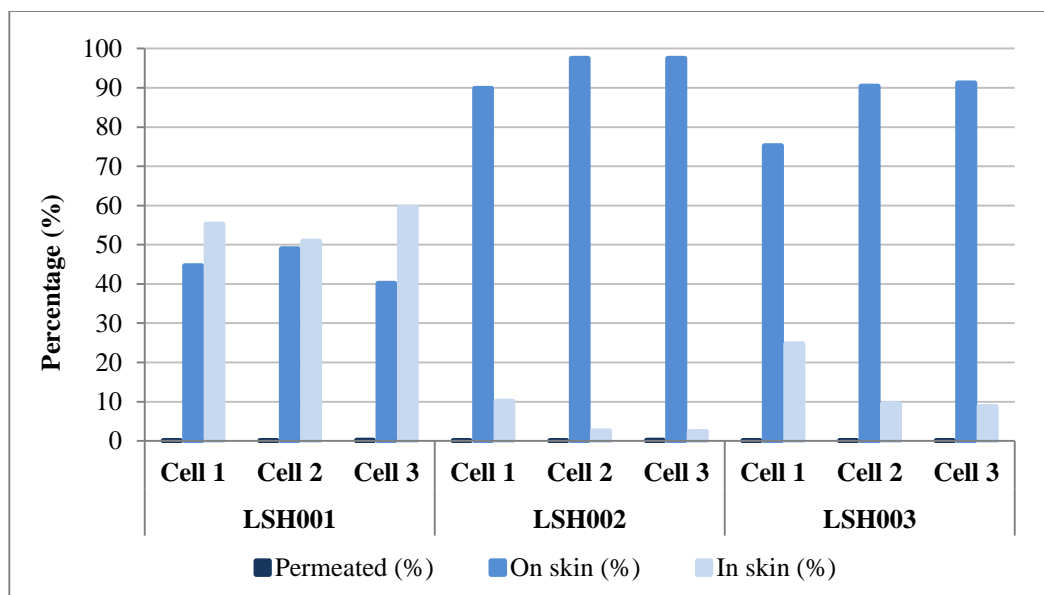
FIGURE 5-17. RESULTS OF THE MASS BALANCE STUDY WITH THE RETRIEVED AMOUNTS OF BENZOXABOROLES EXPRESSED AS PERCENTAGES.

5.4 CONCLUSION

Out of 25 benzoxaboroles tested for anti-leishmanial activity a few had appreciable activity against the 5 species tested. The benzoxaboroles were most potent against *L. tropica*. The Hill coefficient showed negative cooperativity and there was a two-fold difference between the drug-efficacy to cell cytotoxicity for two compounds tested.

The physico-chemical properties of the benzoxaboroles were favourable for skin permeation and the MDCK-MDR1 assay indicated good overall permeability and no Pgp substrates except for two compounds: LSH002 and LSH031.

The benzoxaboroles were degraded to some extent by skin enzymes but were more stable than the paraben compounds. Drug binding to skin components was variable and unbound fractions ranged from 34 to 92%. Permeation evaluation of the benzoxaboroles through reconstructed human epidermis showed LSH002 to be most permeable followed by LSH003 and LSH001. The rank order was replicated in Franz diffusion cells using BALB/c mouse skin when the same experimental conditions were used.

A second assay tested permeation of the compounds after finite dose application in a different vehicle. LSH001 showed the highest permeation followed by LSH003 and LSH002. Furthermore the amount of LSH001 in the skin was statistically significant higher compared to the two other compounds.

Ideally, the outcomes of each experiment would have been related to the chemical structures of the compounds. However it was difficult to allocate one specific outcome to a functional group.

6 EFFICACY OF BENZOXABOROLES AGAINST CL - IN VIVO STUDY

6.1 INTRODUCTION

The previous chapter explains how a range of benzoxaborole compounds was narrowed down to a selection of 3 compounds to be tested *in vivo* against experimental CL.

First, the activity of a series of benzoxaboroles with different chemical structures were tested against intracellular amastigotes of 5 different *Leishmania* species Based on the efficacy results, 18 compounds were subjected to a batch of *in vitro* ADME experiments that focussed on general permeability properties. The partition/distribution coefficient and solubility were determined and the permeability was measured in the MDCK-MDR1 assay. In a second phase, more stringent *in vitro* ADME experiments focussed on dermatopharmacokinetic parameters including stability and binding in skin supernatant and permeation assays with the EpiDerm® model. Finally, a last permeation using BALB/c mouse skin was conducted followed by a mass balance study, whereby the amounts of drug left in and on the skin where analysed.

To summarize, the 3 selected compounds showed (i) anti-leishmanial activity against a range of species, (ii) a physico-chemical profile conductive to skin permeation, (iii) acceptable stability in skin homogenate supernatant; (iv) variable binding in skin homogenate supernatant and (v) different skin disposition profiles from one another.

The next step is the *in vivo* efficacy testing of the selected benzoxaborole compounds LSH001, LSH002 and LSH003 against experimental CL upon oral and topical administration. Literature describes different CL rodent models, however, mainly mice are used. Generally, the course of infection and clinical symptoms depend on the genetic background of the mouse, the parasite strain, the place of injection and inoculum injected[354, 355]. For this study, susceptible BALB/c mice were infected subcutaneously with *L. major* (MHOM/SA/85/JISH118) which resulted in the development of large ulcers that did not heal without intervention.

There are different methods available to assess the leishmanicidal effect of a treatment in models. As a minimum, the progression of the lesion size is followed by measuring the diameter in two directions using callipers. This technique is non-invasive and allows daily evaluation. Expansion of the lesion, however, is three dimensional and therefore,

volume measurements would be more correct. Unfortunately they are difficult to obtain in practical situations.

Moreover lesion size could misrepresent the parasite load as inflammation and secondary infection contribute to volume and diameter increase[354]. Hence, determination of parasite loads in addition to lesion size measurements represent a more rigorous way to evaluate drug efficacy. The establishment of the parasite burden, as described below, requires tissue sampling and thus requires extra animals or is only performed at the end of the treatment to compare parasite loads between different treatment groups at the end of the study.

Determination of the parasite burden can be performed by microscopic techniques that determine the viable parasite counts with[356] or without[357] prior staining but these methods are time consuming, subjective and accuracy can vary when the parasites are not homogeneously dispersed[358]. Limiting dilution assays[355, 359, 360] are more sensitive but remain labour-intensive[361]. More recently recombinant bioluminescent *Leishmania* parasites were generated to follow the infection *in vivo* [362-365] but is limited by a lengthy optimisation. We therefore developed a real-time quantitative polymerase chain reaction (qPCR) method as it allows quick, sensitive and accurate quantification of the parasite load in a CL lesion.

6.1.1 REAL-TIME QUANTITATIVE PCR

The traditional end-point polymerase chain reaction (PCR) is a semi-quantitative technique that produces a high number of target sequences that can be visualised by subsequent agarose gel separation with ethidium bromide. This type of PCR typically has poor precision and low sensitivity and real-time qPCR was developed to circumvent these limitations.

The first report on the use of real-time qPCR originated in the early 1990's and described how a video camera recorded the increase in fluorescence for each PCR cycle[366]. Further use of this technique was delayed by the high price and limited commercial availability of thermocyclers but now, qPCR is widely used for a number of applications including measuring mRNA expression levels, DNA copy numbers and allelic discrimination[367].

Real-time qPCR allows the detection and quantification of the target products as they are generated during each cycle of the polymerase chain reaction. The numbers of DNA copies are proportionate to the amount of template in the sample prior to the start of the PCR process when measured in the exponential phase of the reaction. The use of a standard curve that is prepared from dilution series of a known concentration of template, allows the quantification of the DNA material in the unknown sample.

The amount of DNA generated is measured using a fluorescent signal that is obtained by adding dyes to the reaction. Two main groups of dyes are available: probes and SYBR® Green. SYBR® Green displays a relatively low fluorescence that increases by 1000-fold when bound to double-stranded DNA. The more binding sites available for the dye, the higher the fluorescent signal.

Alternatively, a more specific level of detection is obtained using probes with a specific target sequence. When unbound, the fluorescent probe is not hybridized and remains quenched. There is no fluorescence detectable. Upon the presence of the target sequence, the probe will bind to the DNA and the quencher will be removed. A fluorescent signal is detectable (Figure 6-1).
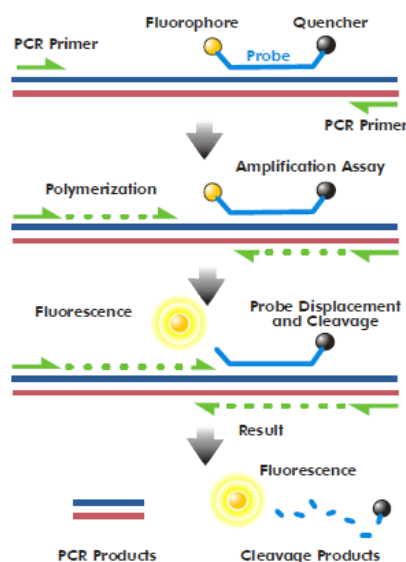
FIGURE 6-1. DUAL-LABELLED PROBE CHEMISTRY MECHANISM. THE PROBE RELIES ON THE 5'-3' NUCLEASE ACTIVITY OF THE DNA POLYMERASE TO RELEASE THE FLUOROPHORE DURING THE HYBRIDISATION TO THE TARGET SEQUENCE (ADAPTED FROM [368])

The first real time qPCR methods used to quantify *Leishmania* parasites in tissue were described a little over 10 years ago[358, 369]. Bretagne et al designed a qPCR assay using TaqMan probes targeting *Leishmania* and mouse DNA sequences to relatively quantify

the number of *L. infantum* present in mouse liver. The outcome of the assay was compared with the results obtained from a culture microtitration conducted in parallel and showed a correlation coefficient of 0.66[358]. Another publication described how a conventional PCR method was adapted into a real-time qPCR method. This method targeted kinetoplast DNA (kDNA) and used SYBR® green I to follow the amplification of the target sequence in time. They reported successful quantification up till 0.1 parasite per reaction for four different *Leishmania* species in mouse tissue[369].

Later, Van Der Meide et al compared 3 methods for the detection and quantification of *Leishmania* parasites in blood and CL skin tissue from patients in Brazil[370]. All methods targeted an 18S ribosomal gene, a multiple-copy gene that is homologous for all *Leishmania* species[371]. Two methods, quantitative nucleic acid sequence-based amplification (QT-NASBA) and quantitative real-time reversed transcriptase PCR (qRT-PCR) detected and amplified ribosomal RNA (rRNA), while the other method, real-time qPCR, amplified ribosomal DNA (rDNA). Because rRNA copy numbers are approximately 100 times more abundant than rDNA[372], a lower sensitivity was expected for the latter method.

qRT-PCR is similar to qPCR but the reaction requires a reversed transcriptase step that transcribes the RNA into the complementary DNA. QT-NASBA is similar to the qRT-PCR method but it is based on an isothermal reaction and does not require a thermocycler. Overall QT-NASBA and qRT-PCR performed better than real-time qPCR with a higher regression coefficient and a higher reaction efficiency for qRT-PCR. Furthermore they showed a 10-fold higher sensitivity with a limit of detection of 100 parasites/ml compared to the real-time qPCR method as was expected because the latter only targeted DNA.

The real-time qPCR that we developed for our project targeted the same 18S ribosomal target gene that was described in the Van Der Meide paper discussed above. We chose to target DNA and not RNA because the data obtained when using real-time qPCR is more robust and generally applicable[373]. This is because the information within the genome is the same for every cell whereas the transcriptome (RNA) expression is variable.

6.2 MATERIALS AND METHODS

6.2.1 MATERIALS

TABLE 6-1. DETAILS OF THE MATERIALS USED FOR THE EXPERIMENTS DESCRIBED IN CHAPTER 6.

Compound	Specifications	Supplier
Chemicals and test reagents		
LSH001, 002, 003	LC-MS/MS and ^{1}H-NMR identification	Anacor Pharmaceuticals
Leshcutan	15% paromomycin sulfate, Teva (Israel)	IsraelPharm
AmBisome®	-	DNDi donation
Propylene glycol	500 ml	Sigma Aldrich
Ethanol	99.7-100%, AnalaR	VWR International
Dextrose	Anhydrous	Sigma Aldrich
Sodium carboxymethylcellulose	Mw ~ 250,000	Sigma Aldrich
Benzylalcohol	99.8%, anhydrous	Sigma Aldrich
TWEEN® 80	-	Sigma Aldrich
Sodium chloride	> 99.5%, anhydrous	Sigma Aldrich
PCR and qPCR		
DNeasy® Blood and Tissue kit	50 reactions	Qiagen
KAPA probe fast universal	500 reactions, KK4702	Anachem
KAPA 2G Hot Robust mix	100 reactions, KK5532	Anachem
Forward primers mouse/leish	Sequences specified below, 25nmoles	Sigma Aldrich
Leishmania probe	FAM fluorophore, 100μM	LifeTechnologies
Other materials		
Bunion cushions	Self-adhesive, Superdrug	Superdrug

6.2.2 DRUGS AND FORMULATION PREPARATION

AmBisome®, a liposomal formulation of amphotericin B for injection was kindly provided by DNDi (Geneva) and prepared according to manufacturer's recommendations. Briefly, AmBisome® powder was reconstituted with 12ml of cold sterile MilliQ water to produce a 4 mg/ml amphotericin B liposomal suspension. This suspension was vigorously shaken and incubated at 65ºC for 10 minutes after which it was allowed to cool to room temperature. This dispersion was diluted with sterile 5% dextrose solution (w/v) to obtain a final suspension of 0.5mg of amphotericin B/ml.

The experimental topical formulations containing LSH001, LSH002 and LSH003 respectively were prepared 24 hours prior to the start of dosing. For each test compound, the following procedure was conducted. An excess amount of the test compound was added to a 1:1 (v/v) mixture of propylene glycol (PG) and ethanol (Ethanol). The mixture was left to stir overnight after which it was centrifuged at 13000

rpm for 15 minutes. The supernatant, i.e. a saturated solution was pipetted into a clean vial and used to apply on mice.

The standard suspension vehicle used to prepare the oral formulations was prepared by weighing and adding each component (0.5% (w/v) carboxymethylcellulose, 0.5% (v/v) benzyl alcohol, 0.4% Tween 80 (v/v) in a 0.9% (v/v) NaCl solution) into a clean recipient. The mixture was left to stir overnight at room temperature prior to sterilisation by autoclaving. The experimental oral formulations containing either LSH001, LSH002 or LSH003 in the vehicle were prepared by adding the appropriate amount of test compound to the vehicle in order to obtain a final concentration of 2.5mg/ml. The suspension was sonicated for 30 minutes and was used as such. All formulations were stored at 4˚C throughout the experiment.

6.2.3 EXPERIMENTAL CL MODEL

For this study, 60 female BALB/c mice (6-8 weeks old; Charles River Ltd., UK) were infected as described previously in section 3.1.3. Approximately 7 days post infection, small nodules were visible. The lesion size was recorded daily and when they reached a diameter of 5 mm, the mice were randomly allocated in groups of 6 and drug administration was started.

In an attempt to increase the contact time between the topical formulations and the CL lesion, an auto-adhesive corn plaster was cut to appropriate size and stuck on the skin around the nodule as seen in Figure 6-2. This prevented the mice from licking and thus removing the topical formulation.

FIGURE 6-2. CORN PLASTER ON THE RUMP OF A MOUSE.

Formulations were administered over a period of 10 days. The details of the administration regimens are shown in Table 6-1. Figure 6-3 shows the experimental design of the *in vivo* study including the different test groups.

Treatment efficacy was evaluated by lesion size progression. To do so, the lesion diameter was measured in 2 directions on a daily basis using digital callipers. The average diameter was plotted as a function of time. Statistical differences between the average diameters per group on the last day of treatment was performed using one-way

ANOVA with post-hoc Tukey test (SPSS software version 19.0). Three days after the end of treatment, the mice were sacrificed and the lesion was excised and stored at-80ºC until the parasite load was quantified using real-time qPCR. Statistical differences in the average parasite numbers amongst different groups were analysed using one-way ANOVA with Tukey post-hoc test (SPSS software, version 19.0)

6.2.4 EXPERIMENTAL DESIGN

Day 0 - Infection

- *L. major* JISH 118

- 200μl - $2x10^7$ promastigotes

- s.c injection on rump

Day 11 – Start drug administration

Controls:

    Group 1 - Untreated control (negative control)

    Group 2 - Topical vehicle control

    Group 3 - AmBisome® (positive control)

    Group 4 - Leshcutan® ointment (topical positive control)

Experimental formulations:

    Group 5 - Topical administration with LSH001

    Group 6 - Topical administration with LSH002

    Group 7 - Topical administration with LSH003

    Group 8 - Oral administration with LSH001

    Group 9 - Oral administration with LSH002

    Group 10 - Oral administration with LSH003

Day 20 – Last dose

Day 23 – Sacrifice animals

Collection lesions

FIGURE 6-3 SHOWS THE DESIGN OF THE *IN VIVO* STUDY CONDUCTED WITH THREE COMPOUNDS OF INTEREST LSH001, LSH002 AND LSH003.

Group	Formulation	Active compound	Vehicle	Administration route	Treatment regimen
1	Untreated control	None	None	None	None
2	AmBisome®	Amphotericin B	Dextrose 5%	IV	25mg/kg/b.i.d, 5 doses
3	Leshcutan®	Paromomycin sulphate 15%	Methylbenzethonium chloride 12% in vaseline	Topical	0.1ml 2/day for 10 days
4	Vehicle control	N/A	PG/Ethanol (1:1)	Topical	2x50µl/day for 10 days
5	Topical formulation 1	LSH001			
6	Topical formulation 2	LSH002	Saturated drug solution in PG/Ethanol (1:1)	Topical	2x50µl/day for 10 days
7	Topical formulation 3	LSH003			
8	Oral formulation 1	LSH001			
9	Oral formulation 2	LSH002	Standard suspended vehicle	Oral	2x25mg/kg/day for 10 days
10	Oral formulation 3	LSH003			

6.2.5 *QUANTIFICATION OF THE PARASITE LOAD IN A CL SKIN LESION*

1.1.1 PRIMERS AND PROBES

The primer pair and probe, previously designed and validated by Van Der Meide et al[370] targeted a 170-bp region in the *Leishmania* 18S ribosomal gene and are specific for all *Leishmania* species. The respective sequences are shown in Table 6-3.

TABLE 6-3. THE SEQUENCES OF THE PRIMER AND PROBES USED IN THE PCR AND qPCR REACTIONS.

	Gene	Primer/probe	Primer Sequence
***Leishmania* species**	18S rDNA (170-bp)	Forward primer	5'-C CAA AGT GTG GAG ATC GAA G-3'
		Reverse primer	5'-GGC CGG TAA AGG CCG AAT AG-3'
		Probe	5'-6FAM ACCATTGTAGTCCACACTGC-NFQ-MGB

6.2.5.1 DNA EXTRACTION FROM THE CL LESION

On the day of extraction the lesions were defrosted and cut into 2. One half was weighed and cut into fine pieces with a surgical blade before placing in a microcentrifuge tube. The DNA was then extracted using the DNeasy® blood and tissue kit (Qiagen).

Briefly, for each 25mg of tissue, 20µl of proteinase K and 180µl of ATL buffer were added and mixed, after which the mixture was incubated in a water bath at 56°C for 5 hours. At regular time intervals, the sample was vortex-mixed to obtain a homogeneously digested sample. Subsequently, AL buffer was added in the appropriate ratio followed by a further 10 minutes incubation at 56°C. The DNA was precipitated by adding ethanol and the sample was transferred onto a spin column. The DNA was retained on the column during the multiple washing steps and then eluted with the AE buffer. The purity and concentration of DNA was analysed using the nanodrop ND1000 spectrophotometer.

6.2.5.2 CONFIRMATION OF THE PRODUCT SIZE BY PCR

Conventional PCR was performed to confirm the presence of PCR product of the correct size and hence to verify primer efficacy. 1µl of a 1/100 dilution of the DNA extract was amplified in a final volume of 10µl containing 2µl of KAPA 2G buffer (Kapa Biosystems, Wilmington, MA) and primers at a concentration of 0.4µM. The samples were run in a G-Storm GS4 machine (Somerset, UK). The amplification cycle started with a denaturation step at 95°C for 3 minutes followed by 40 cycles of 95°C for 15s, 60°C for 1 minute and 72°C for 30 seconds with a final extension of 72°C for 30 seconds. Each run contained a negative sample whereby the extracted DNA was replaced by MilliQ water and positive cDNA control. The PCR products were separated on a 3% agarose gel stained with ethidium bromide and visualised under UV light. A 100-bp DNA ladder was run in parallel with the samples. The band obtained for the *Leishmania* target sequence was 170bp long.

6.2.5.3 EXPERIMENTAL SETTINGS FOR REAL-TIME QPCR

For the amplification reaction, 2µl of a 1/100 diluted DNA sample was added to 8µl mix containing 5µl KAPA Probe Fast qPCR master mix (2x) (Kapa Biosystems, Wilmington, MA), 0.4 µM of each primer and 0.25µM of the appropriate probe. The tubes were placed in the 72 sample rotor of the instrument (Rotor Gene 3000, Qiagen) and the reaction with the following conditions was initiated: 95°C for 3 minutes followed by 40 cycles of 95°C for 3 seconds and 60°C for 30 seconds. Each run contained a standard curve, a no-template-control and a negative control.

6.2.5.4 STANDARD CURVES FOR LEISHMANIA TARGET DNA

The standard curves were prepared and validated prior to the start of the experiment and were stored at -80ºC.

In preparation of the standard curves, amastigotes were extracted from a BALB/c CL lesion. To do so, the lesion was homogenised in RPMI-1460 medium containing 1% penicillin/streptomycin. The homogenate was centrifuged at 800rpm for 10 minutes in order to remove pieces of skin tissue and other cellular material. The supernatant was transferred to a new vial and centrifuged for 15 minutes at 1500rpm. The amastigotes were washed and re-suspended in PBS.

They were microscopically counted using a Thoma haemocytometer and diluted to 1×10^8 amastigotes/ml. The DNA of 200µl of this suspension was extracted and purified using the DNeasy® Blood and Tissue kit from Qiagen as explained above (6.2.5.1). The amount of DNA and purity of the sample were verified using the Nanodrop ND1000 spectrophotometer. Ten-fold serial dilutions (from 1×10^8/ml to 1 amastigote/ml) were made and analysed in duplicate by real-time qPCR in order to determine: (i) the analytical sensitivity i.e. the minimum number of copies in a sample that can be measured accurately; (ii) the repeatability i.e. the precision and robustness of the assay when the same samples are analysed in the same run, (iii) the reproducibility of the assay i.e. the variation between different runs and (iv) the efficiency of the qPCR assay.

Two quality control samples were prepared by spiking skin homogenate with either a high (2×10^7) or low (2.5×10^3) number of amastigotes. The samples were processed in the same way as the standard curve samples and were included in duplicate to verify the accuracy of the assay. The target variation for accuracy was 80-120%.

Quantification of *Leishmania* parasites was obtained by plotting the parasite concentrations against the C_T values with linear regression (Rotor-Gene Analysis Software 6.1). The amplification efficiency and r^2 value were calculated based on the slope and the intercept of the equation describing the standard curve. The intra- and inter-assay variability was established and calculated as the coefficient of variation for each concentration of parasites and for each duplicate.

6.3 RESULTS AND DISCUSSION

6.3.1 VALIDATION OF THE QPCR METHOD

6.3.1.1 TARGET SEQUENCE VERIFICATION BY PCR

The *Leishmania* DNA sequence band of 170bp was visible. This indicated that the primers had successfully amplified the target sequence.

400 bp

300 bp

200 bp

170 bp – *Leishmania* target sequence

100 bp
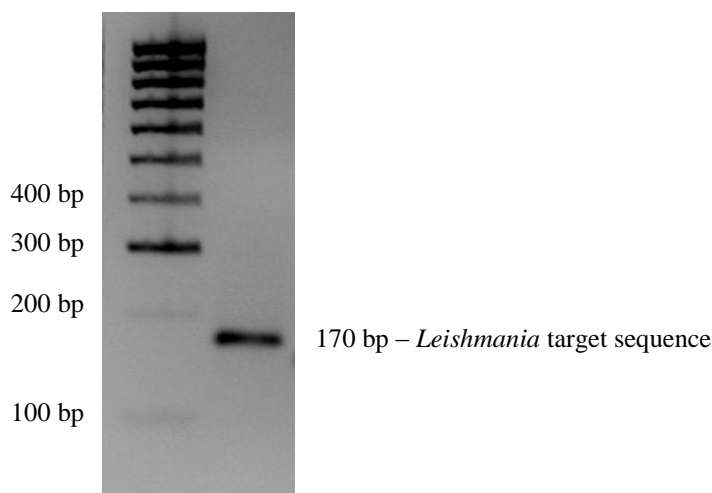
FIGURE 6-4. GEL ELECTROPHORESIS RESULTS SHOWING SUCCESSFUL MULTIPLICATION OF THE *LEISHMANIA* DNA TARGET SEQUENCE BY PCR.

6.3.1.2 VALIDATION OF THE STANDARD CURVES FOR THE LEISHMANIA TARGET SEQUENCE

Table 6-4 shows the coefficient of variation (CV) (standard deviation/average x 100) that was calculated for each amastigote concentration of the standard curve within one run (intra-assay variation) and between three separate runs (inter-assay variation). The intra-and inter-assay variability ranged from 0.11-2.24% and 4.94-15.06% respectively. Both are comparable with values found in literature[370, 372, 374]. The inter-assay is higher especially towards the dilutions that contain more amastigotes. Due to the higher variation seen in the inter-assay variability, it was decided to include a standard curve in each run.

The fluorescent signal for the no-template and negative control did not reached the detection threshold indicating that there was no contamination of reagents and primer dimer did not occur.

Log input (parasites/ml)	Intra-assay variation (%)			Inter-assay variation (%)
	Run 1	Run 2	Run 3	
8	1.63	1.80	0.05	15.06
7	1.49	0.98	1.19	10.47
6	0.94	2.04	0.68	9.41
5	0.73	0.34	0.69	7.90
4	0.22	0.14	1.45	6.86
3	0.11	2.24	0.34	4.94
2	1.95	0.46	0.68	6.06

The CV of accuracy of the method near the detection limits was 8.3 and 17.5% for the sample containing a high and low number of amastigotes respectively. The accuracy was lower for the low amastigote number sample, this could have been caused by a relatively higher loss of DNA for samples containing a low count of amastigotes compared to samples with initially higher DNA material during the extraction/purification process.

Table 6-5 shows the amplification parameters for the qPCR reaction targeting the *Leishmania* 18S rDNA. The high r^2 values confirm the linearity range of the amplification reaction for serial dilutions ranging from 1×10^8 parasites to 100 parasites/ml with the latter as limit of detection. The efficiency of the reaction ranged from 0.88-0.89, these were similar to values found in literature[370].

TABLE 6-5. QPCR PARAMETERS - REGRESSION COEFFICIENTS (R^2), AMPLIFICATION EFFICIENCY AND EQUATIONS OF THE STANDARD CURVES TESTED.
(* E= $(10^{1/SLOPE}-1) \times 100\%$; ** Y=$C_T$ VALUE; X=LOG(NUMBER OF PARASITES))

Parameter	Run 1	Run 2	Run 3
r^2	0.996	0.998	0.998
Efficiency (%)*	89	88	88
Equation**	y=3.606x+42.197	y=-3.654x+39.163	y=-3.662x+42.084

6.3.2 EXPERIMENTAL FORMULATIONS

The 3 topical formulations (Figure 6-5) were applied as saturated solutions with maximal thermodynamic activity of 1. The solubility of the test compounds in the vehicle (PG-Ethanol 1:1) was not measured due to little compound availability. However, LSH002 was more soluble in the vehicle compared to LSH001 and LSH003 and required more drug to obtain a saturated solution. When applying Fick's law to the

passive process of diffusion that occurs upon application of the topical formulation, the concentration gradient between the formulation and the SC is expected to be higher for LSH002 compared to LSH001 and 003.

The oral formulations are shown in Figure 6-5. Even though they are all suspensions, LSH002 was clearly more soluble in the vehicle compared to LSH001 and LSH003. This could influence the bioavailability of the drugs upon administration.
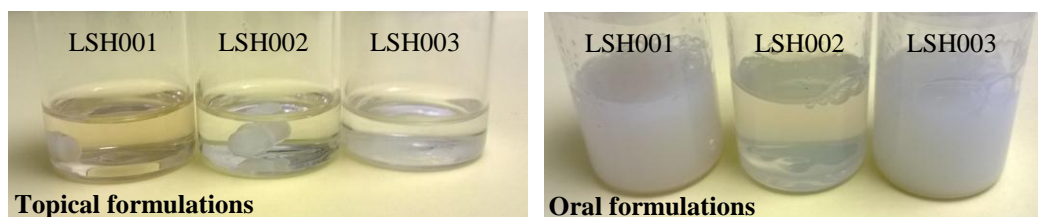
FIGURE 6-5. SHOWS THE EXPERIMENTAL TOPICAL AND ORAL FORMULATIONS.

6.3.3 EVALUATION OF THE LESION SIZE PROGRESSION

Figure 6-6 shows the evolution of the mean lesion size for each group as a function of time. A reduction of lesion size is seen for the groups receiving the AmBisome® and LSH003 oral treatment. LSH001 halted the lesion size growth upon topical application. All other groups showed disease progression as the lesion size increased in time.
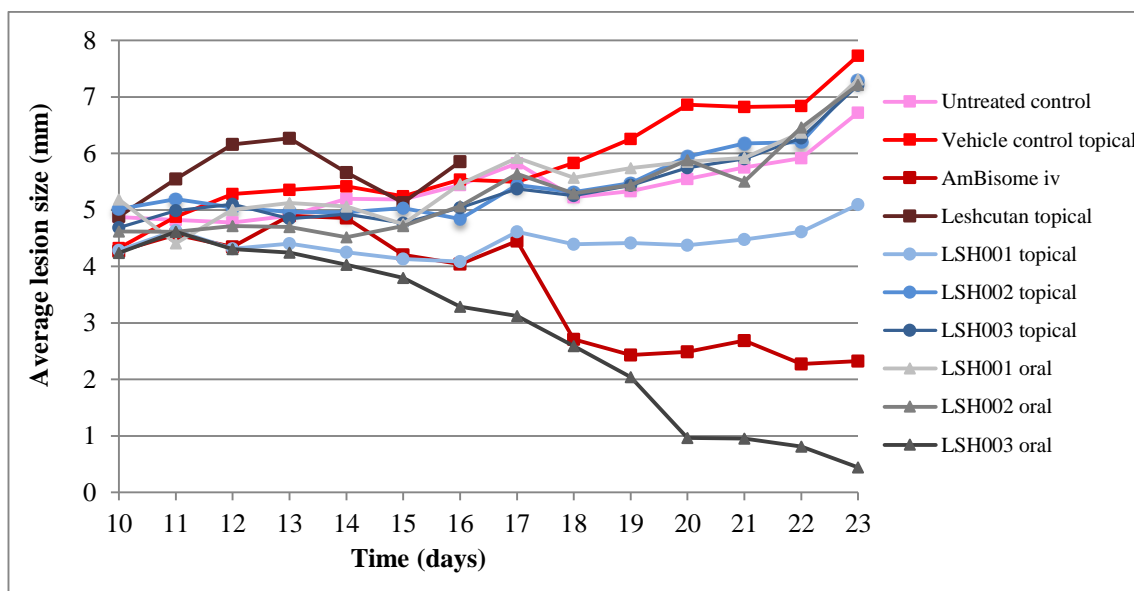
FIGURE 6-6. MEAN LESION SIZE PROGRESSION PER GROUP IN FUNCTION OF TIME POST INFECTION (N=6) (SEE APPENDIX FOR GRAPH WITH ERROR BARS).

The difference in lesion sizes between the groups on day 20 (= last day of drug administration) is also demonstrated in Figure 6-7. A statistically significantly lower lesion size for the experimental groups LSH001 topical and LSH003 oral compared to

the relevant control groups was observed on the last day of treatment (One-way ANOVA, p<0.05). Moreover, there was a statistically significant difference between the average lesion diameter for the AmBisome® and all the other groups (p<0.05) except for the LSH001 topical and LSH003 oral groups (p>0.05).
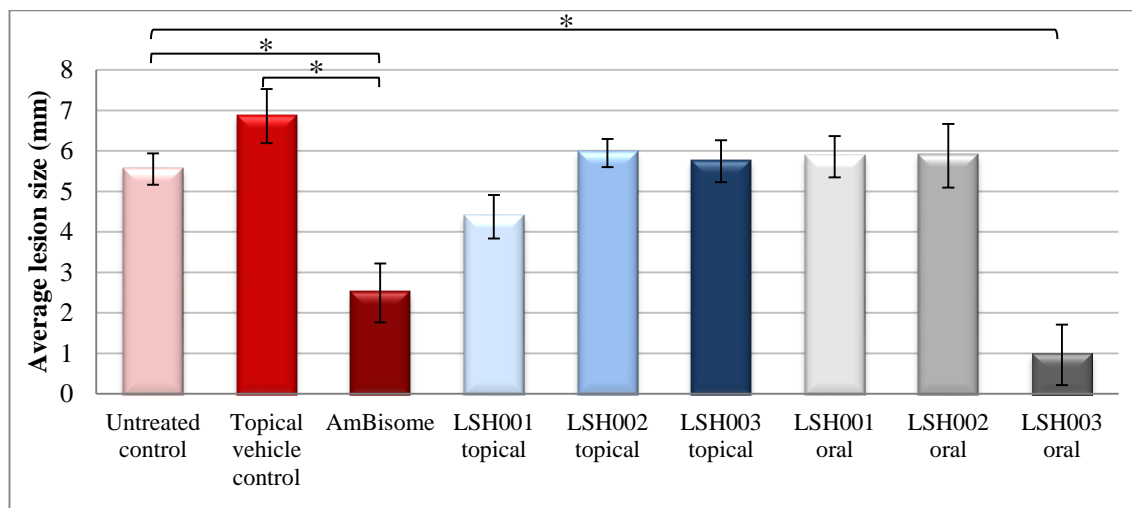
FIGURE 6-7. LESION SIZES (MEAN ±SD, N=6) ON THE LAST DAY OF TREATMENT (ONE-WAY ANOVA, P<0.05 (*)).

When injected with *Leishmania* parasites, the BALB/c mice developed fulminating infections with ulcers that quickly progress to death if left untreated. The LSH001 compound applied topically was able to halt the lesion growth which showed that the drug was able to permeate through the SC and reach the parasites situated in the lower epidermis and dermis. This non-healing BALB/c model is a rigorous test for drugs especially because these drugs were only applied after establishment of the lesion[354]. Therefore lesion size reduction or halt of lesion growth should be regarded as a promising result [354]. Moreover the efficacy of the formulation was probably significantly reduced as the mice were able to quickly remove the formulation by licking the site from day 3-4 of the start of the treatment. Initially, the corn plaster prolonged contact between the formulation and the CL lesion for up to 30 minutes. However as the study progressed, mice were able to remove the plaster quicker and licking the administration site was observed in all groups that received topical administration including the vehicle control group as early as 5-10 minutes after application. As there was no effect on CL progress observed in the LSH001 oral group, it is suggested that the activity seen in the LSH001 topical group is solely due to the drug that was able to permeate the skin.

These results correlate well with the data obtained in chapter 5. An *in vitro* permeation experiment using BALB/c mouse skin followed by a mass balance study showed a higher permeation for LSH001 compared to LSH002 and LSH003. This was only statistically significant higher for LSH001 compared to LSH002. In fact, the main difference between LSH001 and LSH003 was demonstrated in the mass balance study where LSH001 showed to concentrate in the skin after topical application.

It is somewhat surprising that LSH001 and LSH003 showed no effect on the lesion size progression after oral and topical administration respectively. However as mentioned before, this infection model is a real challenge for drugs because it progresses so quickly. Further discussions with the project collaborators revealed that glycol ethers for example PG are known to give rise to peroxide formation which enhances the benzoxaborole ring cleavage[375]. Since PG was only present in the topical formulations, drug degradation most likely reduced the efficacy of the topical formulations. The formulations were analysed by HPLC-UV after the study but this method was not sensitive enough to detect and/or separate the metabolites from the parent compound.

Figure 6-8 shows the CL lesions after 6 days of treatment with Leshcutan® ointment. The application of Leshcutan ointment was stopped 4 days after the start of dosing because of severe skin irritation. Lesion sizes were no longer measurable since the initial nodule was no longer visible. Leshcutan® ointment is formulated with 12% methylbenzethonium chloride, a cationic quaternary ammonium penetration enhancer that facilitates permeation of paromomycin sulfate (Mw > 700g/mol) into the skin by interacting with the intercellular lipid matrix of the stratum corneum[74, 376]. Cationic surfactants are known to damage skin resulting in an increase in transdermal flux[377] and have been reported to be more damaging than anionic or non-ionic surfactants[378]. Therefore they are typically used at a concentration of 0.5-1%, while Leshcutan® ointment contains 12%. Clinical trials using this ointment have frequently reported skin irritation[136]. This study shows that Leshcutan® should not be used as positive control for experiments in mice.

FIGURE 6-8. THE IRRITATIVE EFFECT OF LESHCUTAN OINTMENT ON MOUSE SKIN 5 DAYS AFTER THE START OF APPLICATION.

6.3.4 QUANTIFICATION OF LEISHMANIA DNA IN THE CL LESIONS AFTER DRUG DOSING

Figure 6-9 shows the numbers of amastigotes in the CL lesions three days after application of the last dose. A one-way between-groups analysis of variance was conducted to explore the influence of drug treatment on the reduction of parasite burden per lesion. There was a statistically significant reduction of the parasite burden for the LSH003 oral group compared to the topical vehicle control, LSH001 oral, LSH002 oral and LSH002 topical groups. This indicates that when administered orally, LSH003 was more efficacious killing *Leishmania* parasites *in vivo* compared to the other oral groups. The i*n vitro* activity against intracellular *L. major* amastigotes was ten times lower for LSH002 compared to LSH001 and LSH003 (based on the ED$_{50}$ values). This might explain the difference in activity between LSH003 and LSH002 upon oral administration. However LSH001 and LSH003, exhibited the same *in vitro* activity against *L. major*. It is thus suggested that the difference in efficacy upon oral administration is due to pharmacokinetic variations between LSH001 and LSH003. An oral vehicle control group had not been included as previous experience with this group showed no influence on CL lesions (unpublished data).

The parasite load for the Leshcutan® group was statistically significant lower compared to all groups except LSH003 oral (one-way ANOVA, p<0.05). However it is uncertain if the reduction in parasite load was caused by the activity of PM and/or MBCL, that had shown *in vitro* activity against *Leishmania* parasites[379].

AmBisome® reduced the parasite burden significantly compared to LSH001 and LSH002 oral and the topical vehicle control group (one-way ANOVA, $p < 0.05$). There was no statistically significant difference compared to LSH003 oral (one-way ANOVA, $p > 0.05$), indicating they exhibited a similar *in vivo* anti-leishmanial activity. AmB was reported to reduce parasite burden in CL lesions in mice before[380].

The parasite burden per lesion was not statistically significant reduced for the LSH001, LSH002 and LSH003 groups after topical application even though LSH001 topical showed a lower mean parasite burden compared to the other two topical groups.
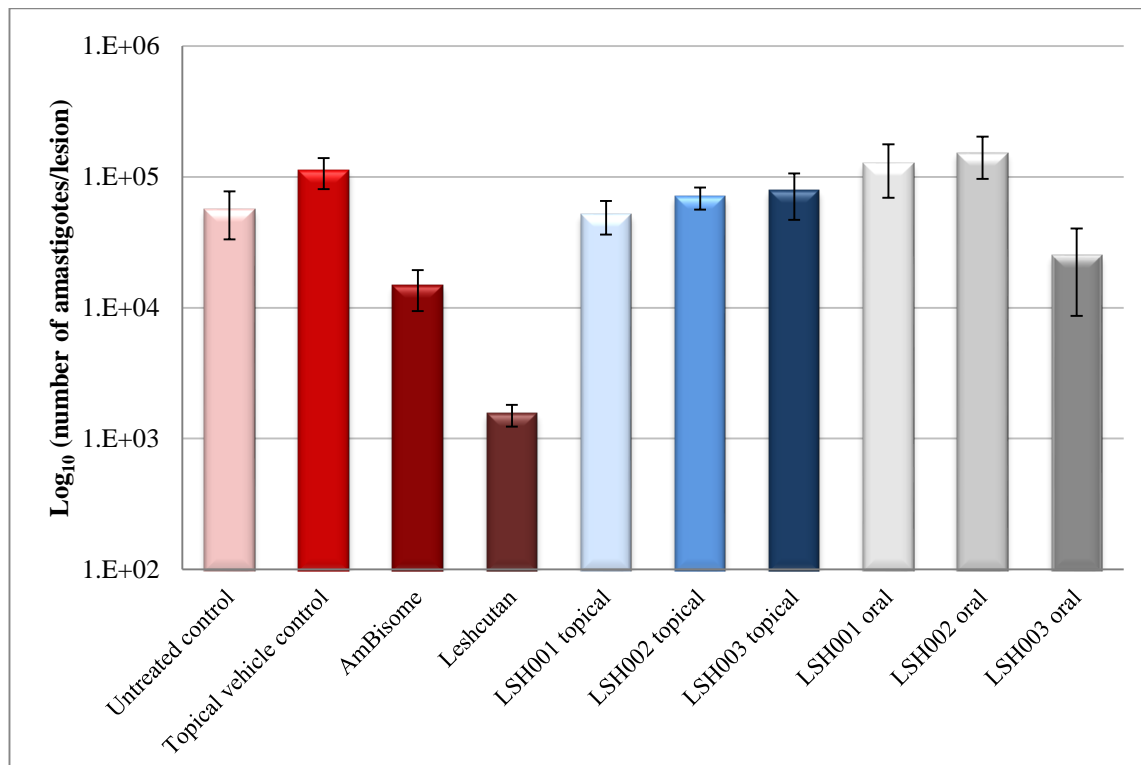
FIGURE 6-9. NUMBER OF AMASTIGOTES PER LESION (MEAN±SD, N=6) THREE DAYS AFTER THE LAST DOSING (ONE-WAY **ANOVA,** P>0.05).

The relationship between the lesion size and the parasite load per lesion on day 23 (three days after last dosing) was investigated using Pearson correlation coefficient (Figure 6-10). There was a strong, positive correlation between the two variables ($r = 0.57$, $p < 0.05$) with large lesion sizes associated with high parasite load. A stronger, positive correlation ($r = 0.73$, $p < 0.05$) was obtained between the logarithm of the parasite load and lesion size.
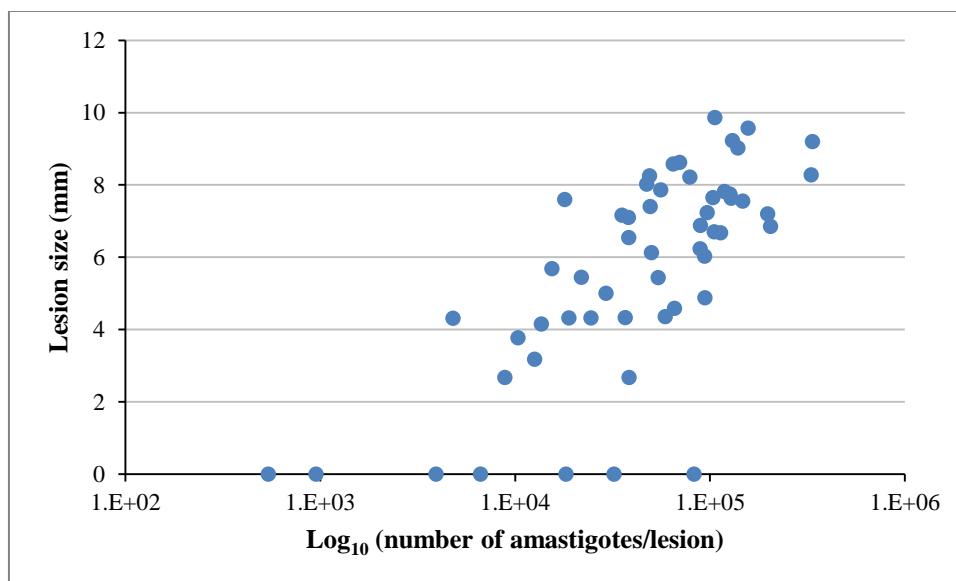
FIGURE 6-10. CORRELATION BETWEEN LESION SIZE AND PARASITE BURDEN ON DAY 23 (R=0.73, P<0.05).

Besides parasite clearance, lesion size reductions can also be caused by anti-inflammatory action of the test compounds. Some benzoxaboroles were reported to show anti-inflammatory activity. In fact AN2728 is currently in phase 3 clinical trials for atopic dermatitis characterised by inflammation[323]. This possible additional anti-inflammatory activity of the benzoxaboroles might explain the statistically significant differences for lesion size reduction while this was not the case for parasite burden per lesion.

6.4 FINAL DISCUSSION

LSH001 and LSH003 exhibited high passive transcellular permeability characterised by a high P_{app} in the MDCK-MDR1 assay. As the *Leishmania* parasites are situated inside the phagolysosome of the macrophage, a high transcellular permeability could give rise to a higher drug concentration inside the macrophage and thus a higher anti-leishmanial activity. For example LSH002 unlike LSH001 and LSH003 showed a low P_{app} and was active against only two *Leishmania* species with an ED_{50} that was 4-fold higher compared to LSH001 and LSH003.

Overall, the *in vivo* study outcome correlates with the results obtained in chapter 5. Amongst the three test compounds, LSH001 showed the highest unbound fraction (87%) in skin supernatant. Moreover, a mass balance study showed that more drug was present in the skin for LSH001 compared to LSH002 and LSH003 and was correlated with a lower lesion size in the *in vivo* study. It could be hypothesized that a high unbound fraction indicates a high anti-leishmanial activity in the dermis.

Additionally, the performance of the LSH001 topical formulation was likely to be enhanced by the reduced barrier integrity of CL affected mouse skin as was indicated in chapter 3.

Yet another important question remains, how the outcome of the *in vivo* mouse study would translate into humans. First, there are physical differences between human and mouse skin for example full-thickness mouse skin appears to be four times thinner compared to human skin while the mouse SC is half the thickness of human skin[381]. Furthermore the number of hair follicles and differences in the composition of the intercellular SC lipids[382] also contribute to the overall higher permeability of mouse skin compared to human skin[383-385].

Skin drug delivery is a complicated multi-factorial process that is affected by drug, formulation and skin related factors[386] including physico-chemical properties of the test compound, drug-vehicle and vehicle-skin interactions, skin physiology etc. For certain factors, data are available and if lucky, *in vitro* or *in vivo* assays with good correlation to humans exist. Developing a topical formulation for CL is therefore not a simple matter of designing one drugs to fit the target but a rational and performance based selection procedure where a collection of compounds with a range of physico-chemical properties are screened and taken forward stepwise. In our project, the selection procedure based

on *in vitro* experiments allowed us to narrow down thirty compounds to a handful of promising candidates for *in vivo* studies thereby increasing the chance of obtaining suitable drug candidates for our formulation and reducing the number of animals required

6.5 FUTURE WORK

Two lead compounds were active *in vivo*, one when administered orally, the other when applied topically. As mentioned before, there is a tendency of peroxide formation in ether solvents such as propylene glycol and polyethylene glycols. This is known to cause instability of the benzoxaboroles. It would be interesting to redo the *in vivo* study but with a different vehicle or repeat the study with the same formulation vehicle but with fresh drug formulations for each day in order to minimise drug metabolism and thus breakdown. When the formulation is optimised, the study will be repeated to assure the effect is reproducible and other New World species might be included for example *L. mexicana*.

LSH003 gave cure, defined as no visible lesion, in 4 out of 6 mice when administered orally. The general *in vitro* ADME tests performed in chapter 5 are suggestive of good membrane permeability. It would be interesting to measure plasma concentrations after oral administration to see if they correlate with these *in vitro* ADME test results and with the outcome of the *in vivo* study.

The mass balance study had shown that high concentrations of LSH001 were found inside the skin. When separating the epidermis and dermis prior to drug extraction, it would be possible to see in which skin layer LSH001 concentrates in particular. Ideally, it would concentrate in the dermis because there is where the parasites reside.

7 FINAL DISCUSSION

Amongst the leishmaniases, CL is perhaps the most neglected disease. It does not cause fatalities but does lead to significant morbidity related to disfiguration and social stigma. A selection of drugs, mainly repurposed, are available to treat these diseases but their usage is limited by toxicity, inefficacy and high cost. Due to these limitations, patients delay seeking treatment and allow the infection to progress increasing the risk of parasite spreading and multiple lesion development, expansion of lesion size, development of ulcers and contribution to transmission. Even if treatment is successful at this stage, scar formation will occur. An effective and safe treatment that the patient can apply or take themselves is expected to change treatment seeking behaviour and hence, avoid scar formation.

To date, there is no literature available on the influence of *Leishmania* infection on the skin barrier integrity and thus drug delivery to the skin. This information is extremely useful as the aim of this work was to investigate drugs that could potentially be used in a topical formulation to treat CL at an early stage. To do so, it was important to know if the barrier function of the skin affected with CL was more or less permeable. Consequently the skin barrier integrity of *Leishmania*-infected mouse skin was compared with uninfected skin. A histopathological evaluation of CL lesions in the nodular stage, before ulceration and skin disruption was observed, indicated epidermal hyperplasia and disruption of the dermal layer by the ingress of abundant inflammatory cells. CL also affected the skin barrier integrity characterised by an increased TEWL value suggesting a damaged inside-outside barrier. More importantly, the permeability of *Leishmania*-infected skin was higher compared to uninfected skin as was shown when performing *in vitro* Franz cell diffusion studies. This was tested for a lipophilic and hydrophilic model permeant and while the permeation of both drugs was enhanced in infected skin, the hydrophilic drug showed a 66 times higher flux through infected compared to uninfected skin, whereas this was only 2-fold higher for the lipophilic drug.

When testing the permeation of leishmanicidal drugs through infected and uninfected skin, this trend was confirmed and indicated that hydrophilic drugs permeated more through infected skin compared to lipophilic drugs. This led to the hypothesis that the inflammatory reaction caused a more hydrophilic environment in the dermis compared to uninfected skin and hence selectively enhancing the permeability of hydrophilic drugs. It

should be mentioned that infected skin remained impermeable for amphotericin B indicating that the barrier integrity was damaged, but not absent. These findings were obtained using mouse skin and as generally known, mouse skin is more permeable than human skin. This work, while it needs to be repeated using human skin, provides the first evidence that *Leishmania* infection of the skin alters the barrier integrity and therefore the dermatopharmacokinetics of drug delivery to skin target sites. This information is valuable in early stages of drug discovery for example when modifying lead molecules, the addition of hydrophilic groups might enhance drug permeation into the *Leishmania*-infected skin.

In a following chapter, the reformulation of miltefosine, an established anti-leishmanial drug, into a topical formulation was evaluated. This drug, available as an oral formulation to treat VL has been increasingly used to treat CL, however, the benefit-risk profile of CL is different compared to VL and due to toxicity and resistance development, the oral administration of miltefosine for CL should be avoided.

This study investigated the permeability of miltefosine formulated in solvents that were reported to enhance permeability of other drugs. For all solvents, miltefosine permeation was limited and mass balance studies showed low concentrations in the skin combined with high amounts left on the skin. The chemical structure of miltefosine indicates similarities with skin lipids and possibly explains the retention of the compound on the skin surface. Moreover this molecule behaves as a surfactant and when used in high concentrations (25% w/v) it was found to solubilise skin (unpublished data).

In parallel, we applied a rational based strategy to evaluate the potential use of benzoxaboroles in a topical formulation to treat CL. Drug discovery requires a multidisciplinary approach and in an area with little pharmaceutical incentive, this methodology has not been described/applied before. Chapter 5 describes the approach that was taken to select lead compounds from a range of benzoxaboroles with different physico-chemical characteristics. First the anti-leishmanial activity of the compounds was evaluated in an *in vitro* intracellular amastigote-macrophage model. The compounds were tested against 5 *Leishmania* species because ideally the lead compounds should show broad range activity. Five compounds had shown activity against at least two Old World and one New World species. Overall, the active benzoxaboroles were less potent than amphotericin B (Fungizone®) but exhibited lower ED_{50} values compared to miltefosine.

L. tropica was more susceptible to the benzoxaboroles compared to the other species. A first series of *in vitro* ADME tests were conducted to determine general physico-chemical properties that are important to establish an overall PK profile for the compound. This included water solubility, log P determination and permeability testing in the MDCK-MDR1 assay. The obtained parameters were similar for the entire range of benzoxaboroles and no 'red flags' were identified.

A second series of *in vitro* tests were more skin specific and determined stability in mouse skin homogenate supernatant and binding to skin components. In the skin supernatant, all benzoxaboroles showed higher stability compared to the paraben compounds that are known substrates for skin esterases and are therefore expected to breakdown. The binding assay demonstrated a range of unbound fractions. At that stage, it was not clear whether a high unbound fraction was beneficial for topically applied drugs as a certain skin retention is required to maintain the compound in the dermis where the parasites reside. The last test in this series of assays evaluated the permeation of the compounds in a reconstructed human epidermis model. This model is readily commercially available in a 6-well format and requires no Franz diffusion cell equipment. Based on the outcome of this study, 3 compounds with a higher permeation compared to testosterone, the lipophilic model permeant that was included, were selected.

The permeation of these 3 compounds was evaluated using full-thickness mouse skin and Franz diffusion cells. At the end of the experiment the amount of drug that was left on the skin was removed by applying several wash and swab cycles. The amount of drug in the skin was recovered by extraction. LSH001 showed high permeation and a high fraction of drugs was recovered from inside the skin. LSH002 and LSH003 showed lower permeation and indicated a high fraction of drugs that was left on the skin.

This chapter described how the efficacy of the selected compounds were tested *in vivo* against CL in BALB/c mice upon topical or oral administration. LSH001 halted the lesion size progression and showed a lower mean parasite burden compared to the topical vehicle control group. These findings led to the conclusion that a high unbound fraction combined with a high skin concentration are important to obtain parasite killing in the dermis. Upon oral administration, LSH003 reduced the lesion size more than AmBisome®. Both results are promising as the non-healing BALB/c model is a rigorous test for drugs

A general body of knowledge on CL is available and *in vitro* PK experiments can be adapted to obtain more target-related information. There is a lack of disease specific *in vitro* models that combine both the activity testing against *Leishmania* parasites and preliminary PK profile evaluation. The current *in vitro* models to test anti-leishmanial activity rely on 2D culture systems that demonstrate activity against the intracellular parasite correlate poorly with results obtained in animal models[387]. This "disconnect" is likely to be caused by the oversimplification of the *in vitro* model that is unable to account for pharmacokinetic drug barriers that occur *in vivo*. *In vitro* 3D culture systems are receiving increasing attention and have demonstrated a better correlation to *in vivo* drug activity.

Dermatopharmacokinetic evaluation of drug formulations after topical application often involves invasive sampling. The two main techniques used are tape stripping, whereby consecutive SC cell layers are mechanically removed and extracted for drugs, and microdialysis, that allows the measurement of unbound drug in the extracellular fluids of skin tissue. A more recent trend involves the use of non-invasive spectroscopy techniques such as Raman spectroscopy and allows the evaluation of drug permeation into the skin layers. This could be used to follow drug permeation in CL models upon application of topical formulations.

The research described in this thesis focused mainly on the development of a conventional topical formulation such as an ointment or cream. Alternatively, a topical formulation may be delivered in spray form. This mode of application could be particularly useful when treating patients with multiple lesions spread over the body. An additional advantage of this contactless application is that it minimises the likelihood of the formulation's contamination by human microflora. Of course, repeated application of the spray on large areas of the body particularly on ulcerated lesions that lack barrier to permeation, may lead to increased absorption of drugs in the systemic circulation resulting in toxicity.

REFERENCES

1. Alvar, J., et al., *Leishmaniasis Worldwide and Global Estimates of Its Incidence.* PLoS One, 2012. **7**(5): p. e35671.
2. El-On, J., et al., *Topical treatment of cutaneous leishmaniasis.* Journal of Investigative Dermatology, 1986. **87**(2): p. 284-288.
3. Croft, S.L. and G.H. Coombs, *Leishmaniasis - current chemotherapy and recent advances in the search for novel drugs.* Trends in Parasitology, 2003. **19**(11): p. 502-508.
4. el-On, J., et al., *Topical treatment of Old World cutaneous leishmaniasis caused by Leishmania major: a double-blind control study.* J Am Acad Dermatol, 1992. **27**(2 Pt 1): p. 227-31.
5. Neal, R.A., et al., *Aminosidine ointments for the treatment of experimental cutaneous leishmaniasis.* Transactions of the Royal Society of Tropical Medicine and Hygiene, 1994. **88**(2): p. 223-225.
6. Neva, F.A., et al., *Non-ulcerative cutaneous leishmaniasis in Honduras fails to respond to topical paromomycin.* Transactions of the Royal Society of Tropical Medicine and Hygiene, 1997. **91**(4): p. 473-475.
7. Arana, B.A., et al., *Randomized, controlled, double-blind trial of topical treatment of cutaneous leishmaniasis with paromomycin plus methylbenzethonium chloride ointment in Guatemala.* American Journal of Tropical Medicine and Hygiene, 2001. **65**(5): p. 466-470.
8. Asilian, A., et al., *Comparative study of the efficacy of combined cryotherapy and intralesional meglumine antimoniate (glucantime) vs. cryothrapy and intralesional meglumine antimoniate (glucantime) alone for the treatment of cutaneous leishmaniasis.* International Journal of Dermatology, 2004. **43**(4): p. 281-283.
9. Croft, S.L., *Monitoring drug resistance in leishmaniasis.* Tropical Medicine & International Health, 2001. **6**(11): p. 899-905.
10. Sherwood, L., *Body defenses* in *Human physiology: from cells to systems*, L. Sherwood, Editor. 2010, Thomas/ Brooks/ cole: Australia, United Kingdom. p. 417-460.
11. Kanitakis, J., *Anatomy, histology and immunohistochemistry of normal human skin.* European Journal of Dermatology, 2002. **12**(4): p. 390-399.
12. Katz, M. and B.J. Poulsen, *Absorption of drugs through the skin*, in *Handbook of experimental pharmacology*, O. Eichler, et al., Editors. 1971, Springer-Verlag: Berlin. p. 103-175.
13. Holbrook, K.A. and G.F. Odland, *Regional differences in the thickness (cell layers) of the human stratum corneum.* Journal of Investigative Dermatology, 1974. **62**(4): p. 415-422.
14. Brody, I., *Ultrastructure of the stratum corneum.* International Journal of Dermatology, 1977. **16**(4): p. 245-256.
15. Downing, D.T., et al., *Skin lipids.* Comparative Biochemistry and Physiology B, 1983. **76**(4): p. 673-678.
16. Norlen, L., et al., *Inter- and intra-individual differences in human stratum corneum lipid content related to physical parameters of skin barrier function in vivo.* Journal of Investigative Dermatology, 1999. **112**(1): p. 72-77.
17. Proksch, E., J.M. Brandner, and J.M. Jensen, *The skin: an indispensable barrier.* Experimental Dermatology, 2008. **17**(12): p. 1063-1072.
18. Becker-Pauly, C., et al., *The alpha and beta subunits of the metalloprotease meprin are expressed in seperate layers of human epidermis, revealing different functions in keratinocyte proliferation and differentiation.* Journal of Investigative Dermatology, 2007. **127**(5): p. 1115-1125.
19. Pearce, R.H. and B.J. Grimmer, *The nature of the ground substance*, in *Advances in Biology of Skin*, W. Montagna, J.P. Bentley, and R. Dobson, Editors. 1970, Appleton-Century-Crofts: New York.
20. Epstein, E.H. and N.H. Munderloh, *Human skin collagen. Presence of type I and type III at all levels of the dermis.* Journal of Biological Chemistry, 1978. **253**(5): p. 1336-1337.
21. Williams, A.C., *Structure and function of human skin*, in *Transdermal and topical drug delivery*. 2003, Pharmaceutical Press: London. p. 1-25.
22. Wilkes, G.L., I.A. Brown, and R.H. Wildnauer, *The biomechanical properties of skin.* CRC Critical Reviews in Bioengineering, 1973. **1**(4): p. 453-495.
23. Shah, V.P., et al., *Principles and criteria in the development and optimization of topical therapeutic products.* International Journal of Pharmaceutics, 1992. **82**(1-2): p. 21-28.
24. Scheuplein, R.J., *Mechanism of percutaneous adsorption. I. Routes of penetration and the influence of solubility.* Journal of Investigative Dermatology, 1965. **45**(5): p. 334-346.

25. Guy, R.H. and J. Hadgraft, *Physicochemical aspects of percutaneous penetration and its enhancement* Pharmaceutical Research, 1988. **5**(12): p. 753-758.

26. Hadgraft, J. and R. Guy, *Feasibility assessment in topical and transdermal delivery: mathematical models and in vitro studies*, in *Transdermal Drug Delivery*, R. Guy and J. Hadgraft, Editors. 2003, Marcel Dekker: New York. p. 383.

27. Scheuplein, R.J., *Mechanism of Percutaneous Absorption.* The Journal of Investigative Dermatology, 1967. **48**(1): p. 79-88.

28. Potts, R.O. and R.H. Guy, *Predicting skin permeability.* Pharmaceutical Research, 1992. **9**(5): p. 663-669.

29. Scheuplein, R.J., et al., *Percutaneous absorption of steroids.* J Invest Dermatol, 1969. **52**(1): p. 63-70.

30. Idson, B., *Percutaneous absorption.* J Pharm Sci, 1975. **64**(6): p. 901-24.

31. Bos, J.D. and M.M. Meinardi, *The 500 Dalton rule for the skin penetration of chemical compounds and drugs.* Exp Dermatol, 2000. **9**(3): p. 165-9.

32. Yano, T., et al., *Skin permeability of various non-steroidal anti-inflammatory drugs in man.* Life Sciences, 1986. **39**(12): p. 1043-1050.

33. Kasting, G.B., R.L. Smith, and E.R. Cooper, *Effect of lipid solubility and molecular size on percutaneous absorption*, in *Skin pharmacokinetics*, B. Shroot and H. Schaefer, Editors. 1987, Karger: Basel. p. 135-138.

34. Pugh, W.J., M.S. Roberts, and J. Hadgraft, *Epidermal permeability - Penetrant structure relationships .3. The effect of hydrogen bonding interactions and molecular size on diffusion across the stratum corneum.* International Journal of Pharmaceutics, 1996. **138**(2): p. 149-165.

35. Hadgraft, J. and W.J. Pugh, *The selection and design of topical and transdermal agents: a review.* Journal of Investigative Dermatology: Symposium Proceeding, 1998. **3**(2): p. 131-135.

36. Farahmand, S. and H.I. Maibach, *Transdermal drug pharmacokinetics in man: Interindividual variability and partial prediction.* International Journal of Pharmaceutics, 2009. **367**(1-2): p. 1-15.

37. Naik, A., Y.N. Kalia, and R.H. Guy, *Transdermal drug delivery: overcoming the skin's barrier function.* Pharmaceutical Science and Technology Today, 2000. **3**(9): p. 318-326.

38. Vecchia, B.E. and A.L. Bunge, *Evaluating the Transdermal Permeability of Chemicals*, in *Transdermal Drug Delivery Systems*. 2002, CRC Press.

39. Roberts, M.S., W.J. Pugh, and J. Hadgraft, *Epidermal permeability: Penetrant structure relationships .2. The effect of H-bonding groups in penetrants on their diffusion through the stratum corneum.* International Journal of Pharmaceutics, 1996. **132**(1-2): p. 23-32.

40. Azzi, C.G., et al., *Topical dermatological vehicles: Engineering the delivery systems*, in *Percutaneous Absorption: Drugs-Cosmetics-Mechanisms-Methodology*, R.L. Bronaugh and H.I. Maibach, Editors. 2005, Taylor & Francis Group: Boca Raton. p. 801-810.

41. Hadgraft, J. and M.E. Lane, *Skin: the ultimate interface.* Physical Chemistry Chemical Physics, 2011. **13**(12): p. 5215-5222.

42. Karande, P. and S. Mitragotri, *Enhancement of transdermal drug delivery via synergistic action of chemicals.* Biochimica et Biophysica Acta (BBA) - Biomembranes, 2009. **1788**(11): p. 2362-2373.

43. Meidan, V.M., M. Al-Khalili, and B.B. Michniak, *Enhanced iontophoretic delivery of buspirone hydrochloride across human skin using chemical enhancers.* Int J Pharm, 2003. **264**(1-2): p. 73-83.

44. Kigasawa, K., et al., *In vivo transdermal delivery of diclofenac by ion-exchange iontophoresis with geraniol.* Biol Pharm Bull, 2009. **32**(4): p. 684-7.

45. McCoy, J.R., et al., *A multi-head intradermal electroporation device allows for tailored and increased dose DNA vaccine delivery to the skin.* Hum Vaccin Immunother, 2014: p. 1-9.

46. Han, T. and D.B. Das, *Permeability enhancement for transdermal delivery of large molecule using low-frequency sonophoresis combined with microneedles.* J Pharm Sci, 2013. **102**(10): p. 3614-22.

47. Subedi, R.K., et al., *Recent advances in transdermal drug delivery.* Archives of Pharmaceutical Research, 2010. **33**(3): p. 339-351.

48. Pearton, M., et al., *Influenza virus-like particles coated onto microneedles can elicit stimulatory effects on Langerhans cells in human skin.* Vaccine, 2010. **28**(37): p. 6104-6113.

49. Funk, J.O., S.H. Dromgoole, and H.I. Maibach, *Sunscreen intolerance. Contact sensitization, photocontact sensitization, and irritancy of sunscreen agents.* Dermatol Clin, 1995. **13**(2): p. 473-81.

50. Reed, B.L., T.M. Morgan, and B.C. Finnin, *Dermal penetration enhancers and drug delivery systems involving same* V. Monash University, Editor. 1997: USA.

51. Finnin, B.C. and T.M. Morgan, *Transdermal penetration enhancers: Applications, limitations, and potential.* Journal of Pharmaceutical Sciences, 1999. **88**(10): p. 955-958.

52. Nicolazzo, J.A., et al., *Synergistic enhancement of testosterone transdermal delivery.* J Control Release, 2005. **103**(3): p. 577-85.

53. Santos, P., et al., *Influence of penetration enhancer on drug permeation from volatile formulations.* International Journal of Pharmaceutics, 2012. **439**(1–2): p. 260-268.

54. Ongpipattanakul, B., et al., *Evidence that oleic acid exists in a separate phase within stratum corneum lipids.* Pharm Res, 1991. **8**(3): p. 350-4.

55. Zatz, J.L. and U.G. Dalvi, *Evaluation of solvent-skin interaction in percutaneous absorption.* Journal of the Society of Cosmetic Chemists, 1983. **34**: p. 327-334.

56. Brendas, B., R.H. Neubert, and W. Wohlrab, *Propylene glycol*, in *Percutaneous Penetration Enhancers*, E.W. Smith and H. Maibach, Editors. 1995, CRC Press, Inc.: Boca Raton. p. 61-75.

57. Watkinson, R.M., et al., *Optimisation of Cosolvent Concentration for Topical Drug Delivery - II: Influence of Propylene Glycol on Ibuprofen Permeation.* Skin Pharmacology and Physiology, 2009. **22**(4): p. 225-230.

58. Mollgaard, B. and A. Hoelgaard, *Vehicle effect on topical drug delivery. II. Concurrent skin transport of drugs and vehicle components.* Acta Pharm Suec, 1983. **20**(6): p. 443-50.

59. Wotton, P.K., et al., *Vehicle effect on topical drug delivery. III. Effect of Azone on the cutaneous permeation of metronidazole and propylene glycol.* International Journal of Pharmaceutics, 1985. **24**(1): p. 19-26.

60. Squillante, E., et al., *Codiffusion of propylene glycol and dimethyl isosorbide in hairless mouse skin.* Eur J Pharm Biopharm, 1998. **46**(3): p. 265-71.

61. Trottet, L., et al., *Effect of finite doses of propylene glycol on enhancement of in vitro percutaneous permeation of loperamide hydrochloride.* International Journal of Pharmaceutics, 2004. **274**(1-2): p. 213-219.

62. Larrucea, E., et al., *Combined effect of oleic acid and propylene glycol on the percutaneous penetration of tenoxicam and its retention in the skin.* European journal of pharmaceutics and biopharmaceutics : official journal of Arbeitsgemeinschaft fur Pharmazeutische Verfahrenstechnik e.V, 2001. **52**(2): p. 113-119.

63. Yamada, M., Y. Uda, and Y. Tanigawara, *Mechanism of enchancement of percutaneous abosorption of molsidomine by oleic acid.* Chemical & Pharmaceutical Bulletin, 1987. **35**(8): p. 3399-3406.

64. Cooper, E.R., E.W. Merritt, and R.L. Smith, *Effect of fatty acids and alcohols on the penetration of acyclovir across human skin in vitro.* J Pharm Sci, 1985. **74**(6): p. 688-9.

65. Komata, Y., A. Kaneko, and T. Fujie, *In vitro percutaneous absorption of thiamine disulfide through rat skin from a mixture of propylene glycol and fatty acid or its analog.* Chem Pharm Bull (Tokyo), 1992. **40**(8): p. 2173-6.

66. Rossi, P. and J.N. Wiechers, *Improved delivery and efficacy with dimethyl isosorbide.* Cosmetic Toiletries, 2005. **120**: p. 107-111.

67. Funke, A.P., et al., *Transdermal delivery of highly lipophilic drugs: in vitro fluxes of antiestrogens, permeation enhancers, and solvents from liquid formulations.* Pharm Res, 2002. **19**(5): p. 661-8.

68. Cevc, G., et al., *Occlusion effect on transcutaneous NSAID delivery from conventional and carrier-based formulations.* Int J Pharm, 2008. **359**(1-2): p. 190-7.

69. Hikima, T. and H. Maibach, *Skin penetration flux and lag-time of steroids across hydrated and dehydrated human skin in vitro.* Biol Pharm Bull, 2006. **29**(11): p. 2270-3.

70. Purdon, C.H., et al., *Penetration enhancement by skin hydration*, in *Percutaneous Penetration Enhancers*, E.W. Smith and H.I. Maibach, Editors. 2006, CRC Press: Boca Raton, FL. p. 67-71.

71. Bouwstra, J.A., et al., *Structural investigations of human stratum corneum by small-angle X-ray scattering.* J Invest Dermatol, 1991. **97**(6): p. 1005-12.

72. Cornwell, P.A., et al., *Wide-angle X-ray diffraction of human stratum corneum: effects of hydration and terpene enhancer treatment.* J Pharm Pharmacol, 1994. **46**(12): p. 938-50.

73. Mak, V.H., R.O. Potts, and R.H. Guy, *Does hydration affect intercellular lipid organization in the stratum corneum?* Pharm Res, 1991. **8**(8): p. 1064-5.

74. Williams, A.C. and B.W. Barry, *Penetration enhancers.* Advanced Drug Delivery Reviews, 2004. **56**(5): p. 603-618.

75. Fox, L.T., et al., *Transdermal drug delivery enhancement by compounds of natural origin.* Molecules, 2011. **16**: p. 10507-10540.

76. Pinnagoda, J. and R.A. Tupker, *Measurement of transepidermal water loss*, in *Handbook of Non-invasive Methods, the Skin*, J. Serup and G.B.E. Jemec, Editors. 1995, CRC Press: London.

77. Ogawa, H. and T. Yoshiike, *Atopic dermatitis: studies of skin permeability and effectiveness of topical PUVA treatment.* Pediatr Dermatol, 1992. **9**(4): p. 383-5.

78. Werner, Y. and M. Lindberg, *Transepidermal water loss in dry and clinically normal skin in patients with atopic dermatitis.* Acta Derm Venereol, 1985. **65**(2): p. 102-5.

79. Imokawa, G., *Surfactant-induced depletion of ceramides and other intercellular lipids: implication for the mechanism leading to dehydration of the stratum corneum.* Exogenous Dermatology, 2004. **3**(2): p. 81-98.

80. Motta, S., et al., *Abnormality of water barrier function in psoriasis. Role of ceramide fractions.* Archives of Dermatology, 1994. **130**(4): p. 452-6.

81. Berardesca, E., et al., *In vivo hydration and water-retention capacity of stratum corneum in clinically uninvolved skin in atopic and psoriatic patients.* Acta Derm Venereol, 1990. **70**(5): p. 400-4.

82. Paige, D.G., N. Morse-Fisher, and J.I. Harper, *Quantification of stratum corneum ceramides and lipid envelope ceramides in the hereditary ichthyoses.* Br J Dermatol, 1994. **131**(1): p. 23-7.

83. Tomita, Y., M. Akiyama, and H. Shimizu, *Stratum corneum hydration and flexibility are useful parameters to indicate clinical severity of congenital ichthyosis.* Exp Dermatol, 2005. **14**(8): p. 619-24.

84. Berry, N., et al., *A clinical, biometrological and ultrastructural study of xerotic skin.* Int J Cosmet Sci, 1999. **21**(4): p. 241-52.

85. Rawlings, A.V. and R. Voegeli, *Stratum corneum proteases and dry skin conditions.* Cell Tissue Res, 2013. **351**(2): p. 217-35.

86. Kezic, S. and J.B. Nielsen, *Absorption of chemicals through compromised skin.* International Archives of Occupational and Environmental Health, 2009. **82**(6): p. 677-688.

87. Chiang, A., E. Tudela, and H.I. Maibach, *Percutaneous absorption in diseased skin: an overview.* J Appl Toxicol, 2012. **32**(8): p. 537-63.

88. Bronaugh, R.L., R.F. Stewart, and M. Simon, *Methods for in vitro percutaneous absorption studies. VII: Use of excised human skin.* J Pharm Sci, 1986. **75**(11): p. 1094-7.

89. Brain, K.R., et al., *Percutaneous penetration of diethanolamine through human skin in vitro: application from cosmetic vehicles.* Food Chem Toxicol, 2005. **43**(5): p. 681-90.

90. Sintov, A.C. and S. Botner, *Transdermal drug delivery using microemulsion and aqueous systems: influence of skin storage conditions on the in vitro permeability of diclofenac from aqueous vehicle systems.* Int J Pharm, 2006. **311**(1-2): p. 55-62.

91. Moon, K.C., R.C. Wester, and H.I. Maibach, *Diseased skin models in the hairless guinea pig: in vivo percutaneous absorption.* Dermatologica, 1990. **180**(1): p. 8-12.

92. Rastogi, S.K. and J. Singh, *Lipid extraction and transport of hydrophilic solutes through porcine epidermis.* Int J Pharm, 2001. **225**(1-2): p. 75-82.

93. Tsai, J.C., et al., *Effect of barrier disruption by acetone treatment on the permeability of compounds with various lipophilicities: implications for the permeability of compromised skin.* J Pharm Sci, 2001. **90**(9): p. 1242-54.

94. Wang, J.C., et al., *The release and percutaneous permeation of anthralin products, using clinically involved and uninvolved psoriatic skin.* J Am Acad Dermatol, 1987. **16**(4): p. 812-21.

95. Anigbogu, A.N., A.C. Williams, and B.W. Barry, *Permeation characteristics of 8-methoxypsoralen through human skin; relevance to clinical treatment.* J Pharm Pharmacol, 1996. **48**(4): p. 357-66.

96. Shani, J., et al., *Skin penetration of minerals in psoriatics and guinea-pigs bathing in hypertonic salt solutions.* Pharmacol Res Commun, 1985. **17**(6): p. 501-12.

97. Rogers, M.E., et al., *Transmission of cutaneous leishmaniasis by sand flies is enhanced by regurgitation of fPPG.* Nature 2004. **430**(6998): p. 463-467.

98. Beil, W.J., et al., *Differences in the onset of the inflammatory response to cutaneous leishmaniasis in resistant and susceptible mice.* J Leukoc Biol, 1992. **52**(2): p. 135-42.

99. Tacchini-Cottier, F., et al., *An immunomodulatory function for neutrophils during the induction of a CD4+ Th2 response in BALB/c mice infected with Leishmania major.* J Immunol, 2000. **165**(5): p. 2628-36.

100. Peters, N.C., et al., *In vivo imaging reveals an essential role for neutrophils in leishmaniasis transmitted by sand flies.* Science, 2008. **321**(5891): p. 970-4.

101. Moore, K.J. and G. Matlashewski, *Intracellular infection by Leishmania donovani inhibits macrophage apoptosis.* J Immunol, 1994. **152**(6): p. 2930-7.

102. Carrera, L., et al., *Leishmania promastigotes selectively inhibit interleukin 12 induction in bone marrow-derived macrophages from susceptible and resistant mice.* J Exp Med, 1996. **183**(2): p. 515-26.

103. Belkaid, Y., et al., *Development of a natural model of cutaneous leishmaniasis: powerful effects of vector saliva and saliva preexposure on the long-term outcome of Leishmania major Infection in the mouse ear dermis.* Journal of Experimental Medicine, 1998. **188**(10): p. 1941-1953.

104. Buates, S. and G. Matlashewski, *General suppression of macrophage gene expression during Leishmania donovani infection.* J Immunol, 2001. **166**(5): p. 3416-22.

105. Kaye, P. and P. Scott, *Leishmaniasis: complexity at the host-pathogen interface.* Nature Reviews Microbiology 2011. **9**(8): p. 604-615.

106. WHO, *Leishmaniasis: worldwide epidemiological and drug access update*. 2012, World Health Organisation.

107. WHO. *Status of endemicity of cutaneous leishmaniasis, worldwide, 2013*. 2014 7/10/2014 [cited; Available from: http://gamapserver.who.int/mapLibrary/Files/Maps/Leishmaniasis_CL_2013.png?ua=1.

108. Alirol, E., et al., *Urbanisation and infectious diseases in a globalised world.* The Lancet Infectious Diseases, 2011. **11**(2): p. 131-141.

109. Alvar, J., et al., *The relationship between leishmaniasis and AIDS: the second 10 years.* Clin Microbiol Rev, 2008. **21**(2): p. 334-59, table of contents.

110. Rangel, E.F., S.M. da Costa, and B.M. Carvalho, *Environmental Changes and the Geographic Spreading of American Cutaneous Leishmaniasis in Brazil*, in *Leishmaniasis - Trends in Epidemiology, Diagnosis and Treatment*, D. Claborn, Editor. 2014.

111. Hayani, K., A. Dandashli, and E. Weisshaar, *Cutaneous Leishmaniasis in Syria: Clinical Features, Current Status and the Effects of War.* Acta Derm Venereol, 2014.

112. Selvapandiyan, A., et al., *Immunity to visceral leishmaniasis using genetically defined live-attenuated.* Journal of Tropical Medicine. , 2012. **2012:631460**.

113. Chappuis, F., et al., *Visceral leishmaniasis: what are the needs for diagnosis, treatment and control?* Nature Reviews Microbiology, 2007. **5**(11): p. 873-882.

114. Alvar, J., S. Croft, and P. Olliaro, *Chemotherapy in the treatment and control of leishmaniasis.* Advances in Parasitology, 2006. **61**: p. 223-274.

115. Kharfi, M., et al., *Mucosal localization of leishmaniasis in Tunisia: 5 cases.* Annales de Dermatologie et de Vénéreologie, 2003. **130**(1 Pt 1): p. 27-30.

116. Akilov, O.E., A. Khachemoune, and T. Hasan, *Clinical manifestations and classification of Old World cutaneous leishmaniasis.* International Journal of Dermatology, 2007. **46**(2): p. 132-142.

117. Goto, H. and J.A. Lindoso, *Current diagnosis and treatment of cutaneous and mucocutaneous leishmaniasis.* Expert Review of Anti-Infective Therapy 2010. **8**(4): p. 419-433.

118. WHO, *Control of the leishmaniases* 2010, World Health Organisation: Geneva. p. 186.

119. Zerpa, O., et al., *Diffuse cutaneous leishmaniasis responds to miltefosine but then relapses.* British Journal of Dermatology, 2007. **156**(6): p. 1328-1335.

120. Mitropoulos, P., P. Konidas, and M. Durkin-Konidas, *New World cutaneous leishmaniasis: Updated review of current and future diagnosis and treatment.* Journal of the American Academy of Dermatology, 2010. **63**(2): p. 309-322.

121. Musa, A.M., et al., *The natural history of Sudanese post-kala-azar dermal leishmaniasis: clinical, immunological and prognostic features.* Ann Trop Med Parasitol, 2002. **96**(8): p. 765-72.

122. Zijlstra, E.E., A.M. el-Hassan, and A. Ismael, *Endemic kala-azar in eastern Sudan: post-kala-azar dermal leishmaniasis.* Am J Trop Med Hyg, 1995. **52**(4): p. 299-305.

123. Zijlstra, E.E., et al., *Post-kala-azar dermal leishmaniasis.* Lancet Infectious Diseases, 2003. **3**(2): p. 87-98.

124. Desjeux, P., et al., *Report of the Post Kala-azar Dermal Leishmaniasis (PKDL) Consortium Meeting, New Delhi, India, 27-29 June 2012.* Parasit Vectors, 2013. **6**: p. 196.

125. Kassi, M., et al., *Marring leishmaniasis: the stigmatization and the impact of cutaneous leishmaniasis in Pakistan and Afghanistan.* Plos Neglected Tropical Diseases, 2008. **2**(10): p. 1-3.

126. Reithinger, R., *Leishmaniases' Burden of Disease: Ways Forward for Getting from Speculation to Reality.* Plos Neglected Tropical Diseases, 2008. **2**(10).

127. Reithinger, R., et al., *Cutaneous leishmaniasis.* Lancet Infectious Diseases, 2007. **7**: p. 581-596.

128. Wyllie, S., M.L. Cunningham, and A.H. Fairlamb, *Dual action of antimonial drugs on thiol redox metabolism in the human pathogen Leishmania donovani.* J Biol Chem, 2004. **279**(38): p. 39925-32.

129. Krauth-Siegel, R.L. and M.A. Comini, *Redox control in trypanosomatids, parasitic protozoa with trypanothione-based thiol metabolism.* Biochim Biophys Acta, 2008. **1780**(11): p. 1236-48.

130. Sereno, D., et al., *Antimonial-mediated DNA fragmentation in Leishmania infantum amastigotes.* Antimicrobial Agents and Chemotherapy, 2001. **45**(7): p. 2064-2069.

131. Sudhandiran, G. and C. Shaha, *Antimonial-induced increase in intracellular Ca2+ through non-selective cation.* Journal of Biological Chemistry. 2003 Jul 4;278(27):25120-32. Epub 2003 Apr 21., 2003. **278**(27): p. 25120-25132.

132. Demicheli, C., et al., *Antimony(V) complex formation with adenine nucleosides in aqueous solution.* Biochimica and Biophysica Acta, 2002. **1570**(3): p. 192-198.

133. Berman, J.D., J.V. Gallalee, and J.M. Best, *Sodium stibogluconate (Pentostam) inhibition of glucose catabolism via the glycolytic pathway, and fatty acid beta-oxidation in Leishmania mexicana amastigotes.* Biochemical Pharmacology, 1987. **36**(2): p. 197-201.

134. Balana-Fouce, R., et al., *The pharmacology of leishmaniasis.* General Pharmacology-the Vascular System, 1998. **30**(4): p. 435-443.

135. Frezard, F., C. Demicheli, and R.R. Ribeiro, *Pentavalent antimonials: new perspectives for old drugs.* Molecules, 2009. **14**(7): p. 2317-2336.

136. González, U., et al., *Interventions for Old World cutaneous leishmaniasis.* Cochrane Database of Systematic Reviews, 2008(4): p. 111.

137. WHO, *Patient receiving intralesional injection for the treatment of cutaneous leishmaniasis in Afghanistan.* 2015.

138. Gonzalez, U., et al., *Interventions for American cutaneous and mucocutaneous leishmaniasis.* Cochrane Database Systematic Reviews, 2009. **15**(2 (CD004834)): p. 1-171.

139. Grogl, M., T.N. Thomason, and E.D. Franke, *Drug resistance in leishmaniasis: its implication in systemic chemotherapy of cutaneous and mucocutaneous disease.* Am J Trop Med Hyg, 1992. **47**(1): p. 117-26.

140. Berman, J.D., et al., *Susceptibility of clinically sensitive and resistant Leishmania to pentavalent antimony in vitro.* Am J Trop Med Hyg, 1982. **31**(3 Pt 1): p. 459-65.

141. Allen, S. and R.A. Neal, *The in vitro Susceptibility of Macrophages Infected with Amastigotes of Leishmania spp. to Pentavalent Antimonial Drugs and Other Compounds with Special Relevance to Cutaneous Isolates*, in *Leishmaniasis*, D.T. Hart, Editor. 1989, Springer US. p. 711-720.

142. Navin, T.R., et al., *Placebo-controlled clinical trial of sodium stibogluconate (Pentostam) versus ketoconazole for treating cutaneous leishmaniasis in Guatemala.* Journal of Infectious Diseases, 1992. **165**(3): p. 528-534.

143. Cohen, B.E., et al., *The water and ionic permeability induced by polyene antibiotics across plasma membrane vesicles from Leishmania sp.* Biochimica and Biophysica Acta, 1986. **860**(1): p. 57-65.

144. Saha, A.K., T. Mukherjee, and A. Bhaduri, *Mechanism of action of amphotericin B on Leishmania donovani promastigotes.* Moleculer and Biochemical Parasitology, 1986. **19**(3): p. 195-200.

145. Gupta, U., H.B. Agashe, and N.K. Jain, *Polypropylene imine dendrimer mediated solubility enhancement: effect of pH and functional groups of hydrophobes.* J Pharm Pharm Sci, 2007. **10**(3): p. 358-67.

146. Sampaio, R.N. and P.D. Marsden, *[Treatment of the mucosal form of leishmaniasis without response to glucantime, with liposomal amphotericin B].* Rev Soc Bras Med Trop, 1997. **30**(2): p. 125-8.

147. Yardley, V. and S.L. Croft, *A comparison of the activities of three amphotericin B lipid formulations against experimental visceral and cutaneous leishmaniasis.* International Journal of Antimicrobial Agents, 2000. **13**(4): p. 243-248.

148. Balasegaram, M., et al., *Liposomal amphotericin B as a treatment for human leishmaniasis.* Expert Opin Emerg Drugs, 2012. **17**(4): p. 493-510.

149. Rodriguez, L.V., et al., *A randomized trial of amphotericin B alone or in combination with itraconazole in the treatment of mucocutaneous leishmaniasis.* Mem Inst Oswaldo Cruz, 1995. **90**(4): p. 525-8.

150. Neves, L.O., et al., *A randomized clinical trial comparing meglumine antimoniate, pentamidine and amphotericin B for the treatment of cutaneous leishmaniasis by Leishmania guyanensis.* An Bras Dermatol, 2011. **86**(6): p. 1092-101.

151. Uberall, F., et al., *Hexadecylphosphocholine inhibits inositol phosphate formation and protein kinase.* Cancer Research 1991. **51**(3): p. 807-812.

152. Achterberg, V. and G. Gercken, *Cytotoxicity of ester and ether lysophospholipids on Leishmania donovani promastigotes.* Mol Biochem Parasitol, 1987. **23**(2): p. 117-22.

153. Croft, S.L. and J. Engel, *Miltefosine - discovery of the antileishmanial activity of phospholipid derivatives.* Transactions of the Royal Society of Tropical Medicine and Hygiene, 2006. **100**(Supplement 1): p. S4-S8.

154. Croft, S.L., et al., *The activity of alkylphosphorylcholine and related derivatives against L. donovani.* Biochemical Pharmacology, 1987. **36**(16): p. 2633-2636.

155. Rakotomanga, M., et al., *Miltefosine affects lipid metabolism in Leishmania donovani promastigotes.* Antimicrob Agents Chemother, 2007. **51**(4): p. 1425-30.

156. Dorlo, T.P., et al., *Miltefosine: a review of its pharmacology and therapeutic efficacy in the treatment of leishmaniasis.* Journal of Antimicrobial Chemotherapy, 2012. **67**(11): p. 2576-2597.

157. Bryceson, A., *A policy for leishmaniasis with respect to the prevention and control of drug resistance.* Tropical Medicine and International Health, 2001. **6**(11): p. 928-934.

158. Sundar, S. and H.W. Murray, *Availability of miltefosine for the treatment of kala-azar in India.* Bulletin of the World Health Organisation, 2005. **83**(5): p. 394-395.

159. Escobar, P., et al., *Sensitivities of Leishmania species to hexadecylphosphocholine (miltefosine), ET-18-OCH3 (edelfosine) and amphotericin B.* Acta Tropica, 2002. **81**(2): p. 151-157.

160. Yardley, V., et al., *The sensitivity of clinical isolates of Leishmania from Peru and Nepal to miltefosine.* American Journal of Tropical Medicine and Hygiene, 2005. **73**(2): p. 272-275.

161. Soto, J., et al., *Miltefosine for new world cutaneous leishmaniasis.* Clinical Infectious Diseases, 2004. **38**: p. 1266-1272.

162. Mohebali, M., et al., *Comparison of miltefosine and meglumine antimoniate for the treatment of zoonotic cutaneous leishmaniasis (ZCL) by a randomized clinical trial in Iran.* Acta Tropica, 2007. **103**(1): p. 33-40.

163. Sundar, S., et al., *Oral miltefosine for Indian post-kala-azar dermal leishmaniasis: a randomised trial.* Trop Med Int Health, 2013. **18**(1): p. 96-100.

164. Ming, X., et al., *Transport of dicationic drugs pentamidine and furamidine by human organic cation transporters.* Drug Metab Dispos, 2009. **37**(2): p. 424-30.

165. Andersen, E.M., et al., *Comparison of meglumine antimoniate and pentamidine for Peruvian cutaneous leishmaniasis.* American Journal of Tropical Medicine and Hygiene, 2005. **72**(2): p. 133-137.

166. Saenz, R.E., H. Paz, and J.D. Berman, *Efficacy of ketoconazole against Leishmania braziliensis panamensis cutaneous leishmaniasis.* American Journal of Medicine, 1990. **89**(2): p. 147-155.

167. Salmanpour, R., F. Handjani, and M.K. Nouhpisheh, *Comparative study of the efficacy of oral ketoconazole with intra-lesional meglumine antimoniate (Glucantime) for the treatment of cutaneous leishmaniasis.* Journal of Dermatological Treatment, 2001. **12**(3): p. 159-162.

168. Alrajhi, A.A., et al., *Fluconazole for the treatment of cutaneous leishmaniasis caused by Leishmania major.* New England Journal of Medicine, 2002. **346**(12): p. 891-895.

169. Neal, R.A., *The effect of antibiotics of the neomycin group on experimental cutaneous leishmaniasis.* Ann Trop Med Parasitol, 1968. **62**(1): p. 54-62.

170. Walter, F., Q. Vicens, and E. Westhof, *Aminoglycoside-RNA interactions.* Curr Opin Chem Biol, 1999. **3**(6): p. 694-704.

171. Maarouf, M., et al., *Ribosomes of Leishmania are a target for the aminoglycosides* Parasitology Research, 1995. **81**(5): p. 421-425.

172. Fernandez, M.M., E.L. Malchiodi, and I.D. Algranati, *Differential effects of paromomycin on ribosomes of Leishmania mexicana and mammalian cells.* Antimicrob Agents Chemother, 2011. **55**(1): p. 86-93.

173. Chawla, B., et al., *Paromomycin affects translation and vesicle-mediated trafficking as revealed by proteomics of paromomycin -susceptible -resistant Leishmania donovani.* PLoS One, 2011. **6**(10): p. e26660.

174. Maarouf, M., et al., *Biochemical alterations in paromomycin-treated Leishmania donovani promastigotes.* Parasitol Res, 1997. **83**(2): p. 198-202.

175. Maarouf, M., et al., *In vivo interference of paromomycin with mitochondrial activity of Leishmania.* Exp Cell Res, 1997. **232**(2): p. 339-48.

176. El-On, J., et al., *Development of topical treatment for cutaneous leishmaniasis caused by Leishmania major in experimental animals.* Antimicrobial Agents and Chemotherapy, 1984. **26**(05): p. 745-751.

177. El-On, J. and A.D. Hamburger, *Topical treatment of New and Old World cutaneous leishmaniasis in experimental animals.* Transactions of the Royal Society of Tropical Medicine and Hygiene, 1987. **81**: p. 734-737.

178. El-On, J., G.P. Jacobs, and L. Weinrauch, *Topical chemotherapy of cutaneous Leishmaniasis.* Parasitology Today, 1988. **4**(3): p. 76-81.

179. Kim, D.H., et al., *Is paromomycin an effective and safe treatment against cutaneous leishmaniasis? A meta-analysis of 14 randomized controlled trials.* PLoS Negl Trop Dis, 2009. **3**(2): p. e381.

180. Asilian, A., et al., *A randomized, placebo-controlled trial of a two-week regimen of aminosidine (paromomycin) ointment for treatment of cutaneous leishmaniasis in Iran.* American Journal of Tropical Medicine and Hygiene, 1995. **53**(6): p. 648-651.

181. Ben Salah, A., et al., *A randomized, placebo-controlled trial in Tunisia treating cutaneous treating cutaneous leishmaniasis with paromomycin ointment.* American Journal of Tropical Medicine and Hygiene, 1995. **53**(2): p. 162-166.

182. Faghihi, G. and R. Tavakoli-kia, *Treatment of cutaneous leishmaniasis with either topical paromomycin or intralesional meglumine antimoniate.* Clinical and Experimental Dermatology, 2003. **28**(1): p. 13-16.

183. Shazad, B., B. Abbaszadeh, and A. Khamesipour, *Comparison of topical paromomycin sulfate (twice/day) with intralesional meglumine antimoniate for the treatment of cutaneous leishmaniasis caused by L. major.* European Journal of Dermatology, 2005. **15**(2): p. 85-87.

184. Grogl, M., et al., *Successful topical treatment of murine cutaneous leishmaniasis with a combination of paromomycin (Aminosidine) and gentamicin.* Journal of Parasitology, 1999. **85**(2): p. 354-359.

185. Gomes, S.F.O., E.A. Nunan, and L.O.M. Ferreira, *Influence of the formulation type (o/w, w/o/w emulsions and ointment) on the topical delivery of paromomycin.* Brazilian Journal of Pharmaceutical Sciences, 2004. **40**(3): p. 345-352.

186. Ben Salah, A., et al., *WR279,396, a third generation aminoglycoside ointment for the treatment of Leishmania major cutaneous leishmaniasis: A phase 2, randomized, double blind, placebo controlled study.* Plos Neglected Tropical Diseases, 2009. **3**(5): p. e432.

187. Ben Salah, A., et al., *Topical paromomycin with or without gentamicin for cutaneous leishmaniasis.* The New England Journal of Medicine, 2013. **368**(6): p. 524-32.

188. Soto, J.M., et al., *Treatment of cutaneous leishmaniasis with a topical antileishmanial drug (WR279396): phase 2 pilot study* American Journal of Tropical Medicine and Hygiene, 2002. **66**(2): p. 147-151.

189. Sosa, N., et al., *Randomized, double-blinded, phase 2 trial of WR 279,396 (paromomycin and gentamicin) for cutaneous leishmaniasis in Panama.* Am J Trop Med Hyg, 2013. **89**(3): p. 557-63.

190. Asilian, A. and M. Davami, *Comparison between the efficacy of photodynamic therapy and topical paromomycin in the treatment of Old World cutaneous leishmaniasis: a placebo-controlled, randomized clinical trial.* Clinical and Experimental Dermatology, 2006. **31**(5): p. 634-637.

191. Asilian, A., et al., *Treatment of cutaneous leishmaniasis with aminosidine (paromomycin) ointment.* Bulletin of the World Health Organisation, 2003. **81**(5): p. 353-359.

192. Iraji, F. and A. Sadeghinia, *Efficacy of paromomycin ointment in the treatment of cutaneous leishmaniasis: results of a double-blind, randomized trial in Isfahan, Iran.* Annals of Tropical Medicine and Parasitology, 2005. **99**(1): p. 3-9.

193. Ozgoztasi, O. and I. Baydar, *A randomized clinical trial of topical paromomycin versus oral ketoconazole for treating cutaneous leishmaniasis in Turkey.* International Journal of Dermatology, 1997. **36**(1): p. 61-63.

194. Armijos, R.X., et al., *Comparison of the effectiveness of two topical paromomycin treatments versus meglumine antimoniate for New World cutaneous leishmaniasis.* Acta Tropica, 2004. **91**(2): p. 153-160.

195. Soto, J., et al., *Topical paromomycin/methylbenzethonium chloride plus parenteral meglumine antimonate as treatment for American cutaneous leishmaniasis: controlled study.* Clinical Infectious Diseases, 1998. **26**(1): p. 56-58.

196. Ro, J., et al., *Pectin Micro- and Nano-capsules of Retinyl Palmitate as Cosmeceutical Carriers for Stabilized Skin Transport.* Korean J Physiol Pharmacol, 2015. **19**(1): p. 59-64.

197. Zhang, J. and E. Smith, *Percutaneous permeation of betamethasone 17-valerate incorporated in lipid nanoparticles.* J Pharm Sci, 2011. **100**(3): p. 896-903.

198. Papakostas, D., et al., *Nanoparticles in dermatology.* Archives of Dermatological Research, 2011. **303**(8): p. 533-550.

199. Romero, E.L. and M.J. Morilla, *Drug delivery systems against leishmaniasis? Still an open question.* Expert Opinion on Drug Delivery, 2008. **5**(7): p. 805-823.

200. Watkinson, A.C., et al., *Nanoparticles do not penetrate human skin-a theoretical perspective.* Pharm Res, 2013. **30**(8): p. 1943-6.

201. Touitou, E., et al., *Liposomes as carriers for topical and transdermal delivery.* Journal of Pharmaceutical Sciences, 1994. **83**(9): p. 1189-1203.

202. Ferreira, L.S., et al., *In vitro skin permeation and retention of paromomycin from liposomes for topical treatment of cutaneous leishmaniasis.* Drug Development and Industrial Pharmacy, 2004. **30**(3): p. 289-296.

203. Jaafari, M.R., et al., *Effect of topical liposomes containing paromomycin sulfate in the course of Leishmania major infection in susceptible BALB/c mice.* Antimicrobial Agents and Chemotherapy, 2009. **53**(6): p. 2259-2265.

204. Nogueira, I.R., et al., *Preparation, characterization, and topical delivery of paromomycin ion pairing.* Drug Development and Industrial Pharmacy, 2011. **37**(9): p. 1083-1089.

205. Salmanpour, R., M.R. Razmavar, and N. Abtahi, *Comparison of intralesional meglumine antimoniate, cryotherapy and their combination in the treatment of cutaneous leishmaniasis.* International Journal of Dermatology, 2006. **45**(9): p. 1115-1116.

206. Sadeghian, G., M.A. Nilfroushzadeh, and F. Iraji, *Efficacy of local heat therapy by radiofrequency in the treatment of cutaneous leishmaniasis, compared with intralesional injection of meglumine antimoniate.* Clinical and Experimental Dermatology, 2007. **32**(4): p. 371-374.

207. Reithinger, R., et al., *Efficacy of thermotherapy to treat cutaneous leishmaniasis caused by Leishmania tropica in Kabul, Afghanistan: a randomized, controlled trial.* Clinical Infectious Diseases, 2005. **40**(8): p. 1148-1155.

208. Navin, T.R., et al., *Placebo-controlled clinical trial of meglumine antimoniate (glucantime) versus localized controlled heat in the treatment of cutaneous leishmaniasis in Guatemala.* American Journal of Tropical Medicine and Hygiene, 1990. **42**(1): p. 43-50.

209. Buates, S. and G. Matlashewski, *Treatment of experimental leishmaniasis with the immunomodulators imiquimod and S-28463: efficacy and mode of action.* Journal of Infectious Diseases, 1999. **179**: p. 1485-1494.

210. Arevalo, I., et al., *Successful treatment of drug-resistant cutaneous leishmaniasis in humans by use of imiquimod, an immunomodulator.* Clinical Infectious Diseases, 2001. **33**(11): p. 1847-1851.

211. Miranda-Verastegui, C., et al., *Randomized, double-blind clinical trial of topical imiquimod 5% with parenteral meglumine antimoniate in the treatment of cutaneous leishmaniasis in Peru.* Clinical Infectious Diseases, 2005. **40**(10): p. 1395-1403.

212. Lee, F., et al., *Isolation of cDNA for a human granulocyte-macrophage colony-stimulating factor by functional expression in mammalian cells.* Proc Natl Acad Sci U S A, 1985. **82**(13): p. 4360-4.

213. Shi, Y., et al., *Granulocyte-macrophage colony-stimulating factor (GM-CSF) and T-cell responses: what we do and don't know.* Cell Res, 2006. **16**(2): p. 126-33.

214. Zhang, L., J. Chen, and C. Han, *A multicenter clinical trial of recombinant human GM-CSF hydrogel for the treatment of deep second-degree burns.* Wound Repair Regen, 2009. **17**(5): p. 685-9.

215. da Costa, R.M., et al., *Quick healing of leg ulcers after molgramostim.* Lancet, 1994. **344**(8920): p. 481-2.

216. Jaschke, E., A. Zabernigg, and C. Gattringer, *Recombinant human granulocyte-macrophage colony-stimulating factor applied locally in low doses enhances healing and prevents recurrence of chronic venous ulcers.* Int J Dermatol, 1999. **38**(5): p. 380-6.

217. Kaplan, G., et al., *Novel responses of human skin to intradermal recombinant granulocyte/macrophage-colony-stimulating factor: Langerhans cell recruitment, keratinocyte growth, and enhanced wound healing.* J Exp Med, 1992. **175**(6): p. 1717-28.

218. Hu, X., et al., *Topically applied rhGM-CSF for the wound healing: A systematic review.* Burns, 2011. **37**(5): p. 729-741.

219. Handman, E. and A.W. Burgess, *Stimulation by granulocyte-macrophage colony-stimulating factor of Leishmania tropica killing by macrophages.* J Immunol, 1979. **122**(3): p. 1134-7.

220. Al-Zamel, F., et al., *Enhancement of leishmanicidal activity of human macrophages against Leishmania major and Leishmania donovani infection using recombinant human granulocyte macrophage colony stimulating factor.* Zentralbl Bakteriol, 1996. **285**(1): p. 92-105.

221. Ho, J.L., et al., *Granulocyte-macrophage and macrophage colony-stimulating factors activate intramacrophage killing of Leishmania mexicana amazonensis.* J Infect Dis, 1990. **162**(1): p. 224-30.

222. Murray, H.W., et al., *Effect of granulocyte-macrophage colony-stimulating factor in experimental visceral leishmaniasis.* J Clin Invest, 1995. **95**(3): p. 1183-92.

223. Almeida, R., et al., *Randomized, double-blind study of stibogluconate plus human granulocyte macrophage colony-stimulating factor versus stibogluconate alone in the treatment of cutaneous Leishmaniasis.* J Infect Dis, 1999. **180**(5): p. 1735-7.

224. Santos, J.B., et al., *Antimony plus recombinant human granulocyte-macrophage colony-stimulating factor applied topically in low doses enhances healing of cutaneous Leishmaniasis ulcers: a randomized, double-blind, placebo-controlled study.* J Infect Dis, 2004. **190**(10): p. 1793-6.

225. Frankenburg, S., et al., *Efficacious topical treatment for murine cutaneous leishmaniasis with ethanolic formulations of amphotericin B.* Antimicrobial Agents and Chemotherapy, 1998. **42**(12): p. 3092-6.

226. Santos, P., et al., *Enhanced permeation of fentanyl from supersaturated solutions in a model membrane.* Int J Pharm, 2011. **407**(1-2): p. 72-7.

227. Bommannan, D., R.O. Potts, and R.H. Guy, *Examination of the effect of ethanol on human stratum corneum in vivo using using infrared spectroscopy.* Journal of Controlled Release, 1991. **16**(3): p. 299-304.

228. Kai, T., et al., *mechanism of percutaneous penetration enhancement: effect of n-alkanols on the permeability barrier of hairless mouse skin.* Journal of Controlled Release, 1990. **12**(2): p. 103-112.

229. Van der Merwe, D. and J.E. Riviere, *Comparative studies on the effects of water, ethanol and water/ethanol mixtures on chemical partitioning into porcine stratum corneum and silastic membrane.* Toxicol In Vitro, 2005. **19**(1): p. 69-77.

230. Vardy, D., et al., *Efficacious topical treatment for human cutaneous leishmaniasis with ethanolic lipid amphotericin B.* Transactions of the Royal Society of Tropical Medicine and Hygiene, 2001. **95**(2): p. 184-186.

231. Zvulunov, A., et al., *Topical treatment of persistent cutaneous leishmaniasis with ethanolic lipid amphotericin B.* The Pediatric Infectious Disease Journal, 2003. **22**(6): p. 567-569.

232. Lavasanifar, A., J. Samuel, and G.S. Kwon, *Micelles self-assembled from poly(ethylene oxide)-block-poly(N-hexyl stearate L-aspartamide) by a solvent evaporation method: effect on the solubilization and haemolytic activity of amphotericin B.* J Control Release, 2001. **77**(1-2): p. 155-60.

233. Hussain, A., et al., *Nanocarrier-based topical drug delivery for an antifungal drug.* Drug Development and Industrial Pharmacy, 2014. **40**(4): p. 527-41.

234. Manosroi, A., L. Kongkaneramit, and J. Manosroi, *Stability and transdermal absorption of topical amphotericin B liposome formulations.* Internation Journal of Pharmaceutics, 2004. **270**(1-2): p. 279-86.

235. Ruiz, H.K., et al., *New amphotericin B-gamma cyclodextrin formulation for topical use with synergistic activity against diverse fungal species and Leishmania spp.* International Journal of Pharmaceutics, 2014.

236. Yardley, V. and S.L. Croft, *Activity of liposomal amphotericin B against experimental cutaneous leishmaniasis.* Antimicrobial Agents and Chemotherapy, 1997. **41**(4): p. 752-756.

237. Barber, E.D., et al., *A comparative study of the rates of in vitro percutaneous absorption of eight chemicals using rat and human skin.* Fundam Appl Toxicol, 1992. **19**(4): p. 493-7.

238. van Ravenzwaay, B. and E. Leibold, *A comparison between in vitro rat and human and in vivo rat skin absorption studies.* Hum Exp Toxicol, 2004. **23**(9): p. 421-30.

239. Santos, C.M., et al., *Amphotericin B-loaded nanocarriers for topical treatment of cutaneous leishmaniasis: development, characterization, and in vitro skin permeation studies.* J Biomed Nanotechnol, 2012. **8**(2): p. 322-9.

240. Corware, K., et al., *Accelerated healing of cutaneous leishmaniasis in non-healing BALB/c mice using water soluble amphotericin B-polymethacrylic acid.* Biomaterials, 2011. **32**(31): p. 8029-8039.

241. Schmidt-Ott, R., et al., *Topical treatment with hexadecylphosphocholine (Miltex) efficiently reduces parasite burden in experimental cutaneous leishmaniasis.* 1999(0035-9203 (Print)).

242. Luque-Ortega, J.R., et al., *In vivo monitoring of intracellular ATP levels in Leishmania donovani promastigotes as a rapid method to screen drugs targeting bioenergetic metabolism.* Antimicrob Agents Chemother, 2001. **45**(4): p. 1121-5.

243. Mantyla, A., et al., *Synthesis, in vitro evaluation, and antileishmanial activity of water-soluble prodrugs of buparvaquone.* Journal of Medicinal Chemistry, 2004. **47**(1): p. 188-95.

244. Croft, S.L., et al., *The activity of hydroxynaphtoquinones against Leishmania donovani. .* Journal of Antimicrobial Chemotherapy, 1992. **30**(6): p. 827-832.

245. Garnier, T., et al., *Topical buparvaquone formulations for the treatment of cutaneous leishmaniasis.* Journal of Pharmacy and Pharmacology, 2007. **59**(1): p. 41-49.

246. Garnier, T., *Topical treatment of cutaneous leishmaniasis*, in *Department of immunology and infection*. 2004, London School of Hygiene & Tropical Medicine. p. 321.

247. DiMasi, J.A., R.W. Hansen, and H.G. Grabowski, *The price of innovation: new estimates of drug development costs.* J Health Econ, 2003. **22**(2): p. 151-85.

248. Morgan, S., et al., *The cost of drug development: a systematic review.* Health Policy, 2011. **100**(1): p. 4-17.

249. Pedrique, B., et al., *The drug and vaccine landscape for neglected diseases (2000?11): a systematic assessment.* The Lancet Global Health, 2013. **1**(6): p. e371-e379.

250. Abazid, N., C. Jones, and C.R. Davies, *Knowledge, attitudes and practices about leishmaniasis among cutaneous leishmaniasis patients in Aleppo, Syrian Arab Republic.* East Mediterr Health J, 2012. **18**(1): p. 7-14.

251. Ruoti, M., et al., *Mucocutaneous leishmaniasis: knowledge, attitudes, and practices among paraguayan communities, patients, and health professionals.* J Trop Med, 2013. **2013**: p. 538629.

252. Arana, B., *Do we need systemic (oral) drugs for CL?* 2014, Drugs for Neglected Diseases Initiative.

253. Visalli, R.J., R.J. Courtney, and C. Meyers, *Infection and Replication of Herpes Simplex Virus Type 1 in an Organotypic Epithelial Culture System.* Virology, 1997. **230**(2): p. 236-243.

254. Jakasa, I., et al., *Altered penetration of polyethylene glycols into uninvolved skin of atopic dermatitis patients.* J Invest Dermatol, 2007. **127**(1): p. 129-34.

255. Jensen, J.M., et al., *Barrier function, epidermal differentiation, and human beta-defensin 2 expression in tinea corporis.* J Invest Dermatol, 2007. **127**(7): p. 1720-7.

256. Cork, M.J., et al., *Epidermal Barrier Dysfunction in Atopic Dermatitis.* Journal of Investigative Dermatology, 2009. **129**(8): p. 1892-1908.

257. Gould, A.R., et al., *Increased permeability of psoriatic skin to the protein, plasminogen activator inhibitor 2.* Arch Dermatol Res, 2003. **295**(6): p. 249-54.

258. Hon, K.L., et al., *Comparison of skin hydration evaluation sites and correlations among skin hydration, transepidermal water loss, SCORAD index, Nottingham Eczema Severity Score, and quality of life in patients with atopic dermatitis.* Am J Clin Dermatol, 2008. **9**(1): p. 45-50.

259. Behne, M.J., et al., *NHE1 regulates the stratum corneum permeability barrier homeostasis. Microenvironment acidification assessed with fluorescence lifetime imaging.* J Biol Chem, 2002. **277**(49): p. 47399-406.

260. Fluhr, J.W., et al., *Generation of free fatty acids from phospholipids regulates stratum corneum acidification and integrity.* J Invest Dermatol, 2001. **117**(1): p. 44-51.

261. Mauro, T., et al., *Barrier recovery is impeded at neutral pH, independent of ionic effects: implications for extracellular lipid processing.* Arch Dermatol Res, 1998. **290**(4): p. 215-22.

262. Yosipovitch, G., et al., *Skin surface pH in intertriginous areas in NIDDM patients. Possible correlation to candidal intertrigo.* Diabetes Care, 1993. **16**(4): p. 560-3.

263. Chikakane, K. and H. Takahashi, *Measurement of skin pH and its significance in cutaneous diseases.* Clinics in Dermatology, 1995. **13**(4): p. 299-306.

264. Brattsand, M. and T. Egelrud, *Purification, molecular cloning, and expression of a human stratum corneum trypsin-like serine protease with possible function in desquamation.* J Biol Chem, 1999. **274**(42): p. 30033-40.

265. Ekholm, I.E., M. Brattsand, and T. Egelrud, *Stratum corneum tryptic enzyme in normal epidermis: a missing link in the desquamation process?* J Invest Dermatol, 2000. **114**(1): p. 56-63.

266. Ekholm, E. and T. Egelrud, *Expression of stratum corneum chymotryptic enzyme in relation to other markers of epidermal differentiation in a skin explant model.* Exp Dermatol, 2000. **9**(1): p. 65-70.

267. Rippke, F., V. Schreiner, and H.J. Schwanitz, *The acidic milieu of the horny layer: new findings on the physiology and pathophysiology of skin pH.* Am J Clin Dermatol, 2002. **3**(4): p. 261-72.

268. Voegli, R. and A.V. Rawlings, *Desquatmation: it is almost all about proteases*, in *Treatment of dry skin syndrome - the art and science of moisturizers*, M. Loden and H.I. Maibach, Editors. 2012, Springer-Verlag: Berlin. New York. p. 149-178.

269. Development, O.f.E.C.-o.a., *Guidance document for the conduct of skin absorption studies.* 2004.

270. Ritter, U. and H. Korner, *Divergent expression of inflammatory dermal chemokines in cutaneous leishmaniasis.* Parasite Immunol, 2002. **24**(6): p. 295-301.

271. Larsen, R.H., et al., *Dermal penetration of fentanyl: inter- and intraindividual variations.* Pharmacology and Toxicology, 2003. **93**(5): p. 244-248.

272. Scott, R.C., et al., *The influence of skin structure on permeability: an intersite and interspecies comparison with hydrophilic penetrants.* J Invest Dermatol, 1991. **96**(6): p. 921-5.

273. Schaefer, U.F., et al., *Models for skin absorption and skin toxicity testing*, in *Drug absorption studies: in skin, in vitro, and in silico models*, C. Ehrhardt and K.J. Kim, Editors. 2008, Springer Science: New York. p. 3-33.

274. Southwell, D., B.W. Barry, and R. Woodford, *Variations in permeability of human skin within and between specimens.* International Journal of Pharmaceutics, 1984. **18**(3): p. 299-309.

275. Liu, P., J.A.S. Nightingale, and T. Kurihara-Bergstrom, *Variation of human skin permeation in vitro: Ionic vs neutral compounds.* International Journal of Pharmaceutics, 1993. **90**(2): p. 171-176.

276. Magnusson, B.M., W.J. Pugh, and M.S. Roberts, *Simple rules defining the potential of compounds for transdermal delivery or toxicity.* Pharm Res, 2004. **21**(6): p. 1047-54.

277. Uranw, S., et al., *Adherence to miltefosine treatment for visceral leishmaniasis under routine conditions in Nepal.* Trop Med Int Health, 2013. **18**(2): p. 179-87.

278. Hadgraft, J. and M. Lane, *Penetration enhancers, solvents and the skin*, in *Drug delivery strategies for poorly water-soluble drugs*, E. Douroumis and A. Fahr, Editors. 2013, John Wiley & Sons, Ltd. p. 359-371.

279. Barratt, M.D., *Quantitative structure-activity relationships for skin permeability.* Toxicol In Vitro, 1995. **9**(1): p. 27-37.

280. Leonard, R., et al., *Randomized, double-blind, placebo-controlled, multicenter trial of 6% miltefosine solution, a topical chemotherapy in cutaneous metastases from breast cancer.* J Clin Oncol, 2001. **19**(21): p. 4150-9.

281. Garnier, T. and S.L. Croft, *Topical treatment for cutaneous leishmaniasis.* Current Opinion on Investigational Drugs, 2002. **3**(4): p. 538-544.

282. Soto, J., et al., *Treatment of American cutaneous leishmaniasis with miltefosine, an oral agent.* Clinical Infectious Diseases, 2001. **33**: p. e57-61.

283. Wiechers, J.N., et al., *Formulating for efficacy.* International Journal of Cosmetic Science, 2004. **26**(4): p. 173-182.

284. Hadgraft, J., *Passive enhancement strategies in topical and transdermal drug delivery.* International Journal of Pharmaceutics, 1999. **184**(1): p. 1-6.

285. Mitragotri, S., *Synergistic effect of enhancers for transdermal drug delivery.* Pharmaceutical Research, 2000. **17**(11): p. 1354-1359.

286. Croft, S.L. and R. Brun, *In vitro and in vivo models for the identification and evaluation of drugs active against Trypanosoma and Leishmania*, in *Drugs against parasitic diseases: R&D methodologies and issues*, A.H. Fairlamb, R.D. Ridley, and H.D. Vial, Editors. 2003, World Health Organisation: Geneva, Switzerland. p. 165-175.

287. Kaufmann-Kolle, P. and E.A. Fleer, *Morphological changes of adherent and nonadherent cells by treatment with hexadecylphosphocholine and 1-O-octadecyl-2-O-methyl-rac-glycero-3-phosphocholine observed by scanning electron microscopy.* Prog Exp Tumor Res, 1992. **34**: p. 47-58.

288. Wieder, T., et al., *The effect of hexadecylphosphocholine on the proliferation of human keratinocytes in vitro and in vivo.* Drugs of Today, 1998. **34**(Suppl F): p. 97-105.

289. Van Krevelen, W. and K. te Nijenhuis, *Cohesive properties and solubility*, in *Properties of polymers: their correlation with chemical structure, their numerical estimation and prediction from additive group contributions*, W. Van Krevelen and K. te Nijenhuis, Editors. 2009, Elsevier. p. 189-228.

290. Lane, M.E., et al., *Rational formulation design.* Int J Cosmet Sci, 2012. **34**(6): p. 496-501.

291. Rakotomanga, M., P.M. Loiseau, and M. Saint-Pierre-Chazalet, *Hexadecylphosphocholine interaction with lipid monolayers.* Biochimica Et Biophysica Acta-Biomembranes, 2004. **1661**(2): p. 212-218.

292. Zia, H., et al., *Cosolvency of dimethyl isosorbide for steroid solubility.* Pharm Res, 1991. **8**(4): p. 502-4.

293. Development, T.O.f.E.C.-o.a. *OEDC guideline for testing of chemicals - Partition Coefficient: High Performance Liquid Chromatography (HPLC) Method (117).* 1989 [cited.

294. Davis, A.F. and J. Hadgraft, *The use of supersaturation in topical drug delivery*. Prediction of Percutaneous Penetration : Methods, Measurements, Modelling, Vol 2, ed. R.C. Scott, et al. 1991. 279-287.

295. Pellett, M.A., A.F. Davis, and J. Hadgraft, *Effect of supersaturation on membrane transport: 2. Piroxicam.* International Journal of Pharmaceutics, 1994. **111**(1): p. 1-6.

296. Benaouda, F., et al., *Triggered in situ drug supersaturation and hydrophilic matrix self-assembly.* Pharm Res, 2012. **29**(12): p. 3434-42.

297. Karande, P., A. Jain, and S. Mitragotri, *Insights into synergistic interactions in binary mixtures of chemical permeation.* Journal of Controlled Release, 2006. **115**(1): p. 85-93.

298. Arora, A., et al., *Multicomponent chemical enhancer formulations for transdermal drug delivery: More is not always better.* Journal of Controlled Release, 2010. **144**(2): p. 175-180.

299. Scheuplein, R.J. and L. Ross, *Effects of surfactants and solvents on the permeability of epidermis.* Journal of the Society of Cosmetic chemists, 1970. **21**: p. 853-873.

300. Rhein, L.D., et al., *Surfactant structure effects on swelling of isolated human stratum corneum.* Journal of the Cosmetic Society of Chemists, 1986. **37**: p. 125-139.

301. van Ruissen, F., et al., *Differential effects of detergents on keratinocyte gene expression.* J Invest Dermatol, 1998. **110**(4): p. 358-63.

302. De Fine Olivarius, F., T. Agner, and T. Menne, *Skin barrier function and dermal inflammation. An experimental study of transepidermal water loss after dermal tuberculin injection compared with SLS patch testing.* Br J Dermatol, 1993. **129**(5): p. 554-7.

303. Shokri, J., et al., *The effect of surfactants on the skin penetration of diazepam.* Int J Pharm, 2001. **228**(1-2): p. 99-107.

304. Alonso, L., et al., *Interaction of miltefosine with intercellular membranes of stratum corneum and biomimetic lipid vesicles.* International Journal of Pharmaceutics, 2012. **434**(1–2): p. 391-398.

305. Kiener, P.A. and S.G. Waley, *Reversible inhibitors of penicillinases.* Biochem J, 1978. **169**(1): p. 197-204.

306. Beesley, T., et al., *The inhibition of class C beta-lactamases by boronic acids.* Biochem J, 1983. **209**(1): p. 229-33.
307. Amicosante, G., et al., *Do inert beta-lactamase inhibitors act as synergizers of beta-lactam antibiotics? Utility of boric and boronic acids.* J Chemother, 1989. **1**(6): p. 394-8.
308. Crompton, I.E., et al., *Beta-lactamase inhibitors. The inhibition of serine beta-lactamases by specific boronic acids.* Biochem J, 1988. **251**(2): p. 453-9.
309. Adams, J., et al., *Potent and selective inhibitors of the proteasome: dipeptidyl boronic acids.* Bioorg Med Chem Lett, 1998. **8**(4): p. 333-8.
310. Teicher, B.A., et al., *The proteasome inhibitor PS-341 in cancer therapy.* Clin Cancer Res, 1999. **5**(9): p. 2638-45.
311. Frankel, A., et al., *Lack of multicellular drug resistance observed in human ovarian and prostate carcinoma treated with the proteasome inhibitor PS-341.* Clin Cancer Res, 2000. **6**(9): p. 3719-28.
312. Hideshima, T., et al., *The proteasome inhibitor PS-341 inhibits growth, induces apoptosis, and overcomes drug resistance in human multiple myeloma cells.* Cancer Res, 2001. **61**(7): p. 3071-6.
313. Jacobs, R.T., et al., *Benzoxaboroles: a new class of potential drugs for human African trypanosomiasis.* Future Medicinal Chemistry, 2011. **3**(10): p. 1259-1278.
314. Jacobs, R.T., J.J. Plattner, and M. Keenan, *Boron-based drugs as antiprotozoals.* Current Opinion in Infectious Diseases, 2011. **24**(6): p. 586-592.
315. Zhang, Y.K., et al., *Synthesis and structure-activity relationships of novel benzoxaboroles as a new class of antimalarial agents.* Bioorg Med Chem Lett, 2011. **21**(2): p. 644-51.
316. Zhang, Y.K., et al., *Benzoxaborole antimalarial agents. Part 2: Discovery of fluoro-substituted 7-(2-carboxyethyl)-1,3-dihydro-1-hydroxy-2,1-benzoxaboroles.* Bioorg Med Chem Lett, 2012. **22**(3): p. 1299-307.
317. Hu, Q.-H., et al., *Discovery of a potent benzoxaborole-based anti-pneumococcal agent targeting leucyl-tRNA synthetase.* Sci. Rep., 2013. **3**.
318. Liu, C.T., J.W. Tomsho, and S.J. Benkovic, *The unique chemistry of benzoxaboroles: Current and emerging applications in biotechnology and therapeutic treatments.* Bioorganic & Medicinal Chemistry, 2014. **22**(16): p. 4462-4473.
319. Elewski, B.E. and A. Tosti, *Tavaborole for the treatment of onychomycosis.* Expert Opin Pharmacother, 2014. **15**(10): p. 1439-48.
320. Nare, B., et al., *Discovery of novel orally bioavailable oxaborole 6-carboxamides that demonstrate cure in a murine model of late-stage central nervous system african trypanosomiasis.* Antimicrobial Agents and Chemotherapy, 2010. **54**(10): p. 4379-4388.
321. Lipinski, C.A., *Drug-like properties and the causes of poor solubility and poor permeability.* J Pharmacol Toxicol Methods, 2000. **44**(1): p. 235-49.
322. Kerns, E.H. and L. Di, *Multivariate pharmaceutical profiling for drug discovery.* Curr Top Med Chem, 2002. **2**(1): p. 87-98.
323. Akama, T., et al., *Discovery and structure-activity study of a novel benzoxaborole anti-inflammatory agent (AN2728) for the potential topical treatment of psoriasis and atopic dermatitis.* Bioorg Med Chem Lett, 2009. **19**(8): p. 2129-32.
324. Del Rosso, J.Q. and J.J. Plattner, *From the Test Tube to the Treatment Room: Fundamentals of Boron-containing Compounds and their Relevance to Dermatology.* J Clin Aesthet Dermatol, 2014. **7**(2): p. 13-21.
325. Jirata, D., et al., *Identification, sequencing and expression of peroxidoxin genes from Leishmania aethiopica.* Acta Trop, 2006. **99**(1): p. 88-96.
326. Gadisa, E., et al., *Leishmania (Kinetoplastida): species typing with isoenzyme and PCR-RFLP from cutaneous leishmaniasis patients in Ethiopia.* Exp Parasitol, 2007. **115**(4): p. 339-43.
327. Janneh, O., et al., *Inhibition of P-glycoprotein and multidrug resistance-associated proteins modulates the intracellular concentration of lopinavir in cultured CD4 T cells and primary human lymphocytes.* J Antimicrob Chemother, 2007. **60**(5): p. 987-93.
328. Jovelet, C., et al., *Influence of the multidrug transporter P-glycoprotein on the intracellular pharmacokinetics of vandetanib.* Eur J Drug Metab Pharmacokinet, 2013. **38**(3): p. 149-57.
329. Kao, J., F.K. Patterson, and J. Hall, *Skin penetration and metabolism of topically applied chemicals in six mammalian species, including man: an in vitro study with benzo[a]pyrene and testosterone.* Toxicology and Applied Pharmacology, 1985. **81**: p. 502-516.
330. Beydon, D., J.P. Payan, and M.C. Grandclaude, *Comparison of percutaneous absorption and metabolism of di-n-butylphthalate in various species.* Toxicol In Vitro, 2010. **24**(1): p. 71-8.
331. Muller, B., et al., *Permeation, metabolism and site of action concentration of nicotinic acid derivatives in human skin. Correlation with topical pharmacological effect.* Eur J Pharm Sci, 2003. **20**(2): p. 181-95.

332. Ozaki, H., et al., *Comparative study of the hydrolytic metabolism of methyl-, ethyl-, propyl-, butyl-, heptyl- and dodecylparaben by microsomes of various rat and human tissues.* Xenobiotica, 2013. **43**(12): p. 1064-72.

333. Morris, A.P., K.R. Brain, and C.M. Heard, *Skin permeation and ex vivo skin metabolism of O-acyl haloperidol ester prodrugs.* Int J Pharm, 2009. **367**(1-2): p. 44-50.

334. Montagna, W., *Histology and cytochemistry of human skin: IX. The distribution of non-specific esterases* The Journal of Biophysical and Biochemical Cytology, 1955. **1**(1): p. 13-16.

335. Baron, J.M., et al., *Expression of multiple cytochrome p450 enzymes and multidrug resistance-associated transport proteins in human skin keratinocytes.* J Invest Dermatol, 2001. **116**(4): p. 541-8.

336. Swanson, H.I., *Cytochrome P450 expression in human keratinocytes: an aryl hydrocarbon receptor perspective.* Chem Biol Interact, 2004. **149**(2-3): p. 69-79.

337. Clausen, J. and M.H. Bickel, *Prediction of drug distribution in distribution dialysis and in vivo from binding to tissues and blood.* J Pharm Sci, 1993. **82**(4): p. 345-9.

338. Netzaff, F., et al., *The human epidermis models EpiSkin (R), SkinEthic (R) and EpiDerm (R): An evaluation of morphology and their suitability for testing phototoxicity, irritancy, corrosivity, and substance transport.* European Journal of Pharmaceutics and Biopharmaceutics, 2005. **60**(2): p. 167-178.

339. Schafer-Korting, M., et al., *Reconstructed human epidermis for skin absorption testing: results of the German prevalidation study.* Altern Lab Anim, 2006. **34**(3): p. 283-94.

340. Schafer-Korting, M., et al., *The use of reconstructed human epidermis for skin absorption testing: Results of the validation study.* Altern Lab Anim, 2008. **36**(2): p. 161-87.

341. Hayden, P., et al., *Poster: skin models as alternatives to animal testing drug metabolizing enzyme activity in human in vitro dermal (EpiDerm™) and airway (EpiAirway™) epithelial models*. 2008.

342. Edwards, J.E., K.R. Brouwer, and P.J. McNamara, *GF120918, a P-glycoprotein modulator, increases the concentration of unbound amprenavir in the central nervous system in rats.* Antimicrob Agents Chemother, 2002. **46**(7): p. 2284-6.

343. Troutman, M.D. and D.R. Thakker, *Novel experimental parameters to quantify the modulation of absorptive and secretory transport of compounds by P-glycoprotein in cell culture models of intestinal epithelium.* Pharmaceutical Research, 2003. **20**(8): p. 1210-24.

344. Thiel-Demby, V.E., et al., *In vitro absorption and secretory quotients: practical criteria derived from a study of 331 compounds to assess for the impact of P-glycoprotein-mediated efflux on drug candidates.* Journal of Pharmaceutical Sciences, 2004. **93**(10): p. 2567-72.

345. Thiel-Demby, V.E., et al., *Biopharmaceutics classification system: validation and learnings of an in vitro permeability assay.* Mol Pharm, 2009. **6**(1): p. 11-8.

346. Mahjour, M., et al., *Effects of propylene glycol diesters of caprylic and capric acids (Miglyol® 840) and ethanol binary systems on in vitro skin permeation of drugs.* International Journal of Pharmaceutics, 1993. **95**(1–3): p. 161-169.

347. *3D human tissue models*. 2010 [cited; Available from: http://www.mbresearch.com/3dtissue.htm.

348. Muller, P.Y. and M.N. Milton, *The determination and interpretation of the therapeutic index in drug development.* Nat Rev Drug Discov, 2012. **11**(10): p. 751-61.

349. Bonina, F.P., et al., *In vitro and in vivo evaluation of polyoxyethylene esters as dermal prodrugs of ketoprofen, naproxen and diclofenac.* European Journal of Pharmaceutical Sciences, 2001. **14**(2): p. 123-134.

350. Harville, H.M., R. Voorman, and J.J. Prusakiewicz, *Comparison of paraben stability in human and rat skin.* Drug Metab Lett, 2007. **1**(1): p. 17-21.

351. Gonzalez, D., S. Schmidt, and H. Derendorf, *Importance of relating efficacy measures to unbound drug concentrations for anti-infective agents.* Clin Microbiol Rev, 2013. **26**(2): p. 274-88.

352. Schreiber, S., et al., *Reconstructed epidermis versus human and animal skin in skin absorption studies.* Toxicology in Vitro, 2005. **19**(6): p. 813-822.

353. Lotte, C., et al., *Permeation and Skin Absorption: Reproducibility of Various Industrial Reconstructed Human Skin Models.* Skin Pharmacology and Physiology, 2002. **15**(**suppl 1**)(Suppl. 1): p. 18-30.

354. Yardley, V. and S.L. Croft, *Animal Models of Cutaneous Leishmaniasis*, in *Handbook of Animals of Infection*, O. Zak, Editor. 1999, Academic Press London. p. 775-781.

355. Kropf, P., et al., *The Leishmaniasis Model*, in *Immunology of infection, 3rd edition*, D. Kabelitz and S.H.E. KAufmann, Editors. 2010, Elsevier: London, UK. p. 307-328.

356. Aguilar Torrentera, F., et al., *Parasitic load and histopathology of cutaneous lesions, lymph node, spleen, and liver from BALB/c and C57BL/6 mice infected with Leishmania mexicana.* Am J Trop Med Hyg, 2002. **66**(3): p. 273-9.

357. Hill, J.O., R.J. North, and F.M. Collins, *Advantages of measuring changes in the number of viable parasites in murine models of experimental cutaneous leishmaniasis.* Infect Immun, 1983. **39**(3): p. 1087-94.

358. Bretagne, S., et al., *Real-time PCR as a new tool for quantifying Leishmania infantum in liver in infected mice.* Clin Diagn Lab Immunol, 2001. **8**(4): p. 828-31.

359. Titus, R.G., et al., *A limiting dilution assay for quantifying Leishmania major in tissues of infected mice.* Parasite Immunol, 1985. **7**(5): p. 545-55.

360. Boitz, J.M., et al., *Leishmania donovani ornithine decarboxylase is indispensable for parasite survival in the mammalian host.* Infect Immun, 2009. **77**(2): p. 756-63.

361. Kobets, T., et al., *Genetics of Host Response to Leishmania tropica in Mice – Different Control of Skin Pathology, Chemokine Reaction, and Invasion into Spleen and Liver.* PLoS Negl Trop Dis, 2012. **6**(6): p. e1667.

362. Lang, T., *The luciferase-expressing L. major-C57Bl/6 mouse model: a standardized model for testing in real time the efficacy of therapeutic regimens*. 2006, Institut Pasteur: Paris.

363. Michel, G., et al., *Luciferase-expressing Leishmania infantum allows the monitoring of amastigote population size, in vivo, ex vivo and in vitro.* PLoS Negl Trop Dis, 2011. **5**(9): p. e1323.

364. Reimao, J.Q., et al., *Parasite burden in Leishmania (Leishmania) amazonensis-infected mice: validation of luciferase as a quantitative tool.* J Microbiol Methods, 2013. **93**(2): p. 95-101.

365. de La Llave, E., et al., *A combined luciferase imaging and reverse transcription polymerase chain reaction assay for the study of Leishmania amastigote burden and correlated mouse tissue transcript fluctuations.* Cellular Microbiology, 2011. **13**(1): p. 81-91.

366. Higuchi, R., et al., *Kinetic PCR analysis: real-time monitoring of DNA amplification reactions.* Biotechnology (N Y), 1993. **11**(9): p. 1026-30.

367. Ginzinger, D.G., *Gene quantification using real-time quantitative PCR: An emerging technology hits the mainstream.* Experimental Hematology, 2002. **30**(6): p. 503-512.

368. Stratagene, *Introduction to quantitative PCR - methods and application guide*. 2004, La Jolla, California: Stratagene.

369. Nicolas, L., et al., *Real-time PCR for detection and quantitation of leishmania in mouse tissues.* J Clin Microbiol, 2002. **40**(5): p. 1666-9.

370. van der Meide, W., et al., *Comparison between quantitative nucleic acid sequence-based amplification, real-time reverse transcriptase PCR, and real-time PCR for quantification of Leishmania parasites.* Journal of Clinical Microbiology, 2008. **46**(1): p. 73-78.

371. van Eys, G.J., et al., *Sequence analysis of small subunit ribosomal RNA genes and its use for detection and identification of Leishmania parasites.* Mol Biochem Parasitol, 1992. **51**(1): p. 133-42.

372. van der Meide, W.F., et al., *Quantitative nucleic acid sequence-based assay as a new molecular tool for detection and quantification of Leishmania parasites in skin biopsy samples.* J Clin Microbiol, 2005. **43**(11): p. 5560-6.

373. Bustin, S.A. and T. Nolan, *Pitfalls of quantitative real-time reverse-transcription polymerase chain reaction.* J Biomol Tech, 2004. **15**(3): p. 155-66.

374. Tellevik, M.G., et al., *Detection of a broad range of Leishmania species and determination of parasite load of infected mouse by real-time PCR targeting the arginine permease gene AAP3.* Acta Tropica, 2014. **137**(0): p. 99-104.

375. Hall, D.G., *Structure, properties, and preparation of boronic acid derivatives. Overview of their reactions and applications.*, in *Boronic acids: preparation and applications in organic Synthesis, medicine and materials.*, D.G. Hall, Editor. 2011, Wiley-VCH Verlag GmbH & Co. p. 1-133.

376. Aoyagi, T., et al., *Polymerization of benzalkonium chloride-type monomer and application to percutaneous drug absorption enhancer.* Journal of Controlled Release, 1990. **13**(1): p. 63-71.

377. Nokhodchi, A., et al., *The enhancement effect of surfactants on the penetration of lorazepam through rat skin.* Int J Pharm, 2003. **250**(2): p. 359-69.

378. Thong, H.Y., H. Zhai, and H.I. Maibach, *Percutaneous penetration enhancers: an overview.* Skin Pharmacology and Physiology, 2007. **20**(6): p. 272-282.

379. El-On, J. and G. Messer, *Leishmania major: antileishmanial activity of methylbenzethonium chloride.* Am J Trop Med Hyg, 1986. **35**(6): p. 1110-6.

380. Costa, I.S., et al., *S-nitrosoglutathione (GSNO) is cytotoxic to intracellular amastigotes and promotes healing of topically treated Leishmania major or Leishmania braziliensis skin lesions.* J Antimicrob Chemother, 2013. **68**(11): p. 2561-8.

381. Wester, R.C. and H.I. Maibach, *In vivo methods for percutaneous absorption measurements*, in *Percutaneous absorption: mechanisms-methodology-drug delivery*, R.L. Brounaugh and H.I. Maibach, Editors. 1989, Marcel Dekker Inc.: New York. p. 215–237.

382. Netzlaff, F., et al., *Comparison of bovine udder skin with human and porcine skin in percutaneous permeation experiments.* Altern Lab Anim, 2006. **34**(5): p. 499-513.
383. Harada, K., et al., *In-vitro permeability to salicylic acid of human, rodent, and shed snake skin.* J Pharm Pharmacol, 1993. **45**(5): p. 414-8.
384. Roy, S.D., et al., *Transdermal delivery of narcotic analgesics: comparative metabolism and permeability of human cadaver skin and hairless mouse skin.* Journal of Pharmaceutical Sciences, 1994. **83**(12): p. 1723-8.
385. Roberts, M.E. and K.R. Mueller, *Comparisons of in vitro nitroglycerin (TNG) flux across yucatan pig, hairless mouse, and human skins.* Pharmaceutical Research, 1990. **7**(6): p. 673-6.
386. Otto, A., J. du Plessis, and J.W. Wiechers, *Formulation effects of topical emulsions on transdermal and dermal delivery.* International Journal of Cosmetic Science, 2009. **31**: p. 1-19.
387. Coelho, A.C., et al., *In vitro and in vivo miltefosine susceptibility of a Leishmania amazonensis isolate from a patient with diffuse cutaneous leishmaniasis.* PLoS Negl Trop Dis, 2014. **8**(7): p. e2999.
388. Lindsay, s. and J. Barnes, *High perormance liquid chromatography.* 2nd ed. 2003, London: John Wiley &Sons Ltd.
389. Jones, D., *Pharmaceutical statistics.* 1st ed. 2002, London: pharmaceutical Press.

APPENDIX

APPENDIX 1: VALIDATION OF HPLC METHODS
- Caffeine, ibuprofen, amphotericin B and buparvaquone -

Preparation of standard solutions

A stock solution of 1 mg/ml was prepared by accurately weighting 10 mg of the drug and diluting that with HPLC grade water in a 10 ml volumetric flask. Standard solutions were obtained by diluting the stock solution. The data is presented as mean ± standard deviation from three different sets of standard solutions.

Details of the HPLC method

TABLE 1. SUMMARY OF THE HPLC ASSAY USED FOR THE DETECTION OF CAFFEINE, IBUPROFEN, AMPHOTERICIN B AND BUPARVAQUONE.

| Compound ID	HPLC column	Injection volume	Mobile phase		Flow rate	Detector wavelength
			A	B		
Caffeine	Phenomenex; Synergi–Hydro RP (250x4.6mm; 5µm)	20	0.1% TFA in water (15%)	ACN (85%)	1.3	273
Ibuprofen	Phenomenex; Synergi–Hydro RP (250x4.6mm; 5µm)	20	0.1% TFA in water (30%)	ACN (70%)	1	227
Amphotericin B	Phenomenex; Synergi–Hydro RP (250x4.6mm; 5µm)	80	2.5mM EDTA in water (68%)	ACN (37%)	1	407 -380
Buparvaquone	Luna C18 (4.6x250mm; 5µm) with Luna guard column	20	5% Water+ acetic acid (pH3.5) (5%)	MeOH (95%)	1.7	250
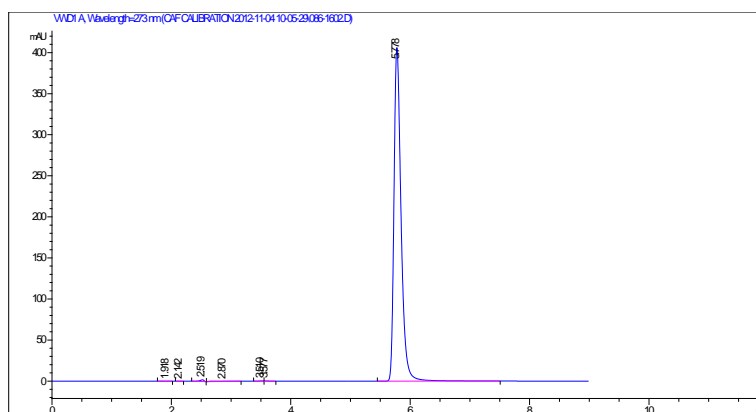
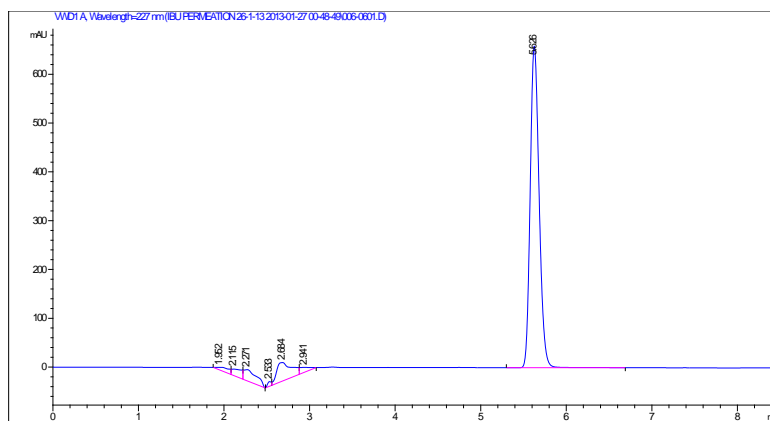FIGURE 1. TYPICAL RP-HPLC CHROMATOGRAM OF 100 µG/ML OF CAFFEINE.

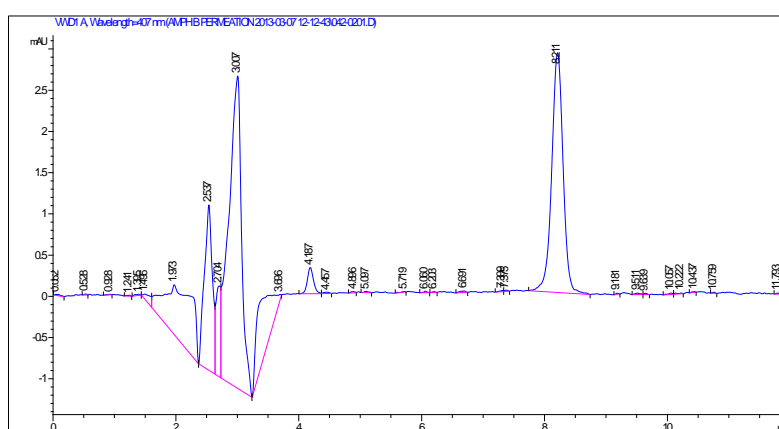**FIGURE 2. TYPICAL RP-HPLC CHROMATOGRAM OF 10 µG/ML IBUPROFEN,**

FIGURE 3. TYPICAL RP-HPLC CHROMATOGRAM OF 160 NG/ML AMPHOTERICIN B
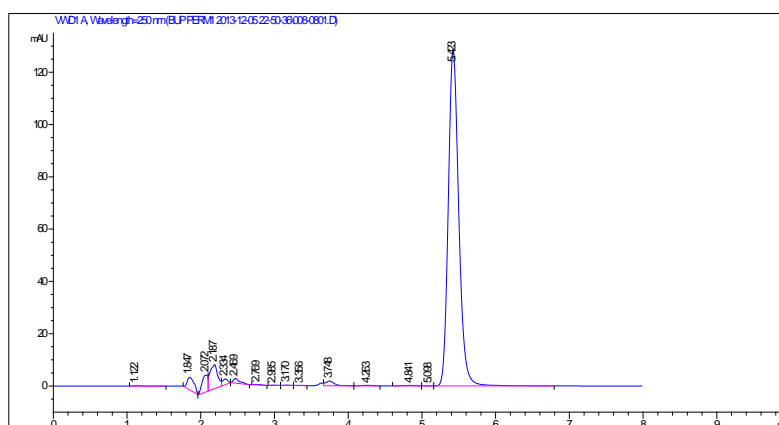

FIGURE 4. TYPICAL RP-HPLC CHROMATOGRAM OF 125 µG/ML BUPARVAQUONE.

Retention time and capacity factor

A compound is eluted from the HPLC column after a period of time known as the retention time (t_R). The retention time is dictated by the flow and nature of the mobile phase as well as the length of the column. If the mobile phase is flowing slowly or the HPLC column is relatively long, then the mobile phase residence time (t_0) is also large. Therefore, the capacity factor (k') which express the elution time of the compound of interest relative to the solvent front is often preferred because it is independent of the column length and mobile phase flow rate [388].

$$k' = \frac{t_R - t_0}{t_0}$$
<div align="right">**EQUATION 9**</div>

A capacity factor between 1 and 5 is often preferred as this implies good separation of the solvent from and the analysed compound without an overly long detection time. The retention time of caffeine, ibuprofen, amphotericin b and buparvaquone are 5.2, 5.6, 8.2 and 5.1 min respectively with corresponding capacity factors of 1.7, 1.9, 3.3 and 1.8 respectively.

Linearity

The linearity of the HPLC detection assays was assessed by plotting the peak area against concentration. The calibration graphs obtained have a linear regression coefficient of > 0.99 for all drugs. The methods are therefore linear over the analysed concentration ranges (1-500 µg/ml for caffeine, 0.5-500 µg/ml for ibuprofen, 0.75-100ug/ml for amphotericin b and 0.1 to 250ug/ml for buparvaquone).
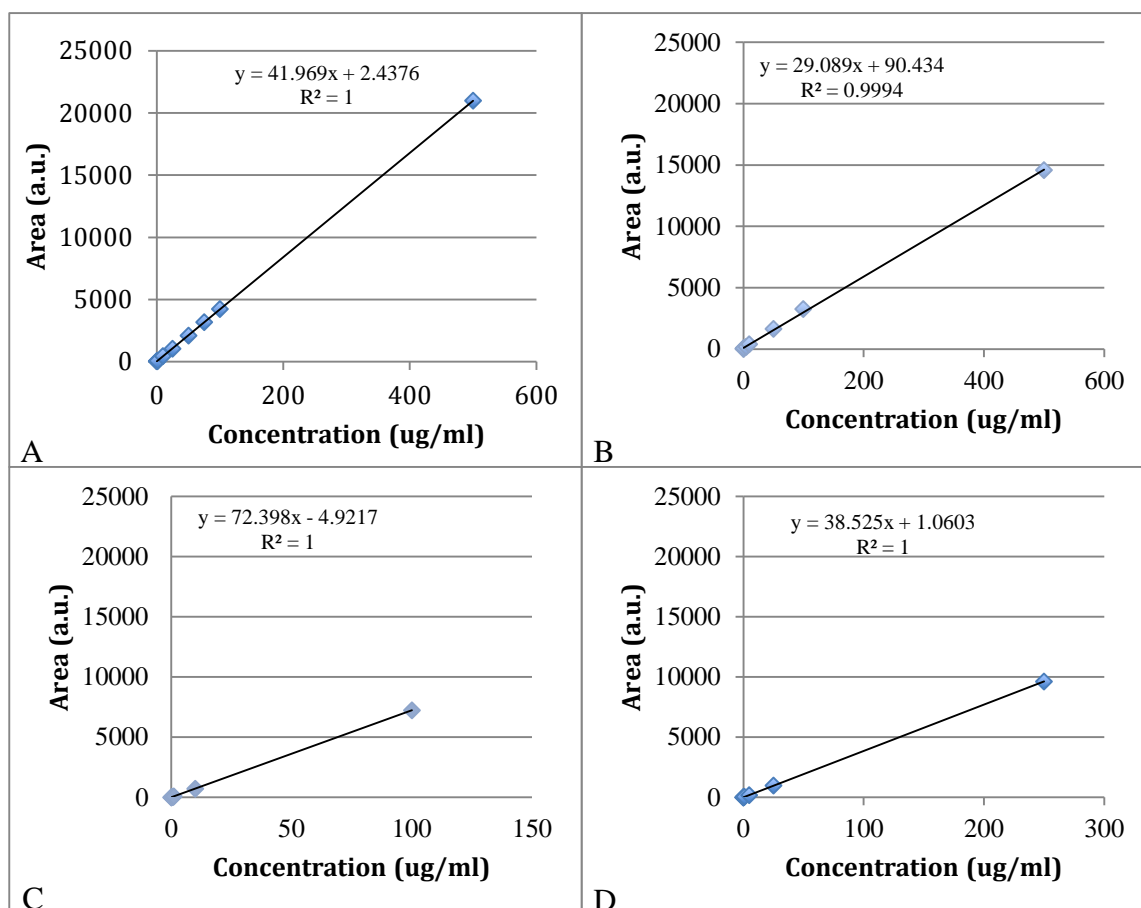
FIGURE5. CALIBRATION CURVES OF: A) CAFFEINE, B) IBUPROFEN, C) AMPHOTERICIN B AND D) BUPARVAQUONE.

Accuracy and precision

Accuracy can be defined as the degree to which a measured value conforms to the true value [389]. In pharmaceutical analysis, an assay is said to be accurate if the mean result is the same as the true value. The accuracy of the analysis obtained for each drug (n=3) expressed as a percentage of the expected concentration, also known as percentage recovery, according to the following equation:

$$Accuracy = \frac{C_c}{C_s} \times 100$$

EQUATION 10

Where C_c is the calculated concentration and C_s is the nominal standard concentration.

Precision, on the other hand, is described as the variability of a set of measurements [389]. Unlike accuracy, this does not provide any indication of the closeness of the obtained results from the true value. High precision is indicative of low variability in

measurements usually demonstrated by low standard deviation values. This is usually reported as a percentage relative standard deviation (%RSD) [389]:

$$\% RSD = \frac{SD}{[Drug]} \times 100 \qquad \text{EQUATION 11}$$

The precision of the method was determined by repeatability (intra-day) and intermediate precision (inter-day). Repeatability was determined by performing three repeated analysis of the same standard solution on the same day, under the same experimental conditions. The intermediate precision of the HPLC methods was assessed by carrying out the analysis on three different days (inter-day). For each drug, the percentage relative standard deviation (%RSD) and the percentage recovery of the standard solutions are reported for each drug (Table 2, 3, 4, 5, 6, 7, 8 and 9).

TABLE 2. THE PRECISION OF THE CAFFEINE HPLC ASSAY.

Standard Concentration (µg/ml)	Intra-day calculated concentration (µg/ml)	Inter-day Calculated concentration (µg/ml)	Intra-day % RSD	Inter-day % RSD
0.5	0.53±0.02	0.51±0.05	3.5	8.87
1	1.02±0.02	1.03±0.09	1.63	9.20
10	9.99±0.07	10.12±0.15	0.73	1.47
25	24.51±0.26	24.83±0.28	1.04	1.13
50	50.49±0.54	50.35±0.73	1.08	1.45
75	75.27±1.86	74.25±1.06	2.47	1.43
100	99.68±1.05	100.42±0.43	1.05	0.42

TABLE 3. THE ACCURACY OF THE CAFFEINE HPLC ASSAY.

Test solutions Concentration (µg/ml)	Calculated concentration (µg/ml)	% recovery
0.75	0.79±0.01	97.1
7.5	21.34±0.17	107.7
80	80.10±0.03	100.0

TABLE 4. THE PRECISION OF THE IBUPROFEN HPLC ASSAY.

Standard Concentration (µg/ml)	Intra-day calculated concentration (µg/ml)	Inter-day Calculated concentration (µg/ml)	Intra-day % RSD	Inter-day % RSD
0.5	-	0.49±0.05	-	9.62
1	0.92±0.01	1.02±0.08	1.46	8.08
5	5.12±0.17	5.21±0.32	0.21	6.20
10	10.26±0.02	10.32±0.51	0.15	4.98
50	50.40±0.05	49.98±1.11	0.09	2.22
100	99.62±0.02	100.04±0.47	0.02	0.47

TABLE 5. THE ACCURACY OF THE IBUPROFEN HPLC ASSAY.

Test solutions Concentration (µg/ml)	Calculated concentration (µg/ml)	% recovery
0.75	0.73±0.01	97.1
20	21.54±0.17	107.7
80	80.10±0.03	100.0

TABLE 6. THE PRECISION OF THE BUPARVAQUONE HPLC ASSAY.

Standard Concentration (µg/ml)	Intra-day calculated concentration (µg/ml)	Inter-day Calculated concentration (µg/ml)	Intra-day % RSD	Inter-day % RSD
0.1	0.11±0.01	0.19±0.01	8.71	6.98
0.25	0.25±0.02	0.33±0.01	6.68	3.73
0.5	0.49±0.03	0.55±0.01	6.42	2.03
1	0.99±0.04	0.99±0.01	4.33	0.56
5	5.08±0.24	4.89±0.00	4.09	0.09
25	25.00±0.08	24.55±0.11	0.07	0.44
125	127.09±0.33	125.77±2.17	0.26	0.02

TABLE 7. THE ACCURACY OF THE BUPARVAQUONE HPLC ASSAY.

Test solutions Concentration (µg/ml)	Calculated concentration (µg/ml)	% recovery
2	2.10±0.39	109.3
60	55.57±1.32	92.6
120	121.85±0.03	101.5

TABLE 8. THE PRECISION OF THE AMPHOTERICIN B HPLC ASSAY.

Standard Concentration (µg/ml)	Intra-day calculated concentration (µg/ml)	Inter-day Calculated concentration (µg/ml)	Intra-day % RSD	Inter-day % RSD
0.75	0.71±0.07	0.79±0.02	9.63	1.97
1	1.03±0.08	0.98±0.01	7.63	0.6
10	9.84±0.10	9.40±0.05	1.04	0.49
50	51.46±1.31	49.96±2.57	2.55	5.14
100	99.29±0.65	100.08±1.29	0.65	1.28

TABLE 9. THE ACCURACY OF THE AMPHOTERICIN B HPLC ASSAY.

Test solutions Concentration (µg/ml)	Calculated concentration (µg/ml)	% recovery
1	0.92±0.07	91.9
50	50.29±1.91	100.1
100	99.90±0.97	99.9

APPENDIX 2: DSC PROFILE
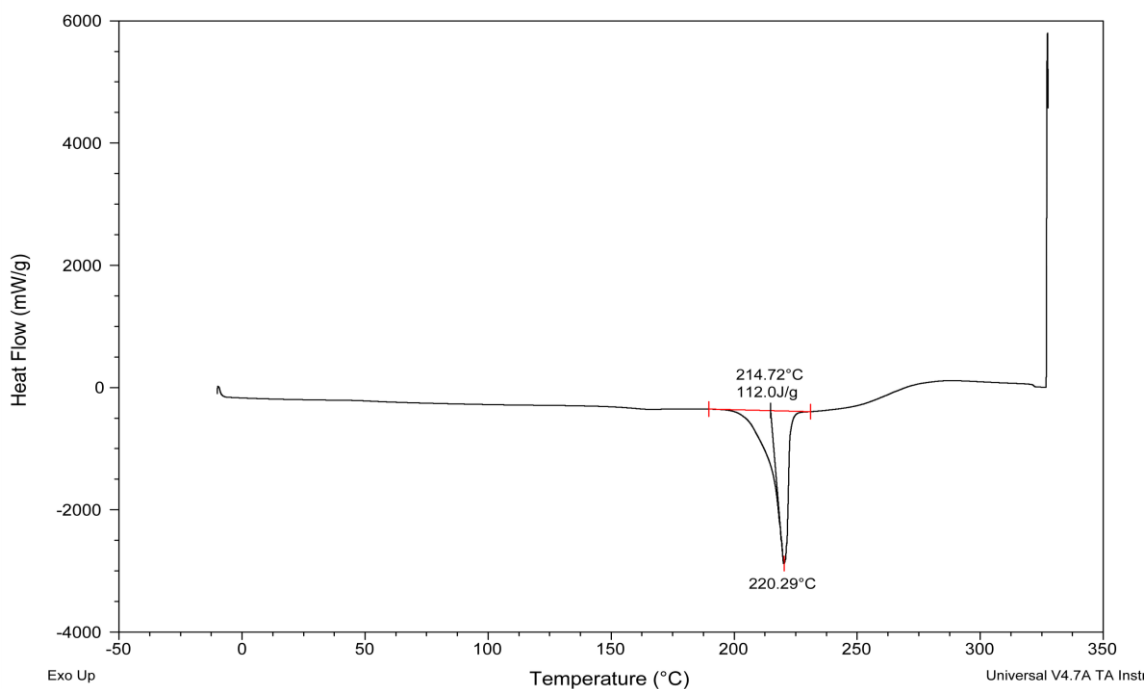
- LSH001, LSH002 and LSH003 -

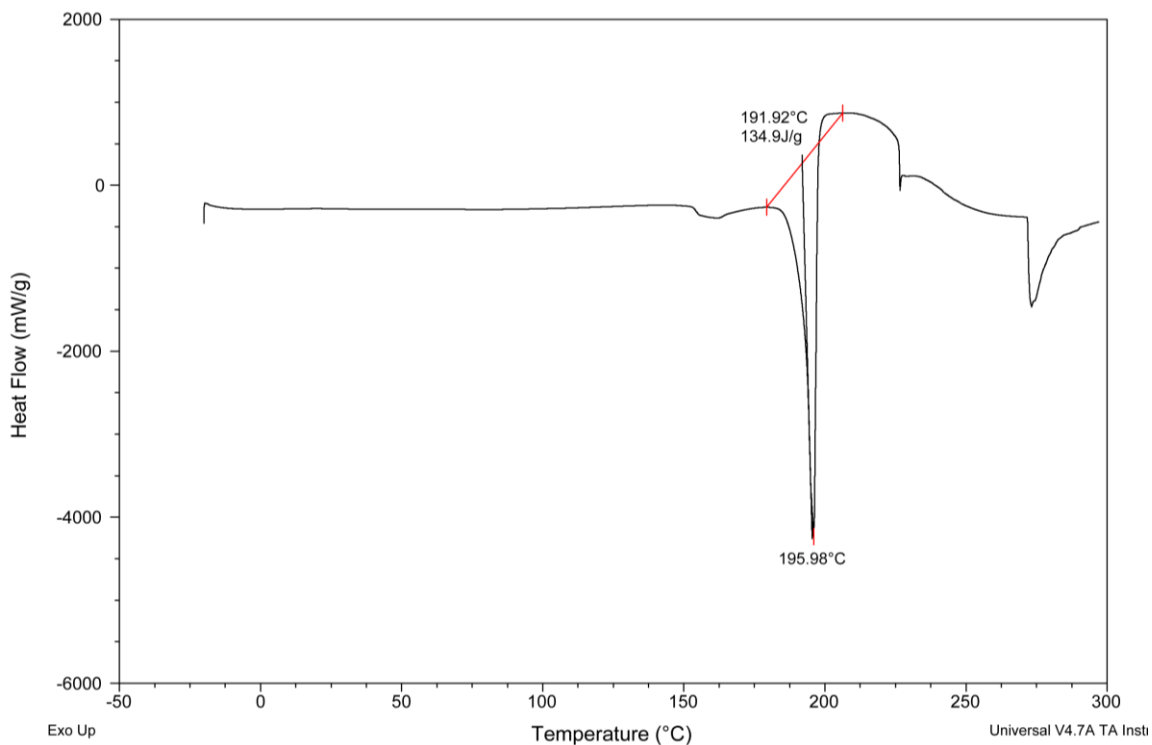**FIGURE 6. DSC PROFILE FOR LSH001.**
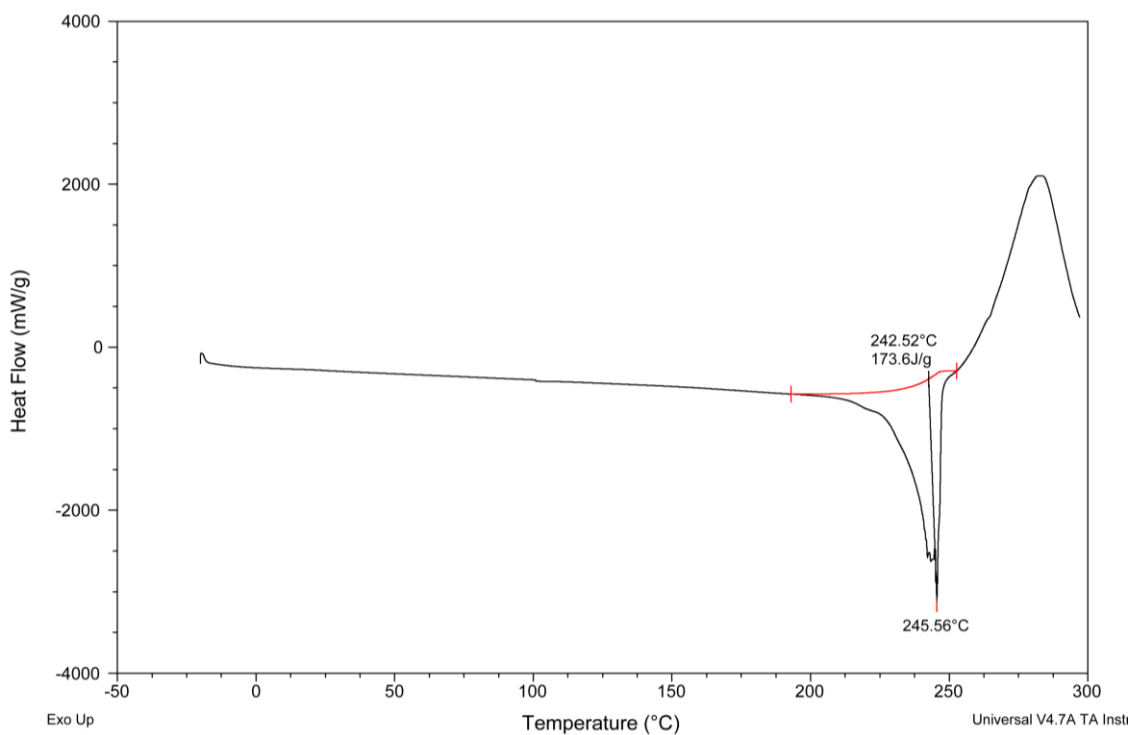

FIGURE 7. DSC PROFILE FOR LSH002.

FIGURE 8. DSC PROFILE FOR LSH003.

APPENDIX 3: *IN VIVO* STUDY

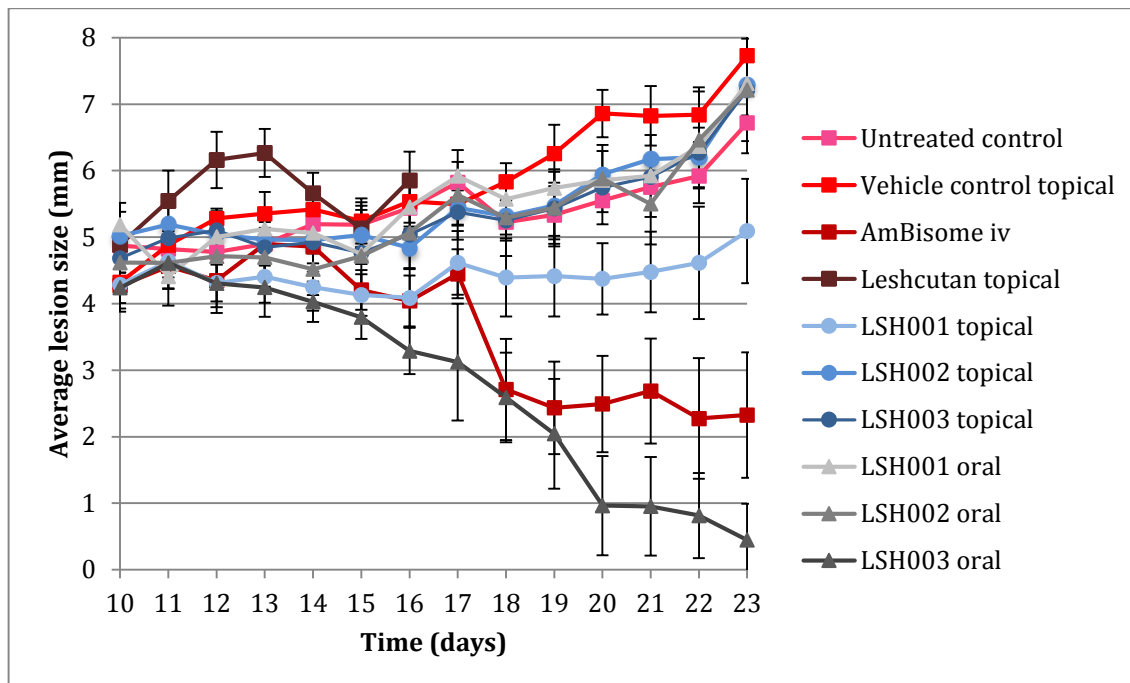## *- Progression of lesion size diameter in function of time -*

FIGURE 9. AVERAGE LESION SIZE PROGRESSION PER GROUP IN FUNCTION OF TIME POST INFECTION.

APPENDIX 4: MISCIBILITY STUDIES

- Solvent ratios for binary and ternary solvent mixtures -

TABLE 10. SOLVENT RATIOS TESTED FOR BINARY SOLVENT MIXTURES.

Ratio (v/v)	Volume (ml)	
	Solvent A	**Solvent B**
1/9	0.1	0.9
2/8	0.2	0.8
3/7	0.3	0.7
4/6	0.4	0.6
5/5	0.5	0.5
6/4	0.6	0.4
7/3	0.7	0.3
8/2	0.8	0.2
9/1	0.9	0.1

TABLE 11. SOLVENT RATIOS TESTED FOR TERNARY SOLVENT MIXTURES.

Ratio (v/v)	Volume (ml)		
	Solvent A	**Solvent B**	**Solvent C**
1/1/8	0.1	0.8	0.8
1/2/7	0.1	0.7	0.7
1/3/6	0.1	0.6	0.6
1/4/5	0.1	0.5	0.5
1/5/4	0.1	0.4	0.4
1/6/3	0.1	0.3	0.3
1/7/2	0.1	0.2	0.2
1/8/1	0.1	0.1	0.1
2/1/7	0.2	0.7	0.7
2/2/6	0.2	0.6	0.6
2/3/5	0.2	0.5	0.5
2/4/4	0.2	0.4	0.4
2/5/3	0.2	0.3	0.3
2/6/2	0.2	0.2	0.2
2/7/1	0.2	0.1	0.1
3/1/6	0.3	0.6	0.6
3/2/5	0.3	0.5	0.5
3/3/4	0.3	0.4	0.4
3/4/3	0.3	0.3	0.3
3/5/2	0.3	0.2	0.2
3/6/1	0.3	0.1	0.1
4/1/5	0.4	0.5	0.5
4/2/4	0.4	0.4	0.4
4/3/3	0.4	0.3	0.3
4/4/2	0.4	0.2	0.2
4/5/1	0.4	0.1	0.1
5/1/4	0.5	0.4	0.4
5/2/3	0.5	0.3	0.3
5/3/2	0.5	0.2	0.2
5/2/3	0.5	0.1	0.1
5/1/4	0.5	0.3	0.3
6/1/3	0.6	0.2	0.2
6/2/2	0.6	0.1	0.1
6/3/1	0.6	0.2	0.2
7/1/2	0.7	0.1	0.1
7/2/1	0.7	0.1	0.1
8/1/1	0.8	0.1	0.1